Novel Carbohydrate-based Materials *via* Sustainable Modification Procedures

Zur Erlangung des akademischen Grades eines

DOKTORS DER NATURWISSENSCHAFTEN

(Dr. rer. nat.)

von der KIT-Fakultät für Chemie und Biowissenschaften

des Karlsruher Instituts für Technologie (KIT)

genehmigte

DISSERTATION

von

M. Sc. Eren Esen

Dekan: Prof. Dr. Manfred Wilhelm

Referent: Prof. Dr. Michael A.R. Meier

Korreferent: Prof. Dr. Pavel Levkin

Tag der mündlichen Prüfung: 09.12 2020

To my parents,

Nihal and Serdar Esen

Die vorliegende Arbeit wurde von November 2017 bis Oktober 2020 unter Anleitung von Prof. Dr. Michael A. R. Meier am Institut für Organische Chemie (IOC) des Karlsruher Instituts für Technologie (KIT) durchgeführt.

Hiermit versichere ich, dass ich die Arbeit selbstständig angefertigt, nur die angegebenen Quellen und Hilfsmittel benutzt und mich keiner unzulässigen Hilfe Dritter bedient habe. Insbesondere habe ich wörtlich oder sinngemäß aus anderen Werken übernommene Inhalte als solche kenntlich gemacht. Die Satzung des Karlsruher Instituts für Technologie (KIT) zur Sicherung wissenschaftlicher Praxis habe ich beachtet Des Weiteren erkläre ich, dass ich mich derzeit in keinem laufenden Promotionsverfahren befinde, und auch keine vorausgegangenen Promotionsversuche unternommen habe. Die elektronische Version der Arbeit stimmt mit der schriftlichen Version überein und die Primärdaten sind gemäß der Satzung zur Sicherung guter wissenschaftlicher Praxis des KIT beim Institut abgegeben und archiviert.

Karlsruhe, 28.10.2020

_____

Eren Esen

Acknowledgements

First of all and at most, I am thankful to Mike for accepting me in this PhD program and supervising me for three years. Anytime I wanted to ask something to him, his door was always open to me. Therefore, I thank him for his advices, patience, kindness and understanding. I learned too many things during my study from him and his impact on my academic skills and my personality is uncountable. Gratefully thank you!

I would like to thank Prof. Selim Küsefoğlu who was my supervisor during my master studies. He encouraged me for my PhD application, and I could not be here without him.

Thank you Luca, Kevin, Roman and Philipp for your comments and corrections. I am especially thankful to Luca for never saying no to me even I sent too many pages and for his immediate corrections.

I would like to thank the whole Meier group, current and former members, for your friendship, help and the coffee/lunch breaks we had. Unfortunately, we could not do our fun BBQ parties this year due to coronavirus and I will miss them a lot! My special thanks go to Lab 409: Pia, Luca and Julian, for the great working atmosphere. The rest of the MZE crew: Philip, Kevin, Marc, Daniel, Jonas, Stefano and Anja, and of course the IOC crew: Roman, Michi, Maxi, Federico and Dennis, thank you for everything! Additionally, I am grateful to Pinar for helping me about the official documents and translations, Becky and Anni for making our life easier. I thank the former group members, Yasmin, Katharina, Rebekka, Gregor and Ben for our fun conversations, and Zafer and Kenny for their advices and helps when I first start my PhD and showing me how amazing the carbohydrate chemistry is.

I am also thankful to Dr. Shouliang Nie for the tensile strength measurement and Johannes Scheiger for the contact angle measurement introductions, and Hans Weickenmeier for the TGA measurements.

My community (Hatice, Meryem, Begüm and Emmerich) in Karlsruhe, I thank you all for the fun times we had with lots of Lambrusco and making me feel at home. I especially thank Hatice who was always the first person when I need an advice.

Benim güzel ailem! Size ne kadar teşekkür etsem az kalir. Bu zamana kadar hep arkamda oldugunuzu bilmek bana hep güc verdi. Sizden uzakta olsam bile zor zamanlarimda sesinizi duymak her zaman önceligim oldu. Bu doktora tezini sizlere adiyorum.

Katja, thank you for everything! You were always there when I need you and I am grateful for the memories we have shared. Thank you for always being supportive and thoughtful!

Abstract

The use of renewable feedstocks for the production of polymer-based materials is receiving ever-growing interest with the objective of a more sustainable circular economy and to decrease the level of dependency of mankind on fossil-based resources. Among the broad range of renewable feedstocks, cellulose and starch offer inherent advantages as excellent candidates for such a substitution due to their high abundancy and unique properties. Inevitably, efforts should be made in order to ensure that these natural polymers could replace synthetic polymers, and to successfully process them using existing industrial-scale technologies. Indeed, it can be achieved *via* post-modification (functionalization) of these natural polymers to generate new, bio-based materials with potential applications. In other words, in order to expand the scope of bio-derived polymers, it is essential to take full advantage of the intrinsic nature of bio-renewable compounds. To achieve the latter, the combination of multicomponent reactions and post-modification should be ideal to realize diversity-oriented polymer synthesis because post-modification can produce various functional polymers starting from a single polymeric sample. Accordingly, in the first part of the thesis, starch was functionalized *via* multicomponent reaction approach. First, starch acetoacetates were synthesized with an efficient and straightforward procedure and subsequently modified by using different renewable aromatic aldehydes and urea *via* the Biginelli multicomponent reaction. After the optimization studies, the processability of the products was also investigated, and glycerol was used as a renewable plasticizer to obtain fully renewable materials.

In the following parts the thesis, cellulose was used as a renewable substrate. In the first approach, cellulose was oxidized to its 2,3-dialdeyhde cellulose (DAC) derivative and subsequently modified *via* the Passerini three-component reaction (P-3CR) employing various renewable carboxylic acids and commercially available isocyanides. P-3CR modification offered the possibility to tune the product's thermal properties by simply varying the acid and isocyanide components in an efficient and catalyst free procedure.

In the last approach, a CO_2-based switchable solvent system was utilized for the transesterification of cellulose using a fatty acid methyl ester. After the optimization of the reaction conditions, the synthesized fatty acid cellulose esters (FACEs) were further modified *via* thiol-ene reactions to investigate the effect of the attached thioether group on the final products' thermal and mechanical properties. With a final modification, two of the thiol-ene products were oxidized to their corresponding sulfone derivatives. Each synthesized product processed into films and their mechanical, thermal and hydrophobic properties were investigated for possible future applications.

Zusammenfassung

Die Verwendung erneuerbarer Rohstoffe für die Herstellung von Polymermaterialien erfährt immer größeres Interesse, mit dem Ziel einer nachhaltigeren Kreislaufwirtschaft und der Verringerung der Abhängigkeit der Gesellschaft von fossilen Ressourcen. Aus der großen Menge erneuerbarer Rohstoffe stechen besonders Cellulose und Stärke aufgrund ihrer breiten Verfügbarkeit und ihrer einzigartigen Eigenschaften als ausgezeichnete Kandidaten heraus. Zukünftig sollte sichergestellt werden, dass diese natürlichen Polymere mittels existierender Technologien im Industriemaßstab erfolgreich verarbeitet werden können, und dass diese synthetische Polymere tatsächlich ersetzen können. Dies kann zum Beispiel durch postsynthetische Modifikation (Funktionalisierung) natürlicher Polymere ermöglicht werden, um neue, biobasierte Materialien für zukünftige Anwendungen herzustellen. Es ist daher notwendig, die inhärenten Eigenschaften biologisch-erneuerbarer Verbindungen maximal auszuschöpfen, um den Anwendungsbereich biobasierter Polymere bestmöglich auszudehnen. Um Letzteres zu erreichen, eignet sich idealerweise die Kombination aus Mehrkomponentenreaktionen und Post-Modifizierungen, um eine diversitätsorientierte Polymersynthese zu realisieren, da hierdurch verschiedenste funktionelle Polymere ausgehend von einem einzigen Vorläuferpolymer hergestellt werden können.

Dementsprechend wurde im ersten Teil dieser Arbeit Stärke mittels einer Mehrkomponentenreaktionsstrategie funktionalisiert. Zunächst wurden Stärkeacetoacetate mit einem effizienten und einfachen Verfahren synthetisiert und anschließend unter Verwendung verschiedener erneuerbarer, aromatischer Aldehyde sowie Harnstoff mittels der Biginelli-Mehrkomponentenreaktion modifiziert. Nach den Optimierungsstudien wurde auch die Prozessierbarkeit der Produkte untersucht und zudem Glycerin als erneuerbarer Weichmacher verwendet, um vollständig erneuerbare Materialien zu erhalten.

Die anschließenden Teile der Arbeit konzentrierten sich auf Cellulose als erneuerbares Substrat. Cellulose wurde im ersten Ansatz zum 2,3-Dialdehyd-

Cellulose-Derivat (DAC) oxidiert und daraufhin mittels der Passerini-Dreikomponentenreaktion (P-3CR) unter Verwendung verschiedener erneuerbarer Carbonsäuren und kommerziell erhältlicher Isocyanide modifiziert. Die P-3CR-Modifikation ermöglichte es, die thermischen Eigenschaften der Produkte durch einfache Variation der Säure- und Isocyanidkomponenten in einem effizienten und katalysatorfreien Verfahren einzustellen.

Im letzten Ansatz wurde ein CO_2-basiertes, schaltbares Lösungsmittelsystem für die Umesterung von Cellulose unter Verwendung von Fettsäuremethylester verwendet. Nach der Optimierung der Reaktionsbedingungen wurden die synthetisierten Fettsäure-Celluloseester (FACEs) über eine Thiol-En-Reaktion weiter modifiziert, um den Einfluss der daraus resultierenden Thioethergruppe auf die mechanischen und thermischen Eigenschaften der Endprodukte zu untersuchen. In einer abschließenden Modifikation wurden zwei der Thiol-En-Produkte zu ihren entsprechenden Sulfonderivaten oxidiert. Jedes synthetisierte Produkt wurde zu Filmen verarbeitet und deren mechanischen, thermischen und hydrophoben Eigenschaften im Hinblick auf zukünftig mögliche Anwendungen untersucht.

Table of Contents

1 Introduction

The United Nations' World Population Prospects report from 2019 discloses that the world population is expected to reach 9.6 billion by 2050, which can be directly related to a drastic increase on vital demands, such as food and energy, as well as daily life products.[1] Fossil resources have been employed to fulfill the energy and raw material demands for industries in today's world. However, with the increasing consumption and our dependency on these resources, they will deplete in the foreseeable future. The expected values for remaining fossil resources are 50 years for natural gas and crude oil, and 132 years for coal with the current consumption rate.[2]

The chemical industry highly depends on crude oil as a raw material for the production of plastics. A modern life without plastics has become impossible, as they have been integrated in almost every part of our daily routine. Since their properties can be tuned, plastics have substituted the consumption of several conventional materials, such as metals, ceramics, glass etc. and this change is still ongoing. Due to their high production rate, plastics are becoming more accessible and making human life easier. However, are they really that innocent?

The global annual production of plastics is estimated as 360 million tons and this number is expected to be doubled in 20 years.[3-4] Additionally, 20% of the crude oil will be used for plastic production, resulting in 15% of the global carbon emission by 2050. Thus, to decrease our dependency on fossil resources and their negative impacts on the environment, immediate actions should be taken. In this regard, the UN released the 2030 Agenda for Sustainable Development in 2015, and as a chemist and also consumer, we are obligated with a considerable number of responsibilities.[5] As Anastas and Warner described in the Twelve Principles of Green Chemistry, the use of renewable resources, minimizing toxic chemicals and derivatizations, increasing the atom efficiency and preventing waste production should be our priorities while designing a synthesis.[6]

Indeed, the utilization of renewable feedstocks for bio-based polymer synthesis has become an important topic, as these resources offer a large variety of compounds

suitable for polymer production, including carbohydrates (such as cellulose, starch and chitin), lignin, vegetable oils, and terpenes (**Figure 1**).[7-8] Biomass is the main source for the renewable feedstocks, and 75% of it consist of carbohydrates, making them very attractive for the chemical industry.[9]

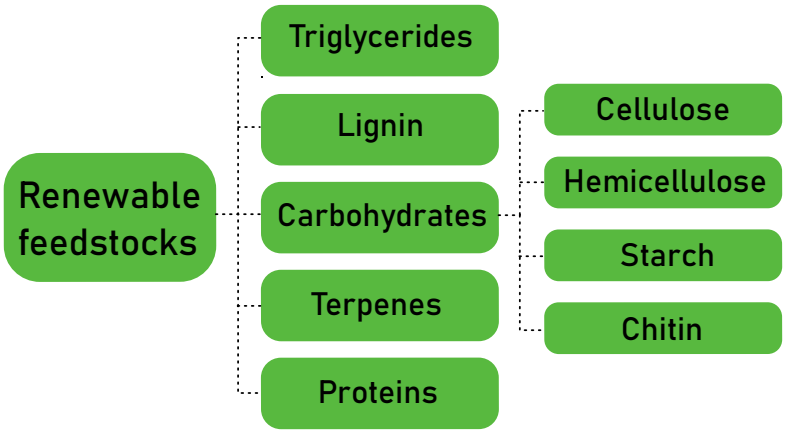

Figure 1: Common renewable feedstocks used in polymer production.

Carbohydrates are mainly biopolymers and can be further functionalized to produce carbohydrate-based materials or converted to building blocks for bio-based polymers production.[8] They have received a considerable interest for bio-based material production, since they are highly abundant, biocompatible, and biodegradable. However, to compete with the existing synthetic polymers and in order to improve their inherent properties they often have to be functionalized. These functionalizations should be performed in a sustainable manner by exploiting renewable components and non-hazardous procedures resulting in low waste production. Thus, reactions should offer high atom efficiency, the possibility to tune the products properties, less waste production and mild reaction conditions, while avoiding toxic or otherwise problematic substances. In this context, among the numerous organic reactions, multicomponent reactions and thiol-ene addition appear as suitable candidates.

2 Theoretical Background

2.1 Cellulose

Cellulose is known to be the most abundant biopolymer on earth, with fascinating properties such as renewability, biocompatibility, biodegradability, low cost and high thermal and mechanical stability, which makes it a very valuable starting material for the chemical industry.[10] It is considered a very crucial biomass component, with an annual production of approximately 1.5 x 10^{12} tons.[10]

Cellulose was first isolated by the French chemist Anselm Payen in 1837.[11-12] In his work, various plant tissues were treated with acids and ammonia, and a fibrous solid was obtained after the extraction with water, alcohol and ether. By elemental analysis, the molecular formula $C_6H_{10}O_5$ was determined and in 1920, its polymeric structure was elucidated by Hermann Staudinger.[13]

Cellulose has been employed to fulfill humankind's energy, clothing or building material demands for thousands of years, mostly in the form of wood, cotton or fibers.[10] However, its first utilization as a raw material dates back over 150 years with the production of the first man made plastic, celluloid.[14] This first thermoplastic material was patented by Hyatt Manufacturing Company and consists of nitrocellulose, obtained by reaction of cellulose with nitric acid/sulfuric acid mixture, and camphor (as a plasticizer).

2.1.1 Structure and Morphology

Cellulose is a linear homopolymer of *β*-1,4 linked D-glucopyranose units. One *β*-D-glucopyranose unit of cellulose is often termed anhydroglucose unit (AGU). The degree of polymerization (DP) of cellulose can vary between 150 and 10000, indicating the number of AGU per cellulose chain, highly depending on the on the source and treatment methods of cellulose.[10]

Table 1: Typical DP values of common types of cellulose[10]

Cellulose type	Degree of polymerization (DP)
Wood pulp	300-1700
Cotton and other plant fibers	800-10000
Bacterial cellulose	800-10000
Regenerated cellulose fibers	250-500
Microcrystalline cellulose	150-300

AGU, as a repeating unit, consists of three hydroxyl groups: one primary hydroxyl group at the C6 position and two secondary hydroxyl group at the C2 and C3 positions. Every AGU of cellulose is connected with each other *via* glycosidic bonds from the equatorial hydroxyl groups of C1 and C4, resulting the formation of the thermodynamically favored $^4C_1$ conformation.[15] The $^4C_1$ conformation indicates the chair conformation of a 6 membered glucopyranose ring, where C2, C3, C5 and the oxygen atom are in the same plane, C4 is above and C1 is below this plane (**Scheme 1**). Every second AGU ring is rotated 180° in the plane to keep the preferred bond angles of the glycosidic bonds. This two AGU rings are connected *via* *β*-1,4 bond and often called as cellobiose unit, which has a length of 1.3 nm.

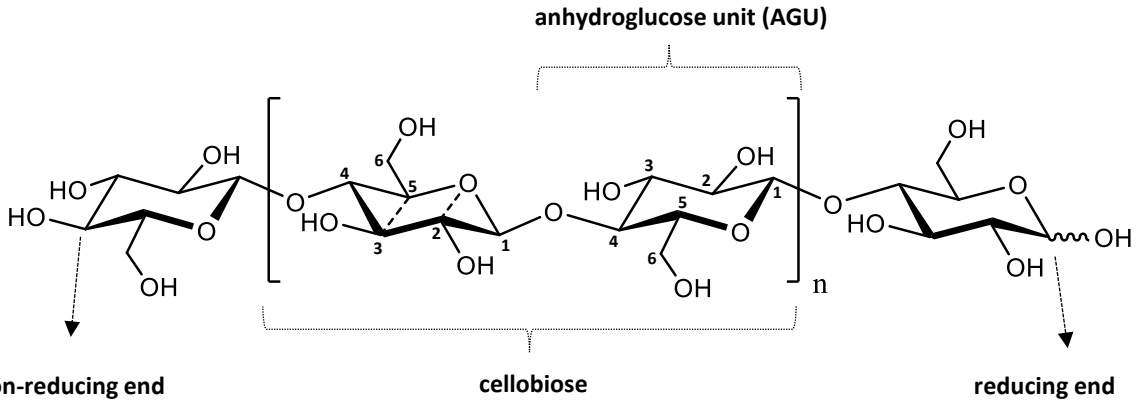

Scheme 1: Structural aspects of cellulose.

The cellulose structure contains two different ends, called reducing and non-reducing end.[16] The reducing end is the hemiacetal moiety in the D-glucopyranose unit, which is in an equilibrium with the corresponding aldehyde function. The stereochemistry of

the anomeric center is not fixed, meaning the C1-OH can be present in α or β conformation. The other end of the cellulose consists of the C4-OH group, the so called non-reducing end. These two end groups have no impact on the overall properties of cellulose, however the reducing end gives the opportunity to modify cellulose selectively.[17-19] These types of modifications (so-called end-wise modifications) include strategies like ligation, reductive amination and Knoevenagel condensation, and have been intensively investigated especially with cellulose nanocrystals (CNCs).[20-23]

One of the most important terms for cellulose chemistry, the degree of substitution (DS), is used to describe how many hydroxyl groups per AGU have been reacted during the chemical modification of cellulose. Thus, DS values can be in the range from 0 to 3. The hydroxyl groups exhibit different reactivity: the primary hydroxyl group at C6 has a significantly higher reactivity compared to the secondary ones positioned at C2 and C3.[10] Additionally, due to different reactivity and steric hindrance, regioselective substitution of cellulose is also achievable, which can affects the final product's properties.[24-26]

Cellulose is universally accepted as a semi-crystalline polymer, as it contains both highly ordered (crystalline) and less ordered (amorphous) regions.[27] The crystallinity of cellulose highly depends on its source. Also, numerous derivatives such as microcrystalline cellulose (MCC), nanofibrillated cellulose (NFC) and nanocrystalline cellulose (NCC) can be prepared *via* different acid treatments.[10, 23, 28]

Looking at the macromolecular arrangement of the carbohydrate chains, cellulose is found in different crystalline allomorphs. In nature, it exist in the cellulose I form (I_α and I_β) and the ratio of I_α and I_β depends on the source of cellulose.[29] For instance, lower organisms like bacteria possess mostly the I_α type, while higher plants show a larger percentage of I_β.[30] Apart from the cellulose I from, cellulose can be also converted to cellulose II, III_I, III_{II}, IV_I and IV_{II} forms. Among the mentioned crystal structures, cellulose II is the thermodynamically most stable structure, which can be obtained *via* regeneration or treatment with aqueous sodium hydroxide solution of cellulose I. By these processes, the cellulose chains which were arranged in parallel

fashion in cellulose I were oriented to antiparallel fashion.[10] Formation of cellulose III can be achieved by liquid ammonia treatment of cellulose I and II, in a reversible process.[29] Lastly, cellulose IV can be prepared by heating cellulose III in glycerol or water.[31]

The crystalline state of cellulose is highly dependent on hydrogen bonding, which can be divided into the intramolecular and intermolecular subgroup, respectively. As **Scheme 2** illustrates, intramolecular hydrogen bonding contains the bonding of O3-H with O5 (red dashed line) and O2-H with O6 (blue dashed line) as well as intermolecular hydrogen bonding of O6-H with O3 (green dashed line) for cellulose I.

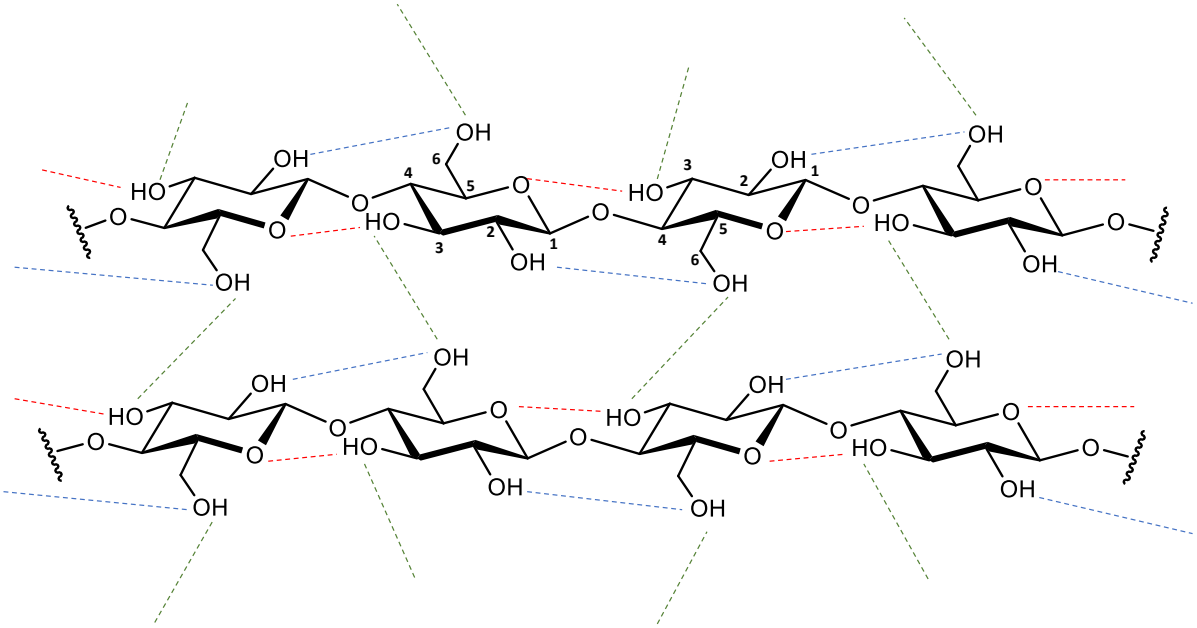

Scheme 2: Schematic representation of the intra- and inter- molecular hydrogen bonding in the cellulose I structure.[32-33] O3-H ··O5 intramolecular (red), O2-H ··O6 intramolecular (blue) and O6-H ··O3 intermolecular (green) hydrogen bonds.

2.1.2 Isolation of Cellulose

Lignocellulosic biomass dominates the biomass feedstocks with an annual production of approximately 170 billion metric tons and it contains non-edible components such as forest and agricultural residues, energy crops and cellulosic waste.[34-35] It has been utilized to produce valuable chemicals and energy, and accepted as a promising candidate to substitute fossil resources.[34, 36] Depending on its sources, the chemical composition can vary; however, its three major components are cellulose, hemicellulose and lignin.[37] Selected sources of lignocellulosic biomasses and their chemical composition are shown in **Table 2**.

Table 2: Selected sources of lignocellulosic biomasses and their chemical composition.[35, 38-39]

Biomass source	Cellulose (%)	Hemicellulose (%)	Lignin (%)
Oak	40.4	35.9	24.1
Eucalyptus	54.1	18.4	21.5
Pine	42.0-50.0	24.0-27.0	20.0
Bamboo	49.0-50.0	18.0-20.0	23.0
Wheat straw	35.0-39.0	23.0-30.0	12.0-16.0
Barley straw	36.0-43.0	24.0-33.0	6.3-9.8
Rice straw	29.2-34.7	23.0-25.9	17.0-19.0
Cotton	85.0-95.0	5.0-15.0	0
Sugarcane bagasse	25.0-45.0	28.0-32.0	15.0-25.0
Grasses	25.0-40.0	25.0-50.0	10.0-30.0

Recently, lignocellulosic biomass has gained more and more interest due to the increasing dependency of mankind on petroleum-based resources. In this regard, many studies have shown that it exhibits a great potential for sustainable chemicals and fuels with in principle net zero carbon emission.[40] Additionally, compared to other biomass examples like fats or starch, lignocellulosic feedstocks are not competing with food production. Other important reasons why it has received considerable attention from chemical industries are because it has low cost (can be collected from forestry and agricultural waste) and can be produced quickly (*i.e. via* fast-growing grasses).[41]

Even though lignocellulosic biomass offers the possibility to produce a wide range of chemicals and possesses many advantages, its utilization is still a challenging issue, especially due to the complex structure and interactions of cellulose.[39] The need for pretreatments increases the cost of the whole process and thus results in the necessity of highly selective and low-cost procedures. For decades, many studies have been conducted aiming for better alternatives and in the following section some of the methods for cellulose isolation will be discussed.

Extracting cellulose from wood is a very challenging process and it can be achieved *via* mechanical or chemical approaches. The common name for the process of isolating cellulose from wood is pulping process.[10] In mechanical pulping, wood can be grinded with rotating stones or refined between two metal discs to obtain the pulp with a 90% yield.[42] However, papers made from the mechanical pulp have a low light stability due to remaining lignin and they exhibit low strength since the fibers are damaged during the isolation process.[42-44] In addition, the whole process requires high amounts of energy, but it can be reduced by the addition of various chemicals like Na_2SO_3/Na_2CO_3 or NaOH.[42]

As an alternative, chemical pulping is a well-established process for pulp industry, representing 77% of the global pulp production.[45] Due to the complex structure of wood, the most challenging part of this process is the separation of cellulose from lignin. Lignin is an aromatic crosslinked polymer network containing mostly carbon-carbon and ether bonds that bind to cellulose. Thus, cellulose with higher purity can only be obtained *via* the degradation of the lignin.[45]

95% of the pulp production *via* chemical pulping originates from the Kraft process. Before the pulping process, wood must be chopped into smaller pieces (wood chips) in order to increase the surface area for the chemical treatment. Later, wood chips are cooked in an aqueous solution containing sodium hydroxide and sodium sulfide at 150-170 °C for 3-4 h. The cooking process degrades the lignin by the cleavage of aryl ether bonds (**Scheme 3**) and after sufficient time its soluble derivatives (polyphenolates) are formed.[45-46] Simultaneously, hemicellulose also partially degrades, and after washing and bleaching the remaining solid, cellulose fibers (so-

called wood pulp) are obtained. Wood pulp has found several application in the industry, mainly in the paper and cardboard industry (92%), production of fibers and films from regenerated cellulose, as well as production of cellulose derivatives (such as esters and ethers).[10]

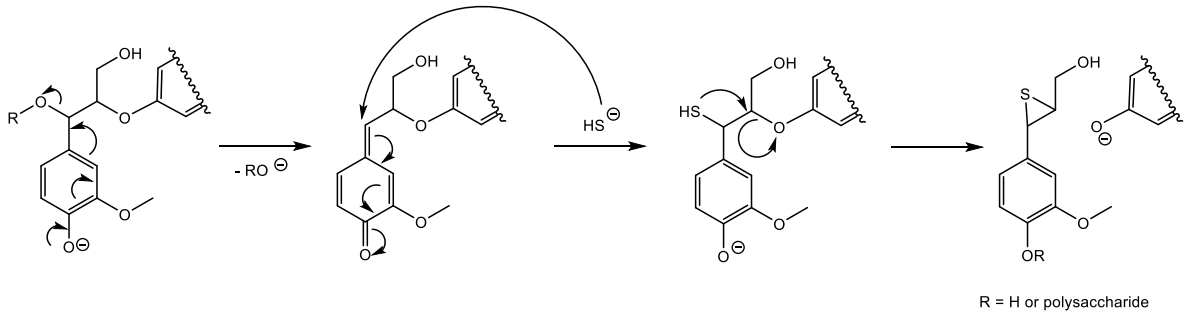

Scheme 3: The cleavage of aryl ether bonds during chemical pulping in the Kraft process.

2.1.3 Cellulose Derivatives

2.1.3.1 Commercial Cellulose Derivatives

The synthesis of the first cellulose derivative dates back to 1845, when the German-Swiss chemist Christian Friedrich Schönbein accidentally discovered cellulose nitrate (nitrocellulose), obtained by treating cellulose with a sulfuric acid/nitric acid mixture.[47-48] This discovery led to several historically important inventions such as Celluloid (the first man-made plastic),[14] Chardonnet silk (the first man-made fiber)[49] and guncotton (an explosive material). The nitrogen content has a pronounced impact on its application possibilities, since with a DS of 2.70, cellulose nitrate is used as an explosive material (gunpowder), while with a DS of 2.35, it is used in ester soluble lacquers.[50]

Cellulose acetate dominates the market of commercial cellulose derivatives with an annual production of 900,000 tons.[51] The first synthesis of cellulose acetate was reported by Paul Schützenberger in 1865 and the commercial production was patented in 1894.[52] The most common industrial versions of cellulose acetate include its pure form and various mixtures with butyrate or propionate (**Scheme 4**). Several applications were implemented, such as cigarette filters, food packaging, membranes, LCD displays, fibers *etc.*[43, 51] It also has a historical importance, since during World

War I, the highly flammable cellulose nitrate coatings on airplane wings were replaced with cellulose acetate.[53]

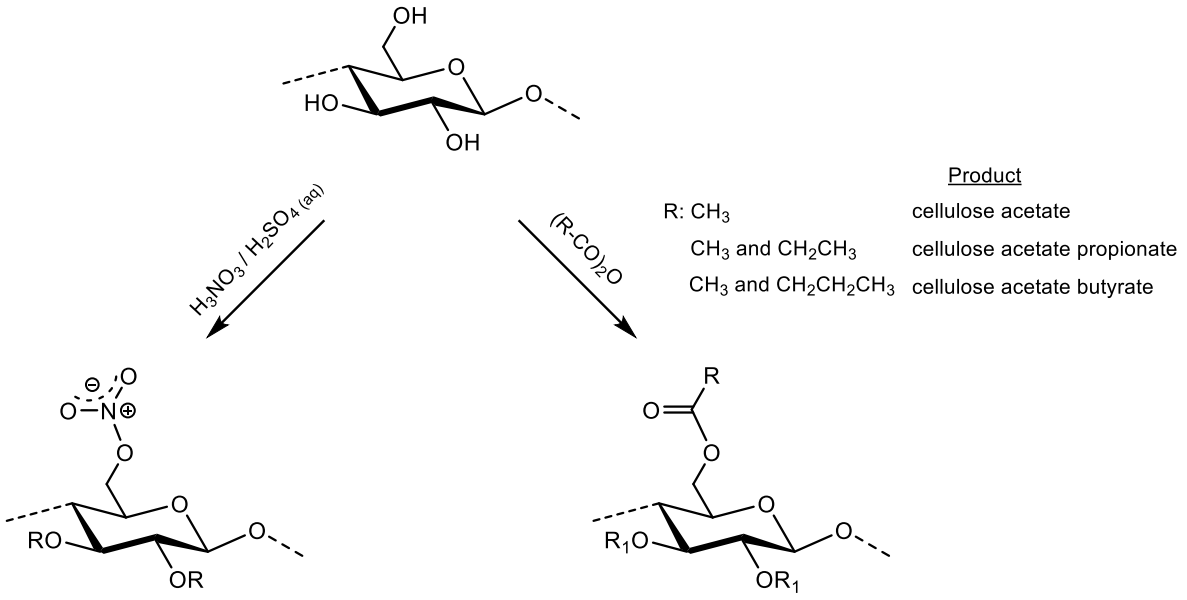

Scheme 4: Synthesis of the most important commercial cellulose esters.

The typical industrial process for cellulose acetate production starts heterogeneously and proceeds homogenously reaching typically resulting in complete functionalization. The production makes use of the mixture of acetic acid and acetic anhydride, together with sulfuric acid as a catalyst. Upon the generation of the acetyl cation, cellulose triacetate is formed, which can be later deacetylated *via* hydrolysis to form the corresponding diacetate.[54] The DS value of cellulose acetate also plays an important role for its properties, as triacetate derivatives are soluble in chloroform, while the low DS ones (0.6-0.9) are soluble in water.[51]

Another important class of derivatives are cellulose ethers, which are employed in various industries including food & beverage, textile, agricultural, cosmetic, textile, construction, and *etc*.[54] The typical synthesis for cellulose ethers are performed under alkaline conditions *via* nucleophilic reactions, such as the Williamson ether synthesis, the ring-opening of epoxides or the oxa-Michael addition reaction (**Scheme 5**). The Williamson ether synthesis is commonly used for the production of derivates such as methyl- or ethyl cellulose with alkyl halides, and carboxymethyl cellulose (CMC) with chloroacetic acid. Well accepted procedures in industry also include the synthesis of

hydroxymethyl- and hydroxypropyl cellulose by ring opening of epoxides and the oxo-Michael reaction in order to obtain cyanoethyl cellulose.

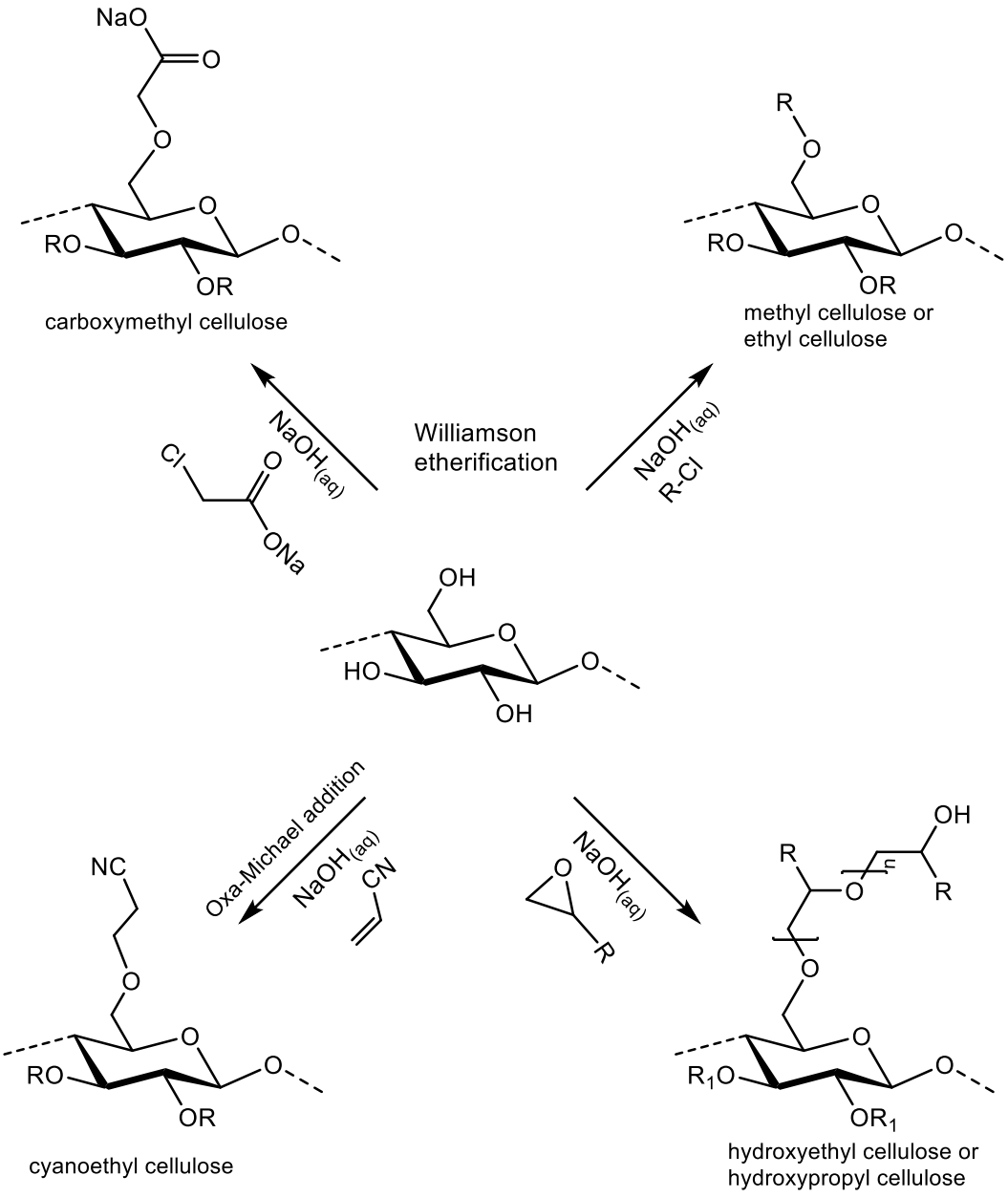

Scheme 5: Synthesis of the most important commercial cellulose ethers.

CMC, in its sodium salt form, is soluble in water and has found several applications in food, beverages and cosmetics as an additive (solution thickener, emulsifier, stabilizer *etc*.), drug formulations, drilling fluids, papers and textiles.[54-55] Due to the electrostatic repulsion between the chloroacetic acid and the increasingly charged cellulose chains,

only a maximum DS of ~1.4 can be achieved in a one-step procedure. Only with subsequent carboxymethylation, substitution can be increased up to a value of 2.9.[54]

2.1.3.2 Oxidized Cellulose Derivatives

Oxidation is a powerful tool to synthesize novel cellulose derivatives by introducing different functional groups such as carboxy, aldehyde and keto groups. Depending on the functionality, the synthesized derivatives are named as carboxy cellulose, (di)aldehyde cellulose and ketocellulose. Additionally, a mixture of the mentioned functionalities can also be present in a single derivative after oxidation, and the typical name for these kinds of products are oxycellulose.[56]

For decades, several oxidizing agents have been adapted to the oxidation of carbohydrates. However, due to the sensitivity of the carbohydrates against strong acidic or basic conditions, there is a limitation regarding the choice of them, and the type of functionalities introduced highly depends on the type of oxidizing agent.[56] Depending on the selectivity of the oxidation, they can be divided into two subgroups: nonselective and selective oxidizing agents. Nitrogen oxides,[57] ozone,[58] alkali metal nitrites and nitrates,[59] peroxides[60] and permanganates[61] are the well-known examples for the nonselective ones and oxidation can take place on both primary and secondary hydroxyls of the cellulose chains. Selective oxidizing agents (periodates[62-63] and nitroxyl radicals[64-65]) on the other hand, offer the possibility to oxidize primary or secondary hydroxyls selectively. In the following chapter, selected methods for cellulose oxidation will be discussed.

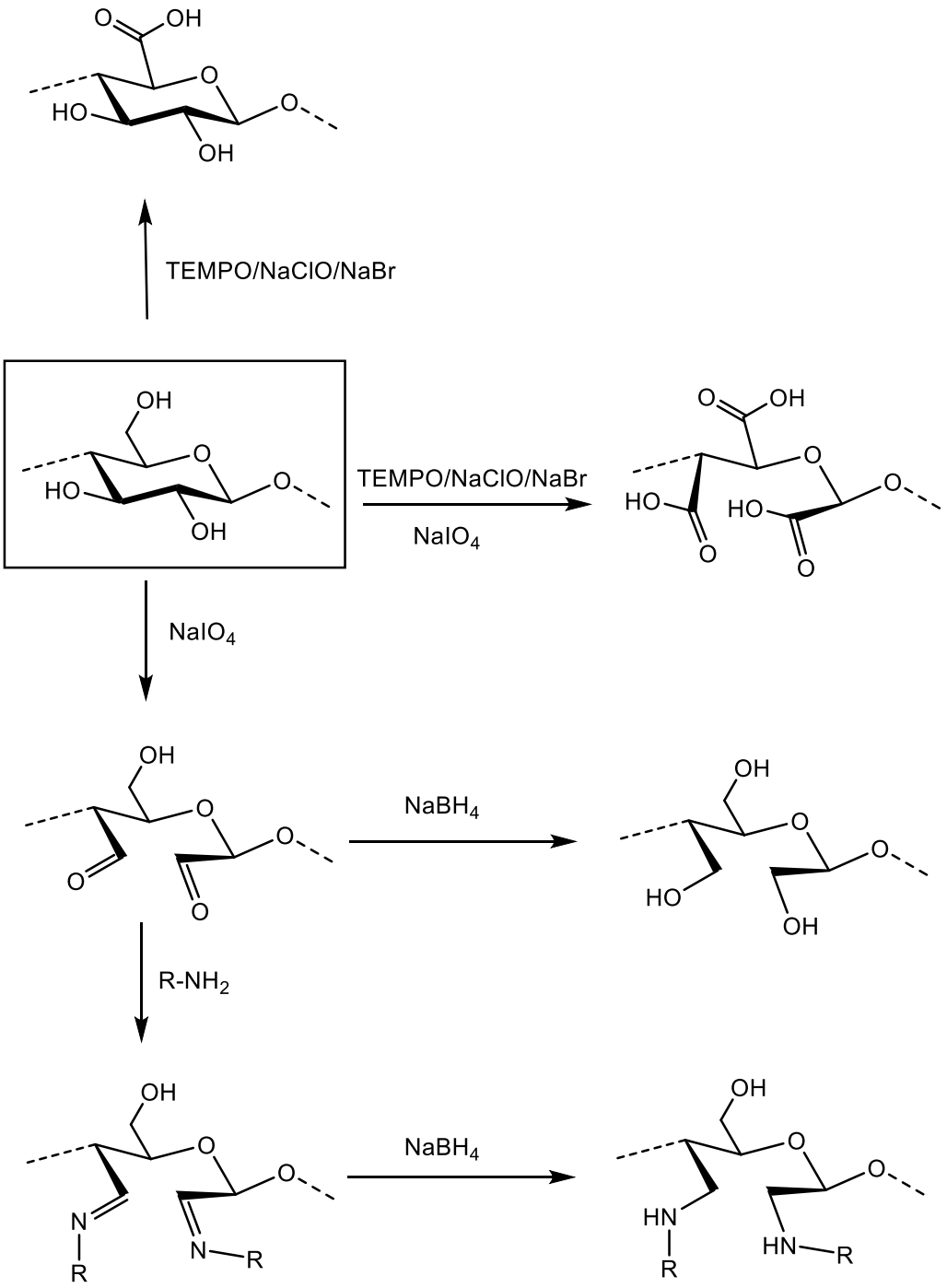

Scheme 6: Selected cellulose modification pathways through oxidation.

Introduction of Carboxy Group *via* Oxidation

Selective oxidation of the hydroxyl group located at the C6 position is the most common way to introduce a carboxy group to the AGU *via* oxidation, forming 6-carboxylcellulose. The obtained products consist of uronic acid units and the ratio

of them in the cellulose chains can vary depending on the degree of oxidation (DO). The confirmation of the carboxy group introduction on the C6 position is commonly performed *via* ^{13}C NMR from the shifting of C6 signal towards lower field.[66]

One of the first examples of 6-carboxylcellulose synthesis dates back to 1942. Kenyon *et al.* reported a unique procedure to oxidize cellulose with nitrogen oxide (the mixture of NO_2 with N_2O_4).[57] The final products revealed a maximum of ~25% carbonyl content, which was calculated by the carbon dioxide evolution after reacting the samples with calcium acetate.

Camy *et al.* reported a similar procedure, dissolving nitrogen dioxide in high pressurized CO_2 medium.[67] The relation between the degree of oxidation and the amount of CO_2 introduced was investigated, and it was assumed that the interaction between CO_2 and NO_2 inhibited the reactivity of NO_2 towards cellulose. By this improvement, degradation of cellulose *via* side reactions could be avoided. However, later studies proved that the oxidation procedures with nitrogen oxide can also lead some aldehyde/ketone formation, classifying the nitrogen oxide as a non-selective oxidizing agent.[56]

In 1994, de Nooy *et al.* introduced the 2,2,6,6-Tetramethyl-1-piperidinyloxy (TEMPO) oxidation into the polysaccharides (potato starch and dahlia inulin) by using a NaClO/NaBr system as the regenerating oxidant (**Scheme 6**).[64] In this system, the nitrosonium ion is the actual oxidizing species and is generated *in situ* by the reaction of TEMPO with oxidants, such as hypobromite ions, which in turn are generated from bromide salts and sodium hypochlorite (**Scheme 7**). After this work, TEMPO oxidation has become the most studied method to obtain 6-carboxylcellulose due to high reaction rate and yield, moderate degradation and high selectivity on the primary alcohol of the cellulose structure.[66, 68-71] In addition to 6-carboxylcellulose synthesis, the same system was also used for the oxidation of water soluble cellulose acetate,[72] chitosan,[73] chitin[65] and several other polysaccharides showing the versatility of procedure.

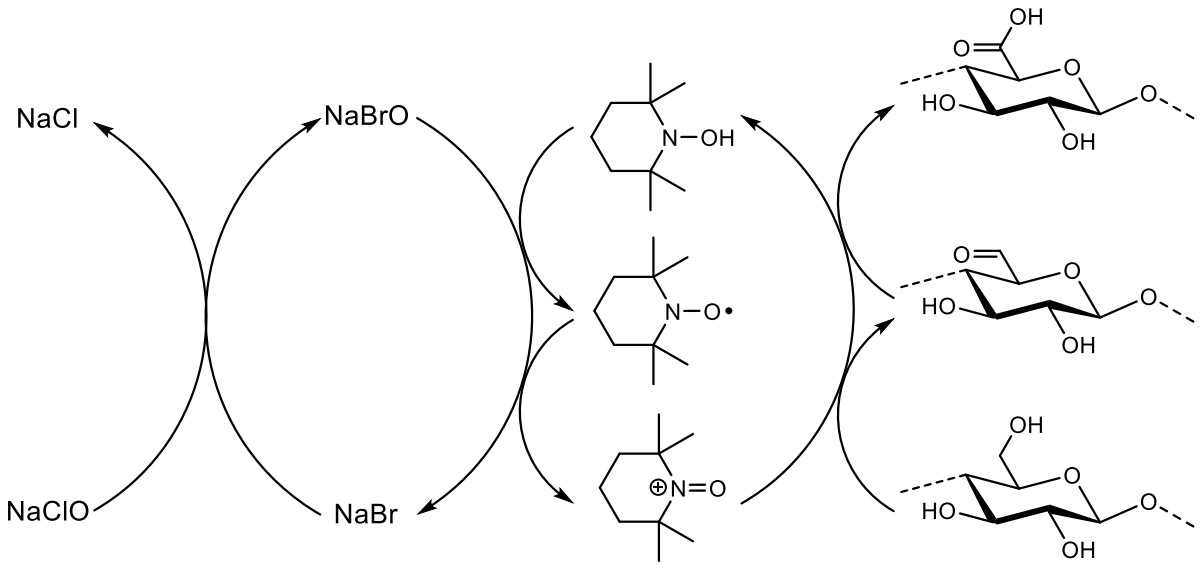

Scheme 7: Scheme of TEMPO-mediated oxidation of cellulose.[74]

As an alternative strategy, hydroxyl groups on the C2 and C3 positions could also be oxidized by the addition of $NaIO_4$ into the TEMPO/NaClO/NaBr system (**Scheme 6**).[75-76] This procedure consists of the combination of two common selective oxidation approaches: nitroxyl mediated oxidation and periodate oxidation. The reactions proceed simultaneously, primary alcohols were oxidized to carboxylic acids and the aldehyde functionalities obtained *via* periodate oxidation of the vicinal diols were further oxidized by the nitroxyl radicals. By this strategy, highly water soluble. 2,3,6-tricarboxylcellulose derivatives were synthesized in a one-pot approach.

Introduction of Aldehyde Group *via* Oxidation

Periodate oxidation is a well-known technique for 1,2 diol oxidation, which cleaves the bonds between the vicinal diols, resulting in two aldehyde functionalities. Therefore, adapting this technique into polysaccharide modification offers manifold possibilities to synthesize novel bio-based materials.[77, 78] Sodium (meta)periodate is the most common periodate used for the synthesis of 2,3-dialdehyde cellulose (DAC). In aqueous medium, the pyranose ring is opened from the C2-C3 bond, leading the aldehyde functionalities at the C-2 and C-3 positions (**Scheme 8**). The reaction should be conducted in the absence of light, which can decompose the periodate. Depending on the reaction parameters such as oxidant equivalent, cellulose concentration,

oxidation temperature and time, the degree of oxidation of the final product can vary. As an example, Varma *et al.* reported the synthesis of 2,3-dialdeyhde cellulose with a DO of 90 % by using 0.95 equivalents of periodate at 55 °C for 8 hours.[79] Similarly, Kim *et al.* used 1.25 equivalents periodate, an increased oxidation time (72 hours) at room temperature and received a DO of 98 % was reached.[80] Many other similar procedures have been investigated for DAC synthesis, including lower or moderate DO values.[63, 81-84]

As an alternative, Hormi *et al.* reported a metal salt assisted periodate oxidation of cellulose at elevated temperatures (65, 75 and 85 °C).[85] LiCl, $ZnCl_2$, $CaCl_2$, $MgCl_2$ and NaCl were employed with short oxidation times (maximum of 3 h), since periodate can decompose at elevated temperatures upon longer times. The metal salts employed in the reaction reduced the hydrogen bonding between the cellulose chains, resulting in a higher aldehyde content in the latter product especially when LiCl was used. Furthermore, the periodate amount could be reduced by the addition of salt. Same working group also investigated the effect of reactive milling during the periodate oxidation.[86] Since the milling process reduced the crystallinity of the cellulose and increased the specific surface area, higher DO values were observed.

Further studies focused on the regeneration of the oxidant, which is a crucial issue in terms of sustainability. In this regard, Liimatainen *et al.* employed sodium hypochlorite as a secondary oxidant to regenerate the periodate after the oxidation process. [87] Within a 10-15 minutes oxidation process, 100% conversion of periodate was achieved by using sodium as a secondary oxidant. A more sustainable method was proposed by Potthast *et al.* using ozone to regenerate the consumed periodate. The regenerated periodate was recycled and reused in new oxidation processes, resulting in 84-90% regeneration efficiency.[88]

The confirmation of the 2,3-dialdehyde structure *via* analytical methods is still a challenging issue. Even with the high DO samples, the carbonyl signal, which is expected to appear at 175-180 ppm, is not visible in the solid-state ^{13}C NMR.[63] To overcome this problem, Kim *et al.* reported a procedure consisting of the further oxidation of the aldehyde groups to carboxylic acids using sodium chlorite. This

modification successfully visualized the carboxyl groups at the C2 and C3 positions, indicating the existence of the former aldehyde functionalities. Since this procedure requires additional work, IR spectroscopy has been accepted as the most practical technique to follow the reaction progress. By using IR spectroscopy, carbonyl groups can be assigned to the band at around 1730 cm^{-1}, and the band at around 800 cm^{-1} to hemiacetals and their hydrates.[63, 80]

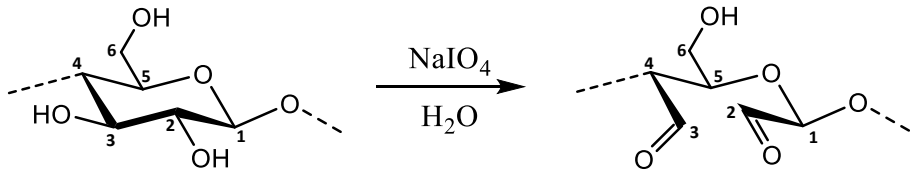

Scheme 8: Periodate oxidation of cellulose.

Although 2,3-dialdeyhdecellulose is usually shown in its dialdehyde from, it has indeed a more complex structure. It was proposed that the aldehyde groups are in an equilibrium with their hydrate, hemialdal and intra- and intermolecular hemiacetals forms(**Scheme 9**).[89-91] This results in a low intensity of the carbonyl band in IR spectroscopy, at it is masked by the abovementioned forms.[92-93]

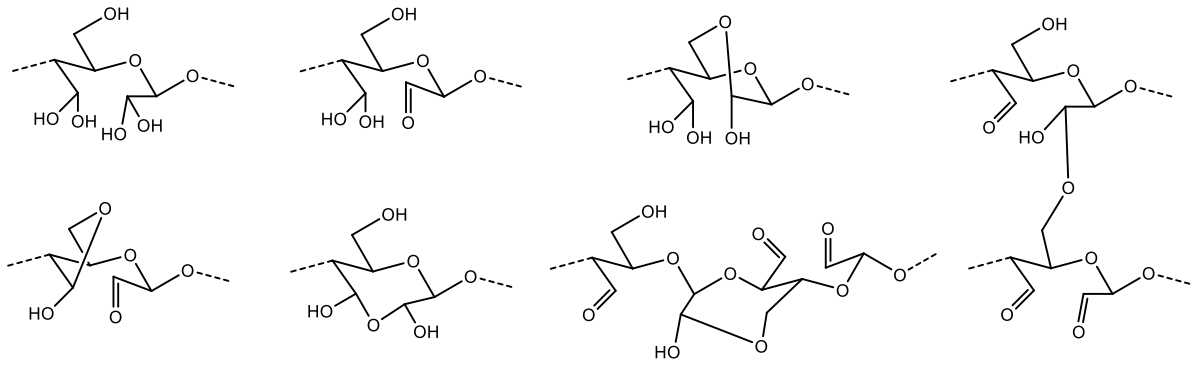

Scheme 9: Selected possible chemical structures of periodate oxidized cellulose.

The determination of the degree of oxidation of 2,3-dialdehydecellulose is another important subject, which must be mentioned. According to the literature, titration, elemental analysis, and UV spectroscopy are the most common methods used for this purpose. Titration method exploits the Schiff base reaction of aldehyde functionality with hydroxylamine hydrochloride, resulting in oxime and hydrochloric acid formation (**Scheme 10**).[80, 94] Thus, the amount of acid formed can be calculated *via* titration

using sodium hydroxide solution. A subsequent elemental analysis of the oxime derivative of the DAC is also widely applied to confirm the DO values using the nitrogen content.[85] Another alternative method is calculating the amount of consumed periodate. Since one periodate can create two aldehyde groups, the aldehyde content can be determined from the absorbance (290 nm) of the remaining periodate in the solution *via* UV spectroscopy.[95]

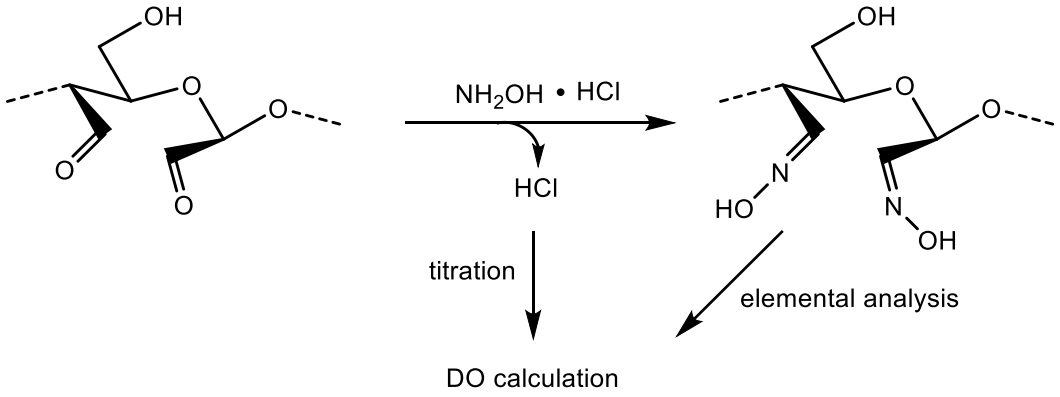

Scheme 10: Schematic representation of the DO calculation *via* titration and elemental analysis methods.

DAC has received remarkable interest in bio-based materials due to its biocompatibility and solubility in hot water. It can be further modified by reduction with sodium borohydride to form a dialcohol,[96-98] oxidation with sodium chlorite to form a dicarboxylic acid,[95, 99] or reaction with amines to form an imine (Schiff base) which is the most common technique reported in the literature (**Scheme 6**). The latter example includes amines with different functionalities,[94, 100-105] enzymes and proteins,[106-109] and biopolymers like collagen,[110] keratin[111] and chitosan[112-114] to synthesize fully bio-based materials. There are also examples of the direct use of DACs such as the preparation of composites[115] and films[89] employing the hemiacetal linkages between the aldehyde groups and the free alcohols, or the use of DAC as a potential bio-based wood adhesive.[83]

2.1.4 Dissolution and Functionalization of Cellulose

2.1.4.1 Dissolution of Cellulose - The Path Towards Ionic Liquids as Solvents

Before the discovery of ionic liquid for cellulose dissolution, several different solvents have been developed, which can be divided into the derivatizing and non-derivatizing solvents subgroups (**Scheme 11**). The first reports for cellulose dissolution included derivative solvents, in which the cellulose had to be derivatized to reach a homogenous solution. The synthesis of the cellulose nitrate in 1846[48] or the solubilization of cellulose using 'Schweizer's reagent' ($[Cu(NH_3)_4](OH)_2$) by Matthias Edward Schweizer can be seen as some of the earliest examples of derivatizing solvents.[116] In 1891, a method to make viscose fibers (rayon) was discovered, called viscose process.[117] The process starts with the treatment of the cellulose pulp with carbon disulfide (CS_2) in alkali solution. Subsequently, the formed cellulose xanthate intermediate becomes soluble and is extruded through spinnerets into a sulfuric acid/sodium sulphate bath to regenerate the cellulose fibers. The invention of cellophane also employed the same concept, using additional baths and glycerol as a plasticizer.[118] However, due to the toxicity of CS_2 and the high amount of waste created by this method, an alternative named CarbaCell, was developed. This variant uses a similar approach to the previous example, creating a cellulose carbamate intermediate with urea or ammonia. In the following years, many other non-derivatizing solvents such as *N*-methylmorpholine-*N*-oxide (NMMO)[119] monohydrate, *N*,*N*-dimethyl acetamide/lithium chloride (DMAc/LiCl),[120] 1-ethylpyridinium chloride[121] and dimethyl sulfoxide/tetrabutylammonium fluoride (DMSO-TBAF)[122] have been investigated for cellulose dissolution. Especially, NMMO has received great attention for fiber production and the process is named Lyocell process. However, most of the abovementioned solvents face sustainability issues such as toxicity and poor recovery, thus ionic liquids were proposed as alternative solvent systems.

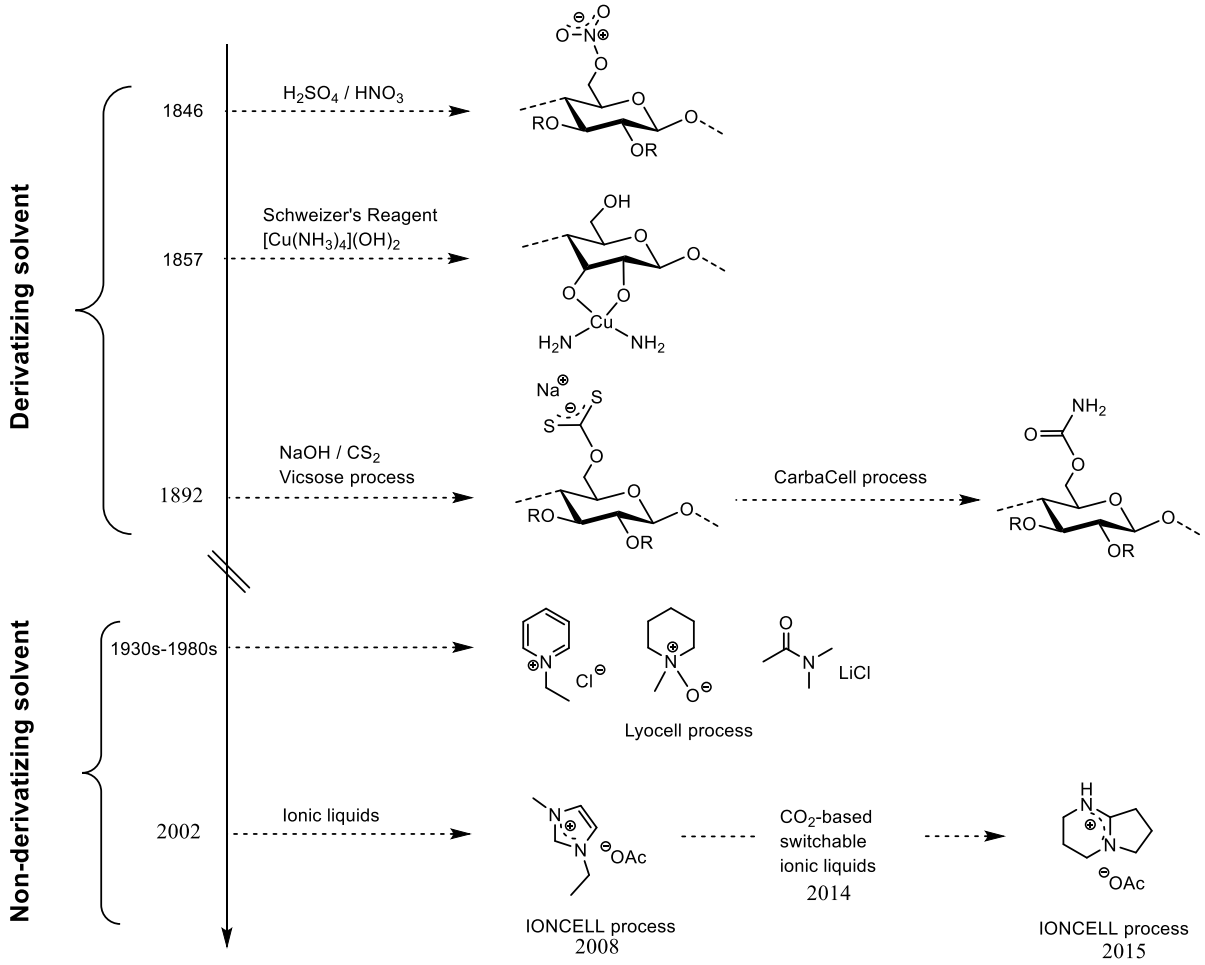

Scheme 11: A brief history of cellulose dissolution strategies through the 19 and 20 centuries.[123]

Ionic liquids (ILs) are classified as special molten salts possessing a melting point below 100 °C. The typical advantages are the low vapor pressure, high thermal and chemical stability, non-flammability and the relatively facile recyclability, which makes them attractive solvents for industrial applications. The introduction of the ILs, then not recognized as such, for cellulose dissolution was first reported in early 1930s by Charles Graenacher.[121] However, ILs for cellulose dissolution and chemistry gained attention from both industry and academia only after the report of Rogers *et al.* in 2002. The group investigated a variety of ionic liquids based on cations like 1-butyl-3-methylimidazolium ([BMIM]), 1-hexyl-3-methyl imidazolium ([HMIM]) as well as 1-octyl-3-methyl imidazolium ([OMIM]) with different anions. A 10 wt% homogenous cellulose solution was obtained using [BMIM][Cl] at 100 °C. The amount was increased to 25 wt% after microwave heating was applied. The authors also

produced 3-7 wt% solutions using other IL combinations. It was reported that the hard chloride anions played an important role in the disturbance of the hydrogen bonding within the cellulose structure. After dissolution, cellulose was regenerated in water and a significant change in the morphology was observed *via* scanning electron microscopy analysis. Overall, these promising results have encouraged many scientists to employ ILs for the cellulose dissolution.

Since ILs offer structural tunability, several variations have been reported for the cellulose dissolution. Some of the common cations and anions are illustrated in **Figure 2**. As one of the most important IL examples, Kilpeläinen *et al.* introduced a distillable ionic liquid constituted of a 1:1 molar ratio of 1,1,3,3-tetramethylguadinine (TMG) and a carboxylic acid.[124] Within this work, various carboxylic acids such as formic, acetic and propionic acid were investigated and up to 10 wt% homogenous cellulose solutions were reported. In order to obtain maximum dissolution, continuous stirring at 100 °C for 20 h was needed. More importantly, the ionic liquid was successfully recovered (99.4%) *via* distillation at 100-200 °C under 1.0 mmHg pressure. Even though this system offered very promising results, its sustainability is still a controversial topic, because of the high energy consumption required by the high vacuum and the elevated temperature.

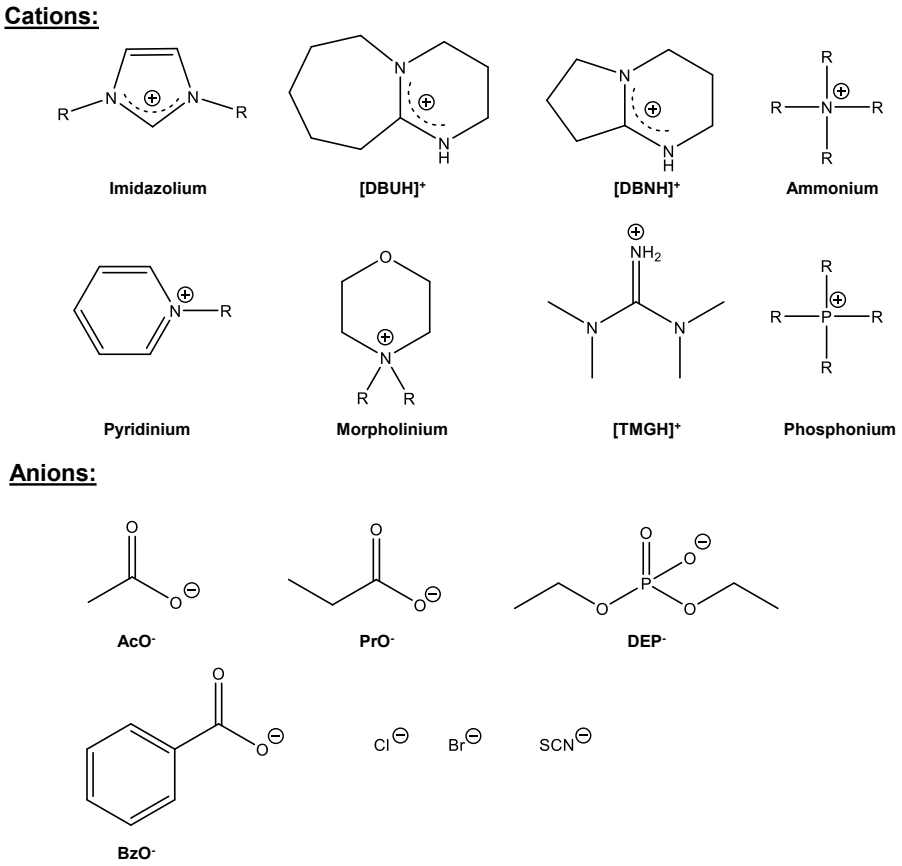

Figure 2: Some of the common cations and anions used in the ionic liquids.[125-126]

2.1.4.2 Homogenous Modification of Cellulose in Ionic Liquids - Selected Examples

Starting from the discovery of ionic liquids for the dissolution of cellulose, many studies have been reported for the homogenous modification of cellulose in these unique solvent systems. These modifications mainly include esterification, transesterification, alkoxycarbonylation and etherification reactions. In the following chapter, selected examples will be discussed to provide an overview.

Cellulose esters are the most studied cellulose derivatives in literature. The typical reagents used for their synthesis are acid anhydrides, acid chlorides and vinyl esters. Zhang *et al.* reported a procedure employing the ionic liquid 1-allyl-3-methylimidazolium chloride ([AMIM][Cl]) as an efficient solvent for the homogenous acetylation of cellulose with acetic anhydride.[127] The reactions were conducted in the absence of catalyst, reaching a maximum DS of 2.74 when 5 equivalents of anhydride/AGU were added at 80 °C for 23 h. The procedure also offered a good control on the DS, as values between 0.64 and 2.71 could be achieved by simple variation of the reaction parameters. More importantly, the ionic liquid could be recovered in a high purity after distillation and reused for new modifications, without losing its solubilizing ability. A very similar approach was used by the working groups of Zhan and Zhang.[128] Differently from the previous work, an additional catalyst (4-dimethylaminopryridine (DMAP)) was employed to synthesize cellulose propionate and cellulose butyrate. The addition of DMAP allowed to perform the reactions at lower temperatures (20-30 °C) with less anhydride equivalent (3 eq per AGU) and in a shorter reaction time (30 minutes). Slightly higher DS values (2.76 to 2.89) were achieved, but the recovery of the solvent was not investigated.

A comprehensive study was reported by Heinze *et al.* using a similar approach.[129] Four different ionic liquids, [BMIM][Cl], 1-*N*-ethyl-3-methylimidazolium chloride ([EMIM][Cl]), 1-*N*-butyldimethylimidazolium chloride ([C_4dmim][Cl]) and 1-*N*-allyl-2,3-dimethylimidazolium bromide ([Admim][Br]), were employed for the acetylation of cellulose with acetic anhydride and acetyl chloride. A complete acetylation (DS: 3) was achieved within 30 minutes using 5 eq of acetyl chloride/AGU in [BMIM][Cl]. In order to achieve a complete acetylation with acetic anhydride, 10 eq /AGU,

120 minutes and the addition of pyridine was needed. After the comparison with the other ionic liquids, the most effective modification was observed with [EMIM][Cl]. Additionally, the authors reported the possibility to recover the ionic liquids by distilling off the water and reusing it for the new syntheses. However, the necessity of an additional freeze-drying process was also mentioned, due to the hygroscopicity of the solvents. Lastly, acetyl chloride exhibited an even higher efficiency than acetic anhydride, but it also led a degradation of the final product and the ionic liquids (except for [BMIM][Cl]). This might be explained by the formation of HCl after the reaction of acid chloride.

Kilpeläinen *et al.* reported a different type of ionic liquid (an acid-base conjugated) for the acetylation of cellulose.[130] Prior to the acetylation, the ionic liquid [DBNH][OAc] was prepared from 1,5-diazabicyclo[4.3.0]non-5-ene (DBN) and acetic acid in a 1:1 molar ratio. Afterwards, cellulose was dissolved in the molten [DBNH][OAc] at 70 °C for 0.5-1 h under argon atmosphere and various reactants including anhydrides (acetic and propionic), vinyl esters (vinyl acetate and vinyl propionate) and isopropenyl acetate were tested for the acetylation reaction. A successful control on the DS values between 0.25 and 2.97 was reported using Ac_2O or isopropenyl acetate within 1 h. However, only a maximum DS of ~ 1.5 was achieved in the case of vinyl esters. Even with an excess of reagents, increased reaction time or higher temperatures, the functionalization could not be improved. Additionally, 1.01 equivalent of the base was required when using Ac_2O to prevent the hydrolysis of cellulose due to the formation of acetic acid as a side product. However, a decrease of the original weight of the starting material (up to 1/3) was still observed for each sample, indicating a great disadvantage of the solvent system. The authors also reported the successful recovery of the ionic liquid *via* fractional distillation. Since the hydrolysis of DBN is known for this solvent's recovery, *n*-butanol was proposed to trap remaining water before distillation.[131] Overall, the results have shown that cellulose esters with high DS values could be efficiently obtained using this unique ionic liquid without the need for additional catalysts. An improved methodology also enabled the recovery of the solvent in a high yield (80%). However, degradation of the products was inevitable,

thus limiting the application potential of this system for the functionalization of cellulose.

Jogunola *et al.* also used the same ionic liquid together with a co-solvent (DMSO, acetone, acetonitrile and DBN) for the synthesis of cellulose acetates.[132] Reactions were performed with acetic anhydride and the influence of the co-solvent was investigated. A maximum DS of 2.89 was achieved using 7 equivalents of anhydride/AGU at 80 °C after 2 h with acetonitrile as a co-solvent. Similar to the abovementioned report, a degradation took place during the acetylation. Furthermore, the ionic liquid was also successfully recovered. As a comparison, methanol was used in the regeneration of the products, thus recovery of the ionic liquid was rather easier by distilling the methanol and co-solvents (only for acetone and acetonitrile) without causing any degradation. However, the use of high equivalents of the reactants and additional solvents led to a less sustainable procedure.

Succinic anhydride has been also used to obtain carboxylic acid containing cellulose derivatives. In this regard, Geng *et al.* employed a [BMIM][Cl]/DMSO mixture for the synthesis of cellulose succinates.[133] Reactions were carried out between 85-100 °C for 5 to 120 minutes. However, even with 12 equivalents of succinic anhydride/AGU, only a maximum DS of 0.54 could be achieved. The authors also reported that the synthesized products degraded significantly, and their crystalline structure was completely lost. An improved procedure was demonstrated by the working groups of Liu and Sun using the ionic liquid [BMIM][Cl] and the additional catalyst DMAP.[134] The use of DMAP was reported as a crucial parameter since a low DS value (0.24) was obtained in its absence. Reactions were conducted between 60-110 °C and the substitution was increased until a temperature of 100 °C (maximum DS of 2.34), while the sample synthesized at 110 °C revealed a lower DS, indicating a possible degradation. Even though it was a promising procedure to obtain cellulose succinates with high DS values, the use of additional catalyst reduced the sustainability.

Most of the esterification reactions in ionic liquids employ activated acids, some of which are toxic and lead to the degradation of the carbohydrate. In this regard, the working groups of Meier and Barner-Kowollik reported a catalytic transesterification of

cellulose in [BMIM][Cl] with methyl esters, which will be discussed in more detail the **Chapter 4.3**.

King *et al.* reported the synthesis of cellulose carbonates using dimethyl carbonate (DMC) and diethyl carbonate (DEC).[135] The reactions were mainly performed in the ionic liquid-electrolyte trioctylphosphonium acetate ([P_{8881}][OAc])/DMSO without any catalyst (**Scheme 12**). However, the authors also reported the same procedure in a more common ionic liquid, [EMIM][OAc], for comparison. Both solvents gave similar results, but a slightly higher modification was achieved with the former solvent. A maximum DS of 1.00 was obtained using both methyl- and ethyl carbonates at 60 °C and 80 °C, respectively. The DS values could not be increased even after the addition of catalysts such as 1,5,7-triazabiycylo[4.4.0]dec-5-ene (TBD), pyridine or indium(III) bromide ($InBr_3$). After the regeneration of the products in methanol, films were prepared for further investigations regarding the mechanical properties of the newly obtained materials. The cellulose methylcarbonate sample revealed a tensile strength value of 35.3 MPa, which was reported as a comparable value to commercial cellulose acetate films (41 MPa).[136] However, a side reaction between the ionic liquid and DMC (forming methyl acetate) was observed, resulting in a difficult recovery of the solvent.

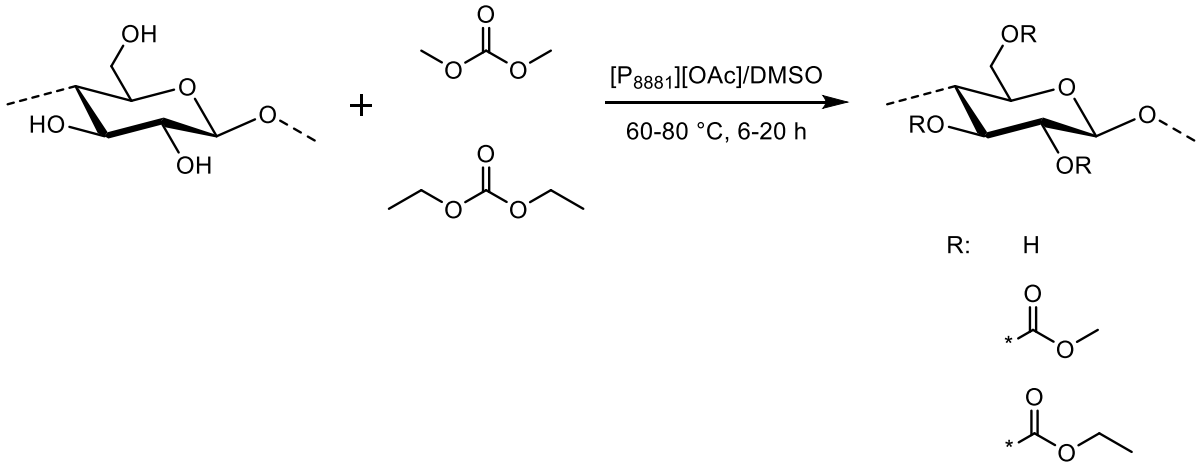

Scheme 12: Synthesis of cellulose carbonates in [P_{8881}][OAc]/DMSO.[135]

Recently, an alternative method was reported by Meier *et al.* for the synthesis of cellulose allyl carbonates.[137] [BMIM][Cl]/DMSO was selected for cellulose dissolution and the reactions were conducted at 80 °C using diallyl carbonate. A maximum DS of

1.32 was achieved using 4 equivalents of reactant/AGU within 18 h. The use of additional catalysts such as TBD and DBU did not increase the obtained DS values, similar to the observation in the above-mentioned report. Since no side reactions were observed between the ionic liquid and diallyl carbonate, a facile and efficient (100%) recovery of the ionic liquid was achieved. Additionally, the introduction of the allylic functionalities offered the possibility to perform a post-modification *via* thiol-ene reaction. The thiol-ene product of cellulose carbonate revealed a glass transition temperature (T_g) of 84 °C, whereas the former derivative did not reveal any thermal transition.

2.1.4.3 CO_2-based Switchable Solvent System for Cellulose Utilization

In 2005, Jessop and coworkers introduced a unique solvent system based on an alcohol and DBU, a non-ionic liquid, which can be switched to an ionic liquid by introducing CO_2 into the mixture (**Figure 3**).[138] This ionic liquid can be switched back to its former non-ionic form upon the release of CO_2 *via* nitrogen or argon gas exposure, as well as by simply leaving it to air. This procedure proposed new opportunities to the chemical community by reducing the cost and environmental impact of several syntheses, where removing or replacing the solvent is necessary after each step.[138]

As the alcohol component, 1-hexanol was chosen, because the respective carbonate salt is formed as a viscous liquid at room temperature, while carbonate salts of other alcohols like methanol are solid, a non-convenient property for the solvent system. After adding CO_2 to the non-ionic and non-polar 1-hexanol/DBU mixture, the polarity changed over 1 hour, caused by formation of the 1-hexyl carbonate/protonated DBU ionic liquid. The change in the polarity was also proven *via* addition of decane into the system and investigating its miscibility in the solvent mixture before and after the addition of CO_2.

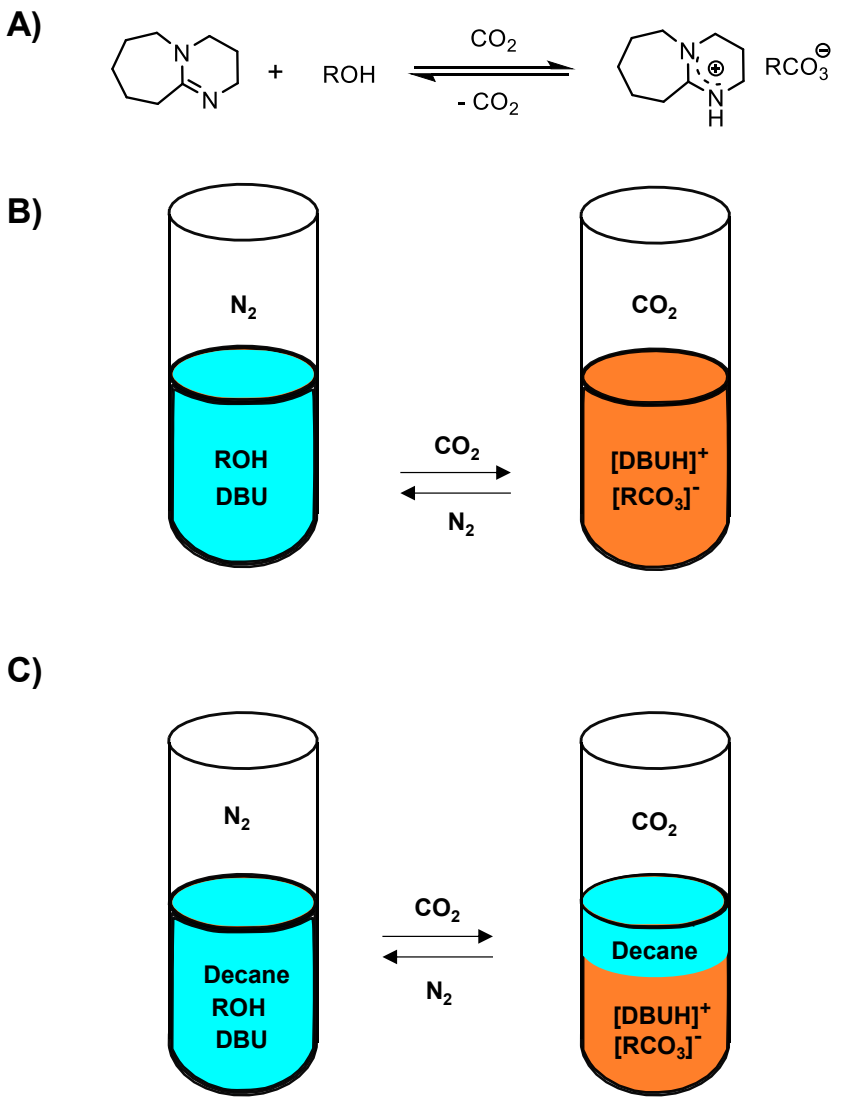

Figure 3: A) Protonation of DBU in the presence of CO_2 and an alcohol, and its deprotonation upon CO_2 release. **B)** Polarity change in the solvent system upon CO_2 exposure and CO_2 release. **C)** Changes on the miscibility of decane in the solvent system before and after CO_2 exposure, adapted from Jessop et al.[138]

8 years after the discovery of this smart solvent system, it was adjusted for cellulose dissolution by Xie *et al.*[139] and Jerome *et al.*[140] almost simultaneously. Although both procedures are based on the same concept, they were divided into a derivative[140] and a non-derivative[139] approach. In the derivative approach, cellulose is suspended in DMSO and CO_2 directly reacts with the hydroxyl groups of the cellulose in the presence of a superbase, such as DBU, TBD, TMG, etc., forming a reversible carbonate complex on the cellulose structure, leading to complete solubility in DMSO.

In the non-derivative approach, however, an additional alcohol is present in the reaction mixture, generating carbonate salt *in situ*, which acts as a good solvent for cellulose dissolution. For both systems, regeneration of cellulose can be performed by releasing the CO_2 from the system, making this solvent system "switchable".

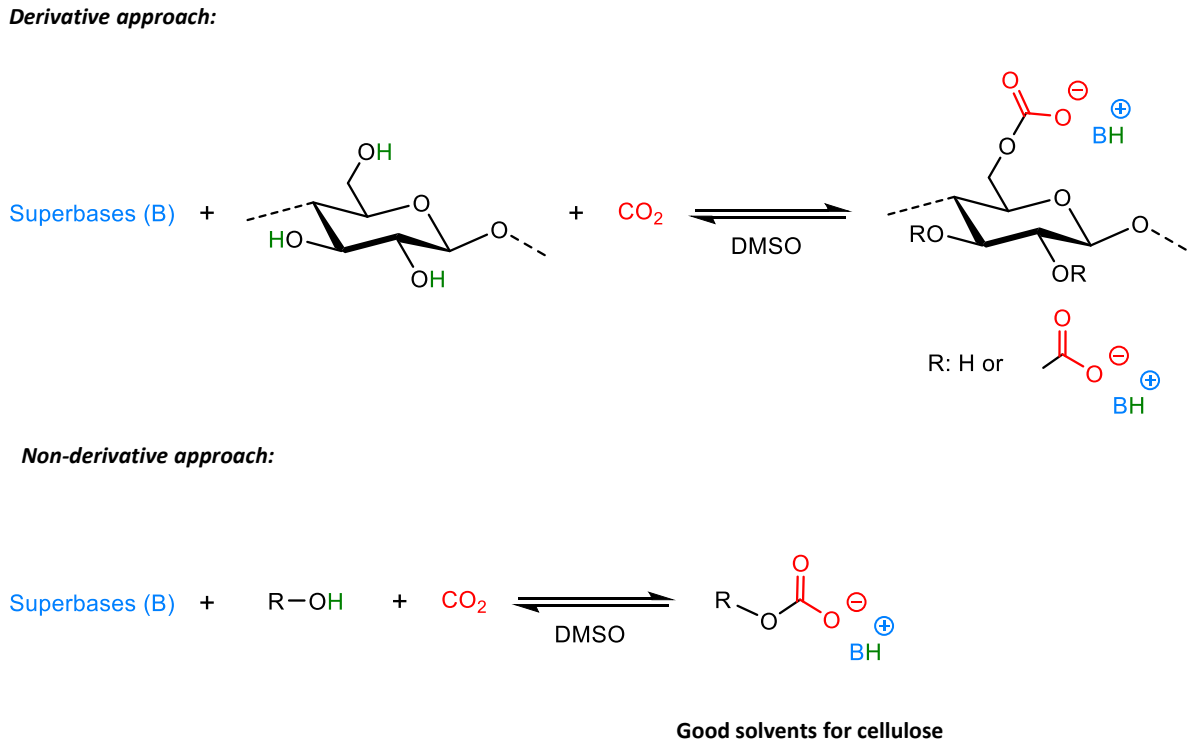

Figure 4: Derivative (top) and non-derivative (bottom) approach of the CO_2-based switchable solvent system for cellulose dissolution

In the first example of the derivative approach, dissolution of cellulose up to 15 wt% at room temperature within 1 h in the presence of CO_2 (2 bar) was achieved.[140] A variety of bases and reaction conditions were investigated to find the optimal parameters for cellulose dissolution. Cellulose dissolution of 3-15 wt% was achieved with different super-base (P2-Et, DBN, TMG, DBU, MTBD, TBD and DABCO) incorporated in the system. Apart from super-bases, also weaker bases such as diethylamine, ethanolamine, adenosine and guanine were tested, however, it was noted that these components were not capable of activating the hydroxyl group on cellulose. After dissolution of cellulose in the presence of DBN, recyclability of the solvent system was studied by addition of ethanol as an antisolvent, leading to the

regeneration of cellulose through precipitation. It was noticed that removal of CO_2 prior to adding ethanol was necessary, while the majority of cellulose was still present in DMSO/DBN mixture. After the regenerated cellulose was filtered off and the ethanol was removed from the filtrate, meaning that the DMSO/DBN mixture could be reused at least three times for new cellulose dissolution without losing its solubilizing ability. This behavior highlighted the sustainability of the developed procedure. Additionally, the authors also observed a decrease in the crystallinity of the regenerated cellulose.

Later, the work of Meier et al. offered a more comprehensive explanation for the derivative approach.[141] DBU, TMG and MTBD were chosen as a super-bases for the switchable solvent and optimized conditions for cellulose dissolution were reported by varying different parameters like temperature, CO_2 pressure, cellulose concentration and solubilization time. Additionally, formation of the *in situ* carbonate intermediates was proven by trapping with benzyl bromide and methyl iodide as well as by *in situ* IR spectroscopy.

In the first example for non-derivative approach, up to 10 wt% of cellulose could successfully be dissolved. Ethylene glycol was used to form the carbonate in the presence of CO_2. Optimization studies were conducted with TMG as a super base and a homogenous cellulose solution was obtained at 60 °C after 1 h under 0.5 MPa CO_2 atmosphere. After adding anti-solvents (*e.g.* methanol and ethanol), the precipitated cellulose was separated and the remaining mixed solvents (DMSO, TMG and ethylene glycol) were recovered almost completely (>99 %). TGA results revealed that regenerated cellulose did not show any residual contaminations from the solvent mixture, however the samples exhibited lower onset temperature, which is possibly caused by a change in the crystallinity. Evidence to support this argument was obtained by ^{13}C CP/MAS NMR, showing the disappearance of cellulose I structure and the formation of cellulose II structure. Additionally, different cellulose sources like α-cellulose, cellulose powder from spruce and sulfate poplar wood pulp were examined, resulting in a 5-10 wt% dissolution, proving the versatility of the solvent system.

Several studies have reported the utilization of these CO_2-based switchable solvent systems for homogenous cellulose modification. Acylation of cellulose with acetic anhydride by using the non-derivative approach is an important example to show the many possibilities of this solvent system.[142] Initially, 5 wt% homogenous cellulose solution was prepared using methanol, DBU and DMSO under 0.5 MPa CO_2 at 60 °C for 3 h. Later, acetic anhydride was added to the reaction mixture under N_2 atmosphere at room temperature and then reaction was conducted at 80 °C for 5 h. In the end, a maximum DS of DS of 2.94 was obtained under considerably mild conditions. Additionally, propionic and butyric anhydride were employed to obtain different cellulose esters with DS values of 2.91 and 2.59, respectively. After completion of the reaction, DBU (91%) and DMSO (93%) were recovered in a facile workup and could be used for new solubilization step.

As an alternative, the derivative approach is a more preferred procedure, since the cellulose is utilized directly, and additional component (alcohol) is avoided increasing the overall sustainability. The same working group, who already reported the procedure for acylation of cellulose *via* a non-derivative approach, also achieved similar DS values (2.89) in a derivative approach by using the higher equivalents of acetic anhydride (5 eq per AGU, in previous study: 3.6).[143] Cellulose dissolution on the other hand was performed in a DBU/DMSO mixture under 2 bar CO_2 atmosphere at a lower temperature (50 °C) for 3 h. Similarly, a good recovery yields for DBU (91%) and DMSO (93%) were observed.

Xie and co-workers employed the derivative CO_2 switchable solvent system approach for preparation of cellulose-*graft*-poly(lactic acid) materials.[144] The grafting method *via* ring opening polymerization (ROP) of L-lactide was initiated by the hydroxyl groups of cellulose without an additional catalyst and under mild conditions. The obtained thermoplastic material revealed varying transition temperatures (T_g) depending on the DS or molar substitution (MS_{PLLA}) of the latter product.

Recently, the sustainable succiniylation of cellulose in derivative CO_2-based switchable solvent system was reported by Meier *et al.* (**Scheme 13**).[145] Cellulose succinates with a maximum DS of 2.59 were successfully obtained by using 4.5

equivalents succinic anhydride per AGU under mild reaction conditions (room temperature and 30 minutes). Furthermore, the introduced carboxylic acids provided the opportunity for post modifications *via* P-3CR and Ugi 4-CR. In the conventional cellulose ester synthesis procedures, more expensive solvents, additional catalysts, and elevated temperatures were needed.[134, 146] Thus, these promising results did pave the way for a more environmentally friendly approach for cellulose ester synthesis.

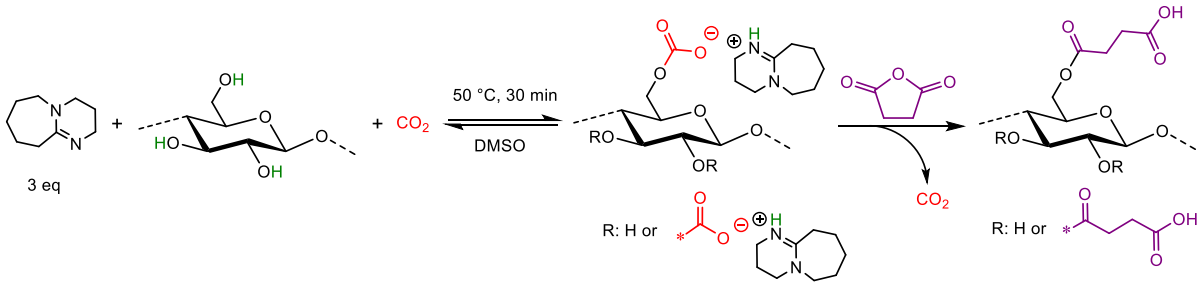

Scheme 13: Dissolution and subsequent reaction of cellulose with succinic anhydride using CO2-based switchable solvent system. [145]

Indeed, a similar approach was employed by Xie *et al.* for the synthesis of fully bio-based cellulose levulinate esters.[147] By using α-angelica lactone, cellulose esters were prepared with easily controllable DS values in the range of 0.14 to 2.04. The authors also reported that small amounts of pseudo-levulinate esters were formed due to the oxo-Michael reaction. Cellulose esters with adequate DS values (>0.89) showed good water solubility, giving an opportunity for the preparation of fully bio-based films with promising mechanical properties.

Synthesis of fatty acid cellulose esters has also been investigated by utilizing high oleic sunflower oil[148] and fatty acid vinyl esters,[149] which will be discussed in **Chapter 4.3**.

This unique solvent system is not only being used for the modification of cellulose but also for the preparation of aerogels[150] and films[151]. Meier *et al.* reported a sustainable and straightforward approach for cellulose-based aerogel preparation.[150] In this work, cellulose was first solubilized, and the homogenous solution was

subsequently coagulated using an anti-solvent. The solvent was then exchanged until the DMSO and the super-base were completely removed. Subsequently, the obtained wet gel was freeze-dried to form the cellulose aerogel.

A very similar approach was used by Xie *et al.* for the preparation of cellulose films.[151] After cellulose dissolution, the homogenous solution was casted onto a glass plate and immersed in different solvents. The solvents were replaced until no traces of DMSO or super-base were detectable. With a final drying process, the formation of the homogenous cellulose films was demonstrated.

2.2 Starch

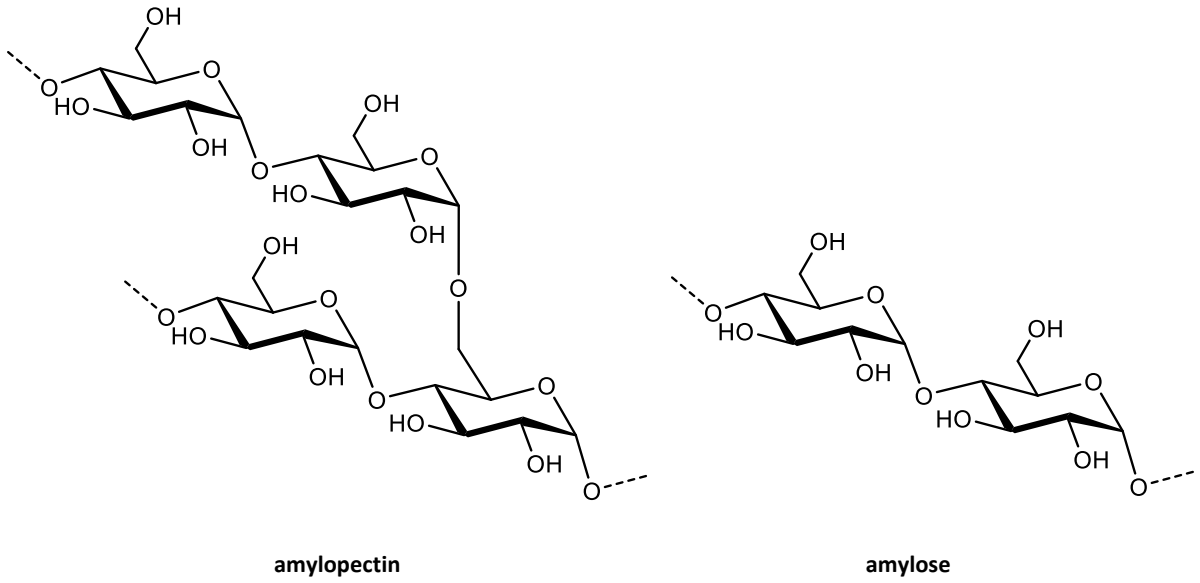

Scheme 14: Structures of starch components: amylopectin and amylose.

Starch is the second most abundant biopolymer on earth with an annual production of >50 million tons production per year.[152] Compared to cellulose, it is relatively easy to isolate in a pure form, making it an attractive renewable feedstock for the chemical industry. It is the end-product of the photosynthesis of plants and found in the leaves of green plants, seeds, roots, tubers and fruits. Starch is an energy and carbon source for plants, as well as, the main component of many animals' dietaries.[153] The main source for agricultural starch production is dominated by corn (maize) with >80% and can be isolated from various crops such as wheat, rice, potato, tapioca *etc*.[154]

Native starch contains a mixture of two types of polysaccharides: amylose and amylopectin (**Scheme 14**), together with trace amounts of lipids, proteins and phosphorous. Both polysaccharides are different from each other in size, chain length, number of side chains, crystallinity, and molecular weight.[154-155] Amylose is a linear polymer with D-glucose units linked *via* α-(1-4) bonds and has a molecular weight of approximately $10^5 – 10^6$ Da.[156] Amylopectin is a larger and heavily branched polymer, composed of shorter linear chains of α-(1-4) linked D-glucose units connected to each

other from branching points *via* α-(1-6) linkages (**Scheme 15**). A typical amylopectin has an approximate molecular weight of 10^7-10^9 Da and the linkage composition is 95% of α-(1-4) bonds to 5% of α-(1-6) bonds.[154, 156] Amylose and exterior chains of amylopectin can be found in double helical form.

Even though amylopectin is known to be the major component in starch composition, the amylose to the amylopectin ratio can be different depending on the sources of starch (**Table 3**).

Table 3: Composition of starch granules from various sources, adapted from Robyt.[157]

Starch source	Amylose (%)	Amylopectin (%)
Maize	25	75
Waxy maize	0	100
Potato	22	78
Wheat	23	77
Rice	19	81
Tapioca	17	83

Starch granules show a semi-crystalline structure, and both amorphous and crystalline areas are located as alternating layers.[158] Significant components of amylose and the long chains of amylopectin locate in the amorphous lamella.[158] Ordered double helical exterior chains of amylopectin are located in the crystalline lamella.[155, 158] Thus, amylopectin is the responsible component for the crystallinity and the degree of crystallinity in starch can differ from 17 to 51%.[155] Crystallinity of the amylopectin can be decreased *via* industrial processes, forming low molecular weight fragments by milling.[159] Amylose can be extracted from starch to obtain high amylopectin containing starch, *i.e.* waxy corn, by aqueous leaching and subsequent precipitation of amylose *via* complex formation with pentanol or 1-butanol.[160-161]

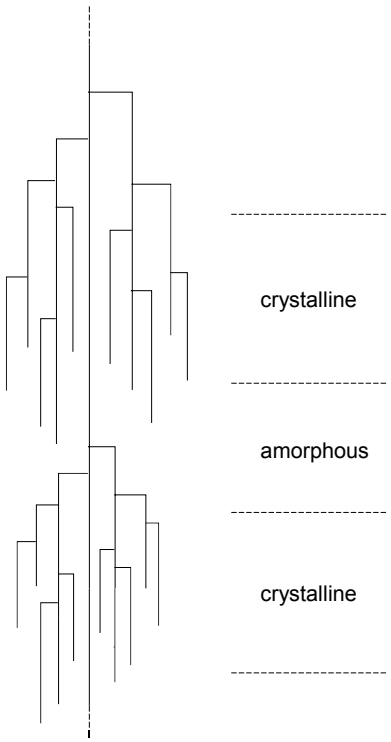

Scheme 15: Schematic representation of amylopectin structure.

Thermoplastic starch (TPS) is a relatively new concept and widely used in the production of biodegradable materials. Due to the intensive inter- and intramolecular hydrogen bonding network, native starch does not exhibit thermoplastic behavior. Indeed, this can be achieved by the addition of plasticizers such as glycerol, sorbitol, ethylene glycol, urea, as well as water, at high temperatures (90-180 °C) under shear.[162-165] By these procedures, it can melt and be processed *via* injection molding, extruder or film blowing machines.

Apart from its consumption as a food, starch is also an attractive feedstock for the chemical industry, since it is highly abundant, nontoxic, cheap and renewable. It is commonly used to produce bioethanol, acetic acid, D-lactic acid and many other organic compounds *via* fermentation process. It has been used for several other areas such cosmetic, paper and textile industries.[166]

Starch possesses fascinating features including biocompatibility, high thermal stability, high strength, durability, as well as biodegradability. Nevertheless, bottlenecks such as low solubility in common organic solvents, high hydrophilicity and

brittleness reduce the feasibility of processing for future applications. Thus, modifications through its free hydroxyl groups are necessary to overcome the abovementioned issues.

By using conventional methods, it can be esterified with anhydrides,[167-169] acids,[170] vinyl esters,[171-172] acid chlorides,[173] plant oils[174] or etherified by the reactions with epoxides,[175] methacrylates[176] etc. Higher molecular weight starch derivatives can be also produced utilizing various approaches such as crosslinking[177-179] and grafting[180-181].

Similar to other polysaccharides, starch can also be oxidized to introduce other functionalities such as carboxy or carbonyl groups. As also discussed for cellulose (**Chapter 2.1.3.2**, **Scheme 6**), primary alcohols can be selectively oxidized to carboxylic acid with TEMPO.[182] Alternatively, dicarboxylic acids derivatives can be obtained using hypochlorite in pH above 7[183] or its 2,3 ketone form can be achieved with bromine solution.[184] With periodates, the vicinal hydroxyl groups can be oxidized to aldehydes *via* C2-C3 bond cleavage.[185] Peroxides also have been used for starch oxidation to obtain a mixture of carboxyl- and carbonyl functionalities on the structure, resulting in water soluble derivatives.[186] All of these starch derivatives can be used for further modifications or blended together with different polymers to create new materials.

Due to its outstanding properties, starch is also used in polymer blends without further modifications to produce biodegradable plastics. Bhattacharya *et al.* reported injection molded blends of starch with various biodegradable polyesters.[187] They observed comparable tensile strength values with the synthetic polyesters when 70% w/w starch was used. Similarly, in the work of Huang *et al*., starch/PVA blends showed good thermal stability, high tensile strength and processability.[188] Many other studies including the well-known biodegradable polymers such as PCL, PHA, PLA and PEG revealed promising results, showing the possibility to obtain biodegradable plastics by using starch as a cheap and renewable component.[189-192]

2.3 Multicomponent Reactions – A Brief Introduction

In organic and polymer chemistry, multicomponent reactions (MCRs) are known to be a powerful tool to obtain multi-functional and highly complex structures in a one-pot approach.[193] They use three or more components, and the resulting product contains all the precursors. Thus, they offer high atom efficiency under considerably mild and sustainable conditions. Furthermore, many other advantages such as versatility, high yield, less waste production, and simple procedures make them a unique and high potential candidate for chemical society.[194-197]

Multicomponent reactions are classified into three types depending on their reaction mechanisms (**Scheme 16**).[193] In type I reactions, each reaction step is reversible, resulting in low yields and difficulties to isolate the desired product. Type II reactions include an irreversible last reaction step, which shifts the equilibrium towards the product formation. Thus, higher yields can be obtained compared to type I reactions. Type III reactions, on the other hand, contain only irreversible steps making it the ideal type and can be found in biochemical (enzymatic) reaction systems.

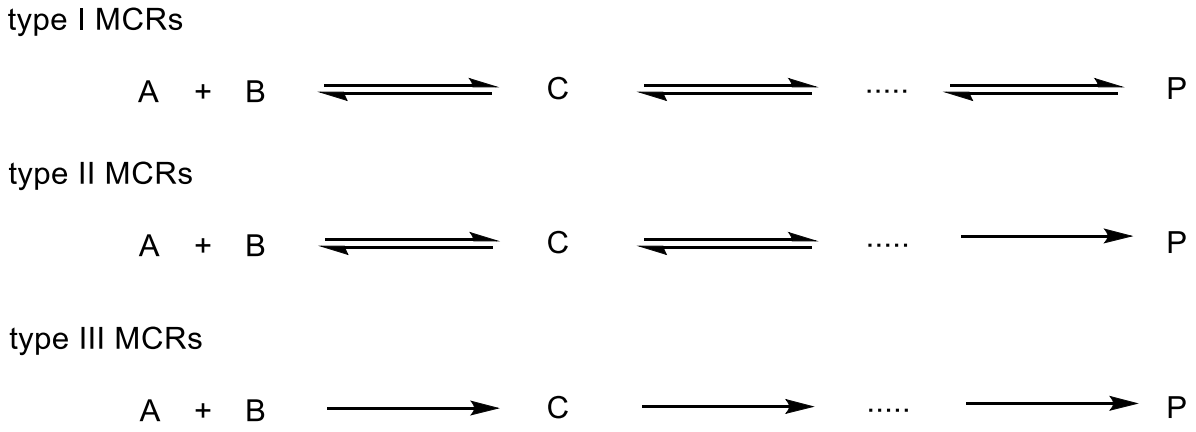

Scheme 16: Three basic types of multicomponent reactions (MCRs).[193]

2.3.1 Non-isocyanide based Multicomponent Reactions (MCRs)

The first known example of a multicomponent reaction was described by Strecker in 1850.[198] The reaction involves the synthesis of an α-amino nitrile by the reaction of an aldehyde, hydrogen cyanide and ammonia (**Scheme 17**). A subsequent hydrolysis

results in the formation of the racemic mixtures of the corresponding amino acids. In 1882, Hantzsch reported a four-component reaction (two equivalents of a β-ketoester, ammonia and an aldehyde) yielding a dihydropyridine (**Scheme 17**).[199] Eight years later, another important MCR, the Hantzsch pyrrole synthesis (H-3CR) was reported.[200] The pyrrole structures are obtained by the reaction of β-ketoesters, ammonia and α-haloketones (**Scheme 17**).

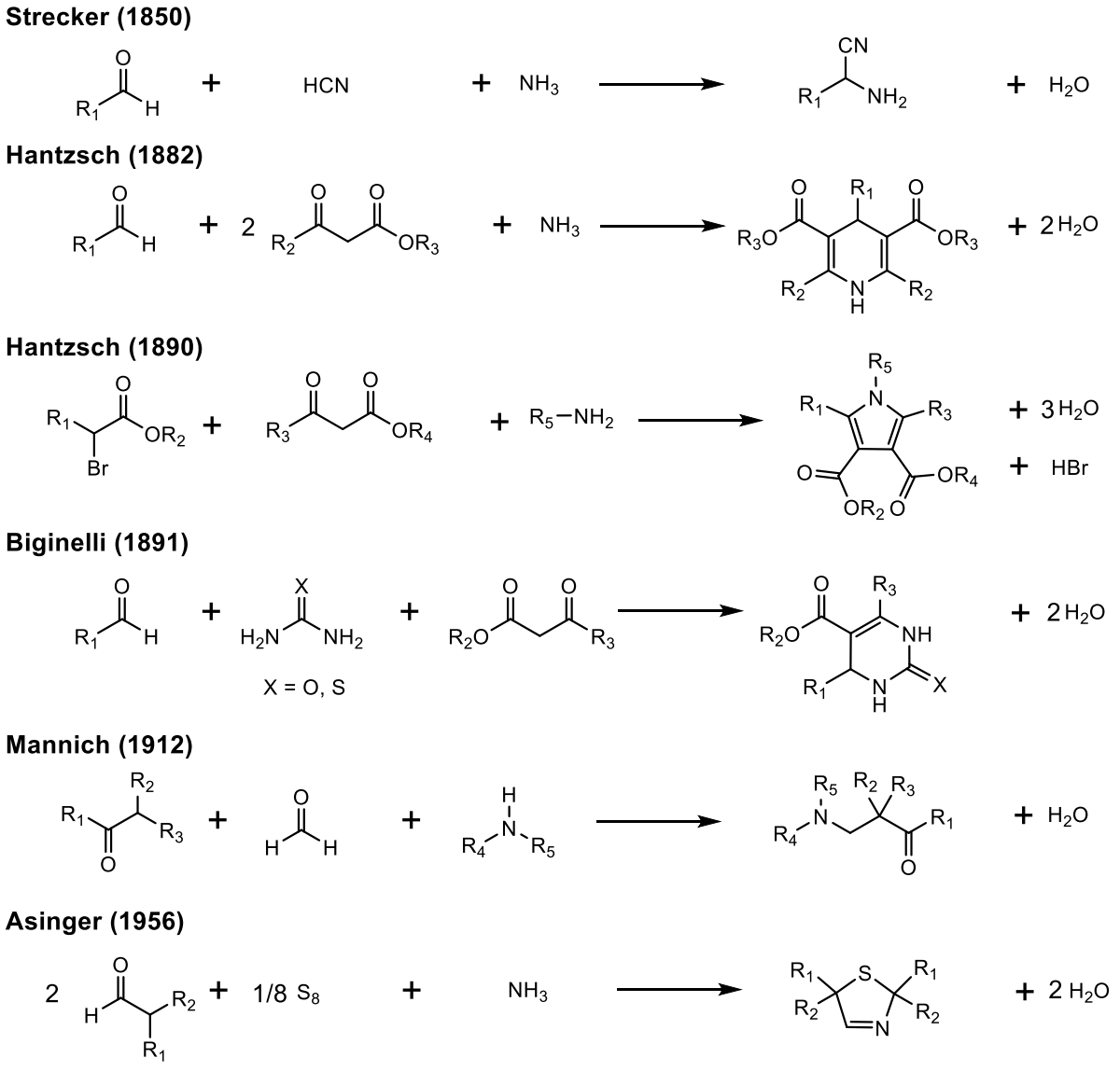

Scheme 17: Selected examples of historically important non-isocyanide based MCRs.[198-203]

In 1893, Pietro Biginelli reported the one-pot synthesis of 3,4-dihydropyrimidin-2-(*1H*)-one (DHPM).[201] The reaction facilitates the formation of

DHPMs by acid-catalyzed reaction of an aldehyde with urea (or thiourea), forming an imine, and subsequent reaction with a β-ketoester (**Scheme 17**). In his first work, benzaldehyde, ethyl acetoacetate and urea were used and under elimination of two equivalents water, the incorporation of all starting components in one product was confirmed *via* elemental analysis.[201] Although the exact structure was not known in the beginning, subsequent investigations revealed the formation of the DHMP structure.[204]

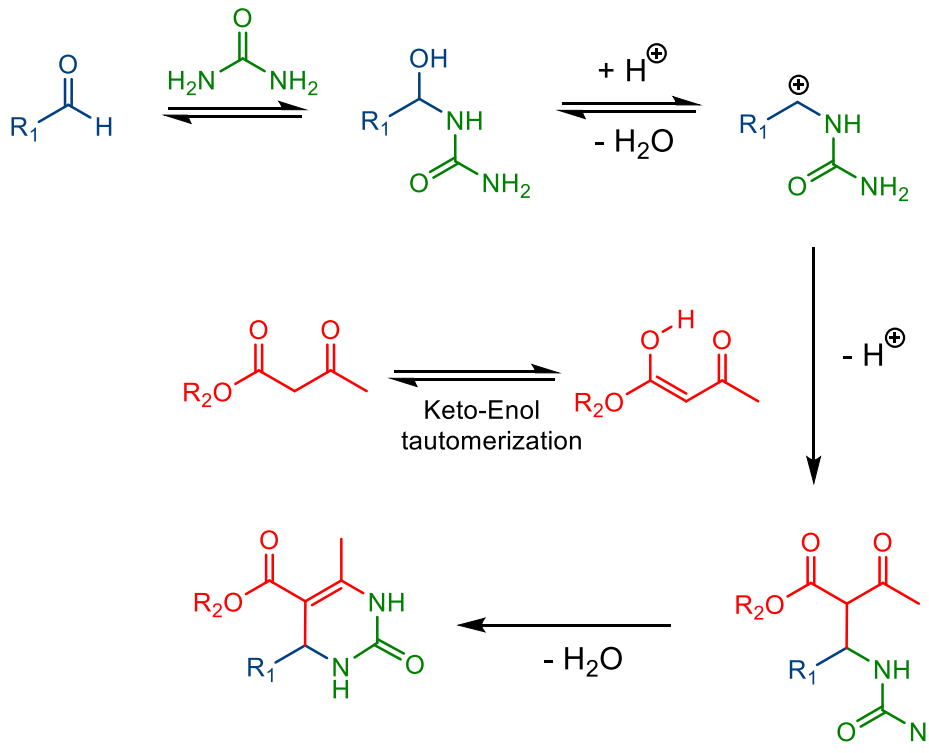

Scheme 18: Proposed mechanism of the Biginelli reaction with an aldehyde, urea and a β-ketoester.[205]

In **Scheme 18**, a simplified mechanism of the Biginelli reaction is illustrated according to the generally accepted mechanism of Kappe *et al*.[205] The reaction starts with the nucleophilic addition of urea to the aldehyde component resulting the corresponding hemiaminal formation. In the subsequent step, an acid promoted dehydration takes place to yield a highly reactive *N*-acyliminium ion. Subsequently, the *N*-acyliminium ion reacts with the 1,3-dicarbonyl compound (through keto-enol tautomerization) to create an ureide intermediate which then undergoes cyclocondensation yielding the

final DHMP component. The resulting DHPMs found various applications, especially in pharmaceutical industry, such as treatment of cardiovascular diseases, epilepsy, cancer or calcium channel blockers.[206-209]

Another literature-known three-component reaction was reported by Carl Mannich in 1912.[202] The reaction involves the formation of the β-amino carbonyl compound by the reaction of formaldehyde, an aldehyde or ketone and an amine under acidic conditions (**Scheme 17**). In 1956, a sulfur containing four-component reaction was discovered by Asinger.[203] In this reaction, two equivalents of carbonyl component react with ammonia and elemental sulfur to form thiazolines (**Scheme 17**).

2.3.2 Isocyanide-based Multicomponent Reactions (IMCRs)

Different from the previous class of multicomponent reactions, IMCRs employ isocyanides in the synthesis, which exhibit an extraordinary reactivity, due to their formally divalent carbon atom. The Passerini three-component reaction (P-3CR) and the Ugi four-component reaction (Ugi-4CR) are the most known examples of IMCRs and will be briefly discussed.

Passerini (1921)

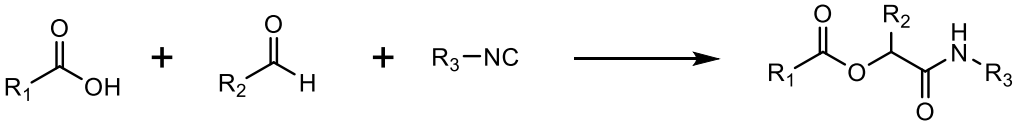

Ugi (1959)

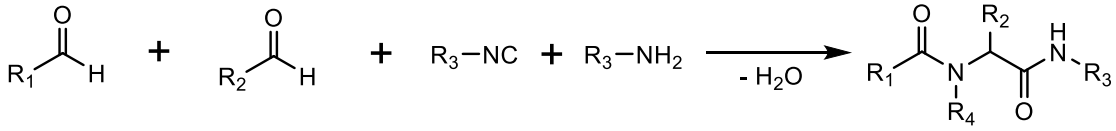

Scheme 19: The most known IMCRs: The P-3CR and U-4CR.[210-212]

The Passerini three-component reaction is the first known IMCR, discovered by Mario Passerini in 1921.[210] It facilitates the formation of α-acyloxyl-amide with the reaction between a carboxylic acid, a carbonyl component (aldehyde or ketone) and an isocyanide as illustrated in **Scheme 19**.

The reaction starts with the activation of the carbonyl component with the carboxylic acid *via* the formation of hydrogen bonding. In the next step, the activated carbonyl carbon is nucleophilically attacked by the carbon atom of the isocyanide (α-addition), resulting a cyclic transition state. In the final step, the P-3CR product is formed *via* an intramolecular rearrangement, the transfer of a proton from the carboxylic acid to the carbonyl component (**Scheme 20**). This commonly accepted mechanism is first proposed by Passerini, which was later confirmed by kinetic studies.[213-214]

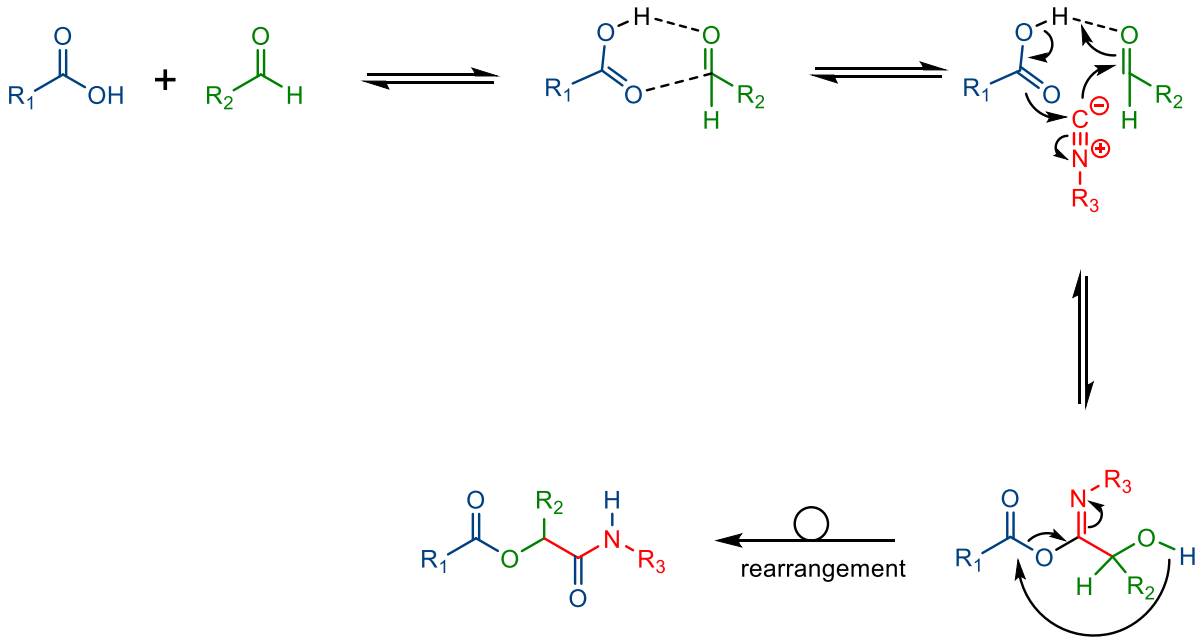

Scheme 20: Proposed mechanism of Passerini-3CR using a carboxylic acid, an aldehyde and an isocyanide.[213-214]

The Ugi four-component reaction was discovered by Ivar Ugi in 1959.[211-212] Here, an additional amine is used compared to P-3CR, forming a α-aminoacylamide (**Scheme 19**).

3 Aims

Following the urge of exploring sustainable methods for the modification of renewable resource by taking advantage of their inherent structural diversity, the present thesis describes new ways for value creation from carbohydrate-based materials. Accordingly, an atom efficient multicomponent reaction approach (the Biginelli reaction) is introduced for the functionalization of starch. Upon the introduction of acetoacetate functionalities on the starch structure, molecularly diverse products are obtained using renewable aromatic aldehydes and urea in a one-pot reaction. Lastly, the processability of the final products is investigated using a hot press instrument by the addition of glycerol as a renewable plasticizer.

In the subsequent approach, an alternative multicomponent reaction is utilized for cellulose modification. For this purpose, cellulose is first oxidized to the corresponding 2,3-dialdehyde derivative, and newly introduced functionalities are employed in the Passerini three component reaction. The versatility of the reaction is demonstrated by using different isocyanides and renewable carboxylic acids. While choosing the components, diverse structures are aimed for to investigate their effect on the final thermal properties.

Since fatty acid cellulose esters (FACEs) have been investigated as an alternative packaging material for petroleum-based examples, an efficient and sustainable procedure employing a CO_2-based switchable solvent system to synthesize FACEs is aimed for in the last approach. To extend the investigation, the products are further modified *via* thiol-ene reaction in the presence of various thiols. In order to obtain fully biobased materials, two terpene-derived thiols are synthesized and further employed in the thiol-ene modification. Moreover, two of the thiol-ene products are additionally oxidized to increase the diversity of the molecular structures. In order to show if the synthesized materials are suitable for packaging material application, thin film properties are investigated.

4 Results and Discussion

4.1 Modification of Starch *via* the Biginelli Multicomponent Reaction

This chapter and the associated sections in the Experimental Part were published previously:

E. Esen, M. A. R. Meier, *Macromol. Rapid Commun.*, **2020**, 41, 1900375.[215]

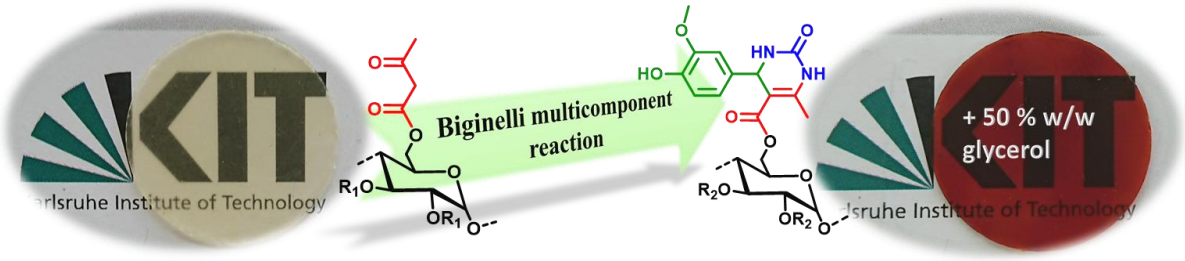

4.1.1 Introduction

As described in **Chapter 2.2**, various methods have been reported for the modification of starch, which are mostly limited to common derivatizations such as esterification, etherification, or grafting. More complex molecular structures during modification cannot be easily achieved by these approaches.

Multicomponent reactions (MCRs) are very powerful tools to synthesize diverse molecular structures in an efficient manner. Thus, they offer great possibilities to synthesize advanced functional materials from polysaccharides in a more sustainable way. Even though several works have been reported for cellulose and chitosan modification *via* MCRs, starch was not studied as a starting material yet.[145, 216-221] Indeed, the only examples of starch in the context of MCRs are its utilization as a catalyst in these reactions.[222-223]

Among the known MCRs, the Biginelli reaction has been recognized as a benchmark non-isocyanide based MCR. It facilitates the synthesis of heterocyclic compounds, the

so-called 3,4-dihydropyrimidin-2(1H)-ones (DHPMs), *via* condensation of an aromatic aldehyde, a β-keto ester and urea (or thiourea), which are known to have antibacterial, antiviral, or antitumor activities.[206, 224]

Very recently, the Biginelli reaction was used for cellulose modification by Sui *et al.* In that work, cellulose acetoacetate was first synthesized in the ionic liquid [AMIM][Cl] and subsequently modified *via* the Biginelli reaction. Even though it was an important example to show the possibility to modify cellulose in an efficient and versatile approach, sustainability of the whole synthesis was not the prior concern.

Within this chapter, an efficient and straightforward modification of starch using fully renewable components is reported. First, starch acetoacetate with a degree of substitution ranging from 0.59 to 2.5 is prepared and subsequently modified *via* the Biginelli reaction with different renewable aromatic aldehydes and urea to show the versatility of this approach. After optimizing the reaction conditions, detailed characterization of the synthesized products is reported. The processability of the products was also investigated using a hot press instrument, revealing that glycerol is a suitable and renewable plasticizer for the Biginelli products.

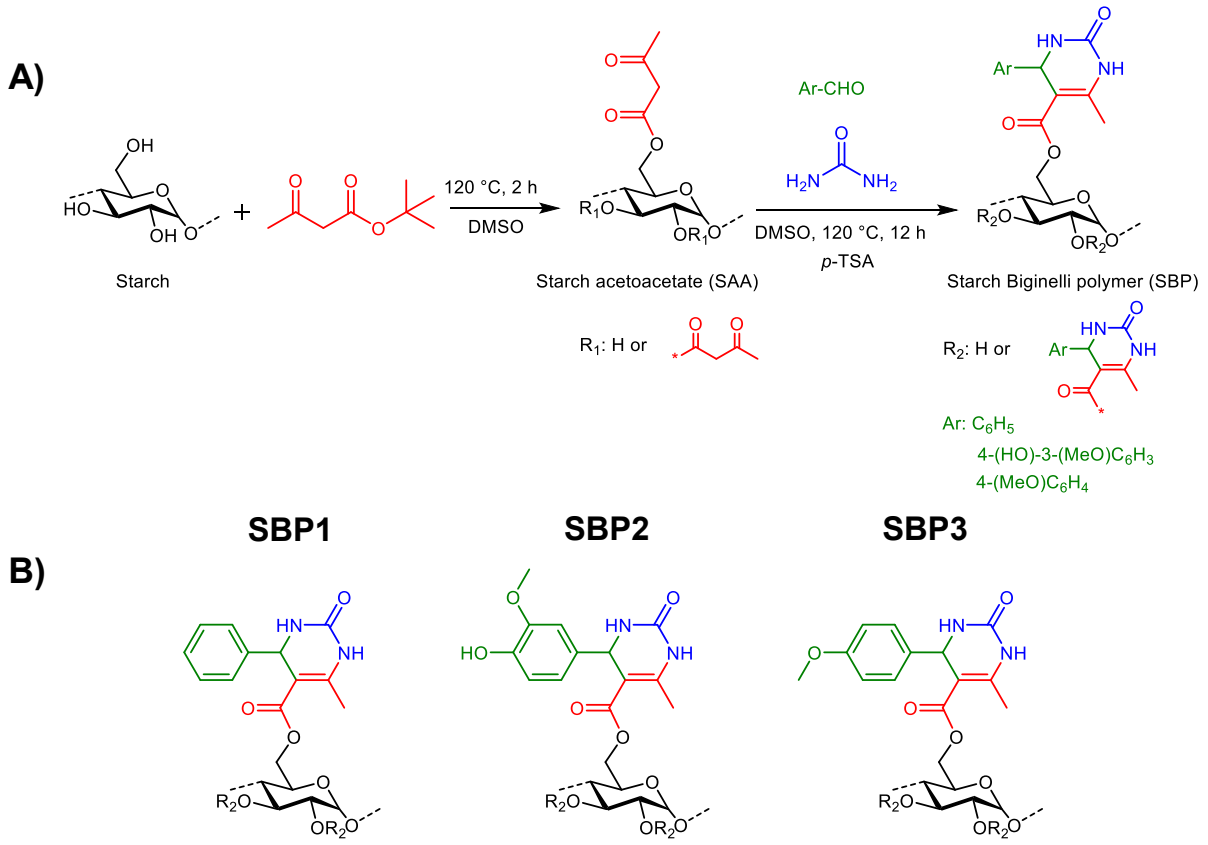

Scheme 21: A) Scheme of the Biginelli modification of starch, **B**) Isolated starch Biginelli polymers (**SBPs**)

4.1.2 Results and discussion

Synthesis and characterization of starch acetoacetate (SAA)

The project was started investigating starch modification *via* acetoacetylation using a straightforward procedure in DMSO at 120 °C without using a catalyst (**Scheme 21A**). The temperature was chosen similar to a reported procedures, where cellulose acetoacetates were synthesized at 110 °C in a ionic liquid ([AMIM][Cl])[225] and at 120 °C in DMAc/LiCl.[226] Even though 2,2,6-trimethyl-4H-1,3-dioxin-4-one (THD) is known to be a better acetoacetylating agent, *tert*-butyl acetoacetate (*t*-BAA) was investigated here to improve the sustainability of the procedure. After purification of the products, initial characterization was performed *via* ATR-IR spectroscopy. Successful acetoacetylation was confirmed by the appearance of two significant bands of the carbonyl stretching vibrations at 1743 and 1710 cm^{-1} (**Figure 5**). In

addition, a decrease of the O-H stretching vibrations intensity on the starch backbone around 3300 cm^{-1} was observed due to the substitution. Similarly, ^{1}H NMR also confirmed the formation of the **SAA** structure by revealing two significant peaks arising from the methylene group of the acetoacetate functionality at 3.61 ppm and the methyl group at 2.18 ppm respectively. The peaks between 5.78 and 3-10 ppm were attributed to protons of anhydroglucose unit (AGU) of starch (**Figure 6**).

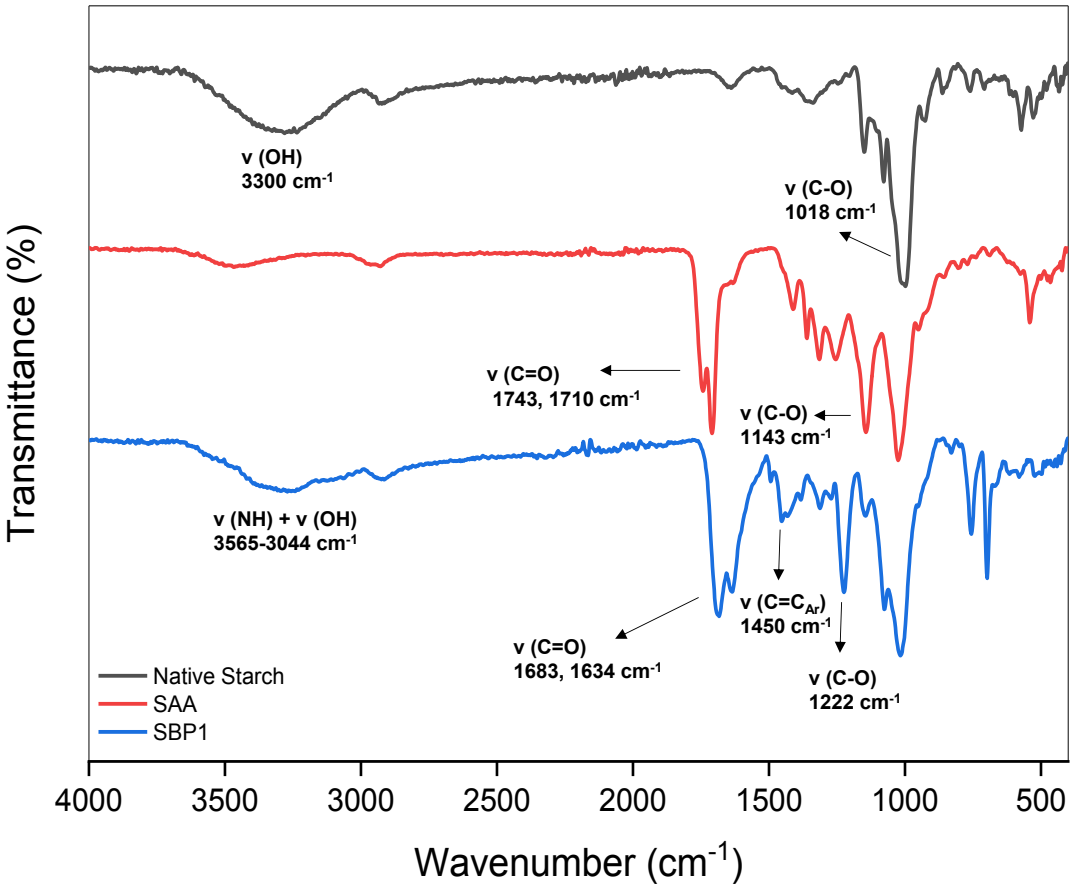

Figure 5: ATR-IR spectra of native starch, **SAA** and **SBP1** (spectra were normalized to the intensity of the C-O stretching vibrations of the pyranose units at 1018 cm^{-1}).

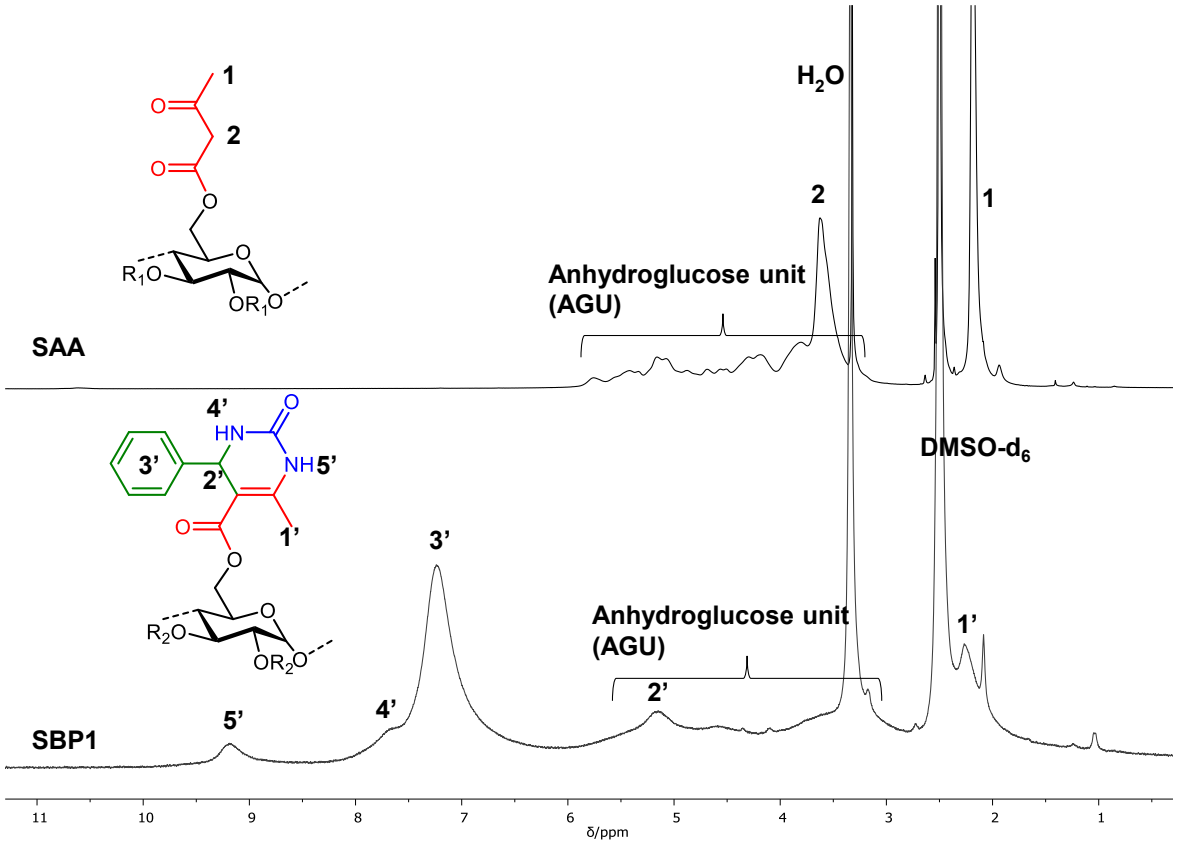

Figure 6: ^{1}H NMR spectra of **SAA** and **SBP1**.

After confirming the **SAA** formation from the first attempts, the reaction optimization was investigated by monitoring the carbonyl stretching vibrations of the acetoacetate group *via* IR spectroscopy. The ATR-IR spectra were normalized to the C-O absorption of the pyranose unit in the starch backbone (1018 cm^{-1}), which is not affected during the starch modification

Because transesterification reactions proceed through an equilibrium, removing one of the products drives the reaction towards higher conversions. Thus, after complete addition of the *t*-BAA, air flow was applied to ease the release of *tert*-butanol, which resulted in a higher conversion (**Figure 7**).Secondly, the influence of the *t*-BAA equivalents (1.00, 3.00 and 6.00 eq per AGU) used in acetoacetylation reaction was studied at 120 °C for 3 hours, revealing that the intensities of the carbonyl bands continuously increased with the *t*-BAA equivalents, as expected (**Figure 8**). Similarly, the intensity of the O-H stretching vibration on the starch backbone around 3000 cm^{-1} decreased significantly.

Additionally, the optimal reaction time was investigated. 1, 2 and 3 hours were chosen as reaction times. The carbonyl intensities increased noticeably from 1 h to 2 h reaction, however after 2 h, no additional conversion was observed, indicating the maximum substitution was reached within 2 h in this system (**Figure 35**).

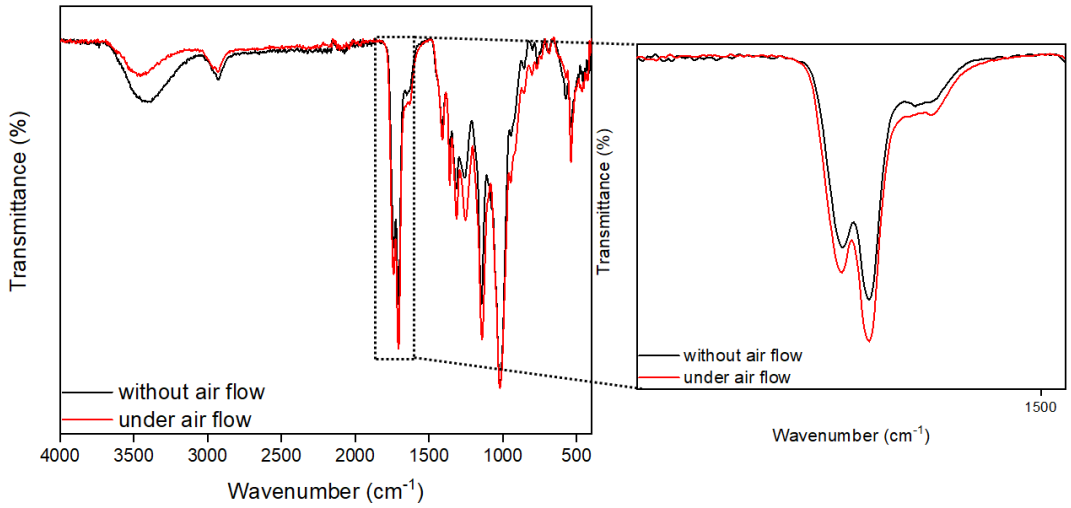

Figure 7: ATR-IR spectra (left) and carbonyl intensities (right) of **SAA**, effect of the air flow (spectra were normalized to the intensity of the C-O stretching vibrations of the pyranose unit at 1018 cm^{-1}).

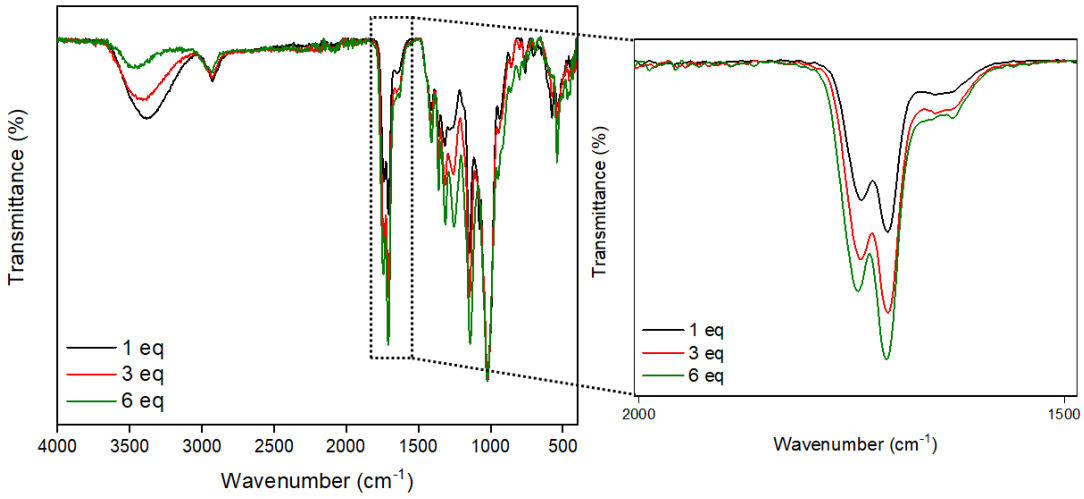

Figure 8: ATR-IR spectra (left) and carbonyl intensities (right) of **SAA** with different *t*-BAA equivalents (spectra were normalized to the intensity of the C-O stretching vibrations of the pyranose unit at 1018 cm^{-1}).

A different type of acetoacetylating agent was not investigated in this work. Apart from being more sustainable and less toxic, *t*-BAA worked quite efficiently in the

acetoacetylation reaction and no side reactions were observed, in contrast to the results reported for the cellulose acetoacetate synthesis procedure with THD.[226]

Degree of substitution (DS) determination of SAAs

The degree of substitution (DS) of the **SAA** products was determined *via* literature known methodology based on ^{31}P NMR.[227] The unreacted hydroxyl groups were thus reacted with the phosphorylating agent, revealing a broad peak between δ = 150-143 ppm in the ^{31}P NMR, which can be attributed to the phosphorylated hydroxyl groups of starch (**Figure 9**). The integration of this peak with respect to and internal standard allows the calculation of the DS according to the above-mentioned procedure. The highest DS was determined as 2.50 when 6 eq *t*-BAA per AGU were used at 120 °C for 2 h (**Table 4**). For the **SAA** samples with lower DS values (below ~1.50), which could be obtained by decreasing the reaction time or the *t*-BAA equivalents, the ^{31}P NMR method was not applicable due to their insolubility in the solvent mixture. Thus, ^{1}H NMR was performed in these cases to determine the DS.

Table 4: Summary of degree of substitution (DS) values of obtained starch acetoacetates (**SAAs**) in DMSO under different reaction conditions.

Sample	Eq. *t*-BAA[b]	Time (h)	T (°C)	DS
SAA1	1.00	2	120	0.59[c]
SAA2	3.00	2	120	1.04[c]
SAA3	6.00	2	120	2.22[c]/2.50[d]
SAA4[a]	6.00	2	120	2.13[d]
SAA5	6.00	1	120	1.40[c]
SAA6	6.00	3	120	2.50[d]

[a]Without air flow. [b]Equivalents of *t*-BAA with respect to AGU. [c]Calculated from ^{1}H NMR spectroscopy. [d]Calculated from ^{31}P NMR spectroscopy.

In some literature examples, DS determination of cellulose acetoacetates were reported by using conventional ^{1}H NMR methodology.[221, 225] However, these values were not representing the exact DS values, while the region between 6.00 and 3.50 ppm was assumed to contain only 7 H (AGU hydrogens) for the calculation. Indeed, the signals from unreacted hydroxyl groups of the cellulose backbone are also present in this area and should be considered. Heinze *et al.* reported more precise

method by measuring the spectrum with the addition of trifluoroacetic acid (TFA).[226] The purpose of the addition of TFA was to shift the water signal and all the exchangeable protons, like the ones from remaining hydroxyl groups on the starch backbone (**Figure 10**), downfield. By doing this, the integral between 5.63-3.22 ppm (AGU region + methylene group) to 2.18 ppm (methyl group) can be used to calculate the DS of the samples. To make a comparison, the same sample used in the ^{31}P NMR was method also tested with this proposed method and the DS was calculated as 2.22, which was comparable but slightly lower than the value obtained from ^{31}P NMR (2.50). However, because the signals were not very sharp in case for the measured ^{1}H NMR, the DS values from ^{31}P NMR were accepted, which is more reliable method due to the better resolution of the signals in the spectra.

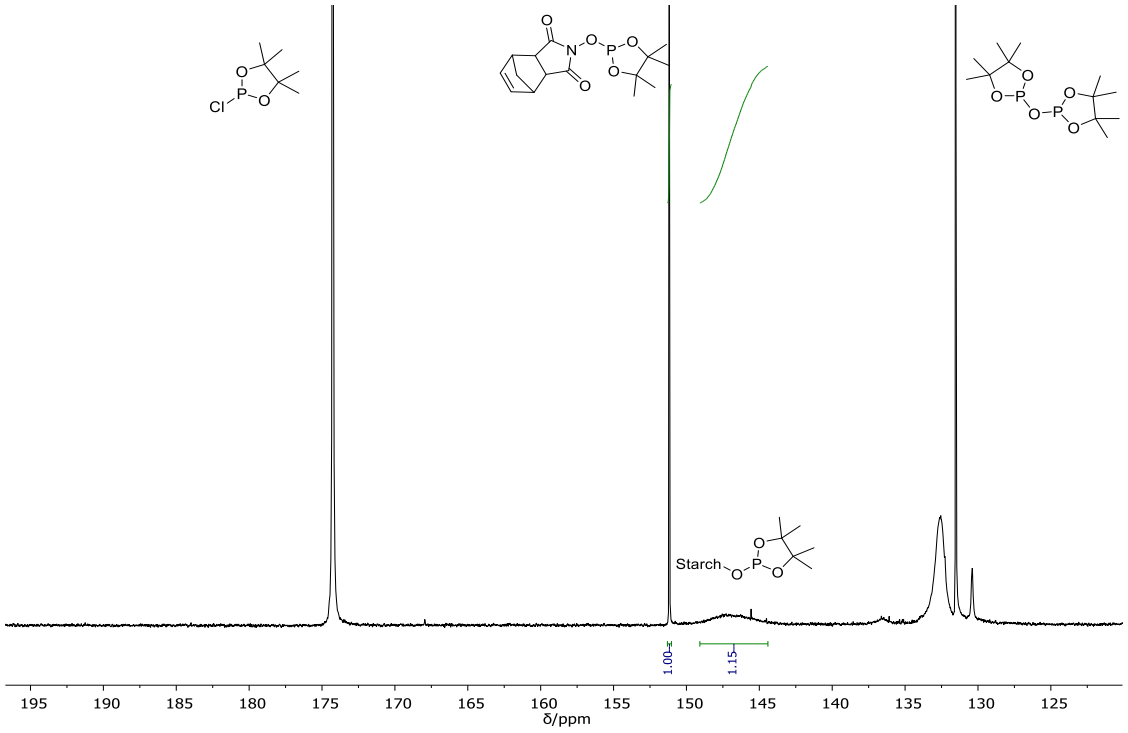

Figure 9: ^{31}P NMR spectrum of **SAA** (DS was calculated as 2.50).

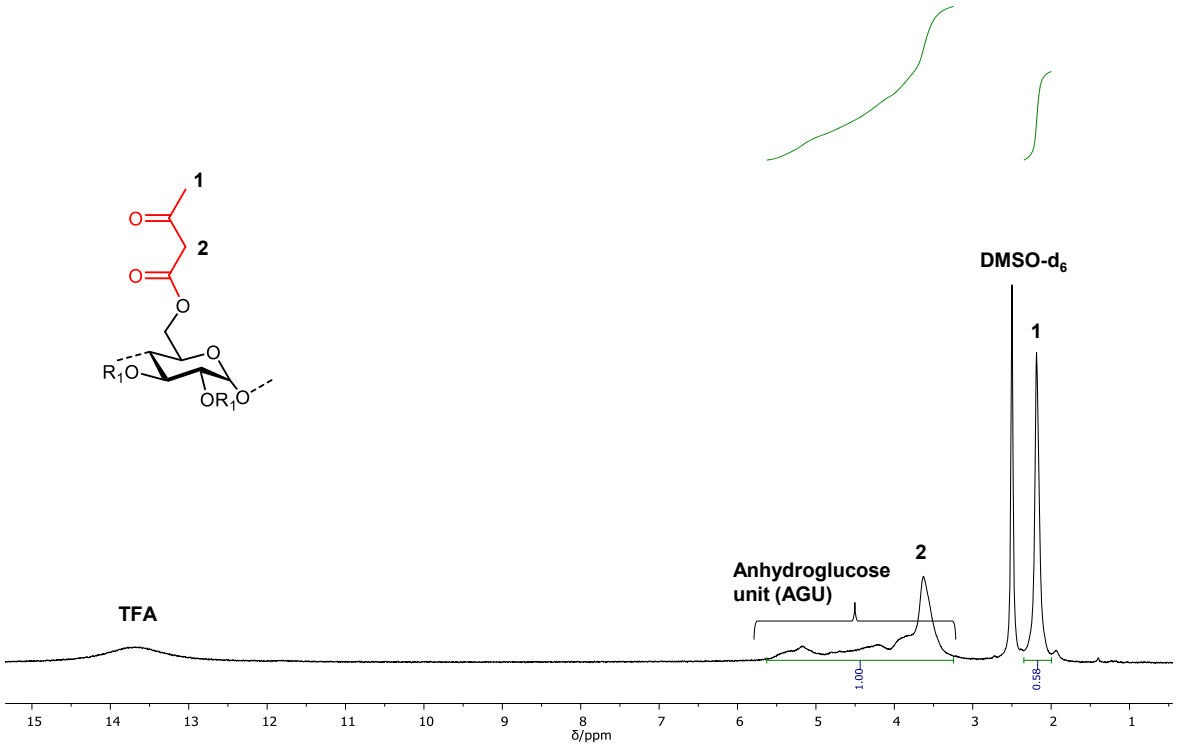

Figure 10: ^{1}H NMR spectrum of **SAA** in DMSO-d_6 containing a drop of TFA (DS was calculated as 2.22).

Synthesis and characterization of the starch Biginelli polymers (SBPs)

In the following step, the **SAA** product with the highest DS (2.50) was modified *via* Biginelli reaction by using an aromatic aldehyde, urea and a catalytic amount of *p*-toluenesulfonic acid (*p*-TSA) in DMSO at 120 °C. The catalyst and temperature in the first trials were chosen according to a literature known procedure.[228] As a model compound, benzaldehyde was chosen as the aldehyde unit to optimize the reaction conditions. Afterwards, vanillin and *p*-anisaldehyde were used with the same reaction conditions to expand the diversity of the final products and to produce fully renewable **SBPs**. After purification, the successful modification was confirmed by ATR-IR spectroscopy, primarily. As an example, the formation of the 3,4-dihydropyrimidin-2(1H)-one structures was validated by the shifting of the initial carbonyl vibrations at 1743 and 1710 cm^{-1} of **SAA** to lower wavenumbers at 1683 and 1634 cm^{-1} for **SBP1**. Moreover, an aromatic vibration at 1450 cm^{-1} became visible due to the incorporation of aromatic aldehyde into the starch backbone (**Figure 5**). Later, ^{1}H NMR spectrum also revealed the characteristic signals of the DHPM structure: the

CONH moieties at 9.2 and 7.7 ppm, in addition to the aromatic signal at 7.2 ppm and the CH peak of heteroatomic ring at 5.2 ppm, confirming the successful modification. Furthermore, the methylene peak of SAA at 3.61 ppm vanished, thus proving the full conversion of **SAA** to **SBPs** (**Figure 6**). The DS determination of the **SBPs** could not be done *via* ^{31}P NMR as it was performed for the **SAAs**. During sample preparation, a precipitate formation was observed, possibly due to the reaction between the phosphorylating agent and the **SBPs**. Nevertheless, the DS values of the **SBPs** were considered same as the **SAA** used for the Biginelli reaction due to the full conversion of **SAA** to **SBPs** (within experimental error of ^{1}H NMR).

Table 5: Molecular and thermal characterization data of the modified starch sample.

Sample	M_n (kDa)[a]	M_w (kDa)[a]	$Đ$[a]	Yield[b] (%)	T_g (°C)	$T_{d,5\%}$ (°C)
SAA	262	612	2.3	88	93	185
SBP1	110	400	3.6	64	-[c]	275
SBP2	143	406	2.8	60	-[c]	277
SBP3	124	452	3.6	61	-[c]	280

[a]SEC in HFIP +0.1 wt% potassium trifluoroacetate (KTFA). [b]Yields were determined taking DS values into consideration. [c]Not observed

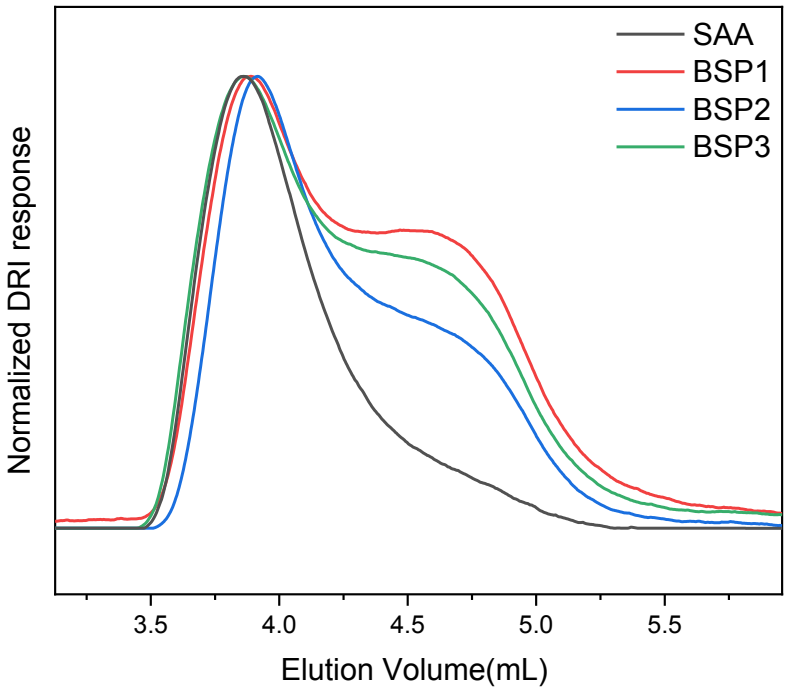

Figure 11: SEC traces of the synthesized products.

Optimization studies for the Biginelli reaction were performed *via* SEC and ATR-IR spectroscopy. Samples were taken from the reaction mixture at different time intervals and after purification, they were initially analyzed by size exclusion chromatography (SEC). Due to the insolubility of the samples with the 1 and 2 h reaction times, analysis was not possible. For the following samples, a lower molecular weight compared to **SAA** was observed, however the molecular weight increased until 12 h reaction time, whereas a slight decrease was dominant for the longer reaction time (24 h). This indicates a possible degradation of the starch backbone due to the long reaction time (lower molecular weight species of ≈ 1 kDa were observed by SEC). Similarly, IR spectroscopy revealed the same trend by a continuous increase in the intensity of the C=O vibration with time until 12 h. Afterwards, a slight decrease was observed for the 24 h reaction time due to some minor degradation. Additionally, already after 1 h, the C=O vibrations of **SAA** disappeared quantitively, which confirmed the efficiency of the modification (**Figure 12**).

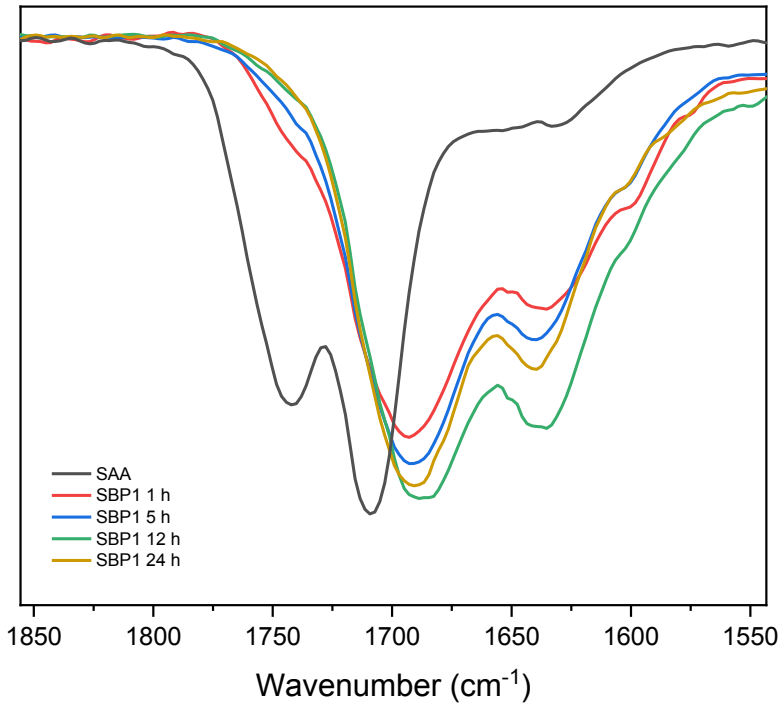

Figure 12: ATR-IR spectra of the carbonyl intensities of **SAA** and **SBP1** with different reaction times (spectra were normalized to the intensity of the C-O stretching vibrations of the pyranose units at 1018 cm^{-1}).

Ensuing investigations were focused on the effect of the reaction concentration. Reactions were conducted in bulk, 5 mL and 10 mL DMSO. Even though the reaction in bulk revealed promising results, higher conversion was observed with 5 mL DMSO (**Figure 40**). On the other hand, the more diluted reaction (in 10 mL) exhibited significantly lower substitution, which is a typical observation for diluted organic reactions. Since, Lewis acids were commonly used as catalysts for the Biginelli reaction, LiBr and $MgCl_2$ were also tested to find an alternative for *p*-TSA.[229-230] They both worked relatively well, however the carbonyl vibration from **SAA** was still present, indicating complete conversion was not obtained under the same conditions as with *p*-TSA (**Figure 41**). This was also in favor of sustainability, as metal catalysts could be avoided for the reaction.

After optimizing the reaction conditions, molecular weight distributions of the synthesized products were investigated *via* SEC by using hexafluoroisopropanol (HFIP) +0.1 wt% potassium trifluoroacetate (KTFA) as an eluent. Analysis revealed that **SAA** (DS: 2.5) shows an M_n of 262 kDa with $Đ$ = 2.3, whereas **SBPs** show lower M_n (110-143 kDa with $Đ$ = 2.8-3.6) (**Table 5**). This difference can be explained by their different (smaller) hydrodynamic volumes in the selected eluent because of the presence of strong hydrogen bonding in the Biginelli products or by the exclusion limit of the SEC columns. The exclusion limit was around 3.7 mL (elution volume), thus molecules with higher molecular weight than the exclusion limit might be detected at higher retention times (**Figure 11**). A control reaction was performed with **SAA** in DMSO/*p*-TSA at 120 °C for 12 h to investigate a possible degradation of the starch backbone under the Biginelli reaction conditions. Unfortunately, after the reaction, very fine insoluble fibers were obtained, possibly due to the aldol condensation of the β-keto-ester. Therefore, SEC analysis was not possible afterwards. A possible degradation thus cannot be ruled out in the optimized conditions, but the results show that the Biginelli reaction proceeds preferred compared to this side reaction and that in any case, high molecular weight modified starches could be confirmed (**Table 5**).

Thermal characterization of the synthesized products

Initial thermal characterization of the synthesized products was conducted *via* thermogravimetric analysis (TGA) to learn about their thermal stabilities (**Figure 13**). In all products, water evaporation was observed between 80 to 175 °C and the **SAA** samples showed a relatively high thermal stability ($T_{d,5\%}$ = 185 °C). The thermal stability of the **SBPs** increased 10–15 °C compared to native starch (**Table 5**). It is worth mentioning that especially at higher temperatures (in this case 320 °C), the Biginelli products only lost 40% of their initial weight, while it was 70% for native starch.

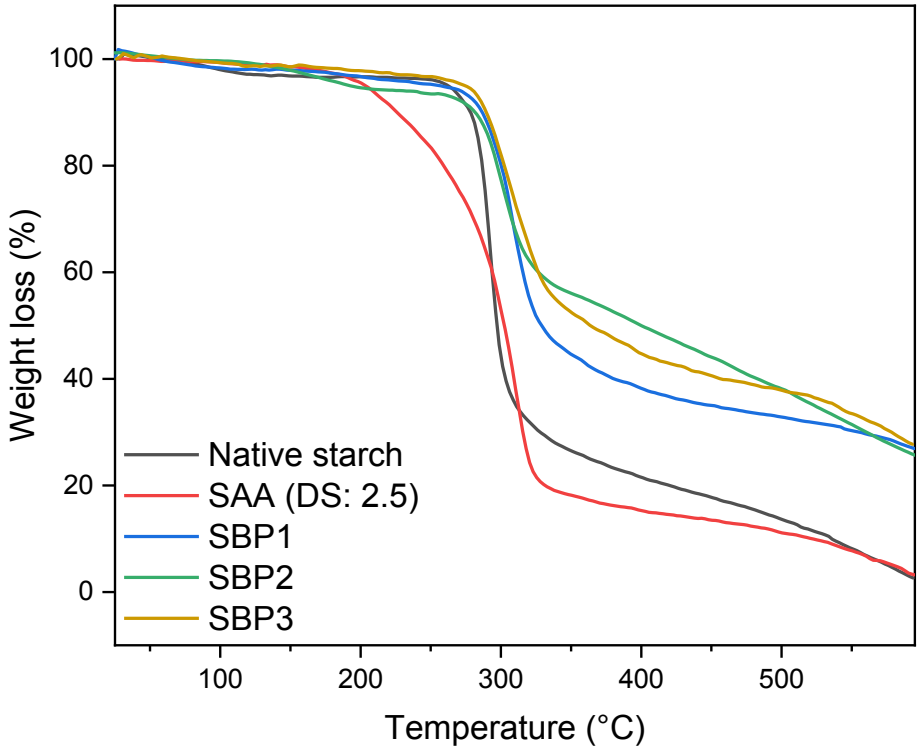

Figure 13: TGA analysis of native starch, **SAA**, **SBP1**, **SBP2** and **SBP3**.

After learning about the thermal stabilities of the products, differential scanning calorimetry (DSC) analysis was performed to investigate their thermal transitions (**Figure 14**). Glass transition temperatures (T_g) between 93 and 131 °C were observed for the **SAA** products, depending on their DS values, which can be easily tuned by changing the reaction time or the *t*-BAA equivalents. On the other hand, a T_g was not observed for the **SBPs** within the measuring range (–25 to 245 °C), probably since

the increase of the inter- and intramolecular hydrogen bonding of the newly introduced DHMP units strongly restricts mobility.

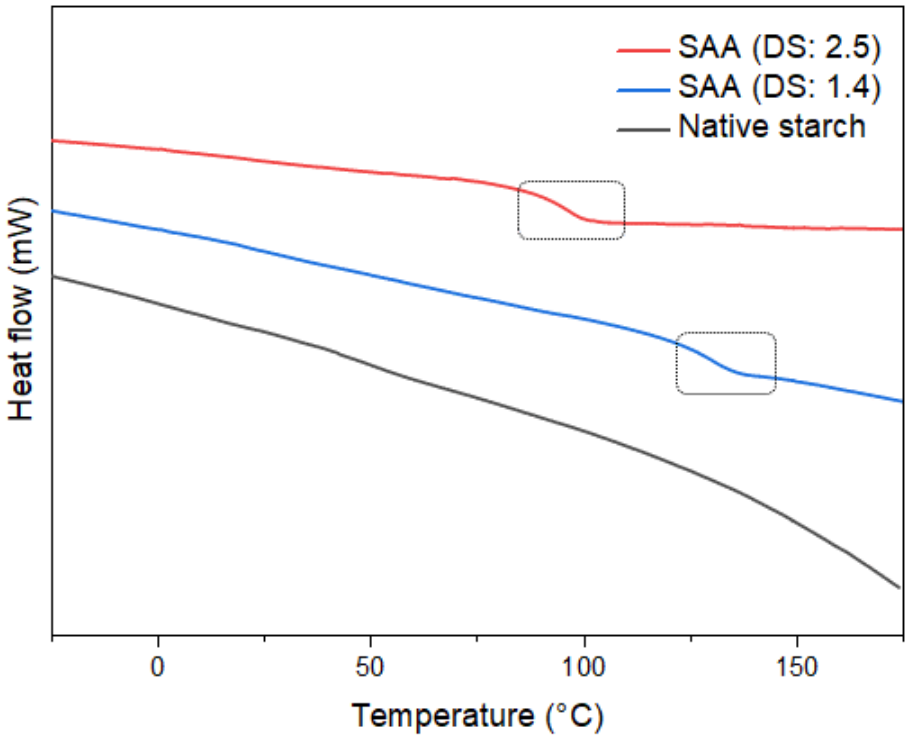

Figure 14: DSC graph of native starch and **SAA** with different DS values.

Processability of the synthesized products

After detailed characterization of the synthesized products, their processability was investigated by using hot press instrument. First, **SAA**s with various DS values were pressed above their T_g and under 5 kN force, resulting in the formation of translucent discs. Afterwards, the same method was applied to the **SBPs**, but since these samples did not show any glass transition below their degradation temperature, processing was difficult. After first trials at 140 °C, discs were obtained but the appearance of the discs was not homogenous (**Figure 15**). In order to overcome this problem, glycerol, which is cheap and renewable, was chosen as a possible plasticizer to obtain some initial results on possible processability of the **SBP** samples. Glycerol is a common plasticizer for starch, introducing thermoplastic behavior *via* hydrogen bonding with the starch hydroxyls, which competes/disturbs the interaction between starch chains.[231-232]

Amount of glycerol was chosen as 20% w/w initially and increased until translucent discs were obtained. With 20% w/w glycerol, samples were too brittle to be taken as one piece out of the press; however, after increasing the glycerol amount up to 50% w/w, homogenous discs could be obtained in one piece. The required glycerol amount (50% w/w) was higher than typically used for plasticized (native) starches.[233-234] Afterwards, the effect of the glycerol addition on the **SBP** polymers' thermal behavior was investigated *via* DSC and a melting point was observed only for **SBP2** at 120 °C (**Figure 45**). This observation also explains why homogenous discs could be obtained only by using **SBP2** with 50% w/w glycerol.

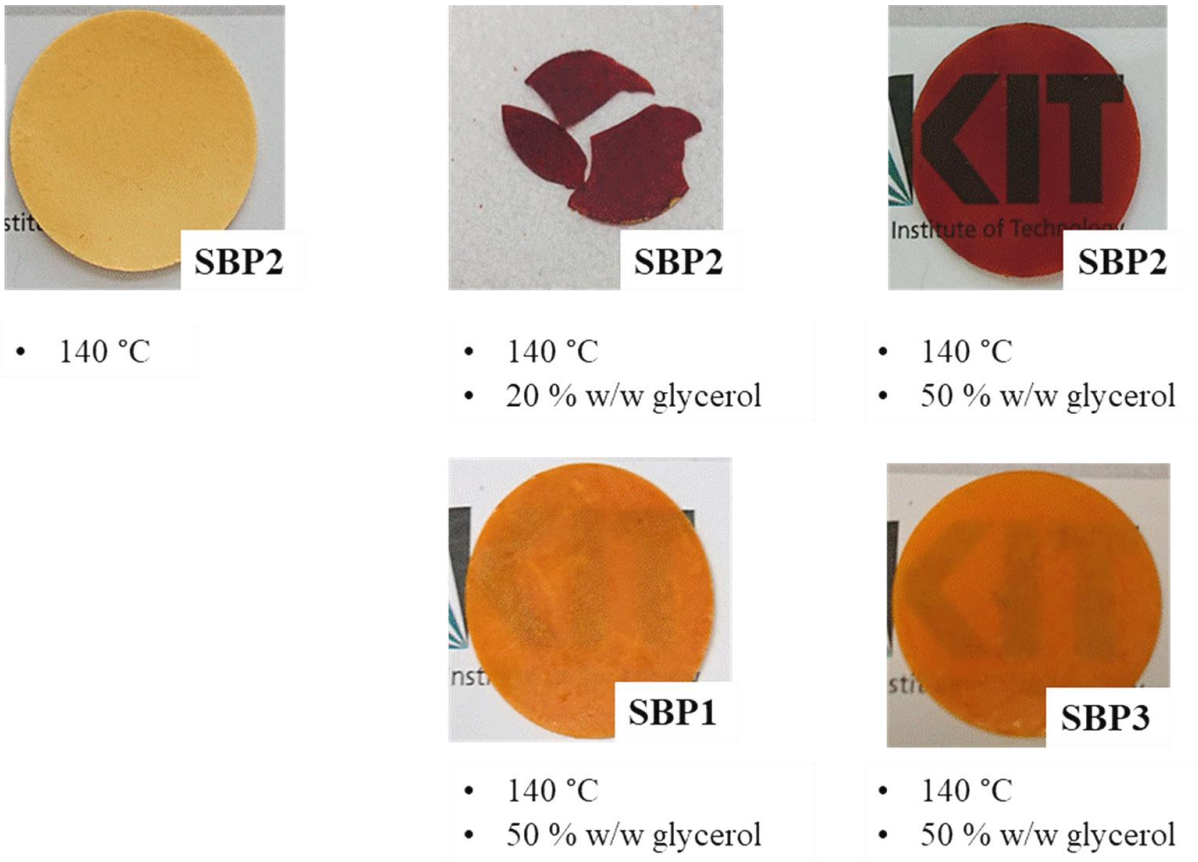

Figure 15: Samples prepared using a hot press instrument.

Later, the obtained discs were cut into 20 mm x 2 mm strips in order to investigate their mechanical behavior using a tensile strength instrument. Only the data from the measurement of **SBP2** with 50% w/w glycerol sample was taken, since the others were still too brittle and started to break in the beginning of the measurements. This

issue could be probably solved by increasing the amount of the plasticizer however further investigations were not conducted. The average values of three measurements showed 16% of elongation at break with a maximum stress value at 5.3 MPa and a Young's modulus (*E*) of 118 MPa (**Figure 16**).

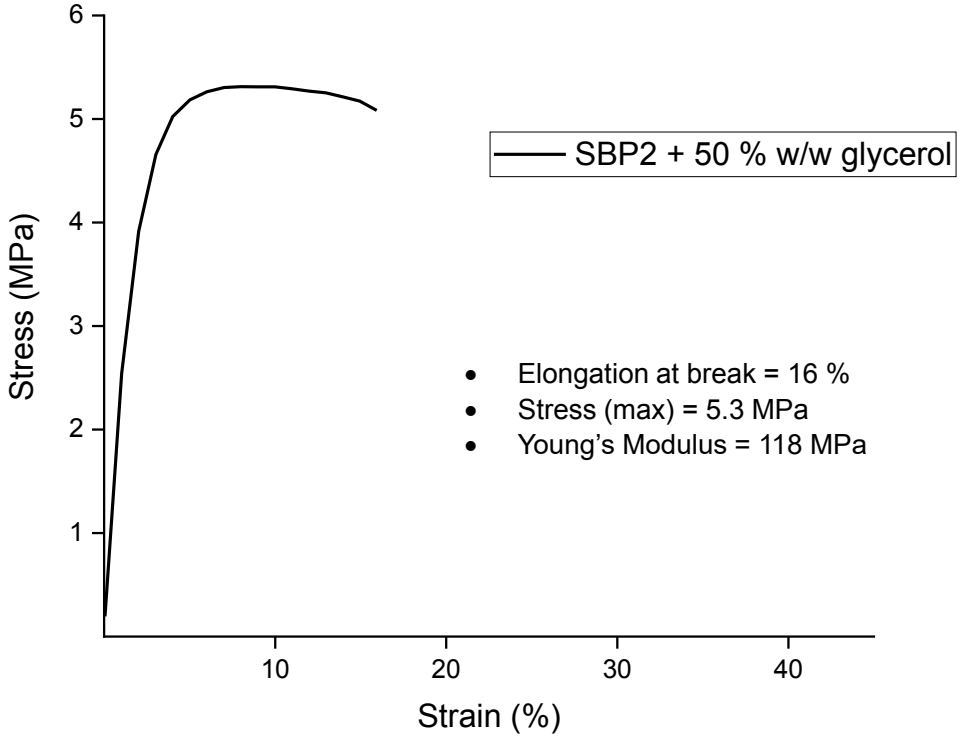

Figure 16: Tensile strength measurement of **SBP2** with 50% w/w glycerol.

4.1.3 Conclusions

In this chapter, a Biginelli type modification of starch is reported by first acetoacetylating starch with a maximum DS of 2.5. and further reacting it with urea and 3 different renewable aromatic aldehydes (benzaldehyde, vanillin and *p*-anisaldehyde) to demonstrate the versatility of this multicomponent reaction approach. In summary, a straightforward and versatile procedure under metal-free and considerably mild conditions was demonstrated. Additionally, starch acetoacetates revealed thermoplastic behavior with a wide range of T_g values (93-131 °C), depending on the degree of substitution, which can be easily tuned by changing the *t*-BAA equivalents and reaction time. After the Biginelli modification, fully

renewable products with high molecular weight (M_n of 110-143 kDa) and high thermal stability ($T_{d,5\%}$ = 275-280 °C) were successfully obtained. Lastly, processability of the Biginelli modified products were investigated by using a hot press instrument. A homogenous disc sample was obtained with **SBP2** by using 50% w/w glycerol as a plasticizer, which was later confirmed to have a melting point at 120 °C *via* DSC measurements.

4.2 Sustainable Functionalization of 2,3-Dialdehyde Cellulose *via* the Passerini Three Component Reaction

This chapter and the associated sections in the Experimental Part were published previously:

E. Esen, M. A. R. Meier, *ACS Sustainable Chem. Eng.*, **2020**, 8, 41, 15755.[220]

4.2.1 Introduction

2,3-Dialdeyhde cellulose (DAC) is one of the most investigated oxidized cellulose derivatives. The most established method to obtain DAC is the periodate oxidation of cellulose, which selectively oxidizes the hydroxyl groups on the C2 and C3 positions of the anhydroglucose unit (AGU), leading to the C2-C3 bond cleavage. Depending on the oxidation conditions (temperature, oxidation time, the use of co-oxidant), the degree of oxidation (DO) of the synthesized DAC can be different. Its solubility in hot water and the aldehyde functionalities promise huge possibilities to obtain new cellulose-based materials. Unfortunately, studies based on DAC are so far limited by the imine formation by the reaction with various amines, including crosslinking with biopolymers. More detailed application examples, as well as preparation procedures were described in **Chapter 2.1.3.2**.

The Passerini three component reaction (P-3CR) is the pioneer of the isocyanide based multicomponent reactions.[210] The mechanism proceed *via* formation of α-acyloxyl-amides by the use of a carboxylic acid, a carbonyl component (aldehyde or ketone) and an isocyanide under catalyst free and mild conditions. The high atom efficiency, versatility and the ability to perform the reaction in a one-pot approach make it a great candidate for sustainable carbohydrate modifications. Indeed, cellulose based hydrogels have been previously synthesized *via* P-3CR by using carboxymethyl cellulose (CMC) as carboxylic acid component.[216] Another approach was presented by Meier *et al.,* in which cellulose was first succiniylated in an efficient and sustainable procedure, and subsequently modified *via* P-3CR.[145] A full

conversion at 50 °C for 24 h was reported, offering new cellulose-based materials showing various thermal transitions The P-3CR was also employed for surface modification of TEMPO-oxidized cellulose nanofibers.[218] In the mentioned publication, thermoresponsive polymers were covalently attached to the oxidized cellulose surface under mild conditions. A more recent example was published by Fleury *et al.*[219] CMC was first dissolved in slightly acidic water and various aldehydes and isocyanides were used to obtain water soluble Passerini-modified derivatives. However, in all of the above-mentioned examples, the carbohydrate substrate was employed as the acid component, thus preventing the use of several different renewable carboxylic acids for the P-3CR modification.

In this chapter, a sustainable and efficient approach for cellulose modification by first oxidizing it to DAC and subsequently modifying it *via* the P-3CR in aqueous medium is described. Various renewable carboxylic acids and commercially available isocyanides were tested to obtain molecularly diverse modifications on the cellulose backbone. After optimizing the reaction conditions, detailed molecular and thermal characterizations are reported for each of the synthesized samples. Overall, this approach demonstrated a novel way to modify DAC *via* a versatile multicomponent reaction strategy under catalyst free and mild conditions.

4.2.2 Results and discussion

Synthesis and characterization of 2,3-dialdehyde cellulose (DAC)

DAC was prepared by using a literature known periodate oxidation procedure of native cellulose at 55 °C for 15 h under protection from light (**Scheme 22**).[79, 83] In most of the literature examples, DAC is purified *via* dialysis for a long time to completely remove the periodate. In this work, the cloudy solution was precipitated in isopropanol, filtered and subsequently washed with ice water, allowing the procedure to skip the dialysis step, saving high amounts of water, the necessary dialysis membranes and time. This improvement can thus be considered a more sustainable purification and is certainly more efficient.

The DAC structure was confirmed by ATR-IR spectroscopy from the formation of the two characteristic peaks at 1730 and 881 cm^{-1}, the carbonyl stretching vibration and the C-O-C vibration of hemiacetal, respectively (**Figure 17**). The carbonyl intensity of the aldehyde functionality is expected to be strong in organic compounds, however this is not the case in DACs, as the aldehyde functionalities are in an equilibrium with their hydrate forms, hemialdal and intra- and intermolecular hemiacetals as described in **Chapter 2.1.3.2**. Optimization studies for the oxidation reaction were not performed in detail due to the sufficient carbonyl intensity from the IR spectra and the optimal solubility of the DAC samples in hot water, which were needed for the subsequent reaction. The degree of oxidation of the DAC samples were measured by using the proposed titration method with NaOH solution, after the reaction of DAC with hydroxylamine hydrochloride.[80, 102] The average value of two analysis was calculated as 1.23, meaning that an average of 1.23 secondary hydroxyls in one AGU was oxidized. The DO value was later confirmed by elemental analysis by using the nitrogen content of the dried oxime derivative of DAC obtained after titration.

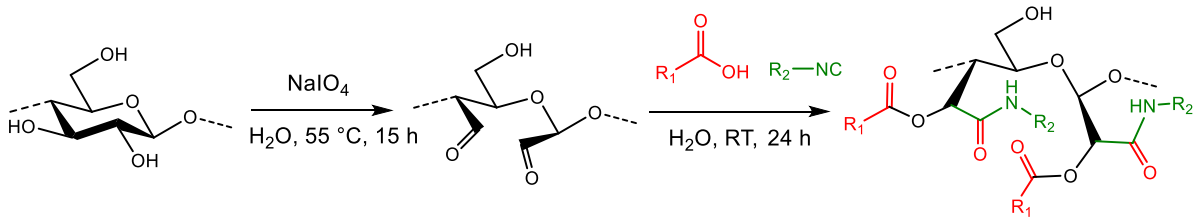

Scheme 22: Periodate oxidation of cellulose and subsequent Passerini 3-CR of DAC.

Synthesis and characterization of Passerini products

In the second step of the project, DAC with a DO of 1.23 was first dissolved in hot water (90-95 °C). Then, a water-soluble carboxylic acid and an isocyanide were added into the reaction mixture and stirred at room temperature for desired time (**Scheme 22**). After approximately 30 minutes, the Passerini product started to precipitate, which proved the efficiency of the reaction. Multicomponent reactions such as the Passerini and Ugi reaction are known to exhibit 300-fold rate accelerations in aqueous media, compared to procedures in organic solvents.[235] Additionally, product formation as a precipitate simplified the subsequent purification step.

Passerini product **P1** (acetic acid and *tert*-butyl isocyanide) was chosen as a model compound for the initial structural characterization. ATR-IR results showed two carbonyl absorbance bands, that are characteristics for the newly introduced ester and amide functionalities at 1744 and 1665 cm^{-1}, respectively (**Figure 17**). In addition, the C-O stretching at 1215 cm^{-1} and the C-H stretching around 2968-2868 cm^{-1} became visible. Further characterization of the **P1** structure was performed by ^{1}H and ^{13}C NMR (**Figure 18**).

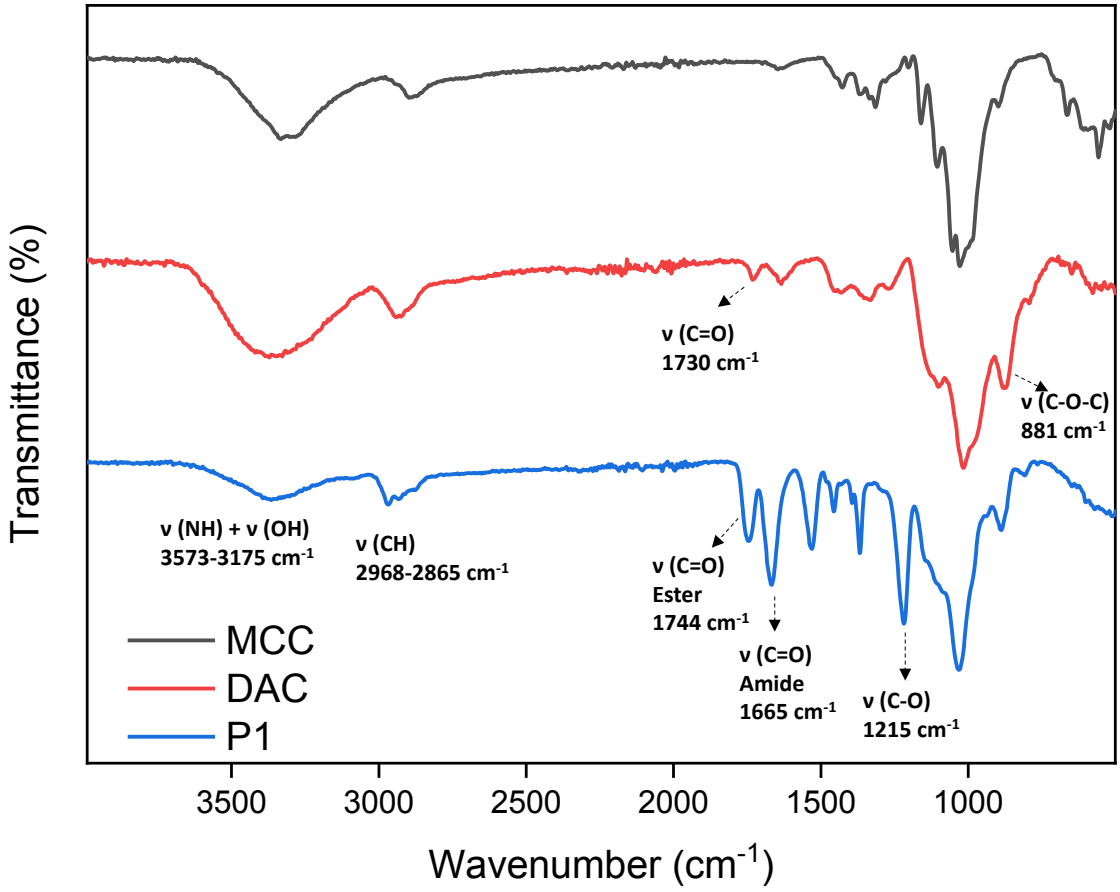

Figure 17: ATR-IR spectra of microcrystalline cellulose (MCC), dialdehyde cellulose (DAC) and **P1**.

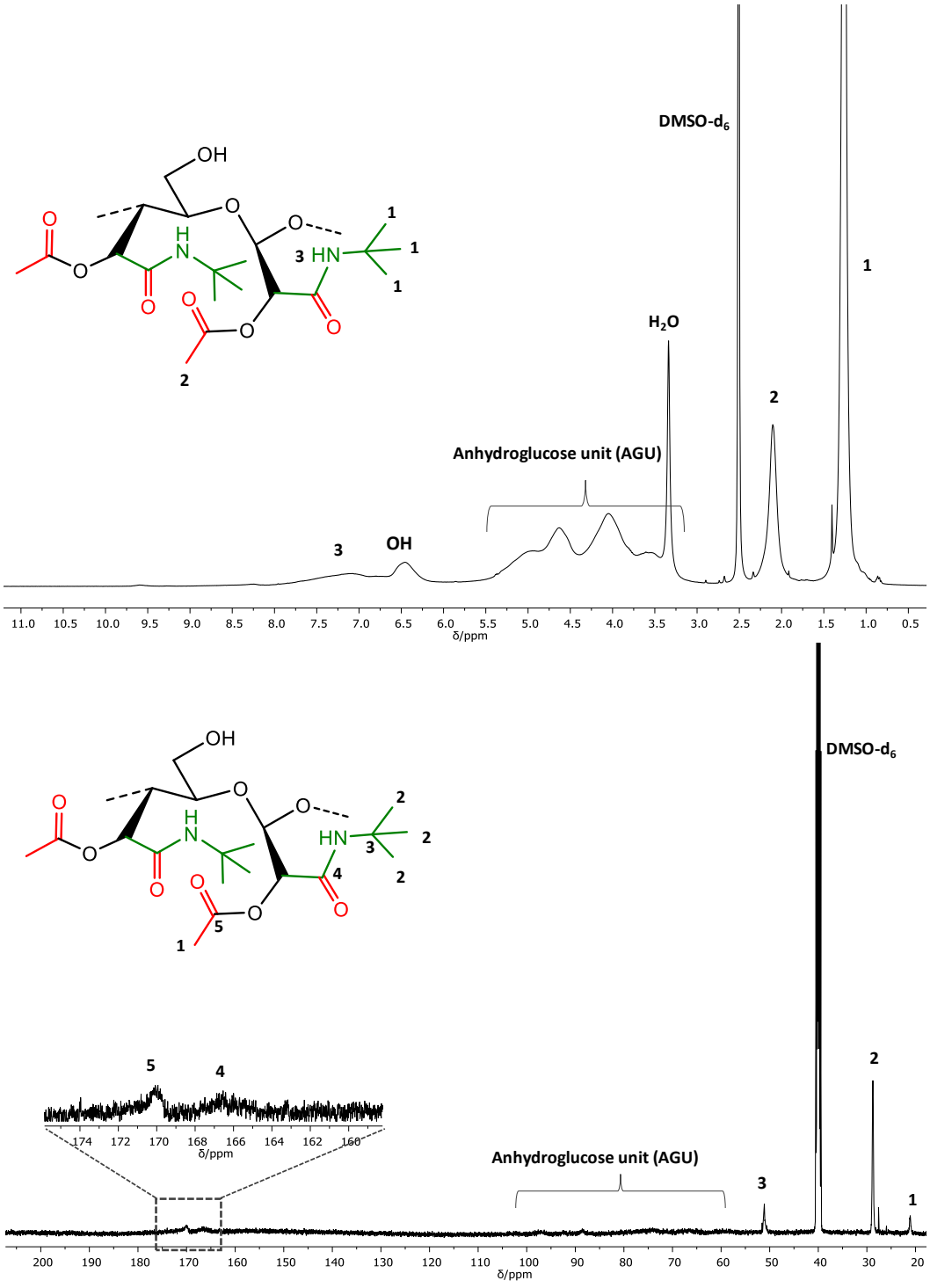

Figure 18: ^{1}H (top) and ^{1}C NMR (bottom) of Passerini product **P1**.

^{1}H NMR revealed a broad peak around 7.21 ppm from the amide moiety, together with CH_3 peaks at 2.10 and 1.25 ppm originating from the acid and isocyanide components, respectively (**Figure 18**). The broad peak at 6.46 ppm can be assigned

to an alcohol peak belonging to intra and/or interchain hemiacetal from the DAC structure, as explained earlier. This peak was later observed in all other Passerini products even though different acid and isocyanide components were used to synthesize these products. It was assumed that the equilibrium between aldehyde and hemiacetals was disturbed by the Passerini reaction, which takes place from the aldehyde functionalities. However, some of the hemiacetals remained in the structure. A similar observation has not yet been reported in literature, as DAC is mostly employed in crosslinking reactions with amines, which makes it impossible to characterize *via* ^{1}H NMR spectroscopy.

In order to confirm this assumption, ^{1}H NMR spectra of **P1** were recorded in different solvents. In THF-d_8, this specific peak was observed at a lower chemical shift (2.83 ppm), while in MeOH-d_4 and DMSO-d_6 containing a drop of trifluoroacetic acid (TFA), the peak was not visible, indicating that the structure possesses an exchangeable proton, in this case from a hydroxyl group (**Figure 56** to **Figure 58**). Additionally, ^{13}C NMR revealed two significant peaks at 170 and 167 ppm, that can be assigned to the carbonyl groups of the ester and amide functionalities of the **P1** structure, respectively (**Figure 18**).

For the optimization of the reaction parameters, **P1** was selected as a model compound. Influence of the reaction temperature was tested initially by preparing four samples with two different reaction temperatures (RT and 50 °C) and two reaction times (2 and 4 hours). After purification, the samples were analyzed *via* SEC. Since no significant difference in molecular weight was observed (**Figure 19**), room temperature was chosen as the optimal reaction temperature to lower the energy consumption and prevent undesired side reactions.

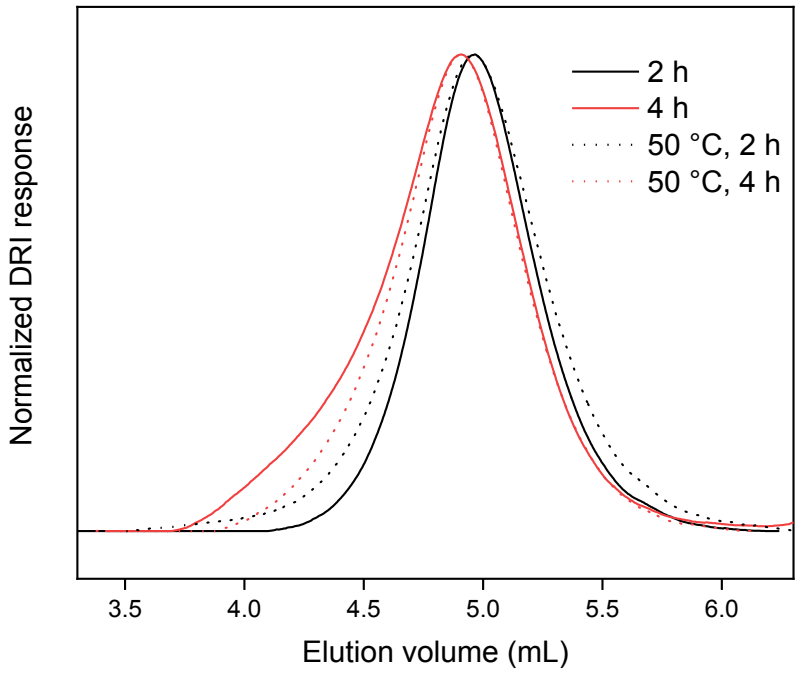

Figure 19: SEC traces for the synthesized **P1** samples for different reaction temperatures and times.

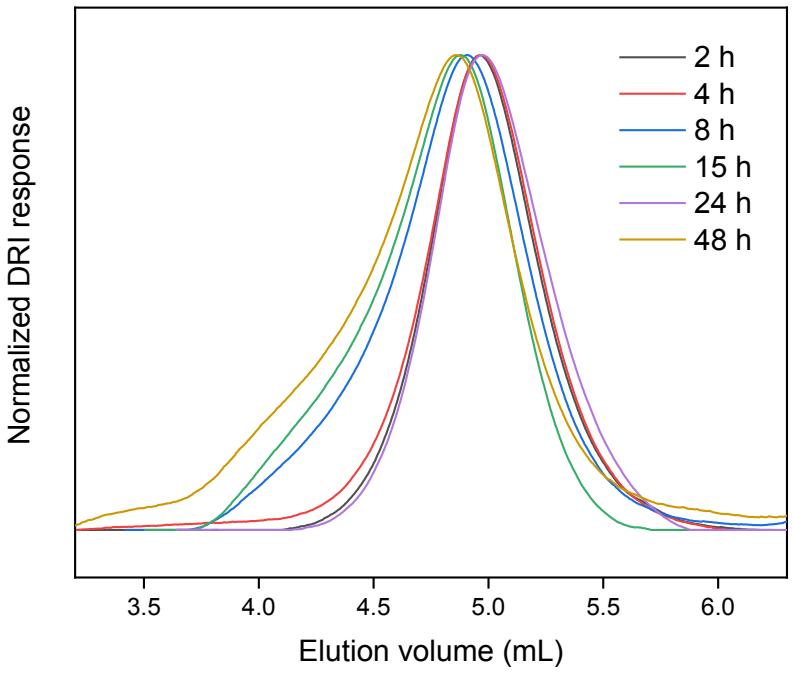

Figure 20: SEC traces of the synthesis of **P1** at different reaction times.

Subsequently, the reaction time was investigated in a more detailed fashion (2, 4, 8, 15, 24 and 48 hours) at room temperature. It is worth mentioning that it was not possible to start with one reaction and take samples in different intervals, since the products started to precipitate after 30 minutes. Thus, each sample was prepared individually and stopped after the desired time. Analysis showed that the molecular weight increased over time, however a decrease was observed at 24 h (**Figure 20**). This observation might be explained by the already discussed intra and/or interchain hemiacetal formation, affecting the sample's hydrodynamic volume in the eluent.

In order to find an explanation for this trend, elemental analysis was performed for each sample. Since the molecular weight can only increase due to the P-3CR, an increase in nitrogen content is an indication of molecular weight increase. As expected, the nitrogen content increased over time (**Table 6**). Calculated DS values were 0.79 for 2-4 h, 0.83 for 8-15 h and 0.94 for 24-48 h, which indicates that 84% of the maximum DS was already achieved within the first 2 hours of the reaction. It is important to emphasize that the reaction proceeded heterogeneously after the formation of the precipitate within 30 minutes, possibly leading to a decrease on the reaction rate. Additionally, a visible increase in the amount of the precipitate was observed until 2 hours. Similar observations related to the reaction kinetics were also reported in the work about the functionalization of carboxymethyl cellulose *via* the P-3CR in aqueous medium.[219] A reaction plateau was reached after 6 h at 50 °C, proving the P-3CR efficiency in aqueous medium.

Table 6: Elemental analysis and calculated degree of substitution (DS) values of **P1** at different reaction times.

Reaction time (h)	C (%)	N (%)	H (%)	DS
2	47.43	4.02	6.88	0.79
4	47.11	3.99	6.84	0.78
8	47.88	4.17	6.96	0.84
15	47.63	4.16	6.87	0.83
24	48.08	4.46	7.05	0.94
48	47.62	4.44	6.96	0.94

Since the reaction conditions seemed promising, the acid and isocyanide equivalents per aldehyde unit were decreased from 2.00 to 1.00 in order to make the procedure more sustainable. However, lower molecular weights were observed for the lower equivalent case, leading to the assumption that an excess of the components is necessary to obtain maximum conversion (**Figure 59**). Even though the P-3CR proceeds very efficiently with a stoichiometric amount of the 3 components for small molecules,[236] complex compounds like cellulose apparently need excess amount of reactants, as also previously reported in another study.[145]

After optimizing the reaction conditions (RT and 24 h), three additional isocyanides (cyclohexyl, 1-pentyl and *n*-octyl) and two additional water-soluble renewable carboxylic acids (2-furoic acid and gallic acid) were employed under the same conditions to expand the diversity of the final products. *n*-Octyl isocyanide was obtained *via* recently reported procedure by Meier *et al.*,[237] which offers a more sustainable way to synthesize isocyanides, and was chosen to present the possibility of obtaining all of the components from renewable sources in a sustainable manner. When 1-pentyl and *n*-octyl isocyanide were used in the reaction, initial precipitation was observed relatively late (4-5 h) compared to the other examples, due to the poor solubility of the alkyl isocyanides in water.

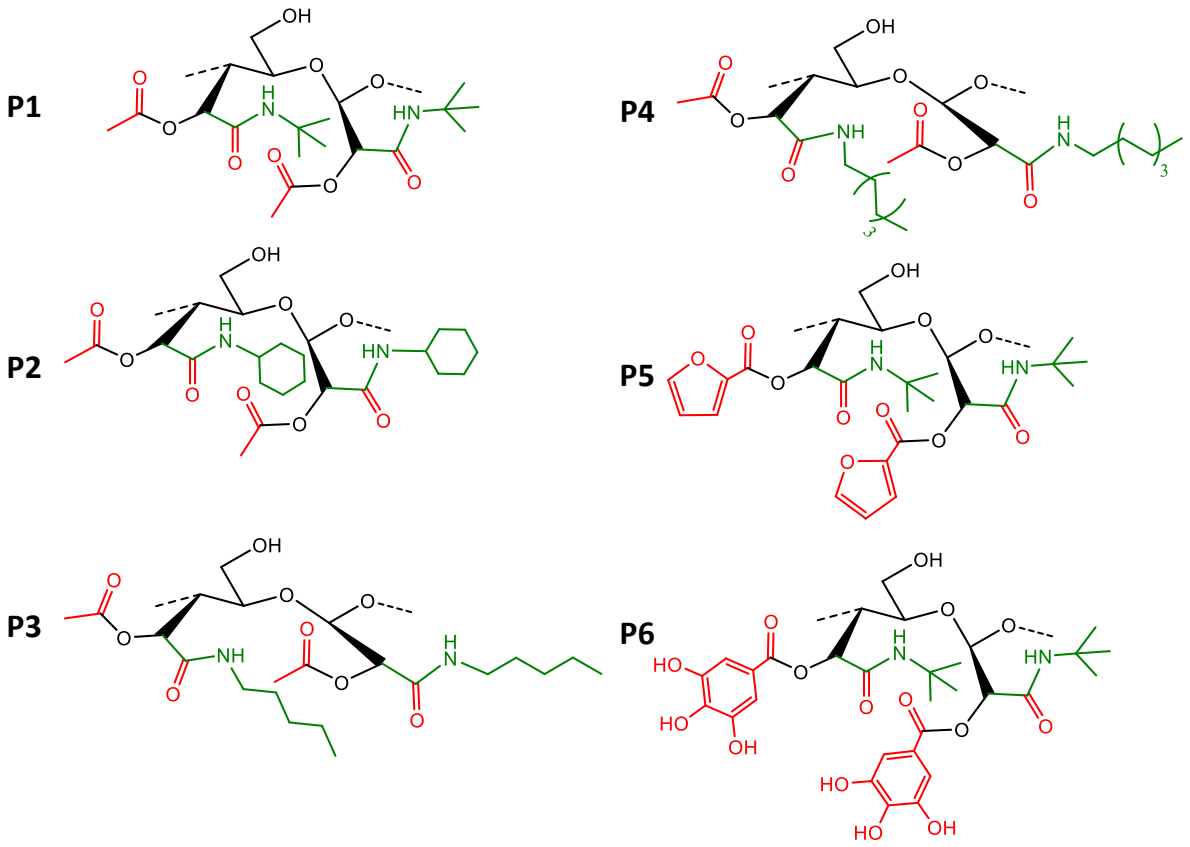

Figure 21: Isolated Passerini products: **P1-P6**.

A more detailed characterization was done *via* size exclusion chromatography (SEC) with hexafluoroisopropanol (HFIP) +0.1 wt% potassium trifluoroacetate (KTFA) as an eluent. As DAC was not soluble in the selected eluent, a comparison between DAC and the Passerini products was not possible. Analysis showed M_n between 16-27 kDa and M_w between 34-126 kDa with a dispersity ($Đ$) of 1.9-4.7 for the Passerini products (**Figure 22**). A small shoulder was observed for the products with long aliphatic chains, i.e. **P3** and **P4**. As the reaction was conducted in aqueous medium, possibly some sort of self-assembly took place, resulting in a molecular weight distribution with higher DS than average, leading to a shoulder in the SEC trace. The molecular weights of the Passerini products are considerably lower compared to other modified cellulose examples in the literature, in which native cellulose is modified directly. This behavior can be explained by the degradation of cellulose during the oxidation process, which was also observed in previous works.[238-239] As Potthast *et al.* reported, M_n of 8.5 kDa and M_w of 19.7 kDa were obtained for highly oxidized MCC *via* SEC/MALLS analysis,

which of course can differ based on the SEC conditions and the DO of the DAC samples.[239] Similarly, in the work of Kim *et al.*, where the molecular weights of DACs were investigated in an aqueous eluent with a pullulan standard, M_w values in a range of 30 to 42 kDa were reported, proving that the molecular weights of the synthesized products are in a reasonable range.[80]

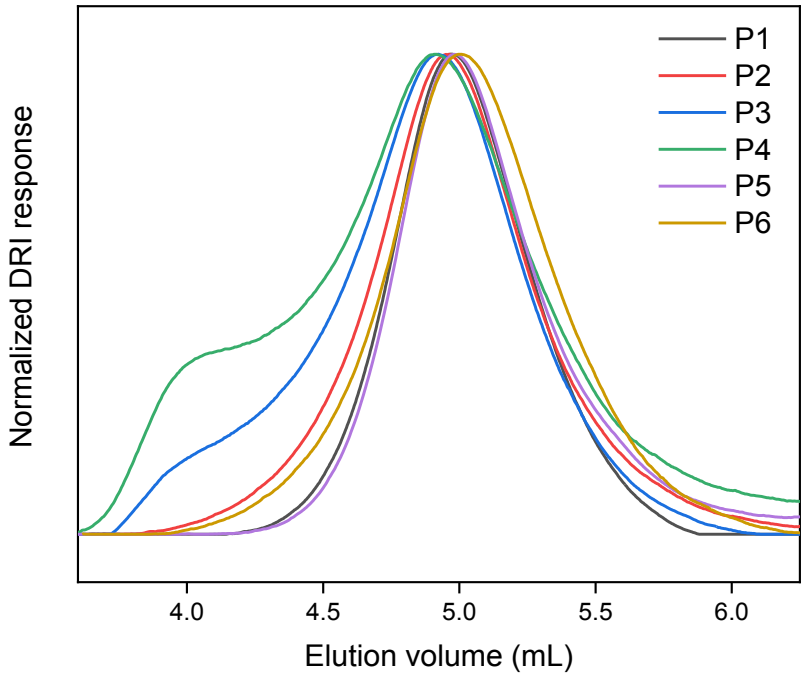

Figure 22: SEC traces of the Passerini products **P1-P6**.

Table 7: Molecular and thermal characterization data of the Passerini products.

Sample	Acid	Isocyanide	M_n [a] (kDa)	M_w [a] (kDa)	Đ[a]	DS[b]	Yield[c] (%)	T_g (°C)	$T_{d,5\%}$ (°C)
P1	acetic	*tert*-butyl	24	46	1.9	0.94	73	166	217
P2	acetic	cyclohexyl	20	51	2.5	0.77	88	159	201
P3	acetic	1-pentyl	27	90	3.2	0.68	91	121	190
P4	acetic	octyl	27	126	4.7	0.75	72	133	198
P5	2-furoic	*tert*-butyl	16	34	2.1	0.82	67	154	211
P6	gallic	*tert*-butyl	18	42	2.3	0.62	68	-[d]	194

[a]SEC in HFIP +0.1 wt% potassium trifluoroacetate (KTFA). [b]Calculated from elemental analysis. [c]Yields were determined taking DS values into consideration. [d]Not observed

Determination of the degree of substitution (DS) of Passerini products

As it was briefly mentioned previously, degrees of substitution (DS) of the Passerini modified samples were calculated *via* elemental analysis. Conventional methods such as ^{1}H or ^{31}P NMR could not be employed in this project, as the exact number of hydrogen atoms in one DAC unit was not known due to the complex structure of DAC, for the ^{1}H NMR case. Meanwhile, for the ^{31}P NMR method, unreacted hydroxyl groups in AGU are reacted with the phosphorylating agent, revealing a broad peak between 145-137 ppm in the ^{31}P NMR spectrum. The ratio of the integration of this peak relative to the internal standard is used in a previously reported equation.[227] However, due to the presence of hemiacetal and/or hemialdal hydroxyl groups this method was also not applicable. Thus, elemental analysis was chosen as a convenient method for DS calculation inserting the nitrogen content in the following equation:

$$\frac{14\alpha}{162 + M\alpha} = \frac{N}{100}$$

α: Degree of substitution

162: Molecular weight of the anhydroglucose unit (AGU)

M: Molecular weight of the Passerini unit

N: Weight percent of nitrogen atoms from elemental analysis

Theoretically, the maximum DS can be 1.23 after the modification, since the degree of oxidation of DAC sample was 1.23. Due to the nature of the P-3CR, the only possibility of the existence of the nitrogen atom on the latter product is the P-3CR product. The maximum DS for the Passerini products was between 0.68-0.94, indicating that the reaction proceeded smoothly (**Table 11**). It is important to remember the ^{1}H NMR discussion provided above in this context, as it is practically impossible to obtain full conversion due to the formation of hemiacetals that decreases the amount of available aldehyde units.

Thermal characterization of the synthesized products

Thermal characterization of the final products was conducted *via* DSC and TGA. First, the thermal stability of the synthesized derivates was investigated by TGA, in which

all the samples revealed a minor water evaporation around 70-135 °C (**Figure 23**). For the DAC sample, thermal degradation started significantly earlier than for native cellulose ($T_{d,5\%}$ = 156 °C *vs* 305 °C), and showed higher thermal stability at higher temperatures (after 330 °C), as also reported in previous studies.[240-241] This can be explained by the decrease of the crystallinity due to the periodate oxidation and the possible side reactions between cellulose chains. After the Passerini modification, however, the thermal stability was increased noticeably ($T_{d,5\%}$ = 190-217 °C) showing a single major degradation step.

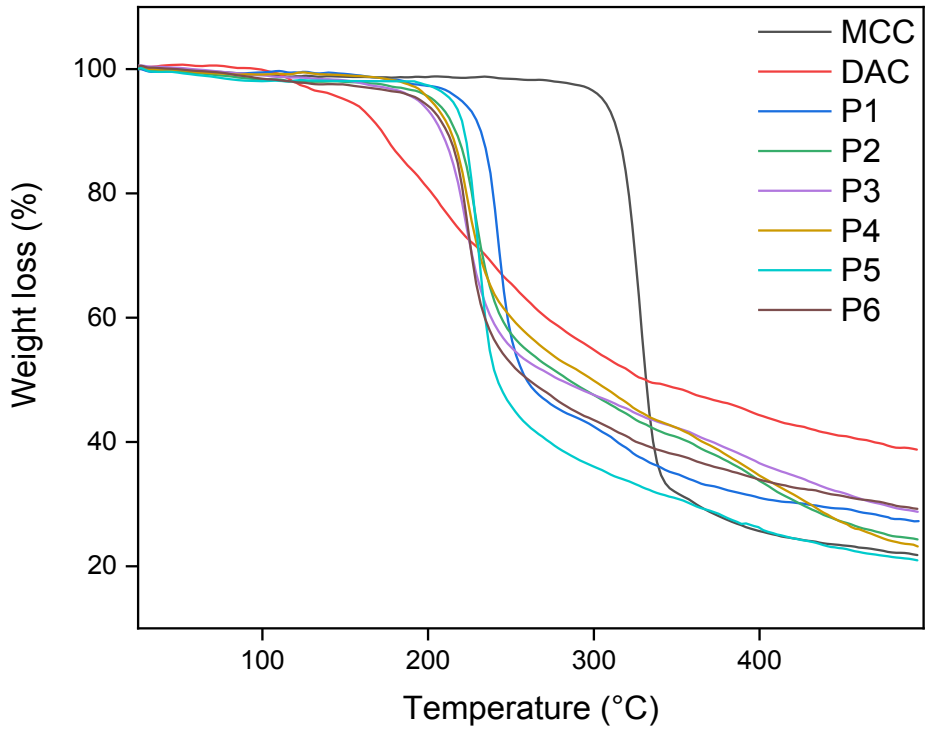

Figure 23: TGA analysis of microcrystalline cellulose (MCC), dialdehyde cellulose (DAC) and Passerini products (**P1-P6**).

Processability is a crucial feature for materials. Thus, after learning about the thermal stabilities of the synthesized products, DSC measurements were carried out to detect thermal transitions. It is known that native cellulose has no thermal transition, and as shown in **Figure 23**, the Passerini modification introduced a new thermal behavior to the products (except for **P6**) by exhibiting a glass transition temperature (T_g) in a range of 121 to 166 °C. From these results, it can be interpreted that the presence of long

alkyl groups (**P3** and **P4**) lowers the T_g, while the rigid, aromatic group on the structure of **P6** possibly restricts the mobility of the chains leading to a non-observable T_g. Thus, the ability to tune this property was achieved by simply changing one of the components during modification.

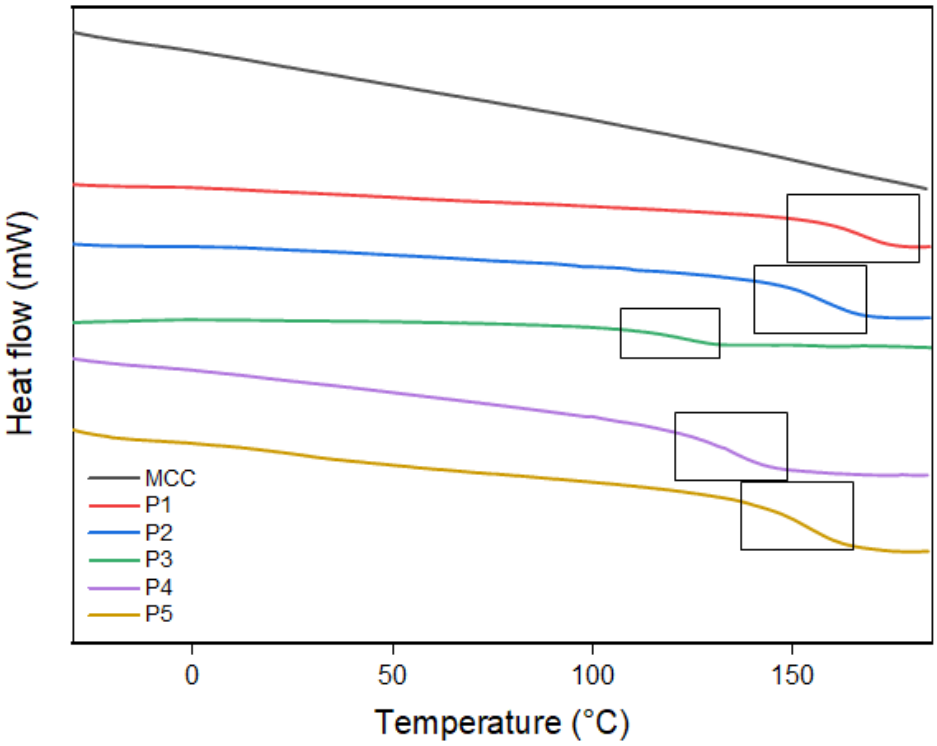

Figure 24: DSC graph of microcrystalline cellulose (MCC), dialdehyde cellulose (DAC) and Passerini products (**P1-P5**).

4.2.3 Conclusions

In this chapter, microcrystalline cellulose was first oxidized to 2,3-dialdehyde cellulose (DAC) with a degree of oxidation of 1.23 and subsequently modified *via* Passerini three component reaction using 4 isocyanides and 3 renewable carboxylic acids. By using elemental analysis, the degrees of substitution (DS) of the Passerini modified products were calculated in a range of 0.62 to 0.94. Additionally, it was proven that 84% of the maximum DS was reached within first 2 hours, which proved the efficiency of the reaction. After a detailed structural characterization of the Passerini products, thermal properties were investigated by TGA and DSC measurements. An

improvement in the thermal stability of the Passerini products ($T_{d,5\%}$ = 190-217 °C) compared to DAC ($T_{d,5\%}$ = 156 °C) was observed *via* TGA analysis. All Passerini products, expect for **P6**, showed glass transition temperatures (T_gs) between 121 and 166 °C, which proved the possibility to tune the final product's thermal transition in this temperature range by simply varying one of the components in the synthesis. Overall, the developed methodology represents a novel way to modify DAC, which have been so far only achieved by imine formation.

4.3 Sustainable Fatty Acid Modification of Cellulose in a CO_2-based Switchable Solvent and Subsequent Thiol-ene Modification

The optimization studies for the first part of this chapter were carried out by Pauline Hädinger in the scope of her bachelor thesis under my co-supervision.

E. Esen, P. Hädinger, M.A.R. Meier, *Biomacromolecules*, **2020**.[242]

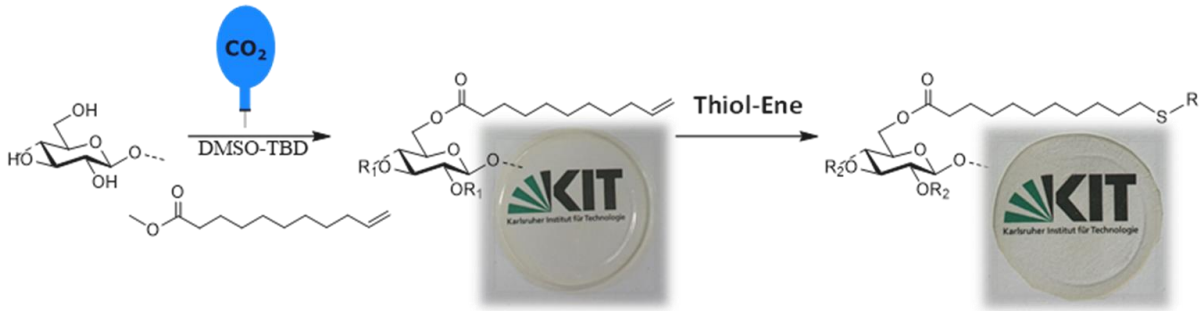

4.3.1 Introduction

Cellulose esters have received especially high interest in several application areas like membranes, films, fibers, coatings, food and pharmaceuticals.[243-244] Among the cellulose esters, fatty acid cellulose esters (FACEs) have been investigated as a sustainable and biodegradable alternative for petroleum based packaging material.[245-247] To compete, not only the final product but also the entire synthesis process should be considered as sustainable. Many studies describe the use of fatty acid chlorides under heterogenous[245-246, 248-249] and homogenous[129, 247, 250-251] conditions. However, the high amounts of waste, the necessity of acid scavengers for the hydrochloric acid byproduct, which can cause degradation to the cellulose backbone, as well as the production of the hazardous acid chlorides clearly show the need for easier and less toxic procedures.

As an alternative, the use of vinyl esters of fatty acids for the transesterification was also studied, which is more efficient and offers milder reaction conditions. Jebrane *et al.* reported a sustainable route for FACE synthesis with vinyl oleate by first activating cellulose in sodium hydroxide solution and subsequent reaction with the vinyl ester in

NMP in the presence of K_2CO_3 as a catalyst.[252] A similar approach was employed by Hauer *et al.* in the ionic liquid [EMIM][OAc], resulting an efficient synthesis of FACEs with a DS in the range of 0.9-3.0.[253] The authors also reported the recovery of the ionic liquid (~90%) improving the sustainability of the process. Recently, another promising procedure by utilizing CO_2-based switchable solvent system was published.[149] In this work, FACEs with a DS of 3 were achieved at 40 °C for 4 hours by using commercially available esters like vinyl octanoate, vinyl palmitate and vinyl laurate. However, the preparation of the vinyl esters is still a challenging issue due to the use of transition metal catalysts such as $[Ir(cod)Cl]_2$ under dry argon,[252] $AuClPPh_3/AgOAc$[254] or Ruthenium based catalysts.[255-256] Therefore, the use of methyl esters is a more practical procedure compared to others. In this regard, working groups of Meier and Barner-Kowollik reported the catalytic transesterification of cellulose using methyl esters in the ionic liquid [BMIM][Cl]/DMSO with TBD as a catalyst.[257] This procedure offered a promising alternative to the conventional esterification of cellulose due to the use of stoichiometric amount of methyl esters and recyclability of the solvent mixture. The reported DS values for the cellulose esters, on the other hand, were not as high as the abovementioned works (a maximum value of 0.69).

Utilization of the CO_2 based switchable solvent system approach was also reported using high oleic sunflower oil during transesterification.[148] The importance of this work lays in the direct use of plant oil in the transesterification without previous derivatization. The reaction was performed under milder and more sustainable conditions (115 °C for 24 h) and resulted in DS values of up to 1.59.

Thus, this chapter focus on the efficient and sustainable synthesis of FACEs with methyl 10-undecenoate in the previously reported CO_2-based switchable solvent system by investigating an improved methodology. The reaction conditions were optimized, and a detailed characterization of the synthesized products is reported. Moreover, the synthesized FACEs were modified *via* thiol-ene addition and mechanical, thermal as well as film forming and hydrophobicity properties of these products were investigated.

4.3.2 Results and discussion

Taking into account the work on sustainable transesterification of cellulose with high oleic sunflower oil[148] and the approach with vinyl esters [149] in a DBU-CO_2 switchable solvent system, the homogenous transesterification of cellulose with methyl 10-undecenoate was investigated in the first part of this work (**Scheme 23**).

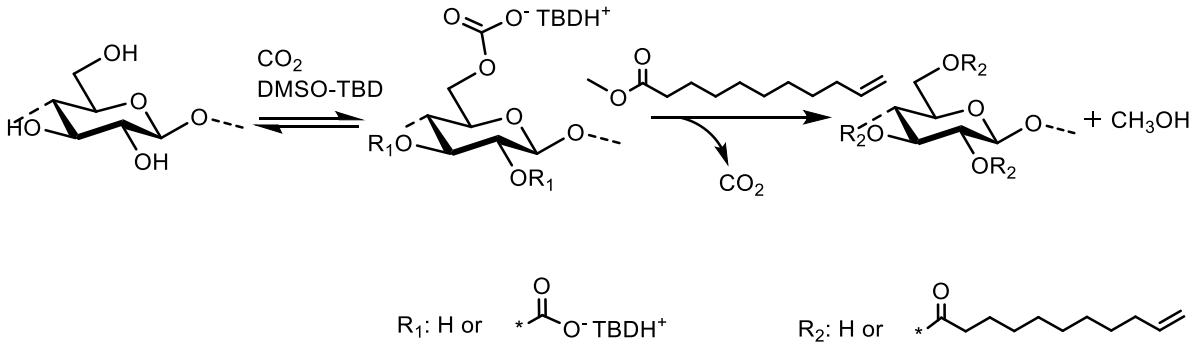

Scheme 23: Dissolution of cellulose in CO_2-based switchable solvent system and subsequent transesterification with methyl 10-undecenoate.

In the first trials, microcrystalline cellulose (MCC) was solubilized in the presence of a super base (DBU) and DMSO under CO_2 (atmospheric pressure) atmosphere according to a method initially proposed by Jerome *et al.*[140] After complete solubilization in 20 minutes, the transesterification reaction was performed by the dropwise addition of methyl 10-undecenoate at 95 °C for 6 hours. As reported in the work of Meier and Barner-Kowollik, transesterification of cellulose using methyl esters was driven by the removal of the methanol.[257] Thus, each reaction was conducted under continuous air flow after complete addition of the methyl ester.

First evidence for the formation of FACE structure was obtained *via* IR spectroscopy (**Figure 25**). After the transesterification, a new C=O stretching vibration at 1740 cm^{-1}, C-O vibration at 1169 cm^{-1} and C-H stretching bands of CH_3 and CH_2 at 2925-2855 cm^{-1} became visible. Additionally, appearance of two significant peaks at 3077 and 1640 cm^{-1} was observed, which are attributed to the =C-H and C=C stretching vibrations, respectively. Moreover, a decrease in the intensity of O-H stretching band of native cellulose around 3300 cm^{-1} confirmed the successful modification of cellulose. However, the intensities of the abovementioned vibrations

were significantly low, indicating a poor functionalization. Therefore, TBD, which is known to be a more efficient catalyst for transesterification reactions than DBU, was tested with the same reaction conditions. Different from previous works,[148-149] TBD revealed higher conversion than DBU. Thus, TBD was used for the reaction optimization studies, while other parameters (cellulose concentration, ester equivalent, reaction temperature and time) were investigated by monitoring the characteristic ester carbonyl absorbance band (1740 cm^{-1}) *via* IR spectroscopy (**Figure 25**). All the IR spectra were normalized to the C-O absorption of the glucopyranose of cellulose (around 1050-1020 cm^{-1}), which is not affected during the modification.

Initially, the effect of cellulose concentration was investigated using 4, 5 and 6 wt% at 95 °C for 6 hours with 6 equivalents of methyl ester per AGU. As IR spectra showed, the 5 wt% sample had the highest C=O absorbance intensity. The 6 wt% sample was highly viscous, leading to a lower conversion if compared to the 5 wt% solution. Afterwards, a higher temperature (115 °C) was tested, again using 6 eq of methyl ester/AGU and 5 wt% cellulose concentration for 6 hours. The results showed slightly higher conversion for the reaction at 95 °C than the one at 115 °C, which is better in the view of energy consumption.

Another important parameter to investigate was the effect of the methyl ester equivalents. Using the optimal conditions from previous trials (95 °C and 5 wt% MCC), methyl ester equivalents were varied from 3 to 9 (per AGU) in 6 hours reactions. As expected, 3 equivalents showed considerably lower functionalization than the others and 9 equivalents showed the highest C=O absorbance intensity between others, but the difference was small compared to 6 equivalents. Additionally, the optimal reaction time was investigated. Even after 3 hours, a pronounced increase in the conversion was observed, while the highest conversion was achieved after 6 hours. A slight decrease in the conversion after 24 hours indicates a possible degradation of the cellulose backbone due to the long reaction time. Finally, the addition rate of the methyl ester into the reaction mixture was observed as an important parameter while a gel formation, subsequently lower substitution, was observed when it was not added

dropwise. Overall, FACEs with different degree of substitutions (DS) were obtained by simply varying the reaction parameters such as ester equivalents, cellulose concentration, reaction time and temperature.

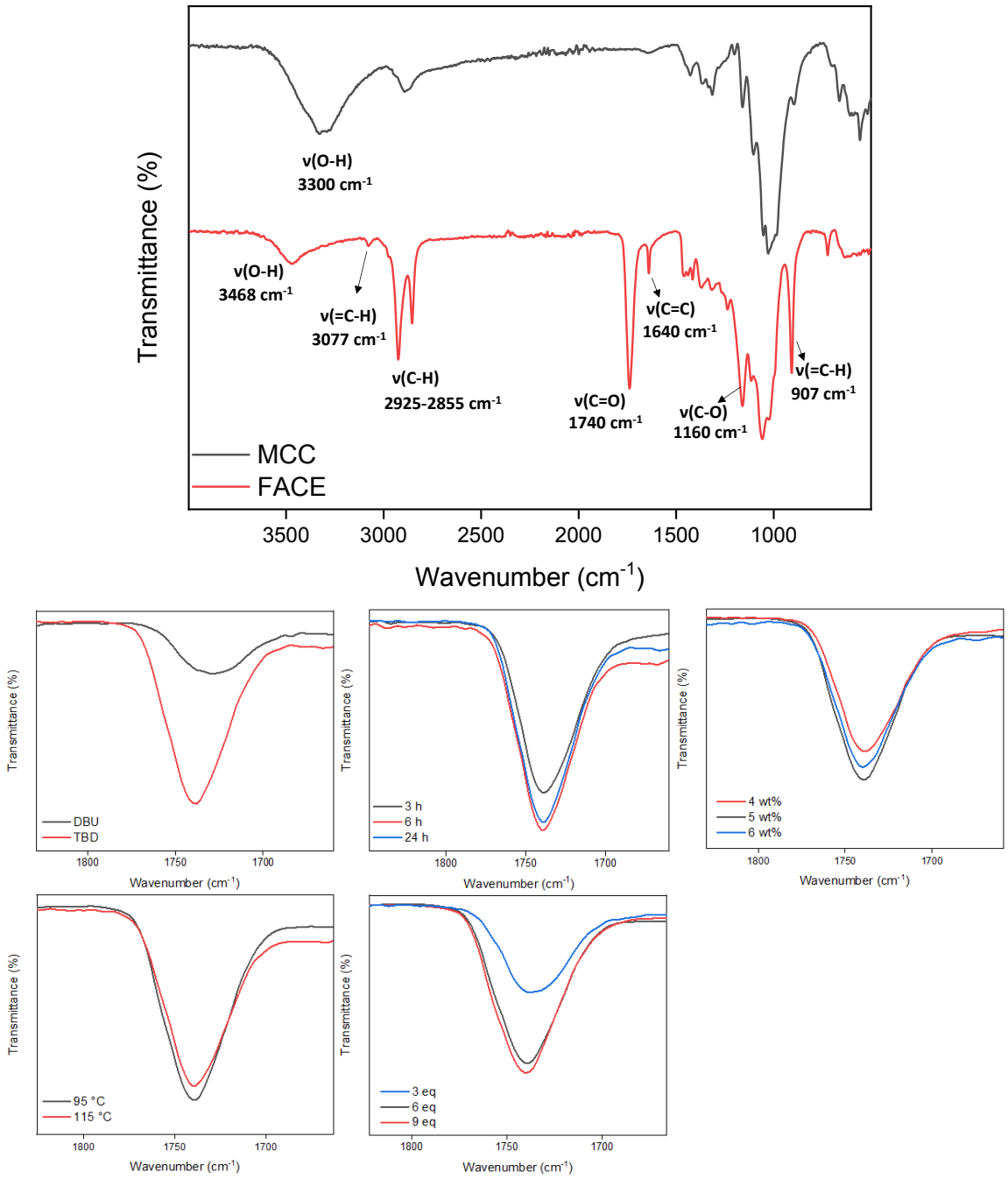

Figure 25: ATR-IR spectra (top) of microcrystalline cellulose (MCC) and FACE. ATR-IR spectra (bottom) of carbonyl intensities of FACEs synthesized with different reaction parameters (spectra were normalized to the intensity of the C-O stretching vibrations of the pyranose unit at 1050-1025 cm^{-1}).

A more detailed characterization of the FACE was performed *via* ^{1}H and ^{13}C NMR spectroscopy (**Figure 26**). As ^{1}H NMR showed, the region between 5.67 and 3.01 ppm is attributed to the protons of the cellulose backbone and the chemical shifts belonging to the terminal double bond protons became visible at 5.77 and 4.95 ppm, together with the adjacent methylene group at 1.99 ppm. Additionally, the signal at 1.24 ppm can be attributed to the alkyl chain can of the fatty acid moiety. Similarly, ^{13}C NMR showed the characteristic signals like the carbonyl group of the ester at 172.01 ppm and the carbon atoms of the terminal double bond at 138.28 and 113.86 ppm.

The degree of substitution (DS) of the synthesized FACEs were determined *via* the literature known methodology based on ^{31}P NMR spectroscopy.[227] The unreacted hydroxyl groups of the cellulose backbone are reacted with the phosphorylating agent, giving a broad peak between 149 and 145 ppm in the ^{31}P NMR. The ratio of the integration of the mentioned signal to the internal standard at 151.30 ppm was used in the equation according to the above-mentioned procedure. These measurements revealed DS values between 0.70 and 1.97 for the FACE samples, depending on the reaction parameters (**Figure 61** and **Figure 62**). The DS of 1.97 was the maximum DS that could be achieved by the described synthesis procedure.

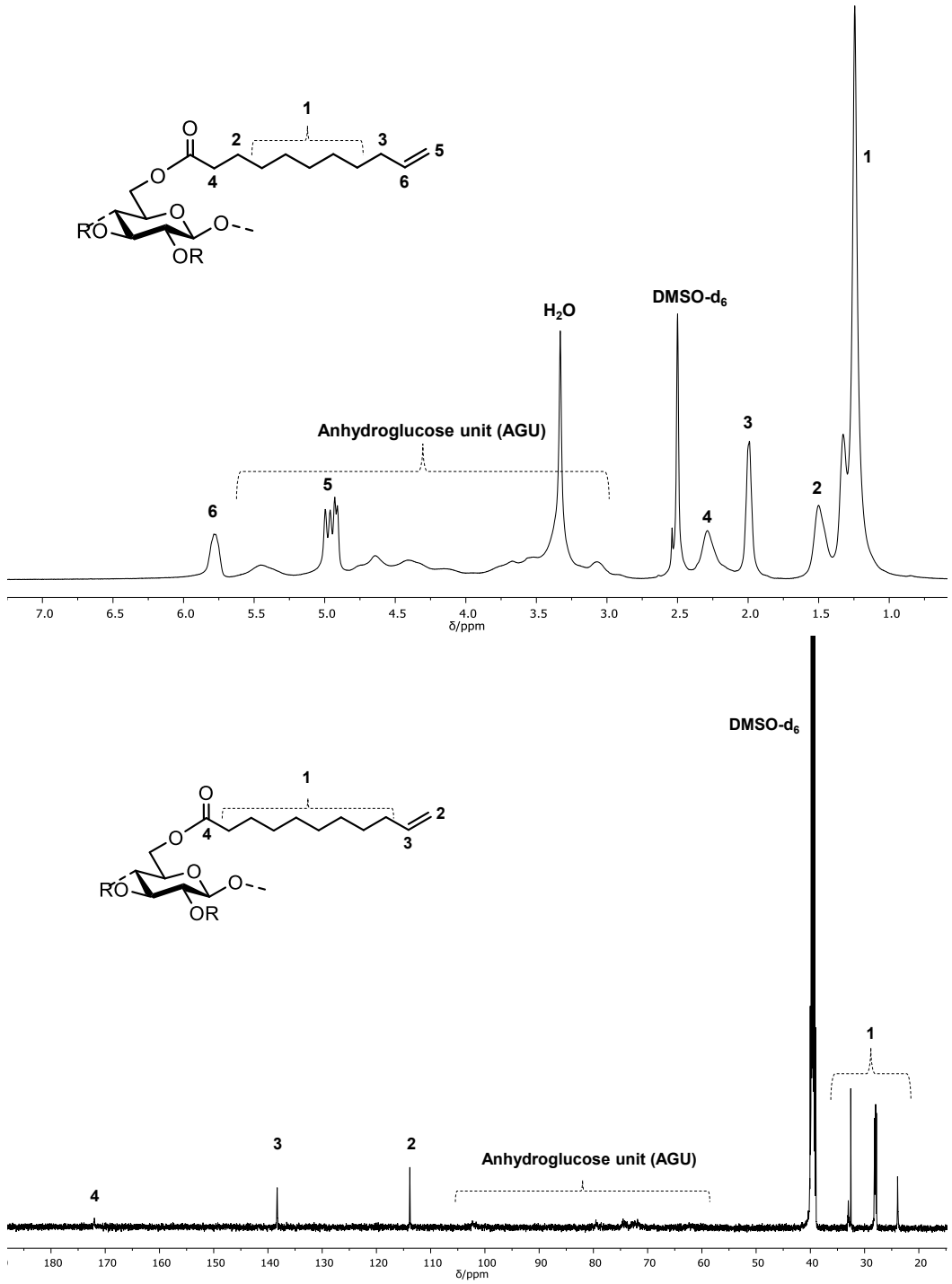

Figure 26: ^{1}H (top) and ^{13}C (bottom) NMR spectra of FACE.

Table 8: Molecular and thermal characterization data of the synthesized products.

Sample	Thiol	M_n[a] (kDa)	M_w[a] (kDa)	$Đ$[a]	Yield[b] (%)	$T_{d,5\%}$[c] (°C)
FACE (DS: 1.97)	-	84	348	4.2	66	225
FACE (DS: 0.70)	-	77	283	3.7	79	234
FACE-TE1	1-butane	86	266	3.1	68	255
FACE-TE2	*tert*-butyl	92	432	4.7	76	270
FACE-TE3	1-hexane	97	327	3.4	84	251
FACE-TE4	cyclohexane	93	351	3.8	76	259
FACE-TE5	β-pinene mercaptan	89	398	4.4	78	254
FACE-TE6	camphene mercaptan	84	314	3.8	71	257
FACE-TE1.Ox	1-butane (sulfone)	84	260	3.5	81	257
FACE-TE3.Ox	1-hexane (sulfone)	92	271	3.0	85	260

[a]SEC in HFIP +0.1 wt% potassium trifluoroacetate (KTFA). [b]Yields were determined taking DS values into consideration. [c]Calculated from thermogravimetric analysis (TGA).

Molecular weight distributions of the FACE products were analyzed *via* size exclusion chromatography (SEC). Because only the samples with high DS values (above ~1.4) were soluble in THF, SEC with hexafluoroisopropanol (HFIP) +0.1 wt% potassium trifluoroacetate (KTFA) as an eluent was used to obtain comparable results (**Figure 27**). Analysis revealed that the FACE with a DS of 1.97 had a M_n value of 84 kDa and M_w of 348 kDa with a dispersity ($Đ$) of 4.2. The FACE with a DS of 0.70 showed lower values with a M_n of 77 kDa and a M_w value of 283 kDa with a $Đ$ of 3.7 (**Table 8**). Furthermore, thermal stability of the samples was determined by thermogravimetric analysis (TGA). Both FACEs showed a single major degradation step with $T_{d,5\%}$ at 225-234 °C, which was lower than for native MCC (305 °C) (**Figure 30**).

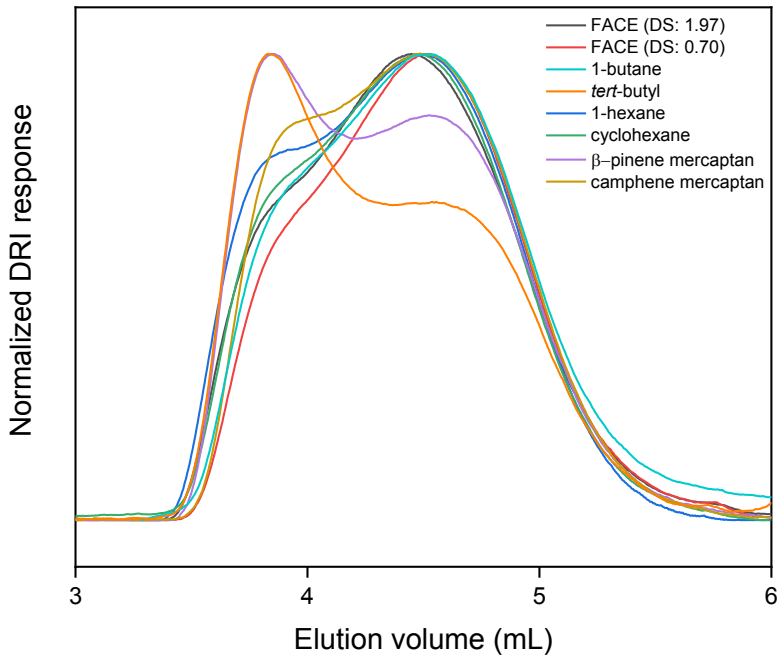

Figure 27: SEC traces of FACEs and **FACE-TE1-6**.

As reported before, increase in the DS of FACEs cause a decrease on the Young's modulus (*E*), which was explained by reduced hydrogen bonding between hydroxyl groups on cellulose backbone.[148, 258] For the same reason, the elongation value (%) was higher for the higher DS samples due to the higher amount of aliphatic chains attached to the backbone, which increased the flexibility of the latter product. Therefore, in the second part of this work, the FACE sample with a lower DS value was chosen for further thiol-ene modification in order to investigate the effect of the attached thioether group on the final products' physical properties.

Thus, 6 different thiols (1-butane thiol, *tert*-butyl thiol, 1-hexane thiol, cyclohexane thiol, mercaptopinene and mercaptocamphene) were used for a thiol-ene modification of the FACE with a DS of 0.70. β-Pinene mercaptan and camphene mercaptan were synthesized according to previously reported procedures to demonstrate the possibility to obtain fully renewable materials.[259-260] Reactions were performed under homogenous conditions in DMSO under 365 nm of ultraviolet light (UV) in the presence of 2.2-dimethoxy-2-phenyl acetophenone (DMPA, 5 mol %) at room temperature (**Scheme 24**). Preliminary trials showed complete consumption of the double bonds *via* IR spectroscopy. However, products were not soluble in any of the

NMR solvents to confirm the final structure. This may be explained by side reactions occurring during radical reactions in the presence of oxygen, which probably resulted in crosslinking.[261] Thus, before every thiol-ene modification, reaction mixtures were degassed for 3-5 minutes and reactions were conducted in a closed system. By using improved system, consumption of the double bonds after modification was first monitored *via* IR spectroscopy by the disappearance of the =C-H and C=C stretching vibrations at 3077 and 1640 cm^{-1}, respectively (**Figure 28**). Further confirmation of the successful modification was obtained *via* ^1H NMR spectroscopy by the disappearance of the two significant signals at 5.77 and 4.96 ppm. As an example, **FACE-TE1** showed new signals for methylene groups adjacent to the sulfur atom at 2.44 ppm and the methyl group at 0.85 ppm (**Figure 29**). To assist with the interpretation of the spectra, a model compound was prepared by the thiol-ene modification of methyl 10-undecenoate with 1-butanethiol and characterized by ^1H NMR spectroscopy (**Figure 81**).

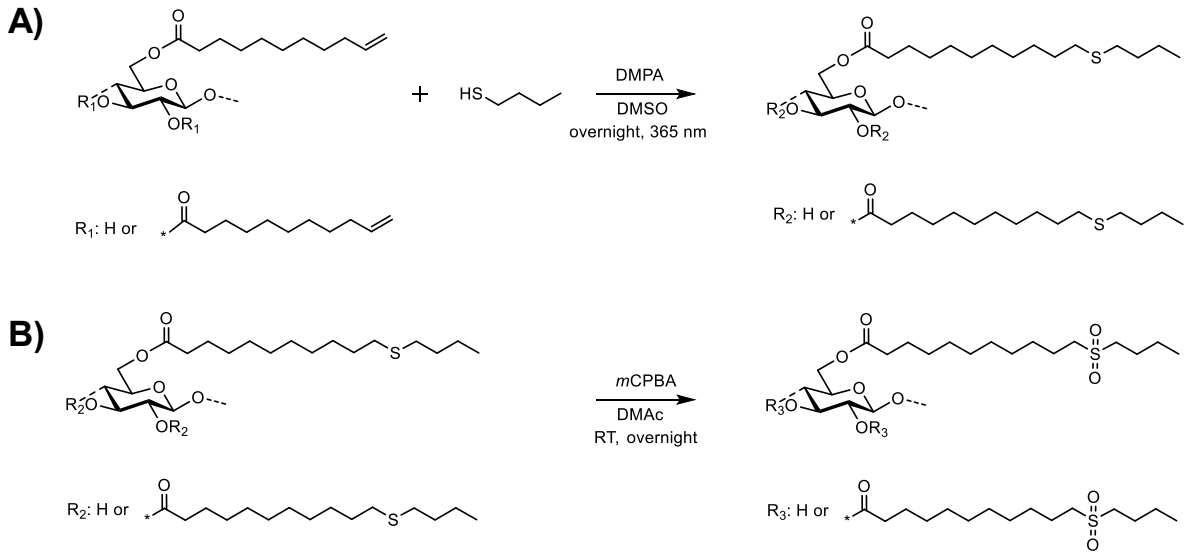

Scheme 24: A) Thiol-ene modification of FACE (**FACE-TE1** as an example). **B)** Oxidation of thiol-ene modified FACE (**FACE-TE1.Ox** as an example).

Additionally, two of the thiol-ene modified FACE samples (**FACE-TE1** and **FACE-TE3**) were chosen for a further modification with *m*CPBA in order to oxidize the sulfide to its corresponding sulfone (**Scheme 24**).[262-263] The aim of this modification was to investigate the effect of sulfone moiety on to the final product properties. Before

*m*CPBA, hydrogen peroxide (H_2O_2) was also tested as a greener alternative; however, oxidation of the cellulose hydroxyls was observed. The reactions were run overnight in DMAc and the successful modification was confirmed by IR spectroscopy after purification. Both samples showed characteristic sulfone absorptions at 1279 and 1125 cm^{-1} (**Figure 28**).

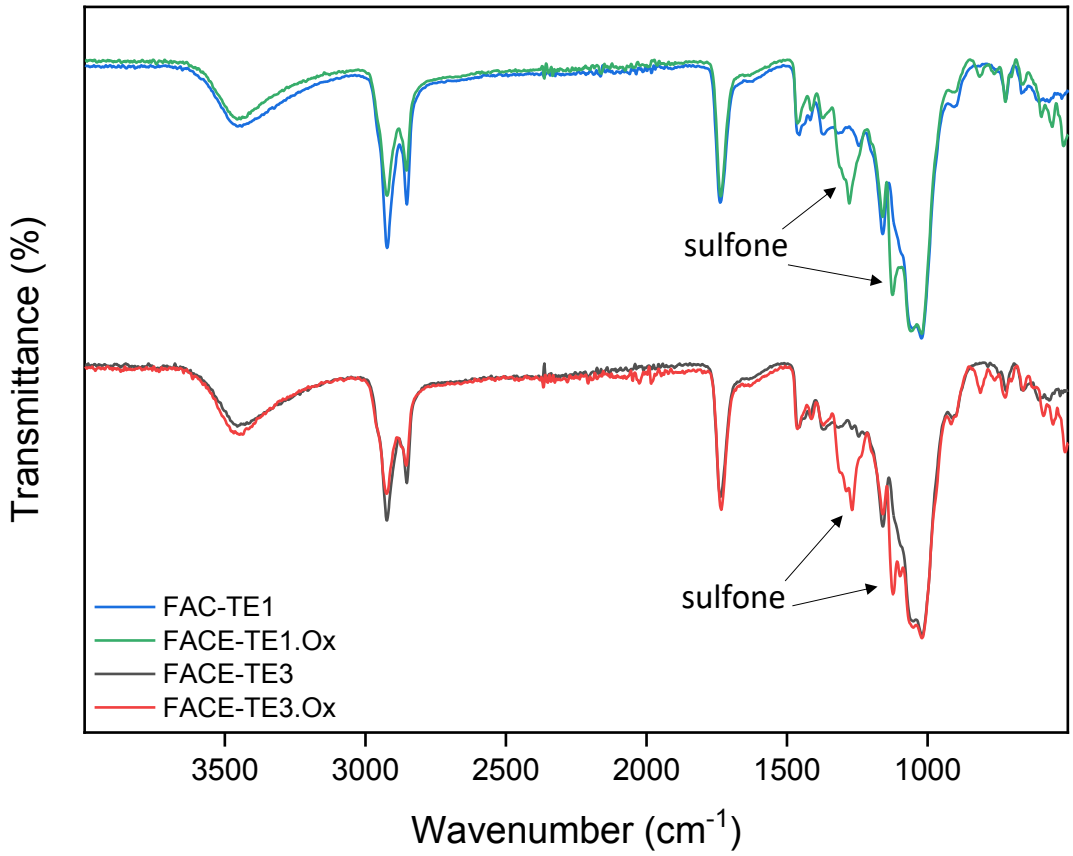

Figure 28: ATR-IR spectra of **FACE-TE1**, **FACE-TE1.Ox**, **FACE-TE3** and **FACE-TE3.Ox**.

Furthermore, ^{1}H NMR spectroscopy also proved the sulfone formation by the shift of the signal for methylene groups adjacent to the sulfur atom towards lower field, at 3.04 ppm (**Figure 29**). A COSY spectrum also showed no coupling at ~2.45 ppm, at which the methylene group of the thiol-ene product was overlapping with the solvent signal (DMSO-d_6), confirming the full conversion of the sulfide to sulfone (**Figure 72**). An additional model compound was also synthetized by the oxidation of the thiol-ene model compound and characterized *via* ^{1}H NMR to support the interpretation (**Figure 82**).

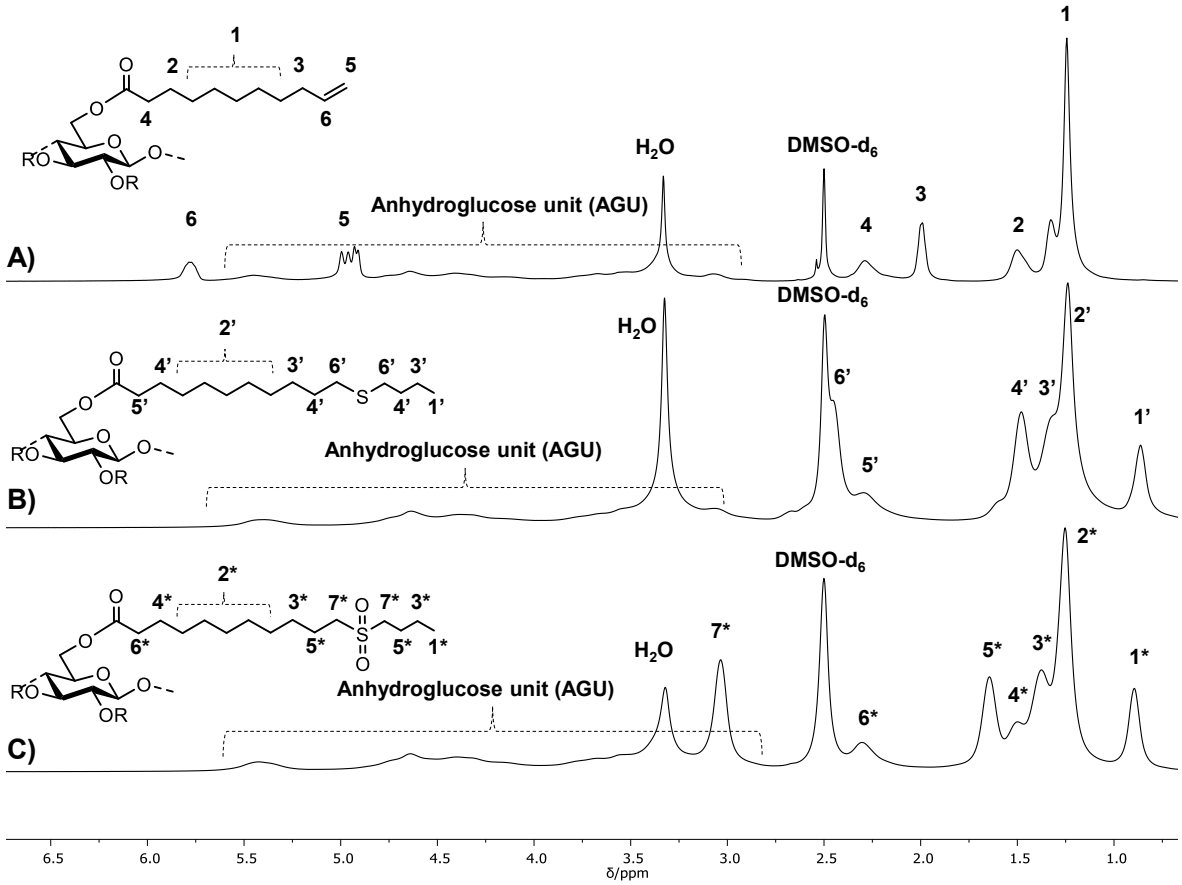

Figure 29: ^{1}H NMR spectra of **A)** FACE, **B)** FACE-TE1 and **C)** FACE-TE1.Ox.

After detailed characterization of the products, SEC was employed to compare the molecular weights of the products (**Figure 27** and **Figure 75**). All products showed higher molecular weights than the former FACE (DS: 0.7). M_n values of 84-97 kDa and M_w values of 260-432 kDa were observed with a dispersity ($Đ$) varying between 3.0 and 4.7 (**Table 8**). Since the exclusion limit of the used SEC columns is at ~3.7 mL (elution volume), separation was unfortunately no longer observed for high molecular weight species. Other SEC systems, *i.e.* using THF as an eluent, could not be used due to solubility issues. A slight decrease in the molecular weight of the **FACE-TE3.Ox** was observed compared to the former **FACE-TE3**, which can be explained by its different behavior in the eluent due to the polarity change on the side chains. Furthermore, TGA analysis showed that thiol-ene modification increased the thermal stability of the former FACE by 17-36 °C (**Figure 30**). Even though the oxidation

process did not have an impact on the $T_{d,5\%}$ values, their thermal stabilities at higher temperatures (after 325 °C) were improved significantly.

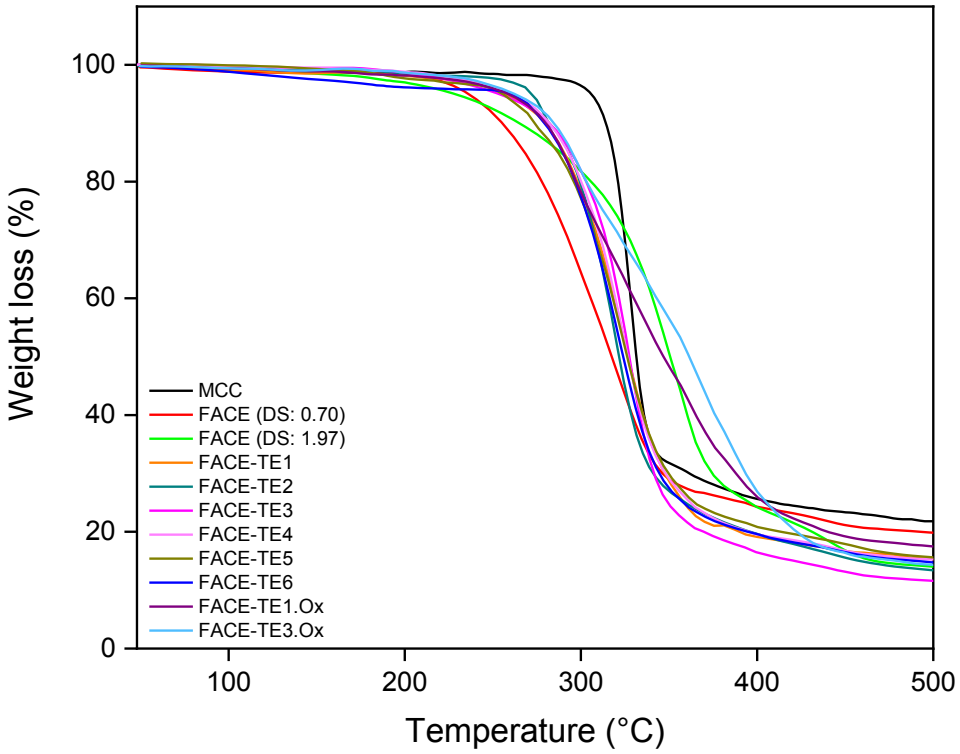

Figure 30: TGA analysis of the synthesized products.

Films of all samples were prepared *via* solvent casting by first dissolving the individual polymer in pyridine or THF and subsequent casting into poly(tetrafluoro ethylene) plates. Films were obtained after the evaporation of the solvent at room temperature for a minimum of 3 days and dried under vacuum at 30 °C for 6 h to ensure complete removal of the solvent. Initially, water contact angle measurements were conducted to investigate the hydrophobicity of the materials (Table 9 and Figure 76). As expected, the FACE with low DS revealed a lower water contact angle compared to the high DS one due to a smaller amount of hydrophobic fatty acid chains on the cellulose backbone (55 vs 78°). Hydrophobicity was increased noticeably compared to former FACE (DS: 0.70) after thiol-ene modification (75-91°), especially for the terpene-based thiols. Additionally**, FACE-TE1.Ox** exhibited lower water contact angle than its sulfide version (**FACE-TE1**) due to the introduction of SO_2 moiety, as expected (75 vs 86°). Surprisingly, **FACE-TE3.Ox** showed higher contact angle than its sulfide

version (**FACE-TE3**) (94 vs 82°). However, when two oxidized samples were compared with each other, similar results were also obtained in the literature.[264] It was previously explained that having longer side groups masked the sulfone moiety and decreased the water affinity of the surface, which could also be the case here. It might be worthwhile investigating with different substrates in the future.

Table 9: Water contact angle data and mechanical characterization of the synthesized products.

Sample	Water contact angle (°)	Young's modulus[a] (MPa)	Maximum stress[a] (MPa)	Elongation at break,[a] strain (%)
FACE (DS: 1.97)	78	90.58 ± 4.5	4.91 ± 0.8	23.14 ± 7.8
FACE (DS: 0.70)	55	626.02 ± 63.1	18.34 ± 3.2	7.85 ± 1.5
FACE-TE1	86	476.34 ± 88.7	16.55 ± 2.4	14.90 ± 2.7
FACE-TE2	78	661.47 ± 98.4	22.48 ± 4.4	5.84 ± 2.2
FACE-TE3	82	393.21 ± 37.2	16.25 ± 2.1	16.35 ± 1.8
FACE-TE4	75	635.2 ± 174.1	22.70 ± 1.7	14.30 ± 6.9
FACE-TE5	86	367.68 ± 56.6	16.62 ± 2.6	14.94 ± 2.1
FACE-TE6	91	395.50 ± 32.6	8.78 ± 1.3	2.46 ± 0.4
FACE-TE1.Ox	75	160.79 ± 35.6	7.35 ± 1.2	10.32 ± 1.7
FACE-TE3.Ox	94	321.73 ± 81.6	12.53 ± 3.1	12.49 ± 0.4

[a]Determined from tensile strength measurements.

After the contact angle measurements, the films were thoroughly dried and used for tensile tests. For each sample, three to four measurements were performed and the average values with their standard deviations were calculated (**Table 9**). As it was already observed before,[148, 258] FACEs with lower DS had significantly higher elastic moduli (626 *vs* 90 MPa) and maximum stress (18.34 *vs* 4.91 MPa) values than the one with higher DS, in addition with a lower elongation at break value (7.85 *vs* 23.14%). FACE (DS: 0.70) revealed a considerably higher elastic modulus and maximum stress value than other literature examples, such as cellulose oleate synthesized in homogenous media with fatty acyl chloride (100 MPa and 7 MPa),[247] cellulose laurate synthesized in LiCl/DMAc with fatty acyl chloride (47 MPa and 12 MPa),[250] and MCC transesterified with high oleic sunflower oil (375 MPa and

16 MPa).[148] Thiol-ene products (except for **FACE-TE2**), on the other hand, possess *E* values between the low and high DS FACEs. Thus, the addition and corresponding enlargement of the side group increased the flexibility (except for **FACE-TE2 and FACE-TE6**). Such mechanical properties could also be obtained by synthesizing a FACE with a DS value between 0.70 and 1.97, however, the water contact angle could then not be as high as for the thiol-ene products, thus demonstrating that the material properties in such FACEs can be finetuned both by DS and subsequent modification.

The oxidation process decreased the mechanical properties if compared to the respective sulfide products, which might be explained by the addition of the bulky polar sulfonyl groups, disturbing the orientation and interaction of the alkyl chains. It is worth mentioning that, the complexity of the structure: polar and high hydrogen bonding capable cellulose chains, nonpolar fatty acid chains, bulky and hydrogen bond acceptor sulfones and subsequent nonpolar chains, makes it difficult to interpretate the obtained results, which should be investigated in detail. In summary, FACE based materials with tunable mechanical and hydrophobicity properties as well as good thermal stability were synthesized in a sustainable and straightforward procedure.

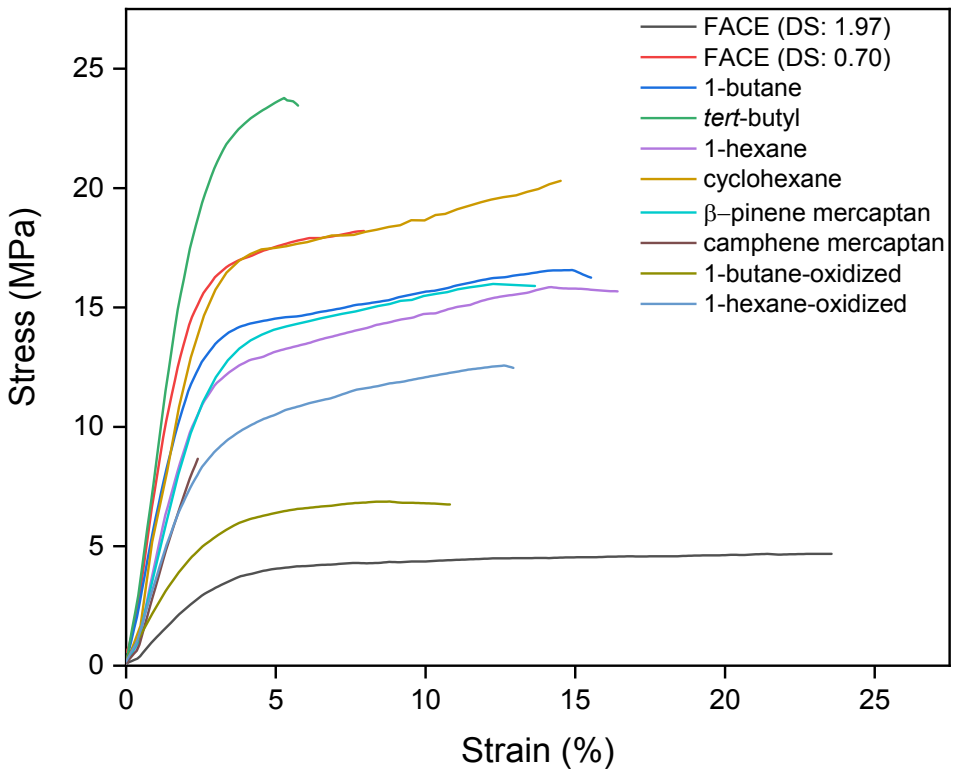

Figure 31: Tensile strength measurements of the films.

4.3.3 Conclusions

In this work, a sustainable and efficient transesterification of cellulose using methyl-10-undecenoate in a CO_2-based switchable solvent system was demonstrated. After complete dissolution of cellulose at 50 °C within 20 minutes, the transesterification reaction was performed with 9 eq methyl ester (per AGU) for 6 hours at 95 °C to reach a maximum degree of substitution (DS) of 1.97. The reported methodology did not require any additional catalyst since TBD not only took an important part in the dissolution of cellulose but also acted as a catalyst. Optimization studies showed the possibility for DS variation of the final product from 0.70 to 1.97, by simply changing reaction parameters. The use of methyl esters of fatty acid offers a more sustainable and less toxic procedure compared to previous examples, where fatty acid chlorides or the respective vinyl esters were employed to obtain cellulose esters (FACEs). Moreover, a FACE with a DS of 0.70 was modified *via* thiol-ene reaction by using 4 commercially available thiols and 2 synthesized terpene-based thiols to investigate

the effect of the thioether functionality on the final products' thermal, hydrophobicity and mechanical properties. Additionally, two of the thiol-ene modified FACEs were oxidized to sulfones for further investigations. All synthesized thiol-ene products showed good thermal stabilities ($T_{d,5\%}$: 225-270 °C) and their mechanical properties could be tuned over a broad range (elastic moduli: 90-661 MPa; elongation at break: 2-23%). Finally, by synthesizing two terpene-based thiols for the thiol-ene modification, a combination of the three major biomass-derived compounds (cellulose, fatty acid and terpene) in one material was presented.

5 Conclusion and Outlook

Within this thesis, a variety of examples of the utilization of carbohydrate-based renewable resources for the synthesis of novel polymeric materials have been described. Particularly, 2 different atom economic multicomponent reactions to modify starch and cellulose in an efficient manner have been applied, as well as the highly efficient thiol-ene addition reaction.

In a first approach, the Biginelli multicomponent reaction was employed to obtain molecularly diverse starch derivatives, which cannot be easily achieved *via* other modifications methods. Prior to the Biginelli modification, starch acetoacetates were synthesized in a straightforward procedure with tunable degree of substitution (DS) values ranging from 0.59 to 2.50. Subsequently, three renewable aromatic aldehydes (benzaldehyde, vanillin and *p*-anisaldehyde) were used in the presence of urea in a metal-free and atom-efficient fashion for the modification. The thermal stability of the products was increased by 10-15 °C compared to native starch, and their processability was investigated using glycerol as a plasticizer.

In the subsequent approach, cellulose was functionalized by first synthesizing 2,3-dialdehyde cellulose (DAC) was synthesized *via* periodate oxidation of cellulose. DAC was subsequently further modified with different aliphatic isocyanides and renewable carboxylic acids (acetic acid, 2-furoic acid and gallic acid) using the Passerini three component reaction. The reactions were performed at room temperate for 24 h and the optimization studies showed that 84% of the maximum DS was reached within 2 h. Since the modification of DAC was previously mainly achieved by imine formation, this new approach offered the possibility to obtain novel cellulose-based materials.

In the last approach, homogenous transesterification of cellulose with a castor oil-based derivative, namely methyl 10-undecenoate, was reported. As an alternative for the existing procedures, the utilization of a CO_2-based solvent system offered sustainable and mild conditions for the synthesis of fatty acid cellulose esters (FACEs) with DS values between 0.7 and 1.97. Later, an efficient post-modifications *via*

thiol-ene reaction and subsequent oxidation allowed to obtain products with a broad range of mechanical properties (*e.g.* elastic moduli: 90-661 MPa) and hydrophobicity (water contact angle of 55-94°). Since the synthesized products revealed promising results, they can for instance be investigated in detail for packaging application with a future work.

Overall, the reported procedures can be used for the production of diverse biobased materials with tunable properties by simply changing the reactants in the investigated highly atom efficient multicomponent or thiol-ene approaches. Additionally, each component can be obtained from renewable feedstocks in a sustainable fashion and depending on the desired application purposes, fully renewable products can be produced.

6 Experimental Section

6.1 Materials

All solvents were used without further purification. Water, when used in the synthesis, was deionized.

The following chemicals were used as received:

Starch (from corn, Sigma-Aldrich) vanillin (98%, Sigma-Aldrich), *p*-toluenesulfonic acid (99%, Acros Organics), *tert*-butyl acetoacetate (97%, Acros Organics), *endo*-*N*-hydroxy-5-norbornene-2,3-dicarboximide (97%, Sigma-Aldrich), potassium trifluoroacetate (KTFA, 98%, Sigma-Aldrich), 1-hexane thiol (95%, Sigma-Aldrich), 2-chloro-4,4,5,5-tetramethyl-1,3,2-dioxaphospholane (2-Cl-TMDP, 95%, Sigma-Aldrich), 1,1,1,3,3,3-Hexafluro-2-propanol (HFIP, 99%, Fluorochem), benzaldehyde (99% Fisher Scientific), *p*-anisaldehyde (99%, TCI), glycerol(99%, abcr GmbH, 99%), microcrystalline cellulose (MCC, Sigma-Aldrich), (-)-β-pinene (99%, Sigma-Aldrich), 3-chloroperbonzoic acid (mCPBA, ≤77%, Sigma-Aldrich), (+)-camphene (mixture of enantiomers, Sigma-Aldrich), cyclohexanethiol (97%, Sigma-Aldrich), 1-butanethiol (99%, Sigma-Aldrich), *tert*-butyl mercaptan (99%, Sigma-Aldrich), 2,2-dimethoxyl-2-phenylacetophenone (DMPA, 99%, Sigma-Aldrich), *N*,*N*-dimethylacetamide (DMAc, 99.8%, Sigma-Aldrich), thioacetic acid (97%, Alfa Aesar), dimethyl sulfoxide (99.7%, Acros Organics), 1,5,7-Triazabicyclo[4.4.0]dec-5-ene (TBD, ≥98%, TCI), methanol (HPLC grade, VWR chemicals), dimethyl sulfoxide-d_6 (99.8%, Eurisotop), 1,8-diazabicyclo[5.4.0]undec-7-ene (DBU, ≥98%, TCI), methanol-d_4 (99.8%, Eurisotop), chloroform-d (99.8%, Eurisotop), cyclohexyl isocyanide (97%, Sigma-Aldrich), 1-pentyl isocyanide (97%, Sigma-Aldrich), *tert*-butyl isocyanide (98%, Sigma-Aldrich), 2-furoic acid (98%, Sigma-Aldrich), sodium periodate (99%, Fisher Chemical), acetic acid (96%, Carl Roth GmbH), ethylene glycol (99.5%, Honeywell™), 10-undecenoic acid (98%, Sigma-Aldrich), gallic acid (98%, Alfa Aesar), hydroxylamine hydrochloride (99%, Acros Organics), tetrahydrofuran-d_8 (99.5%, Eurisotop) trifluoroacetic acid (TFA, 99%, Sigma-Aldrich).

6.2 Instruments

IR Spectroscopy

Infrared spectra of all samples were recorded on a Bruker Alpha-p instrument using ATR technology within the range from 4000 to 400 cm^{-1} with 24 scans.

Nuclear Magnetic Resonance Spectroscopy (NMR)

^{1}H NMR spectra were recorded using a Bruker Avance DRX spectrometer operating at 300 MHz (for modified starch samples) or 400 MHz with 128 scans and a delay time d_1 of 5 seconds at ambient temperature. Data were reported in ppm relative to DMSO-d_6 (2.5 ppm), THF-d_8 (1.73 and 3.58 ppm), D_2O (4.79 ppm), MeOD (3.31 ppm) and $CDCl_3$ (7.26 ppm), ^{13}C NMR spectra of modified cellulose and starch samples were recorded using a Bruker Avance DRX spectrometer operating at 126 MHz (for SAA and FACE samples) or 101 MHz with 30000 (for polysaccharide samples) or 1024 scans and a delay time d_1 of 5 seconds at ambient temperature. Data is reported in ppm relative to DMSO-d_6 at 39.51 ppm. All products were dissolved with a concentration of 40-60 mg mL^{-1}. Correlated spectroscopy (COSY) was carried out when detailed characterization is needed.

^{31}P NMR Method for DS determination

Degree of substitutions (DS) were determined by ^{31}P NMR using a Bruker Avance DRX 400 MHz spectrometer with 1024 scans, a delay time d_1 of 5 seconds and a spectral width of 90 ppm (190−100 ppm). Samples were prepared according to the following procedure: an exact amount of 25 mg of a sample was weighted and dissolved in 0.7-1 mL of pyridine. Next, 1-1.5 mL of $CDCl_3$ were added together with 2-chloro-4,4,5,5-tetramethyl-1,3,2-dioxaphospholane (2-Cl-TMDP, 100 µl, 0.63 mmol). The solution was allowed to homogenize after which the internal standard, endo-N-hydroxy-5-norbornene-2,3-dicarboximide (150 µL, 123.21 mM in Pyridine : $CDCl_3$ / 3:2, 0.0154 mmol) was added and the solution was stirred for further 30 minutes.

Size Exclusion Chromatography (SEC)

SEC measurements were performed in HFIP containing 0.1 wt% potassium trifluoroacetate (KTFA) using with a Tosoh EcoSEC HLC-8320 SEC system. The solvent flow was 0.40 mL min^{-1} at 30 °C and the concentration of the samples was 1 mg mL^{-1}. The analysis was performed on a three-column system: PSS PFG Micro precolumn (3.0 × 0.46 cm, 10000 Å), PSS PFG Micro (25.0 × 0.46 cm, 1000 Å) and PSS PFG Micro (25.0 × 0.46 cm, 100 Å). The system was calibrated with linear poly(methyl methacrylate) standards (Polymer Standard Service, M_p:102-981 kDa).

Gas chromatography (GC)

GC measurements were performed on a Bruker 430 GC instrument equipped with capillary column FactorFour™ VF-5 ms (30.0 m × 0.25 mm × 0.25 mm), using flame ionization detection (FID). The oven temperature program was: initial temperature 95 °C, heated to 200 °C with 15 °C min^{-1}, hold at 200 °C for 4 min, heated to 300 °C with 15 °C min^{-1}, hold at 300 °C for 2 min.

Thin Layer Chromatography (TLC)

Thin layer chromatography was carried out on silica gel coated aluminium foil (TLC silica gel F_{254}, Sigma-Aldrich). Compounds were visualized by staining with Seebach-solution (mixture of phosphomolybdic acid hydrate, cerium(IV) sulfate, sulfuric acid and water).

Thermogravimetric Analysis (TGA)

TGA measurements were performed using a Netzsch STA 409C instrument with Al_2O_3 as a crucible material and reference sample.

For the **Chapter 4.1** samples: The samples (15-20 mg) were heated from 25-600 °C with a heating rate of 5 K min^{-1} under nitrogen flow.

For the **Chapter 4.2** samples: The samples (15-20 mg) were heated from 25-500 °C with a heating rate of 5 K min^{-1} under nitrogen flow.

For the **Chapter 4.3** samples: The samples (15-20 mg) were heated from 25-600 °C with a heating rate of 10 K min^{-1} under nitrogen flow.

Differential Scanning Calorimetry (DSC)

DSC experiments were performed with a DSC821e (Mettler Toledo) calorimeter using 100 µl aluminum crucibles under nitrogen atmosphere.

For the **Chapter 4.1** samples: Two heating cycles of -25-175 °C with heating and cooling rates of 15 K min^{-1} were used with 30-40 mg sample for each measurement. For SBPs, heating cycles of -25-245 °C with heating and cooling rates of 15 K min^{-1} and 30 K min^{-1} for the second heating cycle were used.

For the **Chapter 4.2** samples: Two heating cycles of -50 to 185 °C with heating and cooling rates of 15 K min^{-1} and 30 K min^{-1} for the second heating cycle were used with 30-40 mg sample for each measurement.

Tensile Strength Measurement

For **Chapter 4.1** samples: Tensile strength measurements were performed by using a GABO EXPLEXOR instrument with a 150 N sensor. The initial speed was set at 0.5 mm × min^{-1} and samples were cut into 20×2 mm strips. The average value of the three individual measurements are reported.

For **Chapter 4.3** samples: Tensile strength measurements were performed by using a GABO EXPLEXOR instrument with a 25 N sensor. The initial speed was set at 0.5 mm × min^{-1} and samples were cut into 16×2 mm strips. The average value of the three to four individual measurements are reported.

Contact Angle Measurements

Contact angle measurements were performed with a DSA 25 contact angle goniometer (Krüss) using the sessile drop technique. A water droplet with a size of 5 µL was slowly added on the cast films by a micrometer syringe and contact angles of the cast films against the water droplet were measured The average value of four to five measurements was calculated for each sample with a standard deviation less than 4°.

6.3 Experimental Procedures

6.3.1 Experimental Procedures for Chapter 4.1

General Procedure for Starch Acetoacetate (SAA)

Native starch (0.25 g, 1.54 mmol) was dissolved in 6 mL DMSO at 90 °C for 30 minutes. After complete dissolution, the solution was heated at 120 °C and *tert*-butyl acetoacetate (1.53 mL, 9.24 mmol, 6.00 eq per AGU) was added dropwise under air flow. After 2 hours, the homogenous hot mixture was precipitated into 200 mL isopropanol dropwise. The crude product was filtered and washed with isopropanol. Afterwards, it was dissolved in 10 mL DMSO and reprecipitated in isopropanol. The product was filtered again and dried under vacuum at 85 °C overnight. The degree of substitution (DS) was determined as 2.50 by ^{31}P NMR. The yield was calculated from the DS value as 88%.

ATR-IR ν (cm^{-1}) = 3544-3348 ν(O-H), 1743 and 1710 ν(C=O), 1143 ν(C-O). ^{1}H NMR (300 MHz, DMSO-d$_6$) δ (ppm) = 5.78-3.10 (m, AGU, 7H), 3.61 (br, 2H), 2.18 (br, 3H). ^{13}C NMR (126 MHz, DMSO-d$_6$) δ (ppm) = 200.69, 166.68, 100.37, 95.59, 72.59, 70.08, 68.60, 62.97, 49.15, 29.62.

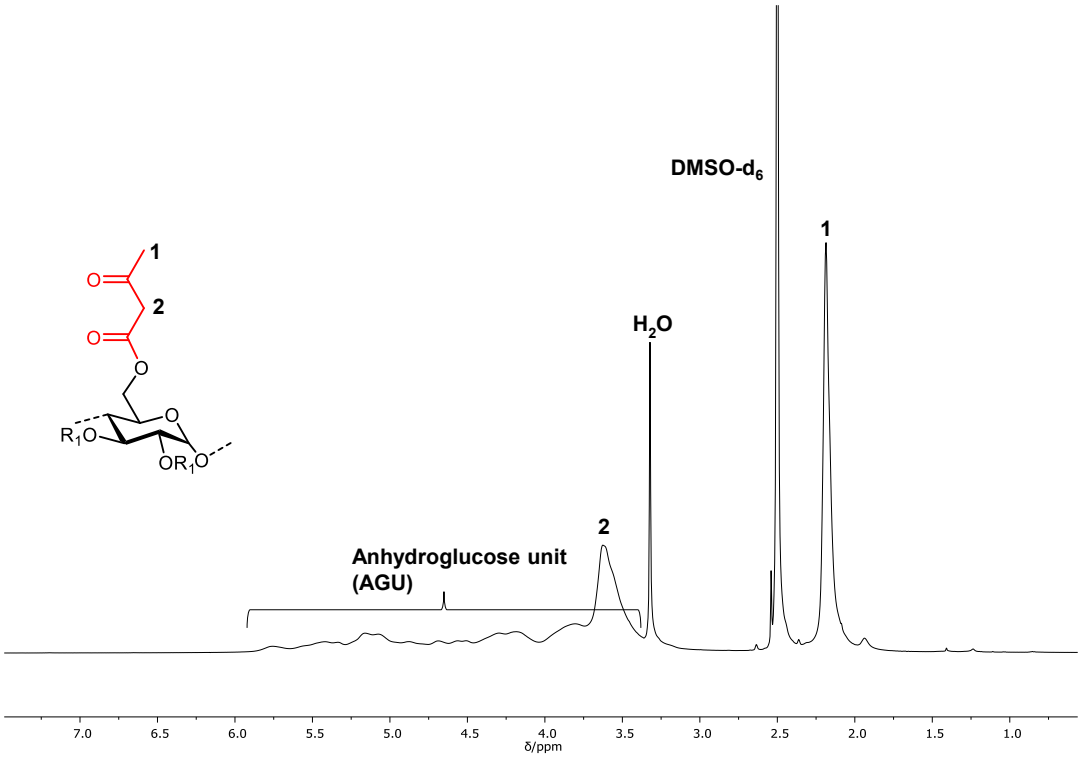

Figure 32: ^{1}H NMR of starch acetoacetate (**SAA**).

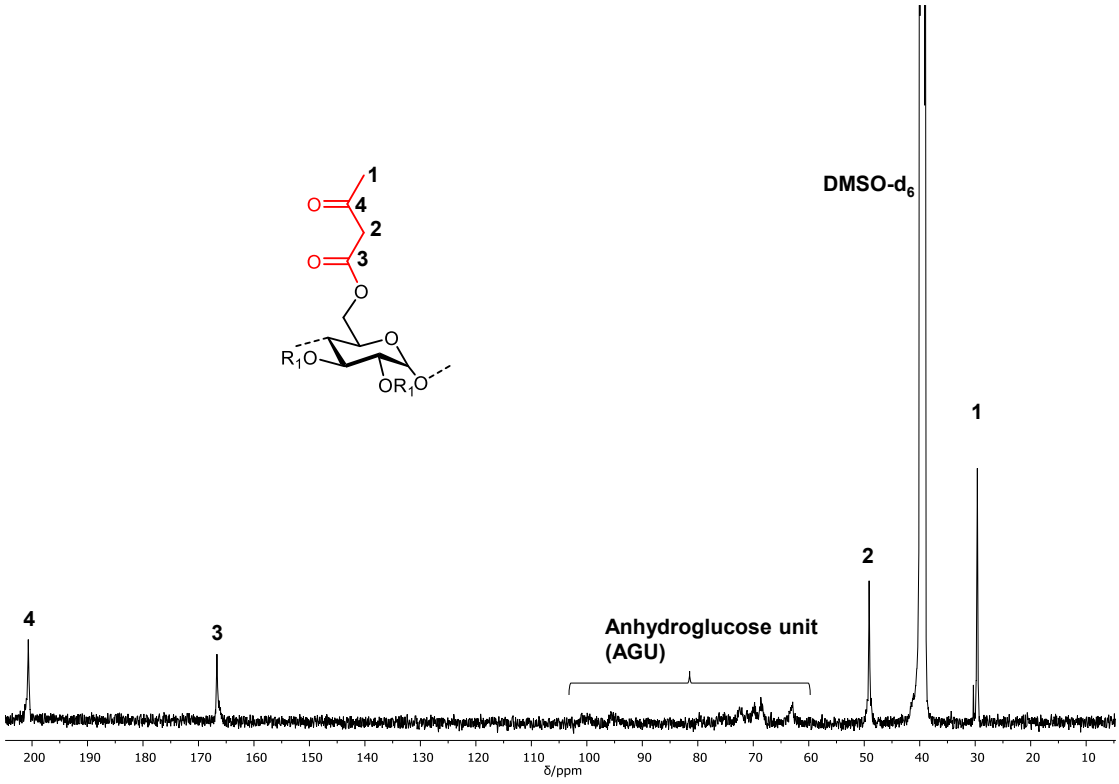

Figure 33: ^{13}C NMR of starch acetoacetate (**SAA**).

DS calculation method

DS of the **SAAs** were calculated by the following procedure of King *et al.*[227]:

$$DS_{31P} = DS_{max} \times \frac{\frac{1}{OH_S} - \frac{1}{OH_C}}{MW_S + \frac{1}{OH_S} - 1}$$

$$OH_S = \frac{IS_{mol} \times IS_{vol} \times I_R}{1000000 \times W_S}$$

MW_s: molecular weight (g/mol) of the substituents without including the oxygen atom between starch and the acetoacetate moiety.

IS_{vol}: volume of the internal standard used, mL.

IS_{mol}: mole of internal standard used, mmol.

I_R: integration ratio of remaining phosphorylated starch hydroxyl groups against the internal standard.

W_s: weight of the sample, mg.

DS_{max}: maximum DS obtainable value of 3.0 for unsubstituted starch.

OH_C: free hydroxyl groups per weight unit of starch = DS_{max} / MW_{AGU} = 3/1.162.16 = 0.01852 mol/g.

OH_S: free hydroxyl groups per weight unit of the substrate (mol/g).

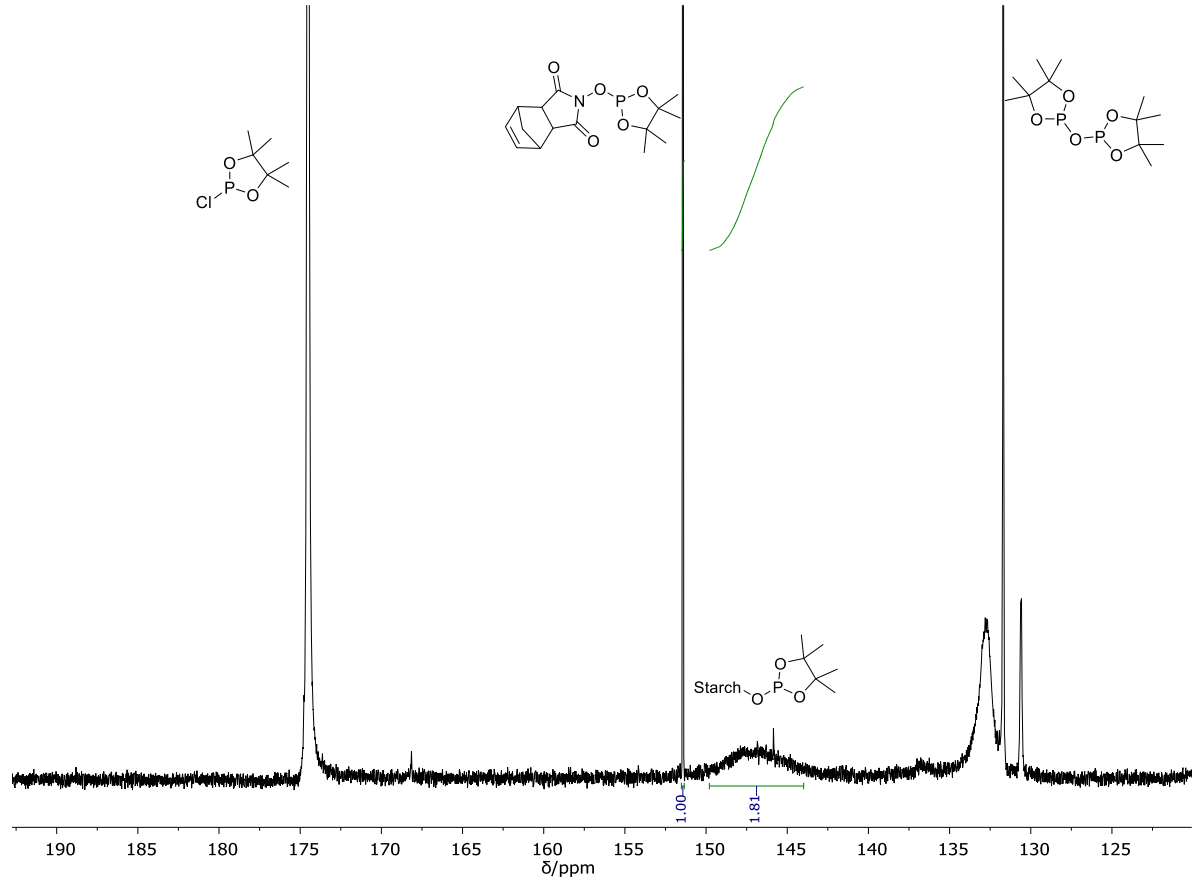

Figure 34: ^{31}P NMR spectrum of **SAA** (DS: 2.10).

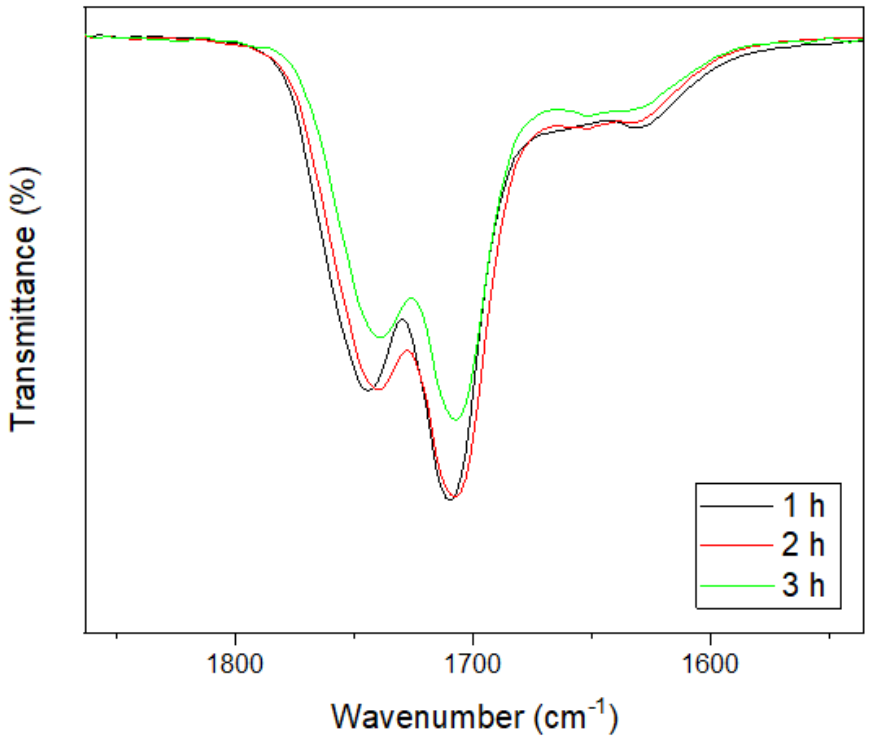

Figure 35: ATR-IR spectra of carbonyl intensities of **SAAs** with different reaction times (spectra were normalized to the intensity of the C−O stretching vibrations of the pyranose units at 1018 cm^{-1}).

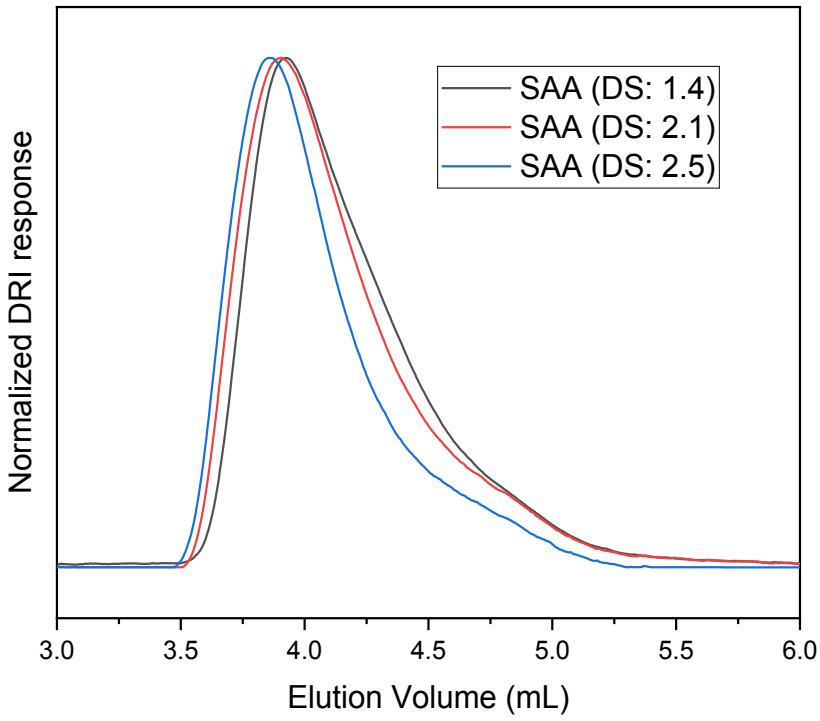

Figure 36: SEC traces of **SAA** samples with different DS values.

General procedure for the synthesis of starch Biginelli polymers (SBPs)

SAA (0.20 g, 0.54 mmol, DS: 2.50) was dissolved in 5 mL DMSO at ambient temperature. 1.75 eq (per acetoacetate group) urea (0.14 g, 2.36 mmol,), benzaldehyde (0.24 mL, 2.36 mmol) and 0.01 eq (per acetoacetate group) *p*-TSA (23.2 mg, 0.135 mmol) were added into the reaction mixture and heated to 120 °C for 12 hours. When the reaction was completed, the mixture was precipitated into cold methanol (200 mL) to obtain fine orange powders. The product was collected by centrifugation and washed several times with methanol. The purified product (**SBP1**) was dried under vacuum at 85 °C overnight. Vanillin (0.36 g, 2.36 mmol) was used for the **SBP2** and *p*-anisaldehyde (0.29 mL, 2.36 mmol) was used for the **SBP3** applying the above-mentioned procedure.

SBP1: Yield: 64% ATR-IR ν (cm^{-1}) = 3565-3044 ν(N-H) and ν(O-H), 1683 and 1634 ν(C=O), 1450 ν(C=C_{Ar}), 1222 ν(C-O) ^{1}H NMR (300 MHz, DMSO-d_6) δ (ppm) = 9.20 (br, NH), 7.69 (br, NH), 7.23 (br, CH_{Ar}), 5.83-3.20 (m, anhydroglucose units, 7H), 5.15 (br, CH), 2.30 (br, 3H).

SBP2: Yield: 60% ATR-IR ν (cm^{-1}) = 3559-3108 ν(N-H) and ν(O-H), 1684 and 1635 ν(C=O), 1453 ν(C=C_{Ar}), 1229 ν(C-O) ^{1}H NMR (300 MHz, DMSO-d_6) δ (ppm) = 8.79 (br, NH), 7.64 (br, NH), 6.81-6.68 (br, CH_{Ar}), 5.71-3.08 (m, anhydroglucose units, 7H), 5.08 (br, CH), 4.47 (br, OH), 3.71 (br, OCH_3), 2.71 (br, 3H).

SBP3: Yield: 61% ATR-IR ν (cm^{-1}) = 3522-3152 ν(N-H) and ν(O-H), 1686 and 1637 ν(C=O), 1448 ν(C=C_{Ar}), 1243 ν(C-O) ^{1}H NMR (300 MHz, DMSO-d_6) δ (ppm) = 9.15 (br, NH), 7.64 (br, NH), 7.15-6.82 (m, CH_{Ar}), 5.83-3.20 (m, anhydroglucose units, 7H), 5.10 (br, CH), 3.68 (m, OCH_3), 2.26 (br, 3H).

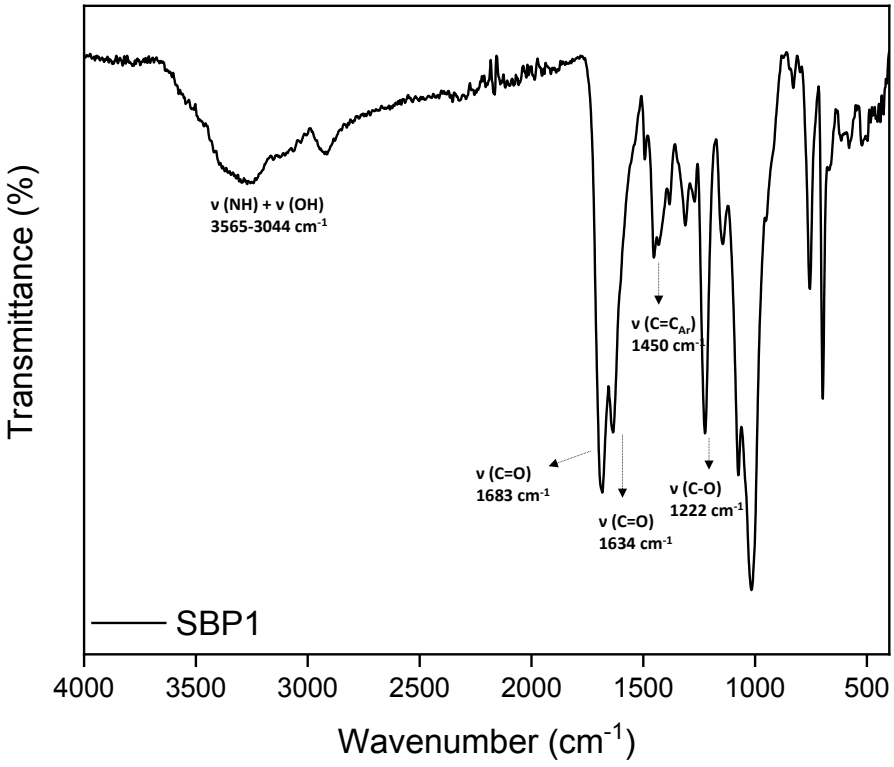

Figure 37: ATR-IR spectrum of **SBP1**.

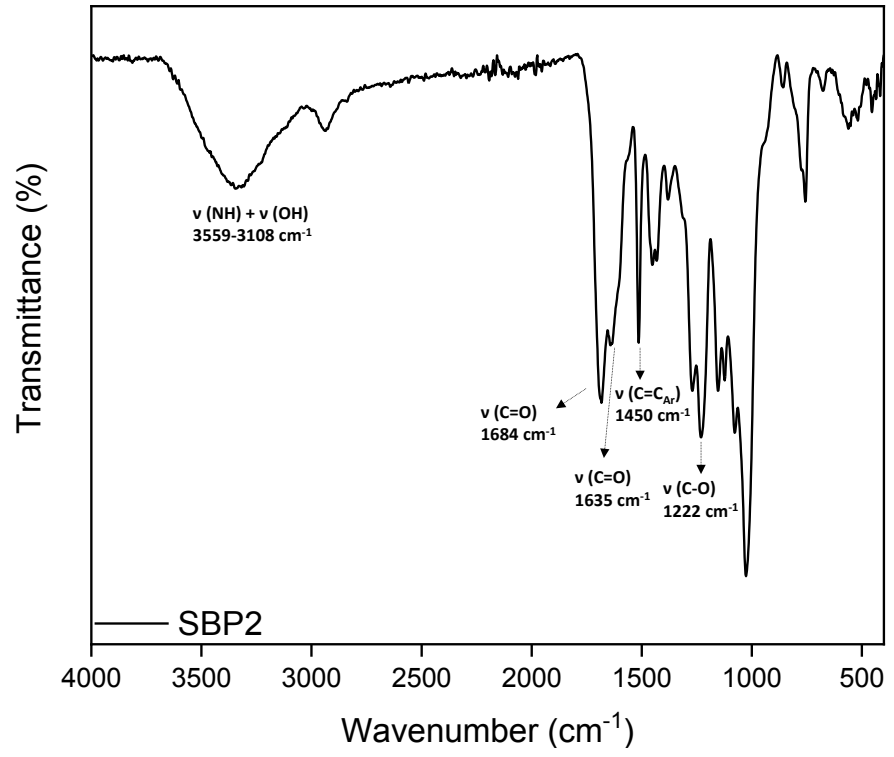

Figure 38: ATR-IR spectrum of **SBP2**.

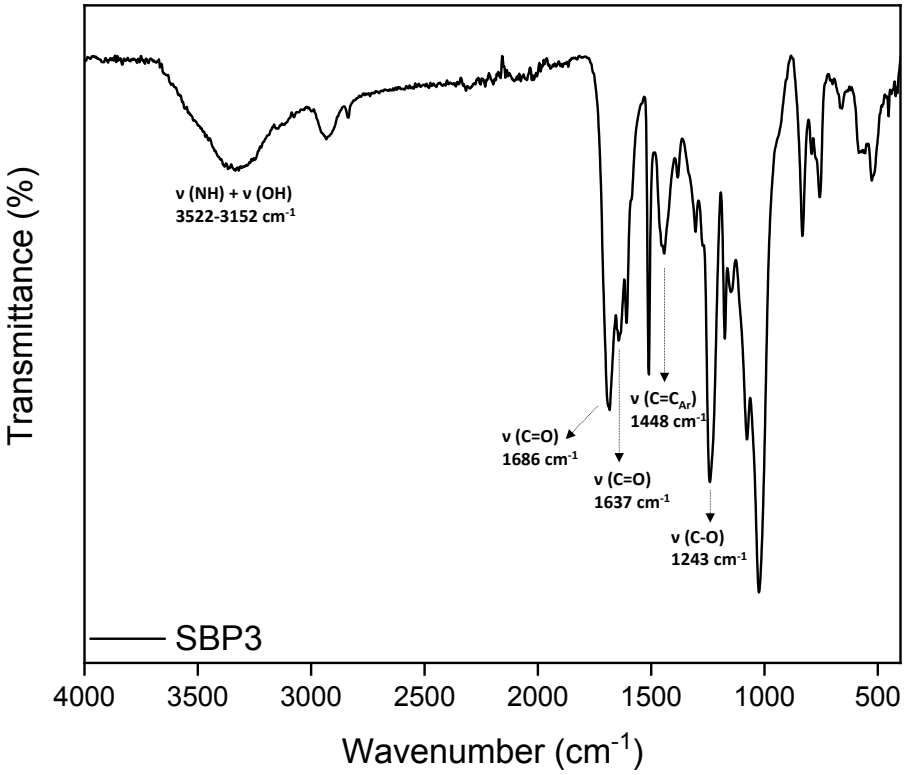

Figure 39: ATR-IR spectrum of **SBP3**.

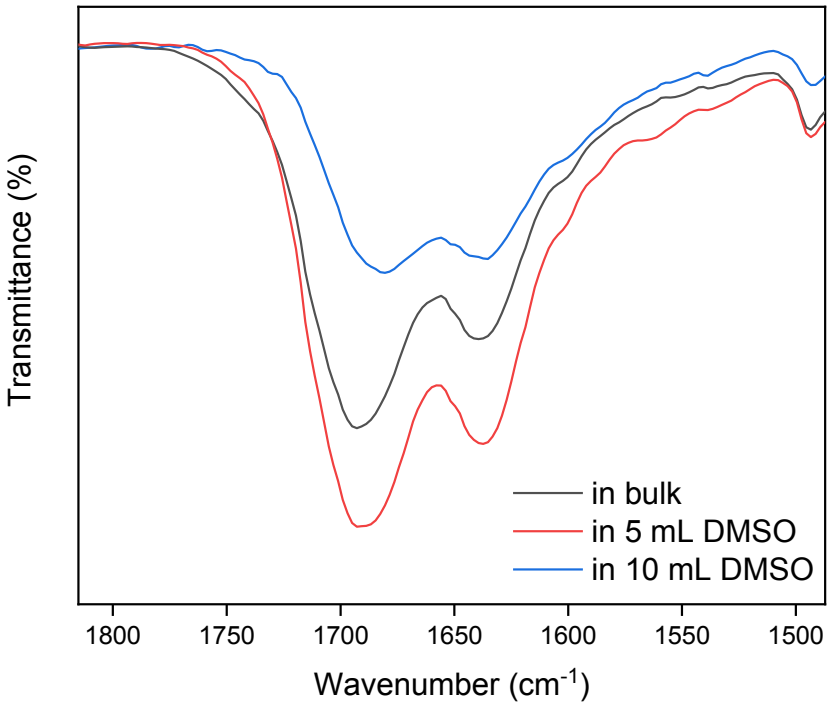

Figure 40: ATR-IR spectra of carbonyl intensities of **SBP1** with different concentrations (spectra were normalized to the intensity of the C−O stretching vibrations of the pyranose units at 1018 cm^{-1}).

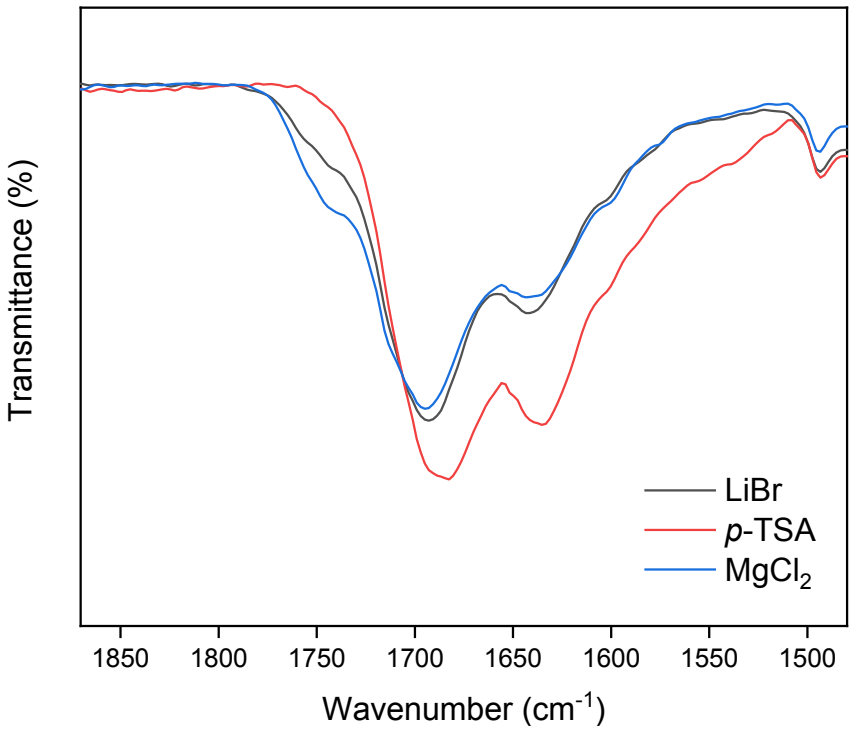

Figure 41: ATR-IR spectra of carbonyl intensities of **SBP1** synthesized with different catalysts (spectra were normalized to the intensity of the C−O stretching vibrations of the pyranose units at 1018 cm^{-1}).

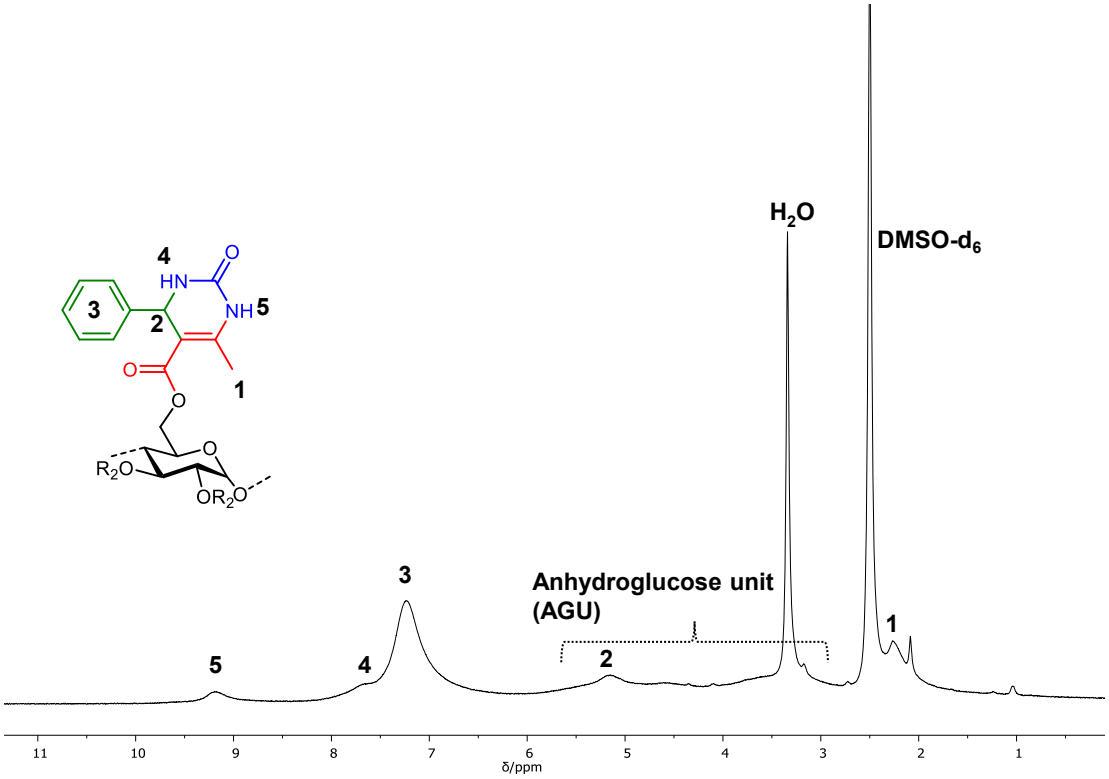

Figure 42: ^{1}H NMR spectrum of **SBP1**.

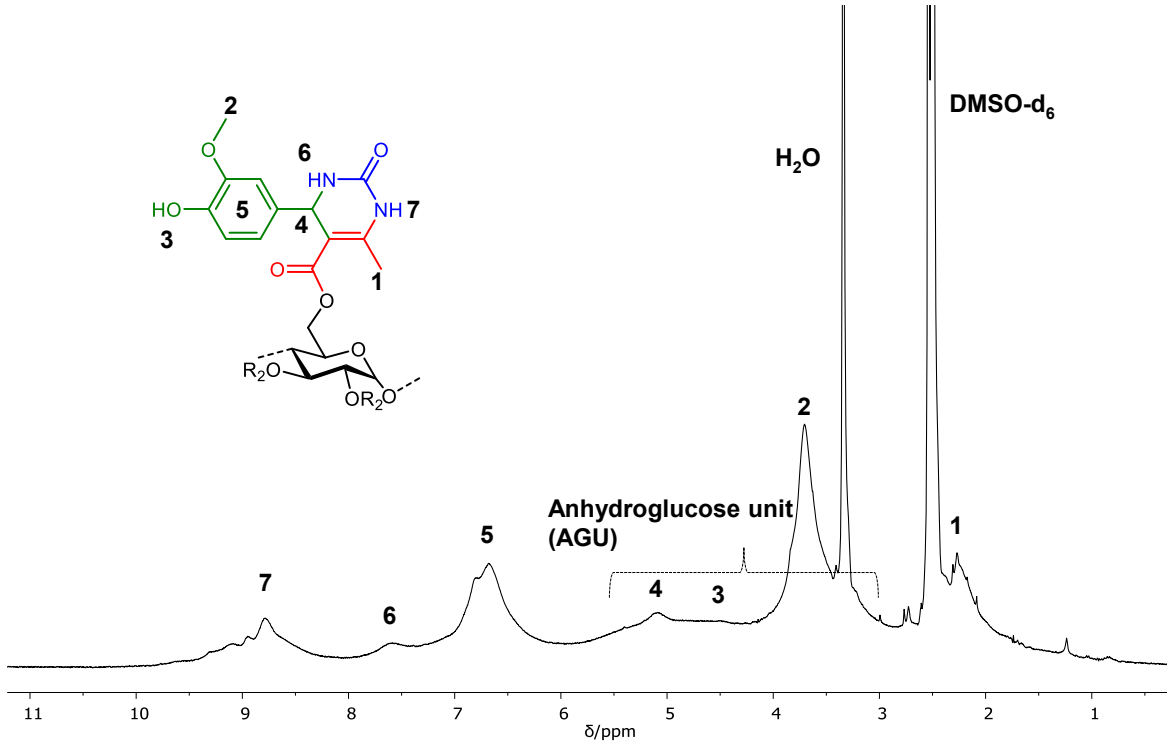

Figure 43: ^{1}H NMR spectrum of **SBP2**.

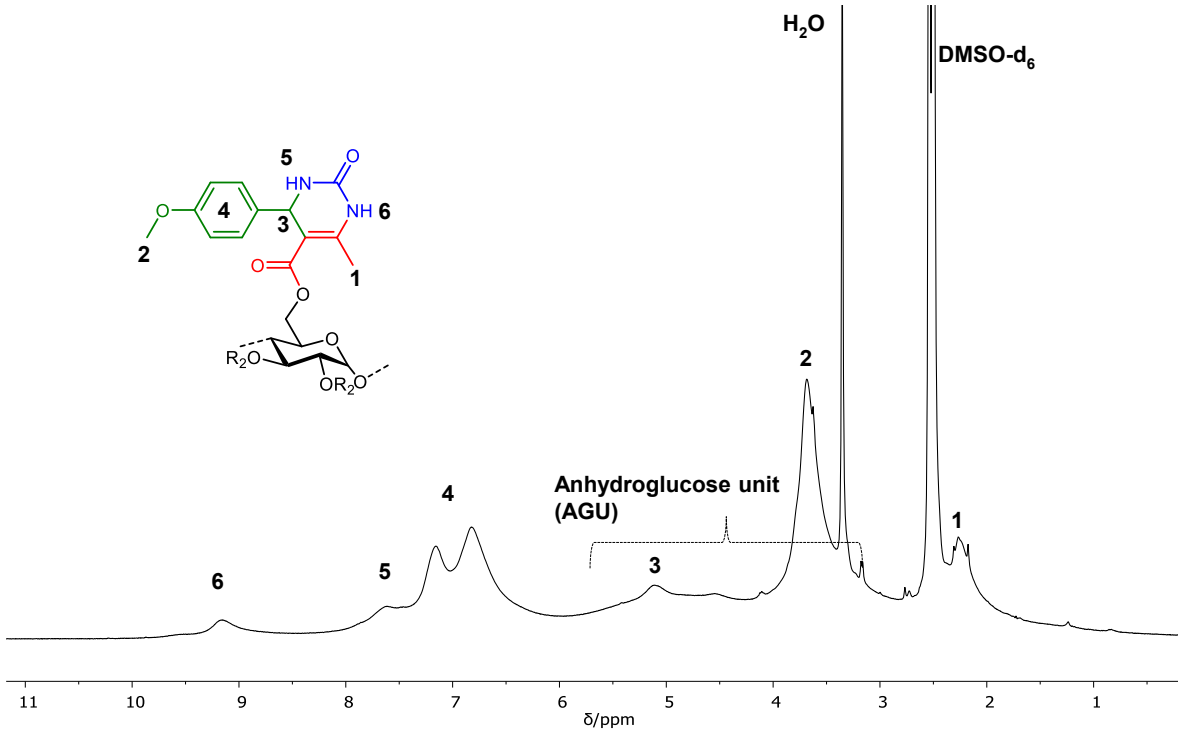

Figure 44: ^{1}H NMR spectrum of **SBP3**.

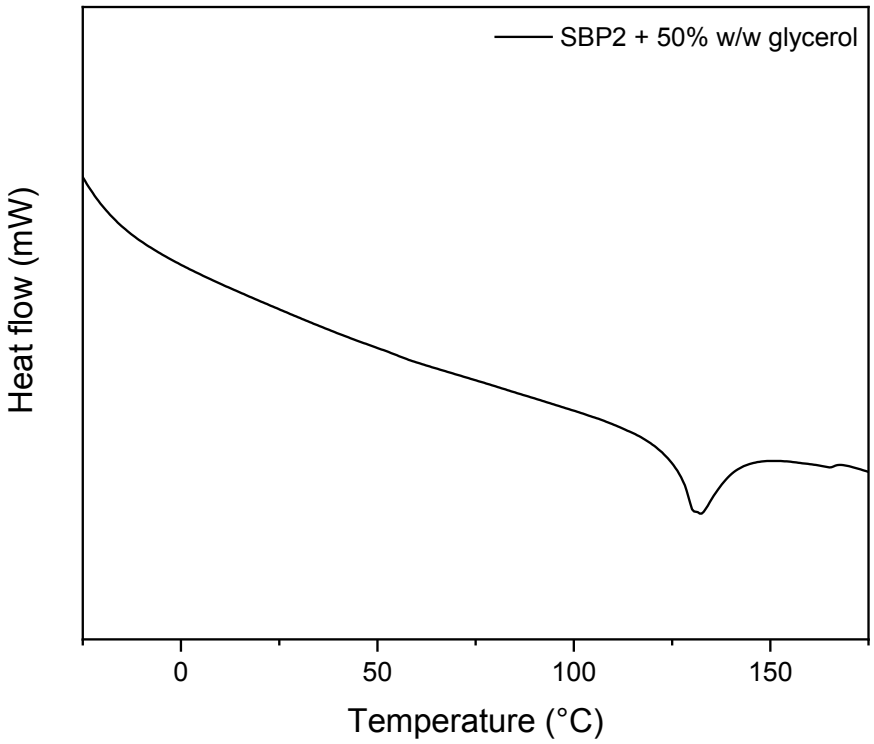

Figure 45: DSC graph of **SBP2** with 50% w/w glycerol.

6.3.2 Experimental procedures for Chapter 4.2

Periodate oxidation of cellulose

MCC (1.00 g, 6.16 mmol) was suspended in 50 mL deionized water. $NaIO_4$ (1.58 g, 7.38 mmol, 1.2 eq per anhydroglucose unit) was added into the suspension and the flask was covered with aluminum foil to prevent periodate decomposition caused by light. The oxidation reaction was performed for at 55 °C for 15 h. Afterwards, ethylene glycol (4.1 mL, 73.8 mmol) was added into the cloudy mixture to quench the unreacted $NaIO_4$. Later, the reaction mixture was precipitated dropwise into 250 mL isopropanol and subsequently filtered. The obtained white precipitate was placed in a flask and further washed with ice water to dissolve the remaining periodate and the side products. The DAC was collected *via* centrifugation from the final suspension, dried under reduced pressure and stored at 4 °C. The degree of oxidation of the DAC sample was measured by using reported methods[80, 102] *via* titration by using hydroxylamine hydrochloride. The dried DAC (0.10 g) was dissolved in 10 mL of water and the pH was adjusted to 3.50 with HCl. Then, 10 mL of hydroxylamine hydrochloride solution (5 wt%) was added and the reaction mixture was allowed to stir for 15 h. Afterwards, the mixture was titrated with 0.05 M NaOH solution until pH 3.50 was reached. Additional confirmation of the DO value was performed *via* elemental analysis by evaluating the nitrogen content of the dried oxime derivative of DAC obtained after titration.

Table 10: Elemental analysis of the DAC-oxime products after titration.

DAC-oxime	C (%)	N (%)	H (%)
1	36.80	9.55	5.33
2	37.61	9.68	5.50

General procedure for the Passerini (3-CR) of DAC

DAC (0.10 g, 0.62 mmol) was dissolved in 4 mL deionized water at 95 °C. After complete dissolution, the reaction mixture was cooled down to room temperature. Then, the carboxylic acid and isocyanide (1.52 mmol, 2.00 equivalents each, with respect to the aldehyde group, DO: 1.23) were added and the mixture was stirred for 24 hours. The product formed as a precipitate and then filtrated and washed with water several times. Thereafter, the solid was dissolved in THF (3 mL) and reprecipitated in cyclohexane (50 mL). This step was repeated 2 times to completely remove unreacted starting materials. The purified white product was then dried under vacuum at 75 °C overnight.

P1: Yield: 73% ATR-IR *v* (cm^{-1}) = 3573-3175 *v*(N-H) and *v*(O-H), 2968-2865 *v*(C-H), 1744 ester *v*(C=O), 1665 amide *v*(C=O), 1215 *v*(C-O) ^{1}H NMR (400 MHz, DMSO-d_6) *δ* (ppm) = 7.11 (br, 1H), 6.46 (br, 1H), 5.33-3.42 (m, AGU, 7H), 2.10 (br, 3H), 1.25 (br, 9H) ^{13}C NMR (126 MHz, DMSO-d_6) *δ* (ppm) = 170.07, 166.54, 51.10, 28.76, 21.06.

P2: Yield: 88% ATR-IR *v* (cm^{-1}) = 3585-3109 *v*(N-H) and *v*(O-H), 2948-2835 *v*(C-H), 1744 ester *v*(C=O), 1654 amide *v*(C=O), 1221 *v*(C-O) ^{1}H NMR (400 MHz, DMSO-d_6) *δ* (ppm) = 7.67 (br, 1H), 6.45 (br, 1H), 5.33-3.42 (m, AGU, 7H), 2.10 (br, 3H), 1.67 (br, 4H), 1.22 (br, 6H).

P3: Yield: 91% ATR-IR *v* (cm^{-1}) = 3588-3078 *v*(N-H) and *v*(O-H), 2973-2829 *v*(C-H), 1744 ester *v*(C=O), 1655 amide *v*(C=O), 1221 *v*(C-O) ^{1}H NMR (400 MHz, DMSO-d_6) *δ* (ppm) = 7.93 (br, 1H), 6.46 (br, 1H), 5.38-3.43 (m, AGU, 7H), 3.05 (br, 2H), 2.13 (br, 3H), 1.40 (br, 2H), 1.25 (br, 4H), 0.85 (br, 3H).

P4: Yield: 72% ATR-IR *v* (cm^{-1}) = 3595-3068 *v*(N-H) and *v*(O-H), 2986-2816 *v*(C-H), 1751 ester *v*(C=O), 1659 amide *v*(C=O), 1219 *v*(C-O) ^{1}H NMR (400 MHz, DMSO-d_6) *δ* (ppm) = 7.90 (br, 1H), 6.45 (br, 1H), 5.38-3.43 (m, AGU, 7H), 3.04 (br, 2H), 2.13 (br, 3H), 1.23 (br, 12H), 0.84 (br, 3H)

P5: Yield: 67% ATR-IR *v* (cm^{-1}) = 3608-3097 *v*(N-H) and *v*(O-H), 2999-2854 *v*(C-H), 1730 ester *v*(C=O), 1672 amide *v*(C=O), 1289 *v*(C-O) ^{1}H NMR (400 MHz, DMSO-d_6) *δ* (ppm) = 7.97 (br, 2H), 7.35 (br, 1H) 6.69 (br, 2H), 5.33-3.42 (m, AGU, 7H), 1.24 (br, 9H) ^{13}C NMR (126 MHz, DMSO-d_6) *δ* (ppm) = 165.95, 157.35, 148.52, 143.88, 119.62, 112.91, 88.46, 51.10, 28.72.

P6: Yield: 68% ATR-IR *v* (cm^{-1}) = 3614-3068 *v*(N-H) and *v*(O-H), 2996-2841 *v*(C-H), 1721 ester *v*(C=O), 1660 amide *v*(C=O), 1204 *v*(C-O) ^{1}H NMR (400 MHz, DMSO-d_6) *δ* (ppm) = 9.28 (br, 2H), 9.02 (br, 1H), 7.00 (br, 3H), 6.46 (br, 1H), 5.38-3.42 (m, AGU, 7H), 1.26 (br, 9H) ^{13}C NMR (126 MHz, DMSO-d_6) *δ* (ppm) = 166.19, 146.07, 139.27, 119.56, 109.58, 50.97, 28.91.

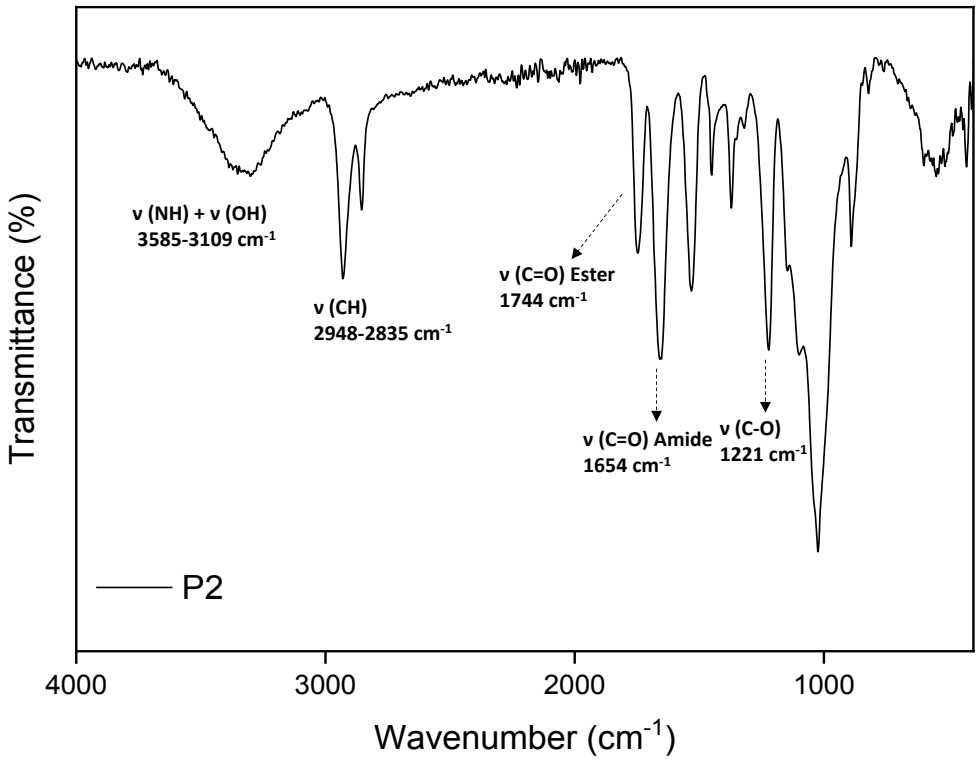

Figure 46: ATR-IR spectrum of Passerini product **P2**.

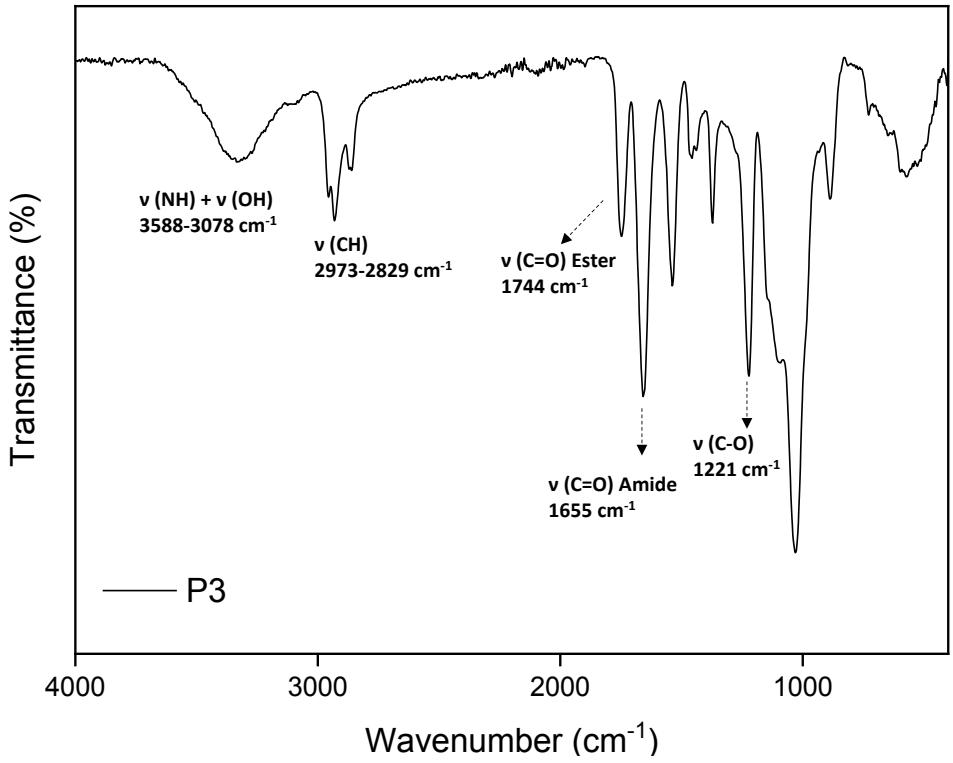

Figure 47: ATR-IR spectrum of Passerini product **P3**.

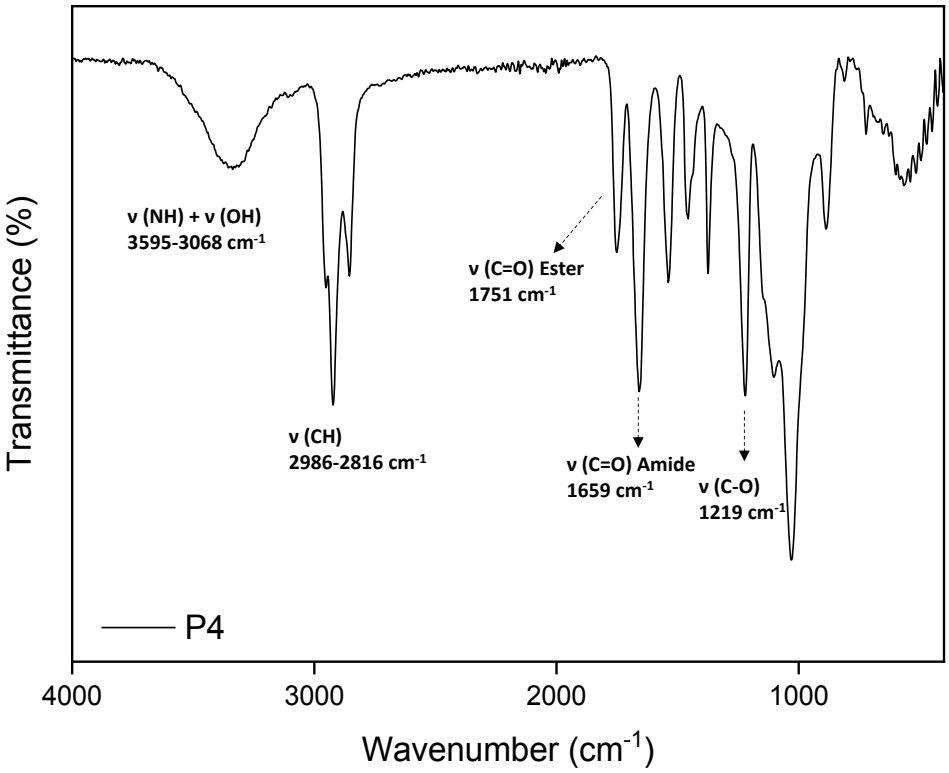

Figure 48: ATR-IR spectrum of Passerini product **P4**.

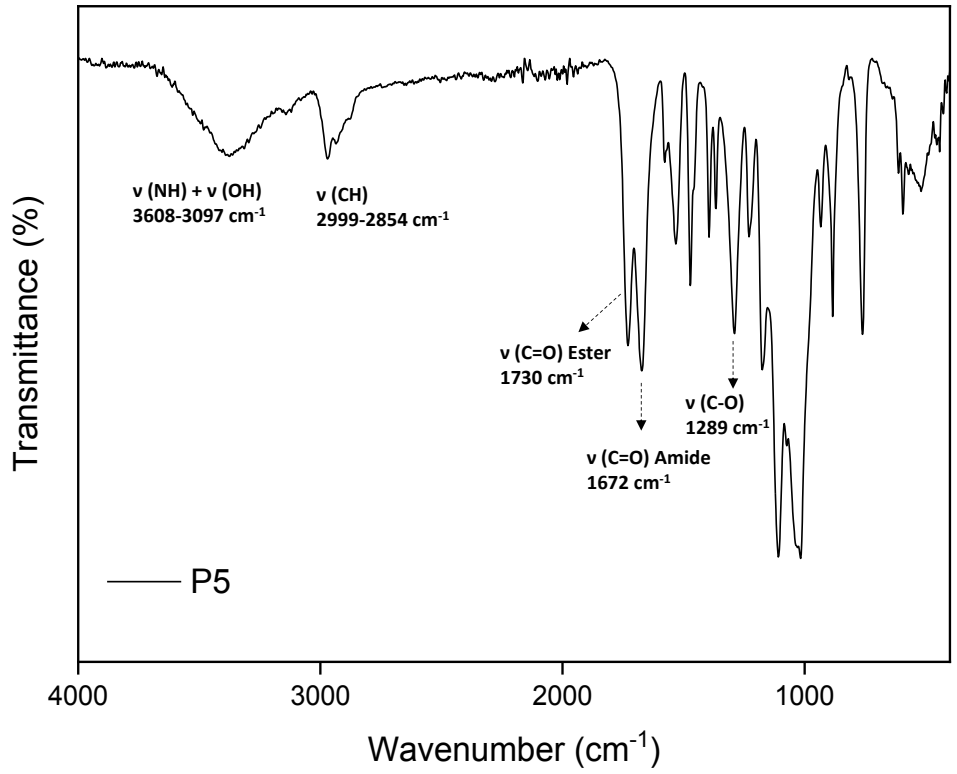

Figure 49: ATR-IR spectrum of Passerini product **P5**.

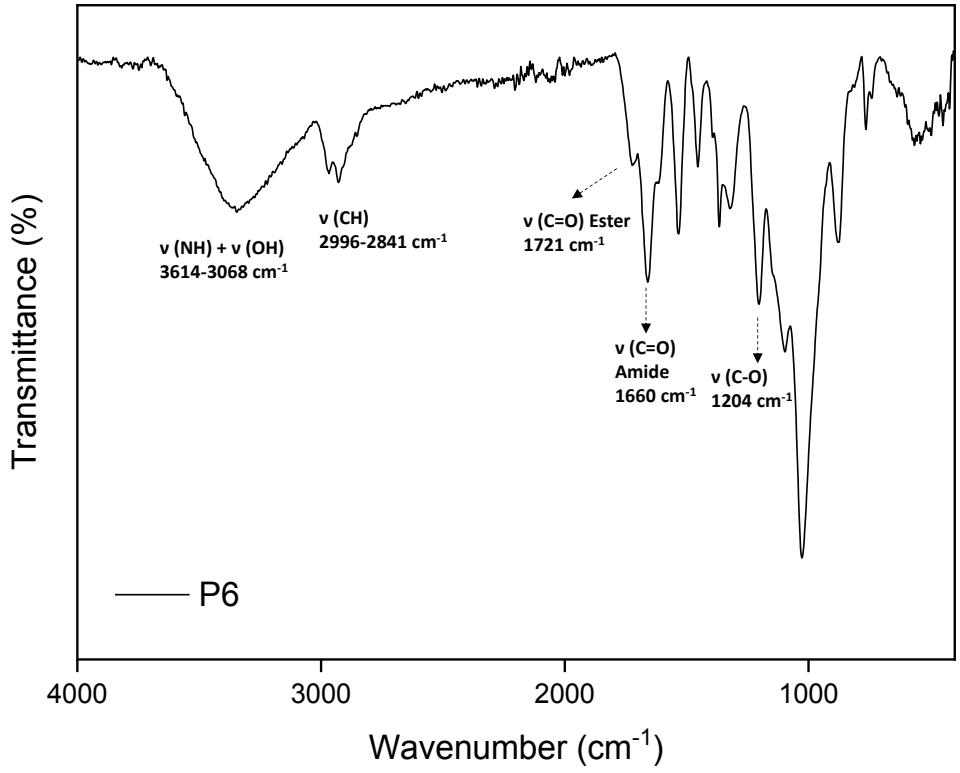

Figure 50: ATR-IR spectrum of Passerini product **P6**.

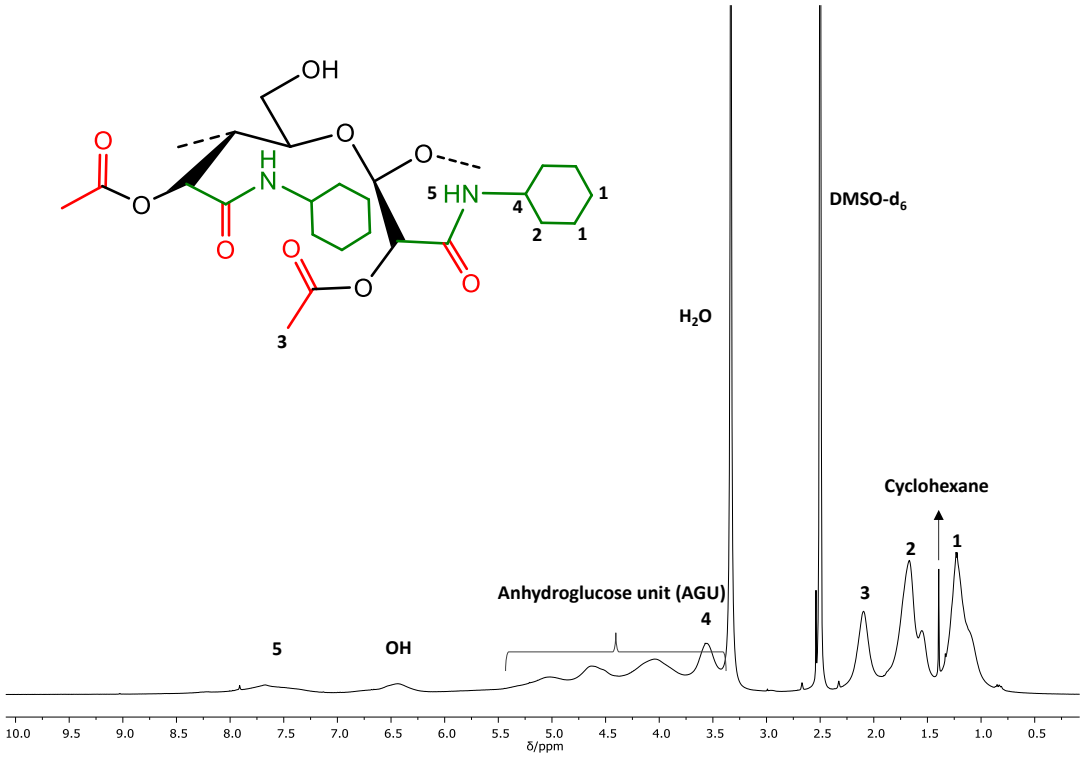

Figure 51: ^{1}H NMR spectrum of Passerini product **P2**.

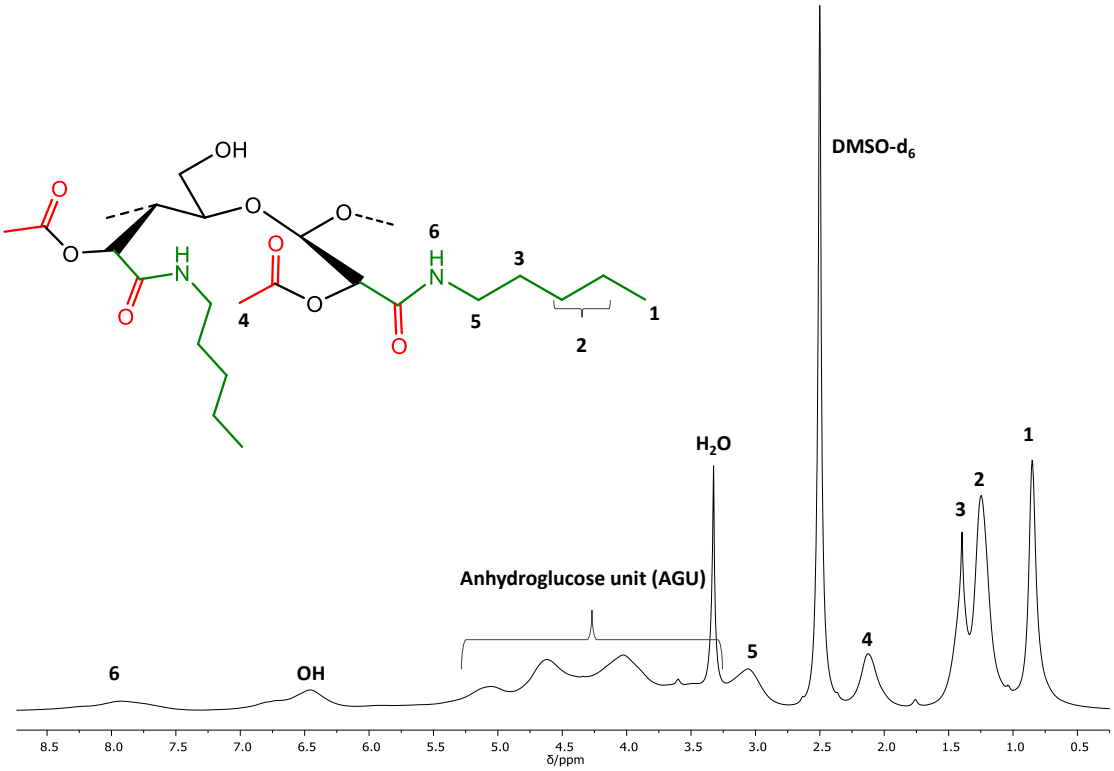

Figure 52: ^{1}H NMR spectrum of Passerini product **P3**.

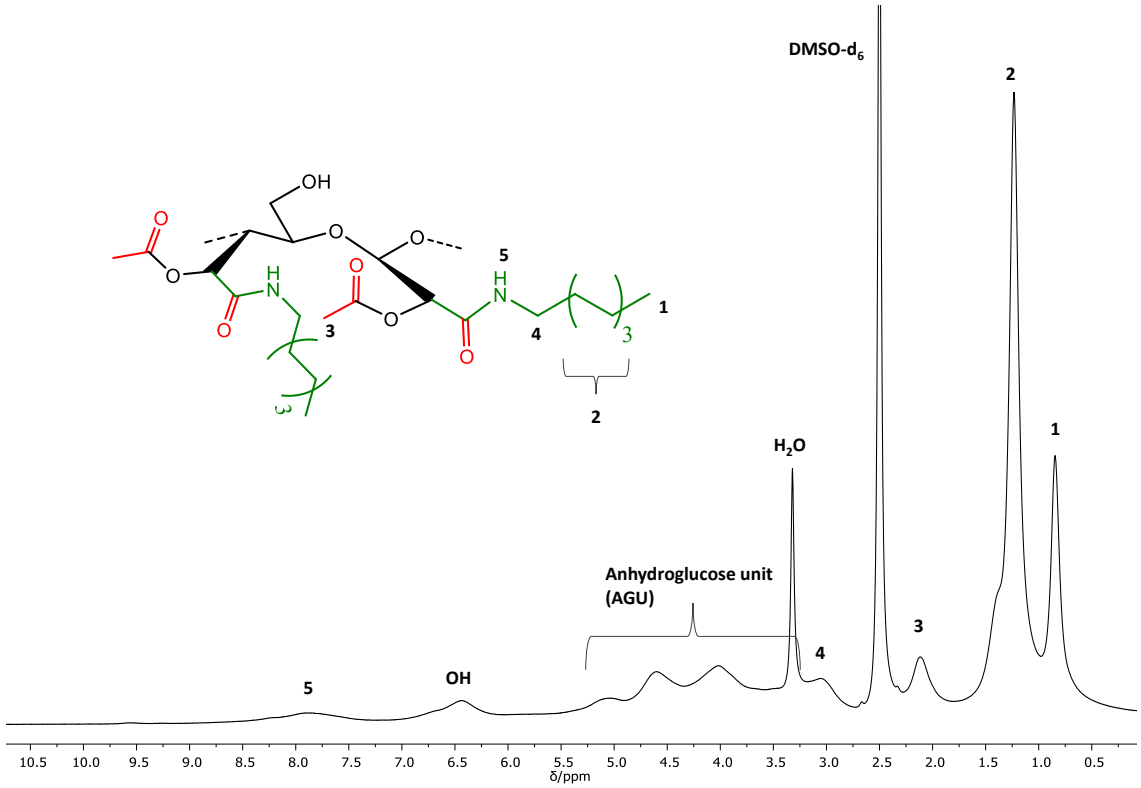

Figure 53: ^{1}H NMR spectrum of Passerini product **P4**.

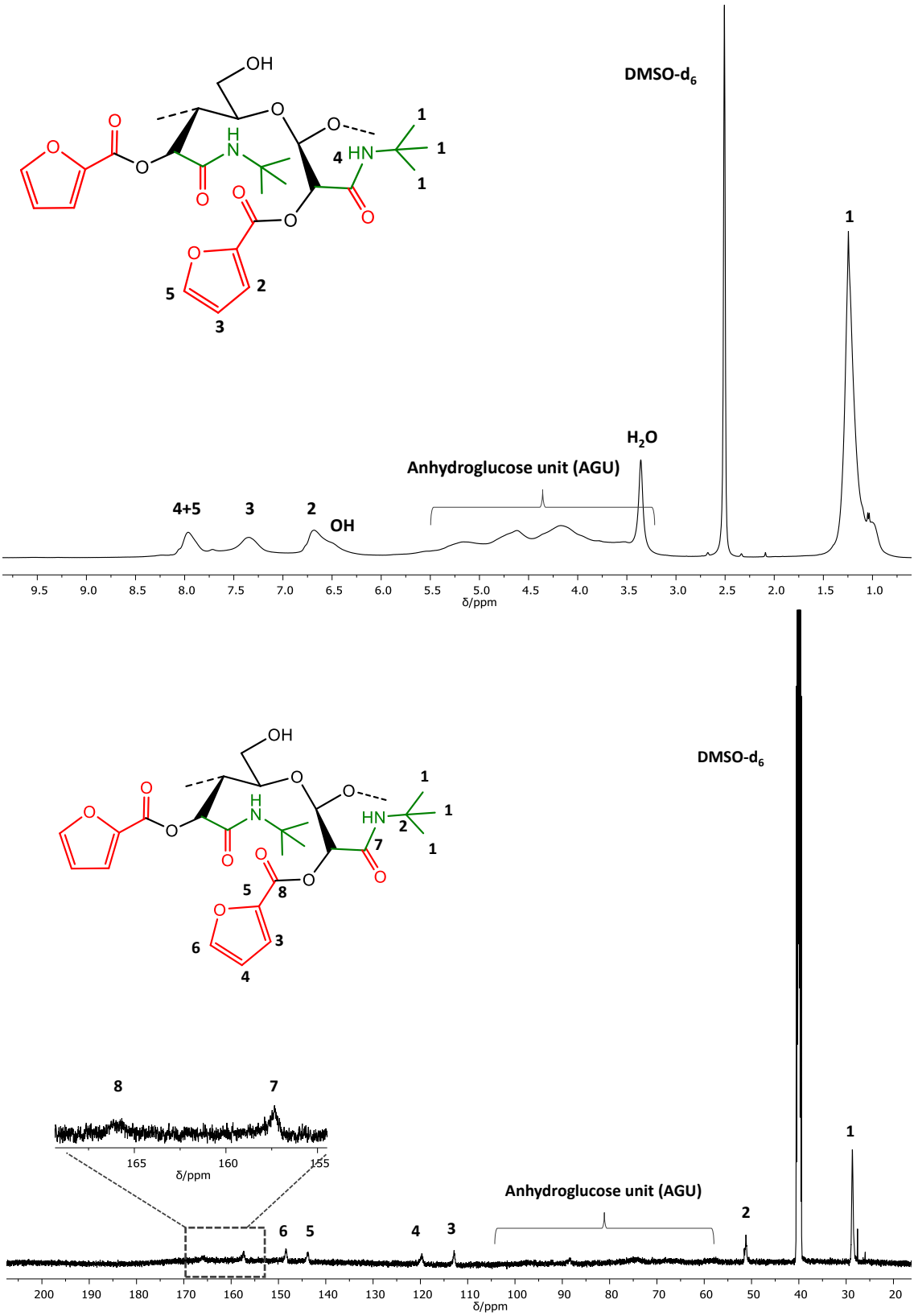

Figure 54: ^{1}H NMR (top) and ^{13}C NMR (bottom) spectra of Passerini product **P5**.

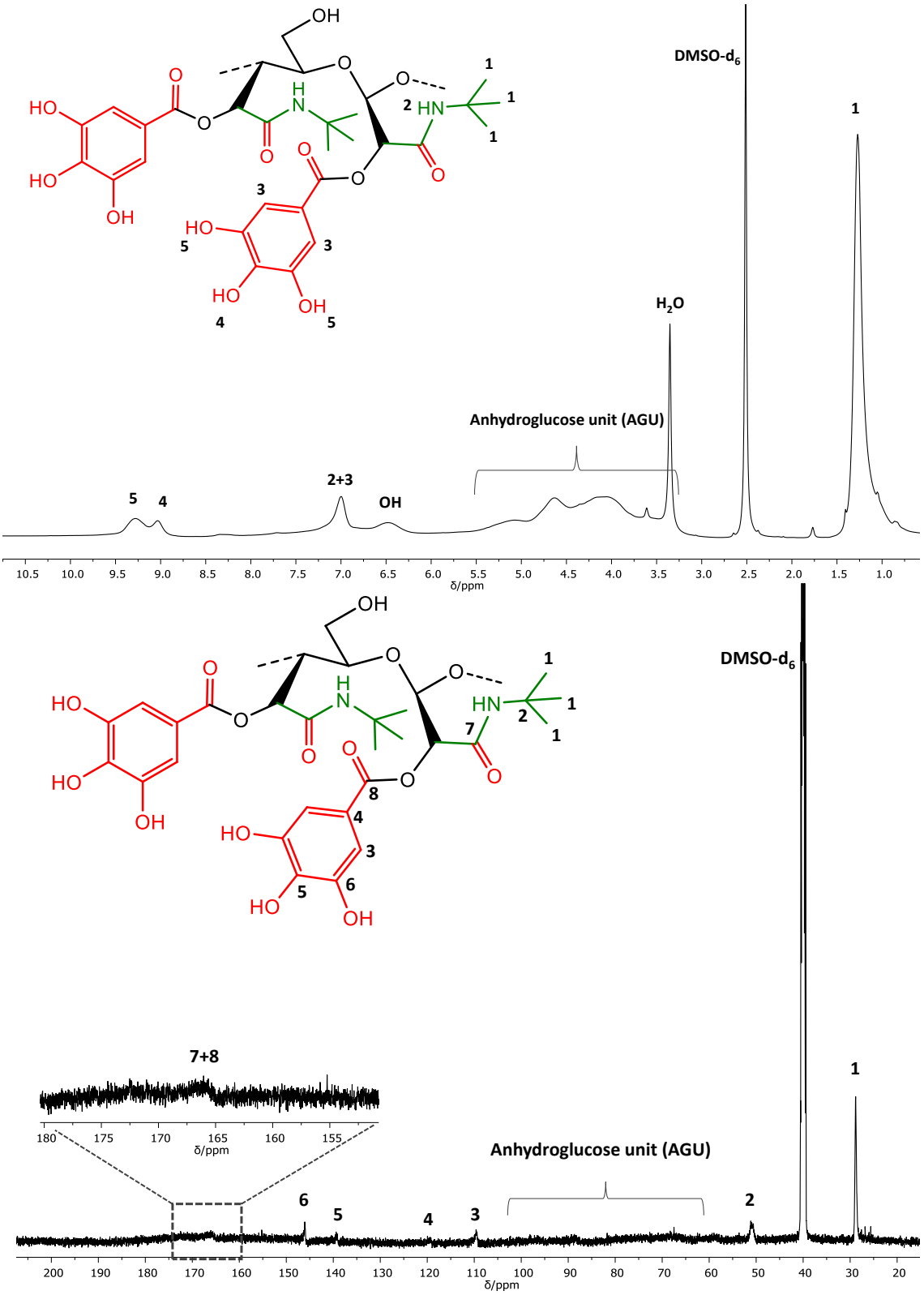

Figure 55: ^{1}H NMR (top) and ^{13}C NMR (bottom) spectra of Passerini product **P6**.

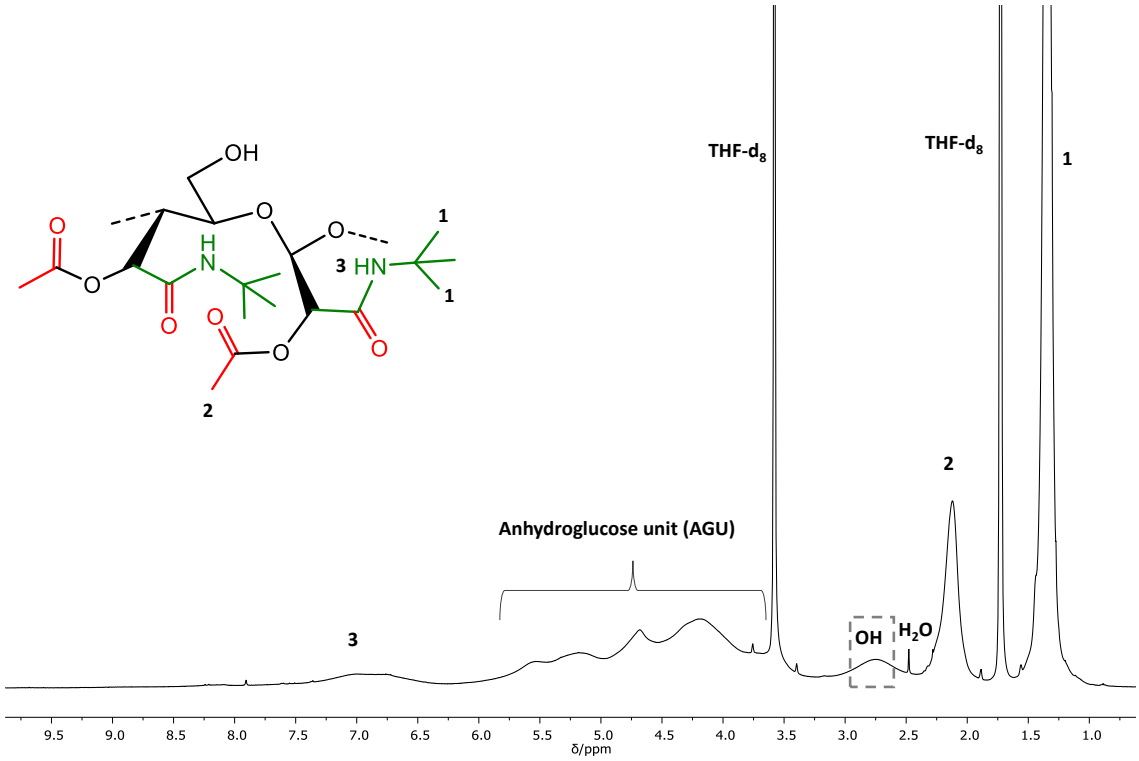

Figure 56: ^{1}H NMR spectrum of Passerini product **P1** in THF-d_8.

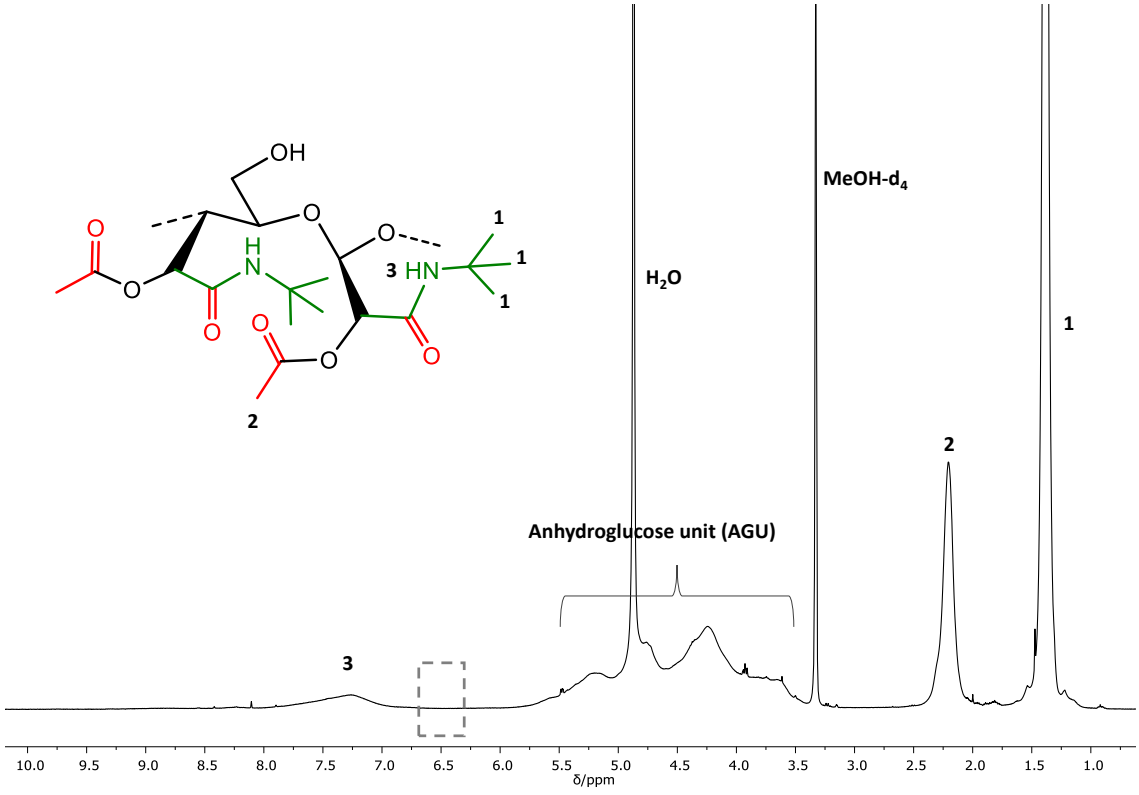

Figure 57: ^{1}H NMR spectrum of Passerini product **P1** in MeOH-d_4.

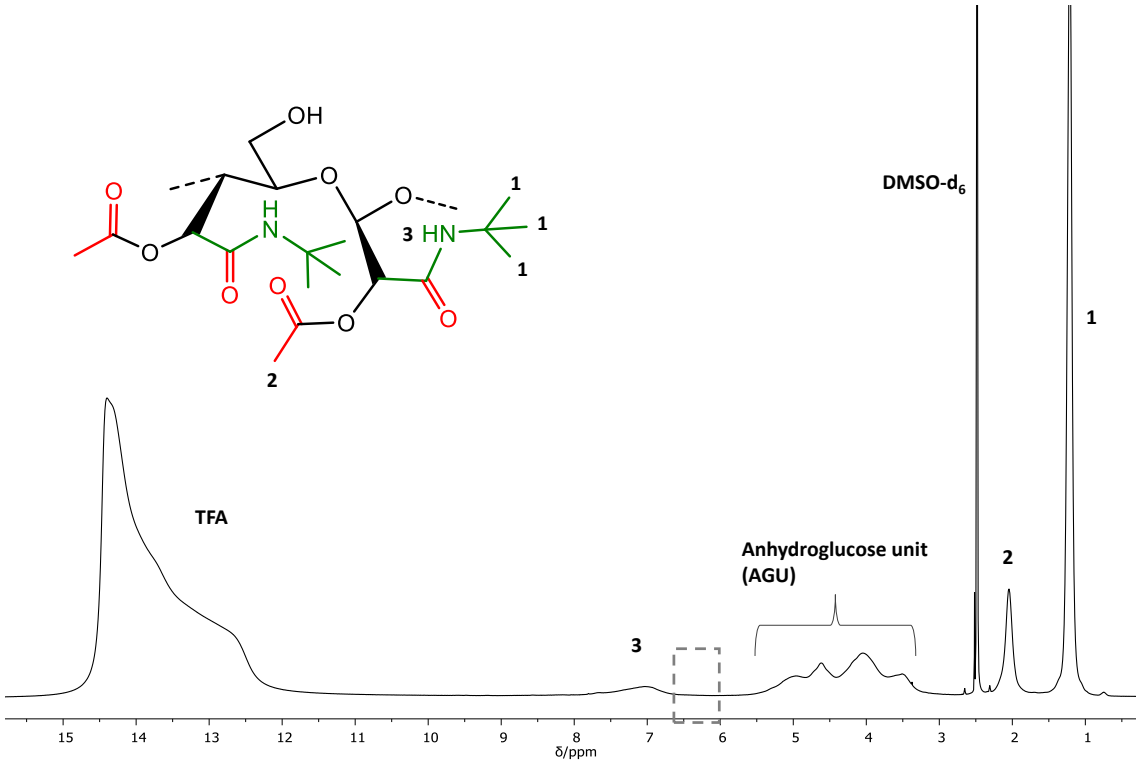

Figure 58: ^{1}H NMR spectrum of Passerini product **P1** in DMSO-d_6 containing a drop of TFA.

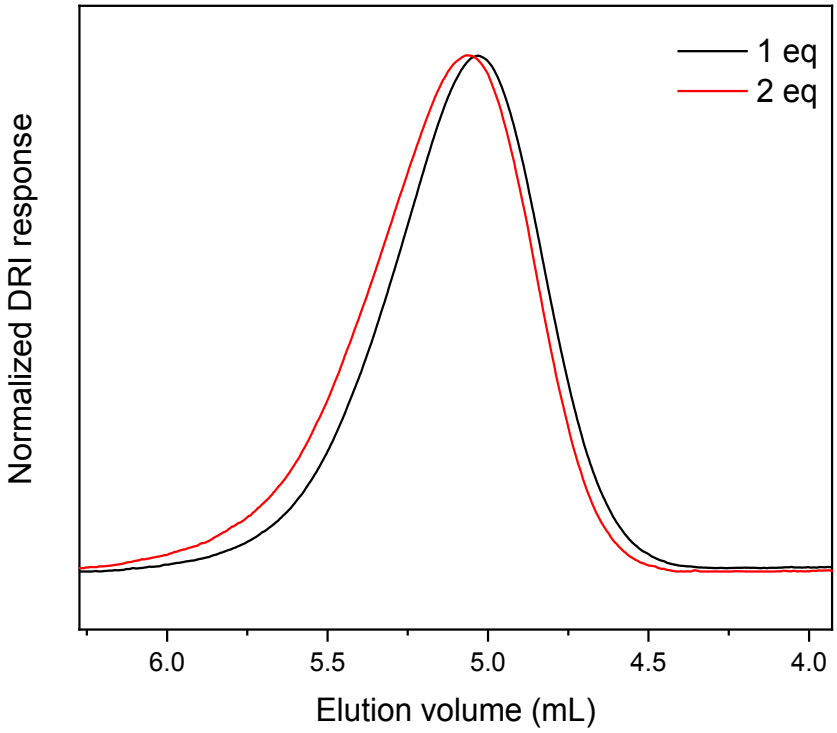

Figure 59: SEC analysis of Passerini product **P1** synthesized with different acid and isocyanide equivalents per aldehyde unit.

Table 11: Elemental analysis of Passerini products **P1-P6**.

Sample	C (%)	N (%)	H (%)
P1	48.08	4.46	7.05
P2	50.72	3.68	7.10
P3	48.75	3.56	6.60
P4	50.36	3.38	7.94
P5	49.91	3.57	5.90
P6	48.90	3.96	6.62

6.3.3 Experimental Procedures for Chapter 4.3

General procedure for the synthesis of Fatty Acid Cellulose Esters (FACEs)

Microcrystalline cellulose (0.5 g, 3.08 mmol) was suspended in 10 mL DMSO (anhydrous 99.9%), followed by the addition of 1,5,7-Triazabicyclo[4.4.0]dec-5-ene as (TBD, 1.28 g, 9.25 mmol). The reaction mixture was then stirred at 50 °C for 20 minutes under CO_2 (atmospheric pressure) until a clear solution was obtained. After solubilization, methyl 10-undecenoate (9 eq. per AGU, 1.83 g, 9.25 mmol) was added dropwise at 95°C and the reaction was carried out for 3 hours under air flow. Then the homogenous hot mixture was precipitated into 200 mL water and the product was filtered. Later, the precipitate was washed with cyclohexane (100 mL) for two times and after filtration, product was dissolved in THF (10 mL). Homogenous solution was then reprecipitated into water to completely remove the undesired compounds. Final product with a DS of 1.97 was obtained after drying under vacuum at 75 °C overnight. Instead of reprecipitation process, additionally washing with MeOH (100 mL) for three times was done for lower DS products. Yields were determined as 66 to 79% by taking DS values into consideration.

ATR-IR: ν (cm^{-1}) = 3582-3293 ν(O-H), 3077 ν(=C-H), 2925-28255 ν(C-H), 1740 ν(C=O), 1640 ν(C=C), 1160 ν(C-O), 1050-1025 ν(C-O) glucopyranose of cellulose. ^{1}H NMR (400 MHz, DMSO-d_6) δ (ppm) = 5.77 (br, 1H), 5.67-3.01 (m, AGU, 7H), 4.95 (m, 2H), 2.29 (br, 2H), 1.99 (br, 2H), 1.49 (br, 2H), 1.39-1.02 (br, 10H). ^{13}C NMR (126 MHz, DMSO-d_6) δ (ppm) = 172.01, 138.28, 113.86, 102.21, 79.56, 74.48, 71.81, 62.28, 32.98, 32.53, 28.17, 27.97, 27.80, 23.93.

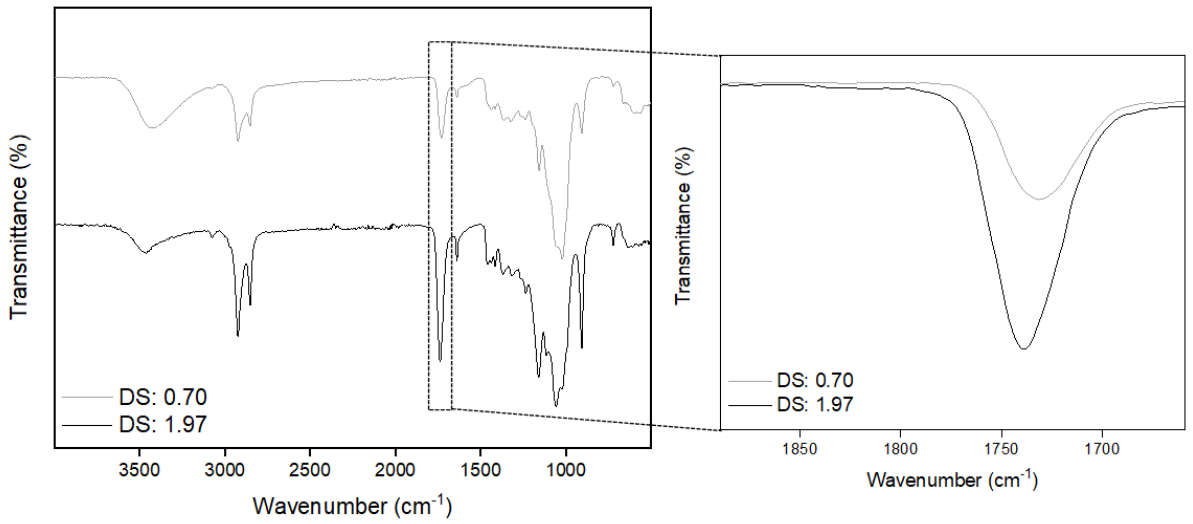

Figure 60: ATR-IR spectra (left) and zoom to carbonyl intensities (right) of FACEs with different DS values (spectra were normalized to the intensity of the C-O stretching vibrations of the pyranose unit at 1050-1025 cm^{-1}).

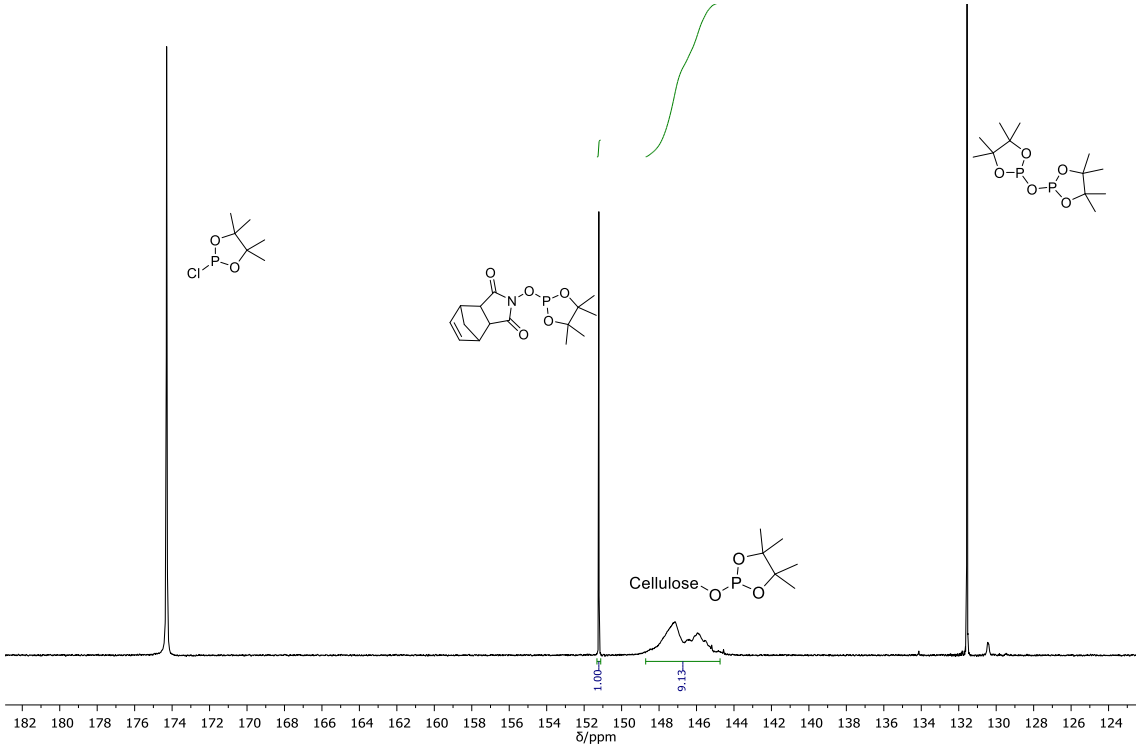

Figure 61: ^{31}P NMR spectrum of FACE (DS: 0.70), obtained with 5 wt.% MCC, 3 eq. methyl 10-undecenoate, 95 °C, 3 h.

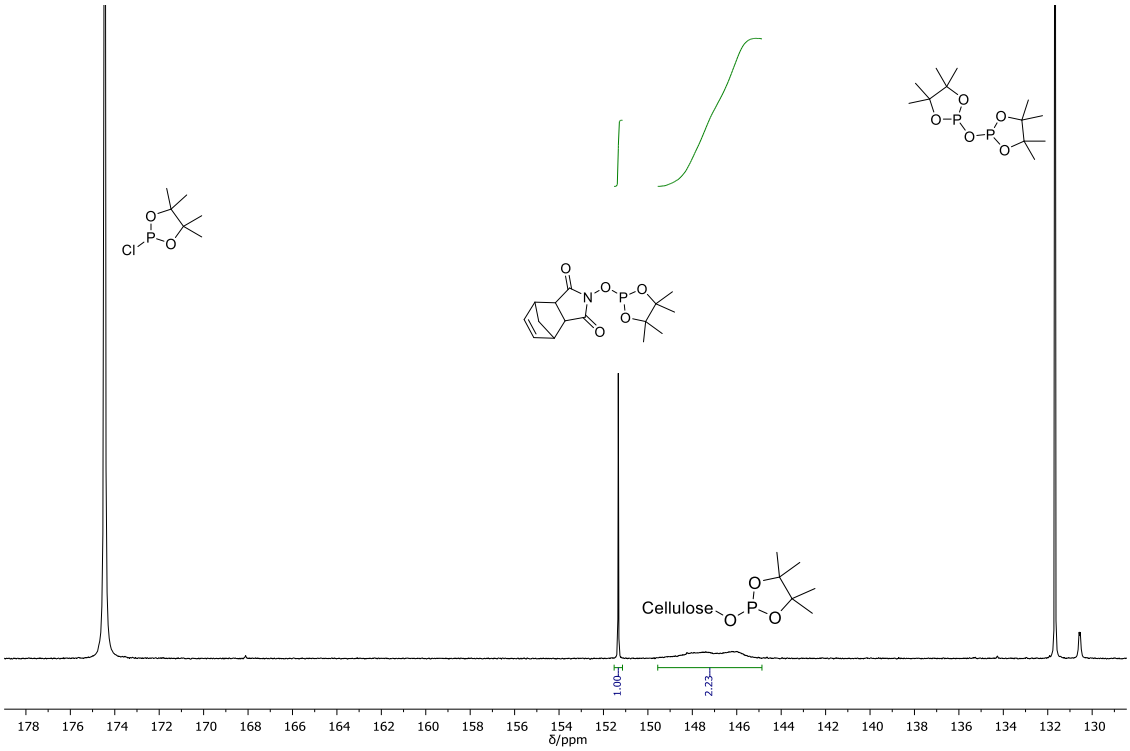

Figure 62: ^{31}P NMR spectrum of FACE (DS: 1.97), obtained with 5 wt.% MCC, 9 eq. methyl 10-undecenoate/AGU, 95 °C, 6 h.

Procedure for Thiol-ene Modification of FACE

FACE (DS: 0.70, 0.20 g, 0.71 mmol) is dissolved in 4 mL DMSO. After complete dissolution, 1.5 eq of thiol (1.06 mmol) and DMPA (5 mol%, 10 mg, 0.04 mmol) were added at room temperature. Solution was degassed for 3-5 minutes and stirred for 12 hours under UV radiation (365 nm). After reaction was completed, homogenous solution was precipitated into water (200 mL), filtrated and washed with isopropanol (100 mL) for 2 times. Precipitate was dried under vacuum at 75 °C overnight with a yield between 68 and 84%.

FACE-TE1: Yield: 68% ATR-IR: *v* (cm^{-1}) = 3582-3132 *v*(O-H), 2968-2818 *v*(C-H), 1740 *v*(C=O), 1160 *v*(C-O), 1050-1025 *v*(C-O) glucopyranose of cellulose. ^{1}H NMR (400 MHz, DMSO-d$_6$) *δ* (ppm) = 5.67-3.01 (m, AGU, 7H), 2.45 (br, 4H), 2.29 (br, 2H), 1.62-1.49 (br, 6H), 1.38-1.03 (br, 14H) 0.86 (br, 3H). ^{13}C NMR (101 MHz, DMSO-d$_6$) *δ* (ppm) = 172.50, 51.12, 50.83, 33.23, 31.30, 31.15, 30.84, 29.18, 28.84, 28.71, 28.52, 28.27, 24.40, 24.45, 22.18, 21.46, 21.35, 13.52.

FACE-TE2: Yield: 76% ATR-IR: *v* (cm^{-1}) = 3582-3132 *v*(O-H), 2968-2818 *v*(C-H), 1740 *v*(C=O), 1160 *v*(C-O), 1050-1025 v(C-O) glucopyranose of cellulose. ^{1}H NMR (400 MHz, DMSO-d_6) *δ* (ppm) = 5.67-3.01 (m, AGU, 7H), 2.48 (br, 4H), 2.29 (br, 2H), 1.47 (br, 4H), 1.38-1.16 (br, 12H) 1.13 (s, 9H).

FACE-TE3: Yield: 84% ATR-IR: *v* (cm^{-1}) = 3582-3132 *v*(O-H), 2968-2818 *v*(C-H), 1740 *v*(C=O), 1160 *v*(C-O), 1050-1025 *v*(C-O) glucopyranose of cellulose. ^{1}H NMR (400 MHz, DMSO-d_6) *δ* (ppm) = 5.58-3.01 (m, AGU, 7H), 2.45 (br, 4H), 2.29 (br, 2H), 1.49 (br, 6H), 1.40-1.08 (br, 18H) 0.85 (br, 3H).

FACE-TE4: Yield: 76% ATR-IR: *v* (cm^{-1}) = 3582-3132 *v*(O-H), 2968-2818 *v*(C-H), 1740 *v*(C=O), 1160 *v*(C-O), 1050-1025 *v*(C-O) glucopyranose of cellulose. ^{1}H NMR (400 MHz, DMSO-d_6) *δ* (ppm) = 5.58-3.01 (m, AGU, 7H), 2.62 (br, 1H), 2.48 (br, 2H), 2.30 (br, 2H), 1.93-1.83 (br, 2H), 1.67 (br, 4H), 1.49 (br, 4H) 1.36-1.11 (br, 16H).

FACE-TE5: Yield: 78% ATR-IR: *v* (cm^{-1}) = 3582-3132 *v*(O-H), 2968-2818 *v*(C-H), 1740 *v*(C=O), 1160 *v*(C-O), 1050-1025 *v*(C-O) glucopyranose of cellulose. ^{1}H NMR (400 MHz, DMSO-d_6) *δ* (ppm) = 5.58-3.01 (m, AGU, 7H), 2.50 (br, 2H), 2.43 (br, 2H), 2.37-1.39 (m, 8H), 2.31 (br, 2H), 1.48 (br, 4H), 1.37-1.20 (br, 12H), 1.16 (br, 3H), 0.96 (br, 3H), 0.90-0.74 (m, 1H).

FACE-TE6: Yield: 71% ATR-IR: *v* (cm^{-1}) = 3582-3132 *v*(O-H), 2968-2818 *v*(C-H), 1740 *v*(C=O), 1160 *v*(C-O), 1050-1025 *v*(C-O) glucopyranose of cellulose. ^{1}H NMR (400 MHz, DMSO-d_6) *δ* (ppm) = 5.57-3.01 (m, AGU, 7H), 2.50 (br, 2H), 2.45 (br, 2H), 2.44-0.77 (m, 15H), 2.29 (br, 2H), 1.49 (br, 4H), 1.41-1.15 (br, 12H).

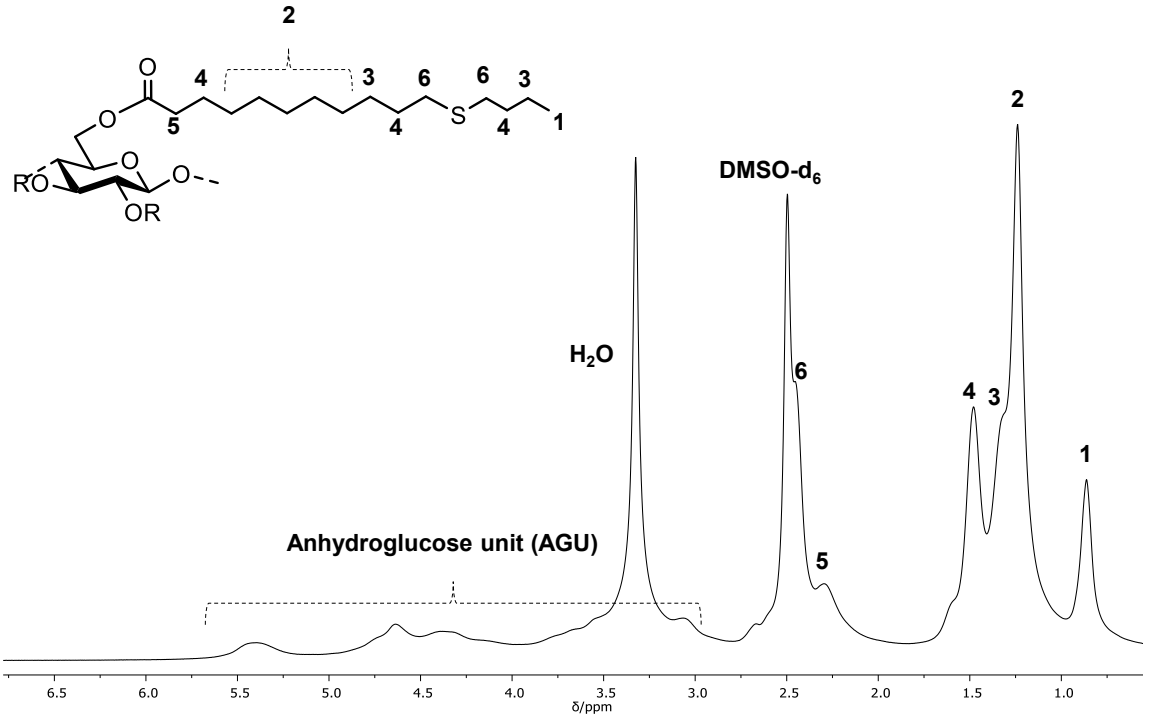

Figure 63: ^{1}H NMR spectrum of **FACE-TE1**.

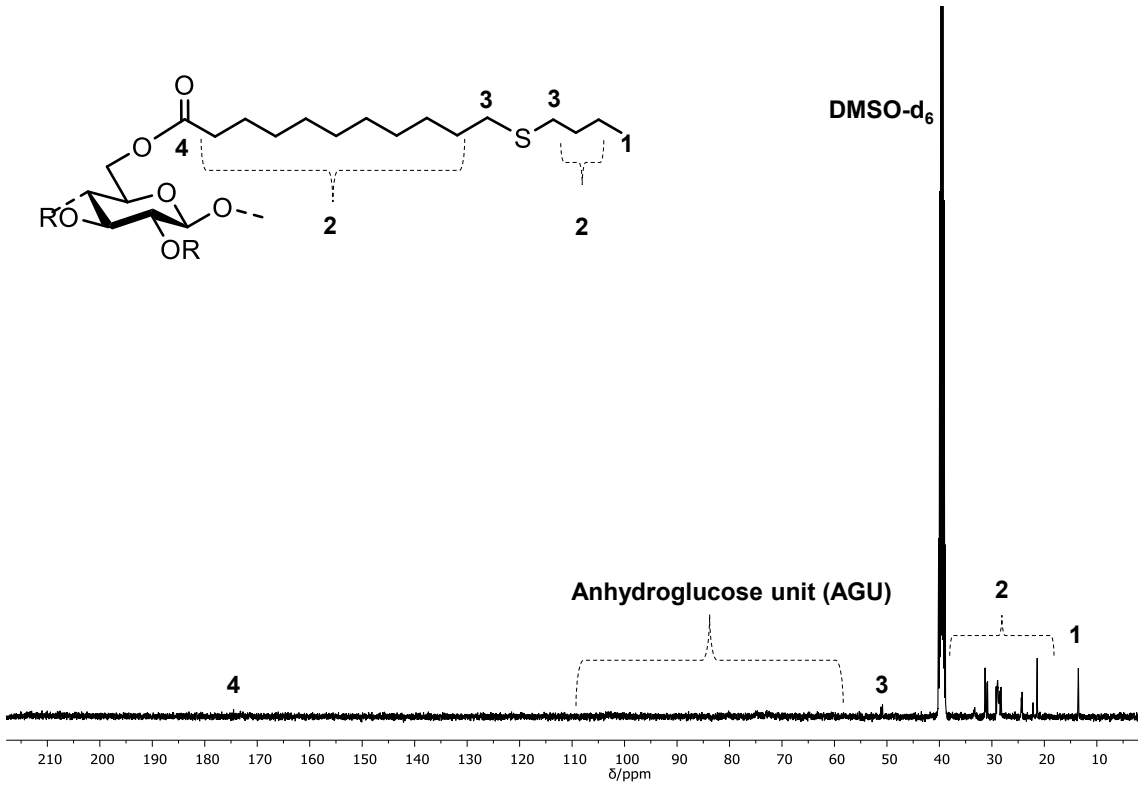

Figure 64: ^{13}C NMR spectrum of **FACE-TE1**.

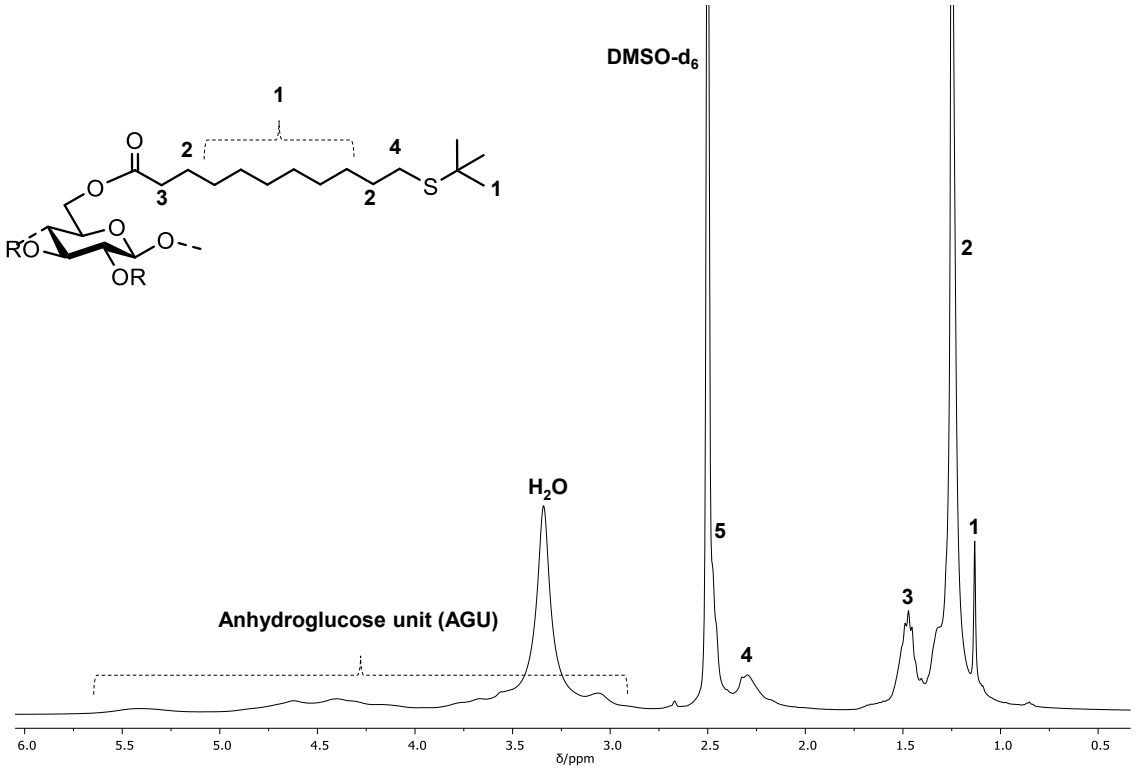

Figure 65: ^{1}H NMR spectrum of **FACE-TE2**.

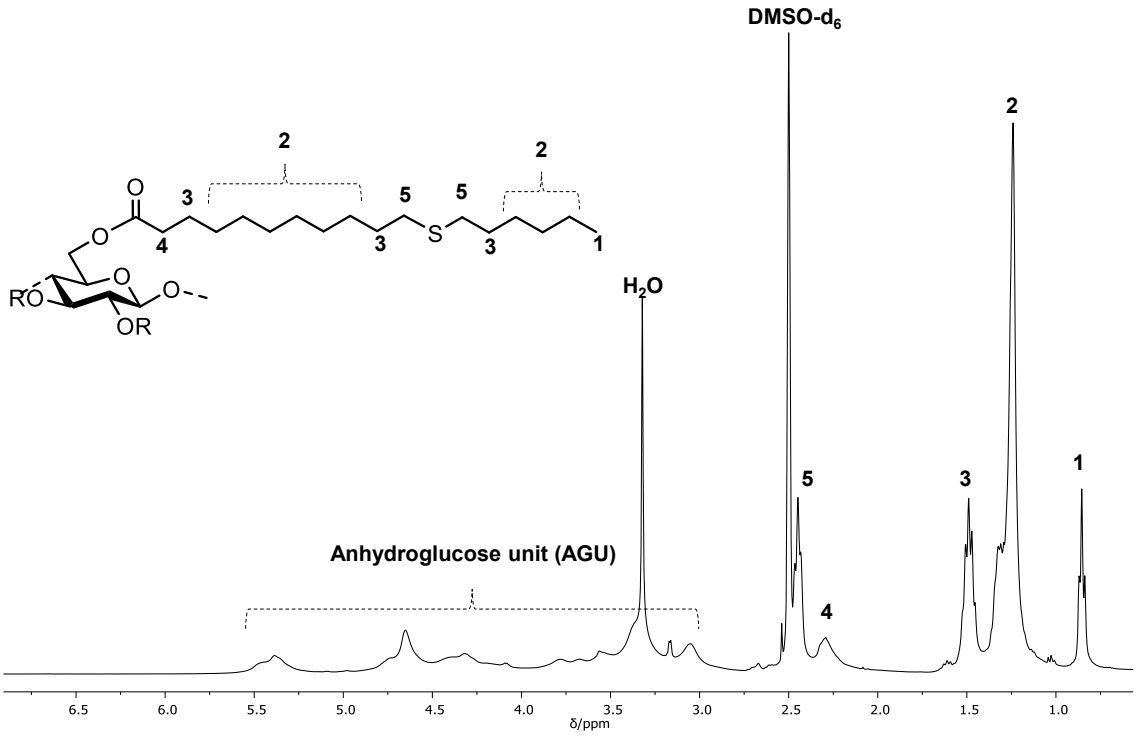

Figure 66: ^{1}H NMR spectrum of **FACE-TE3**.

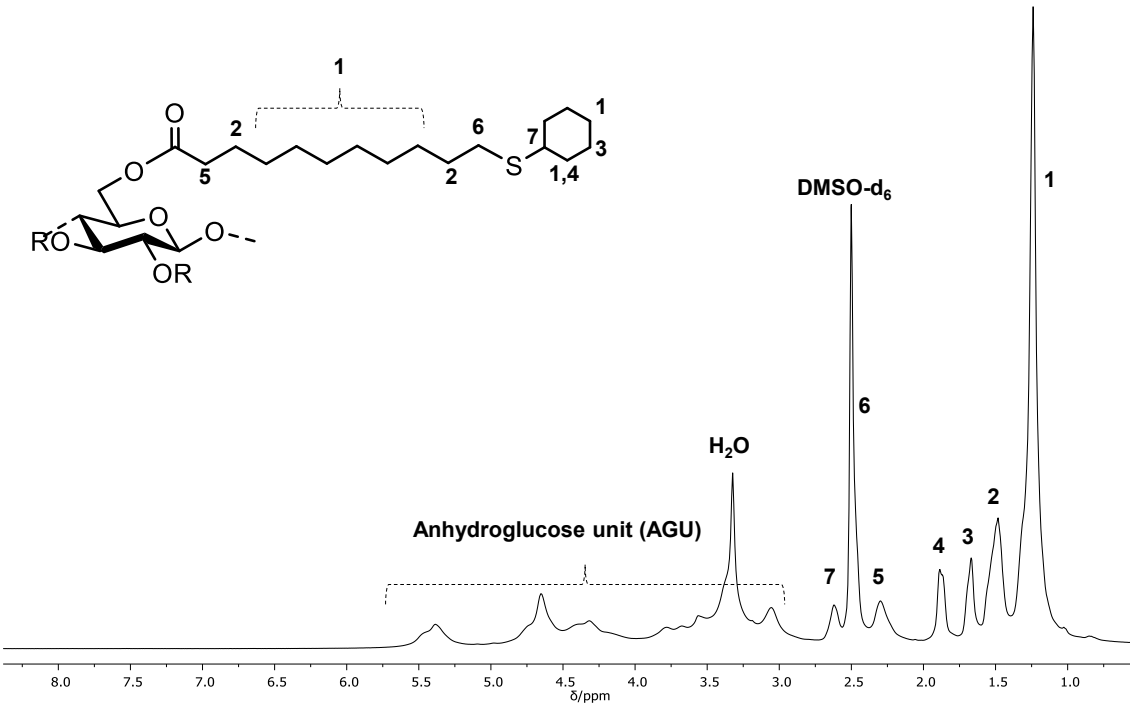

Figure 67: [1]H NMR spectrum of **FACE-TE4**.

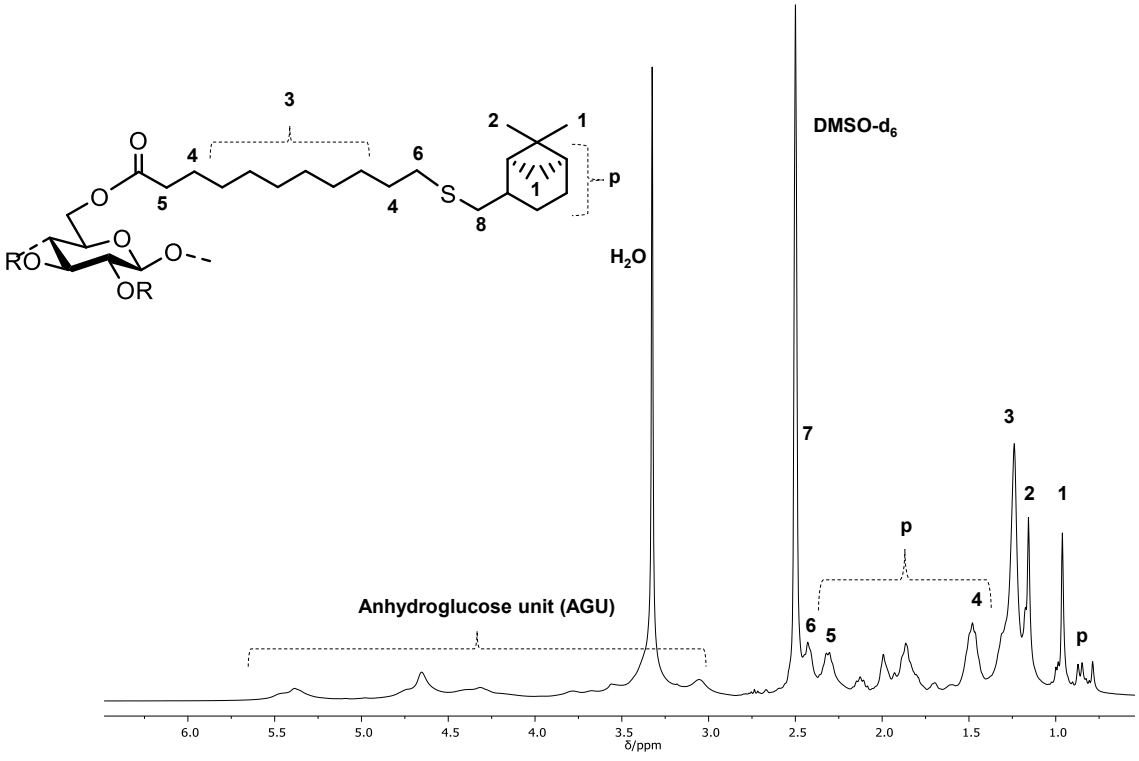

Figure 68: [1]H NMR spectrum of **FACE-TE5**.

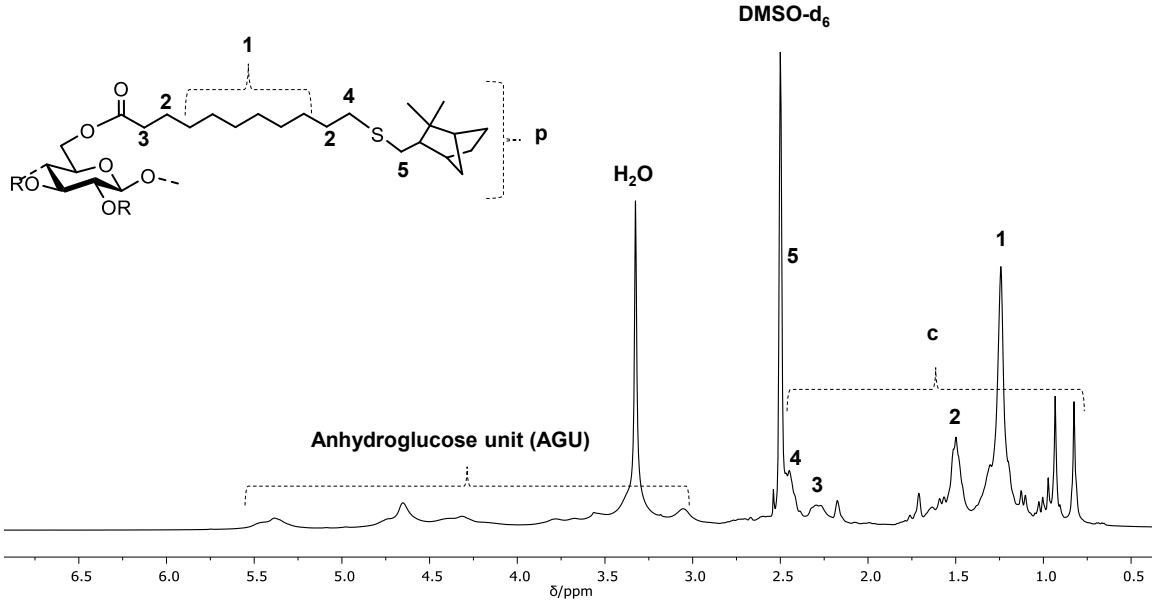

Figure 69: ^{1}H NMR spectrum of **FACE-TE6**.

Procedure for Oxidation of Thiol-ene Products

Selected thiol-ene modified FACE product (FACE-TE1 and FACE-TE3) (DS: 0.7, 0.3 mmol) was dissolved in 2 mL DMAc. After complete dissolution, *meta*-chloroperoxybenzoic acid (*m*CPBA) (0.26 g, 1.5 mmol) was added and the solution was stirred at room temperature overnight. The resulting mixture was poured to saturated sodium sulfite solution to quench the remaining oxidizing agent. Precipitate was filtered and washed with water (200 mL) and isopropanol (100 mL). Remaining white product then dried under vacuum at 75 °C overnight with a yield between 81 and 85%.

FACE-TE1.Ox: Yield: 81% ATR-IR: *v* (cm^{-1}) = 3582-3132 *v*(O-H), 2968-2818 *v*(C-H), 1740 *v*(C=O), 1329-1250 *v*(S=O), 1160 *v*(C-O), 1123 *v*(S=O), 1050-1025 *v*(C-O) glucopyranose of cellulose. ^{1}H NMR (400 MHz, DMSO-d$_6$) *δ* (ppm) = 5.67-3.01 (m, AGU, 7H), 3.03 (br, 4H), 2.29 (br, 2H), 1.64 (br, 4H), 1.49 (br, 2H), 1.37 (br, 4h), 1.32-

1.08 (br, 10H), 0.89 (br, 3H). ^{13}C NMR (101 MHz, DMSO-d_6) *δ* (ppm) = 172.74, 51.56, 51.29, 33.24, 28.78, 25.52, 24.40, 23.26, 21.24, 21.03, 13.46.

FACE-TE3.Ox: Yield: 85% ATR-IR: *v* (cm-1) = 3582-3132 *v*(O-H), 2968-2818 *v*(C-H), 1740 *v*(C=O), 1329-1250 *v*(S=O), 1160 *v*(C-O), 1123 *v*(S=O), 1050-1025 *v*(C-O) glucopyranose of cellulose. 1H NMR (400 MHz, DMSO-d_6) δ (ppm) = 5.65-3.01 (m, AGU, 7H), 3.03 (br, 4H), 2.30 (br, 2H), 1.64 (br, 4H), 1.51 (br, 2H), 1.35 (br, 4h), 1.32-1.06 (br, 14H), 0.87 (br, 3H).

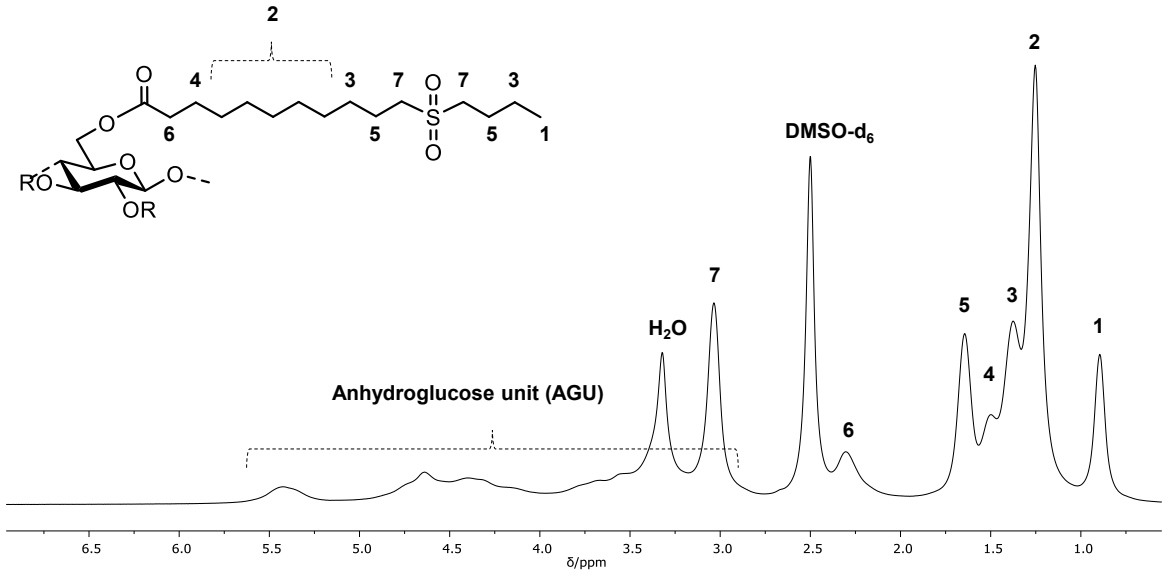

Figure 70: ^{1}H NMR spectrum of **FACE-TE1.Ox**.

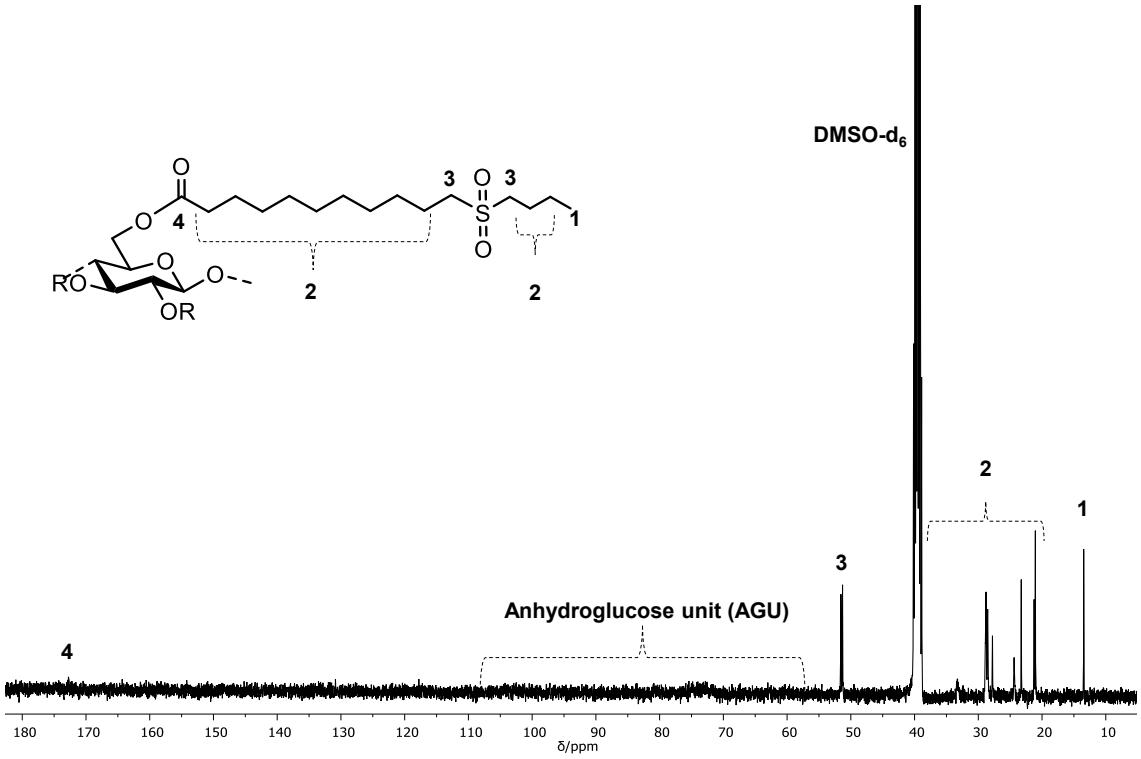

Figure 71: ^{13}C NMR spectrum of **FACE-TE1.Ox**.

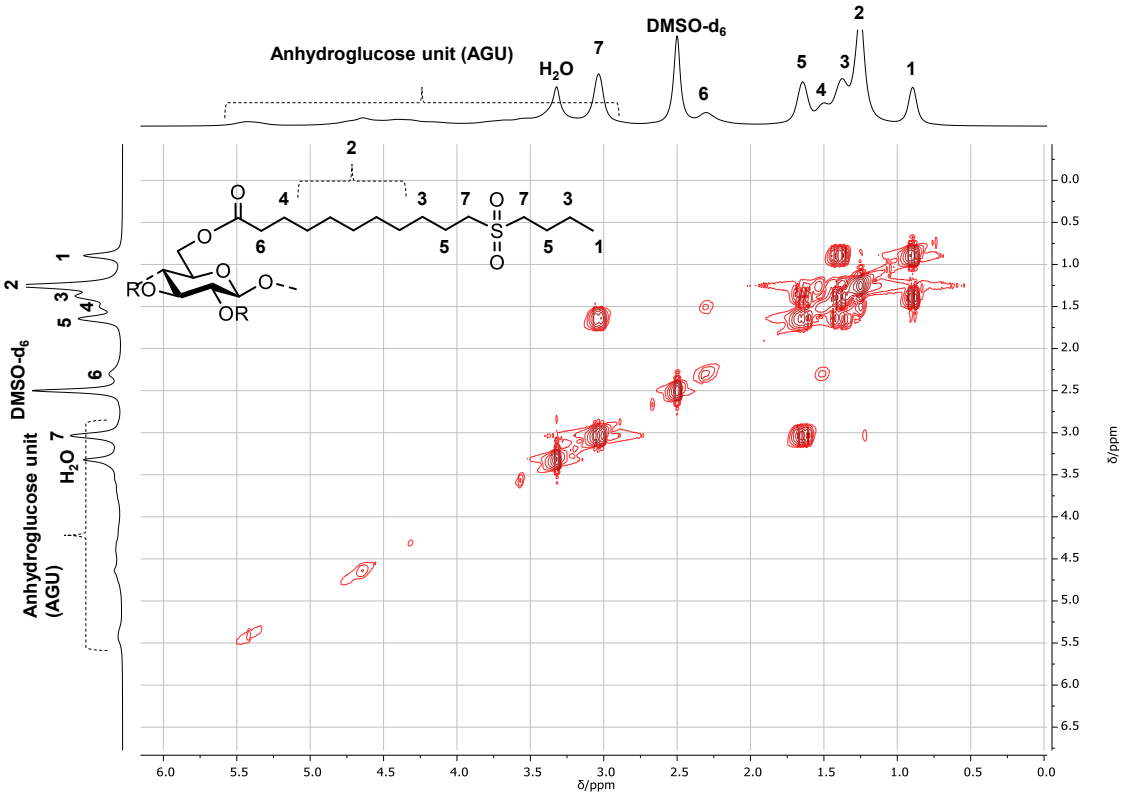

Figure 72: COSY spectrum of **FACE-TE1.Ox**.

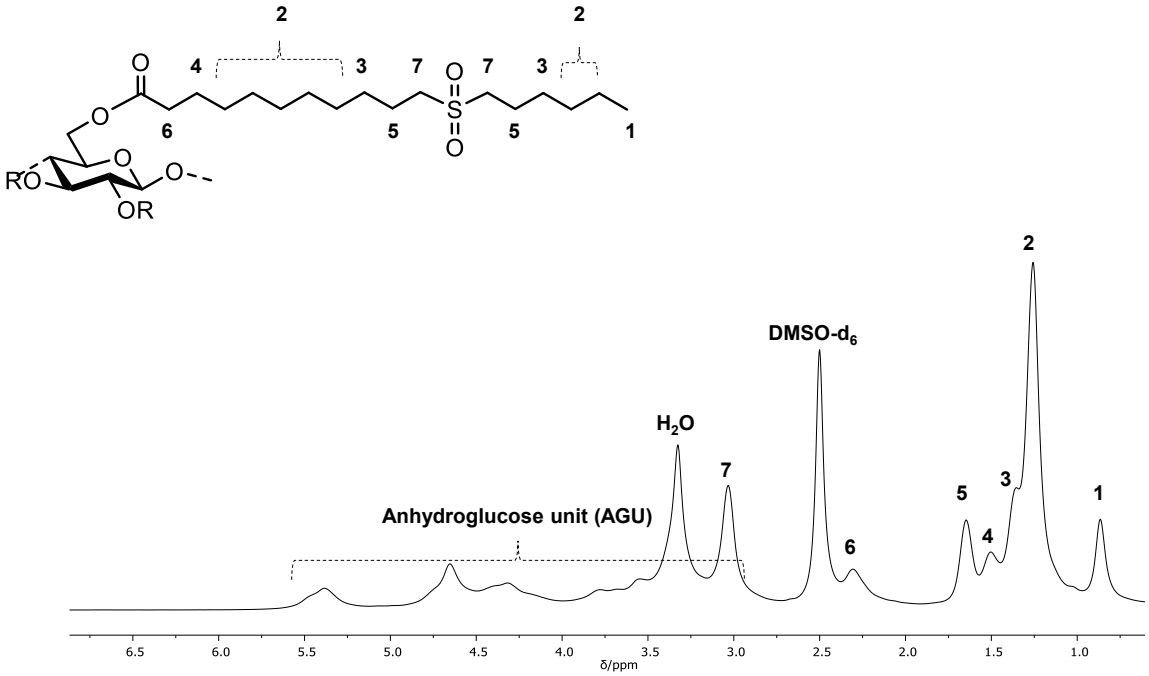

Figure 73: ^{1}H NMR spectrum of **FACE-TE3.Ox**.

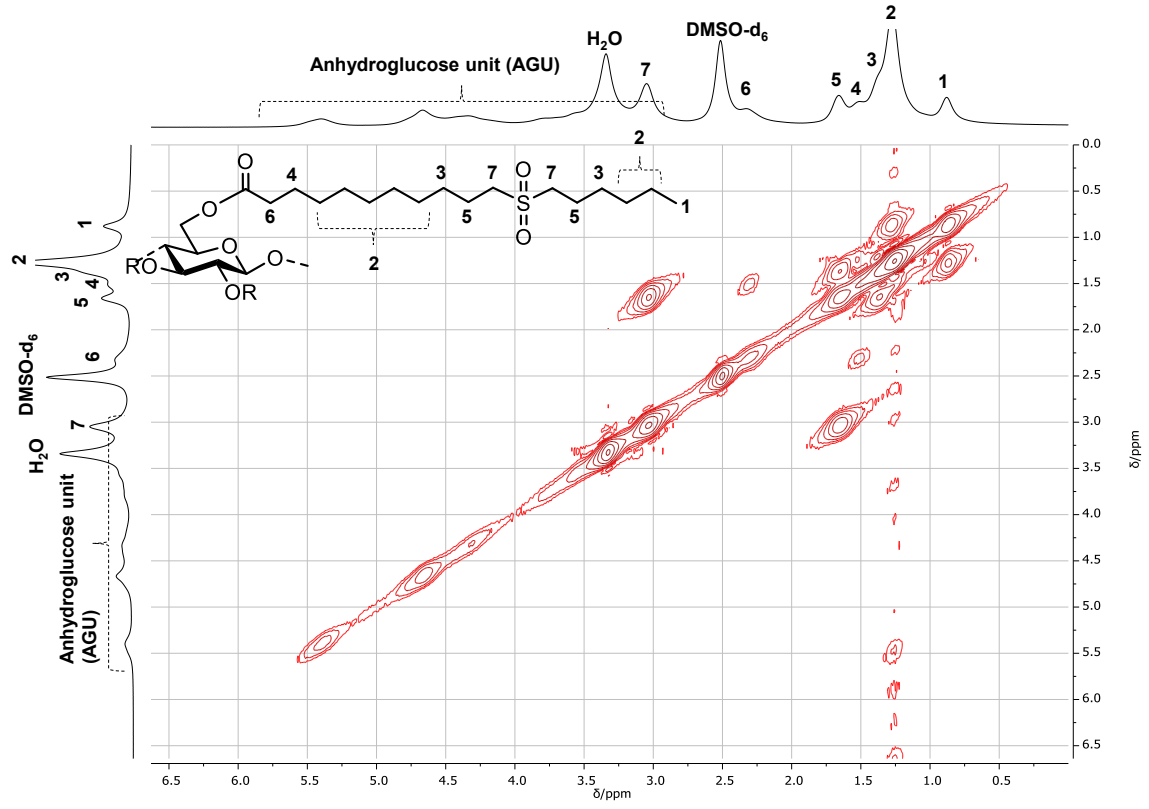

Figure 74: COSY spectrum of **FACE-TE3.Ox**.

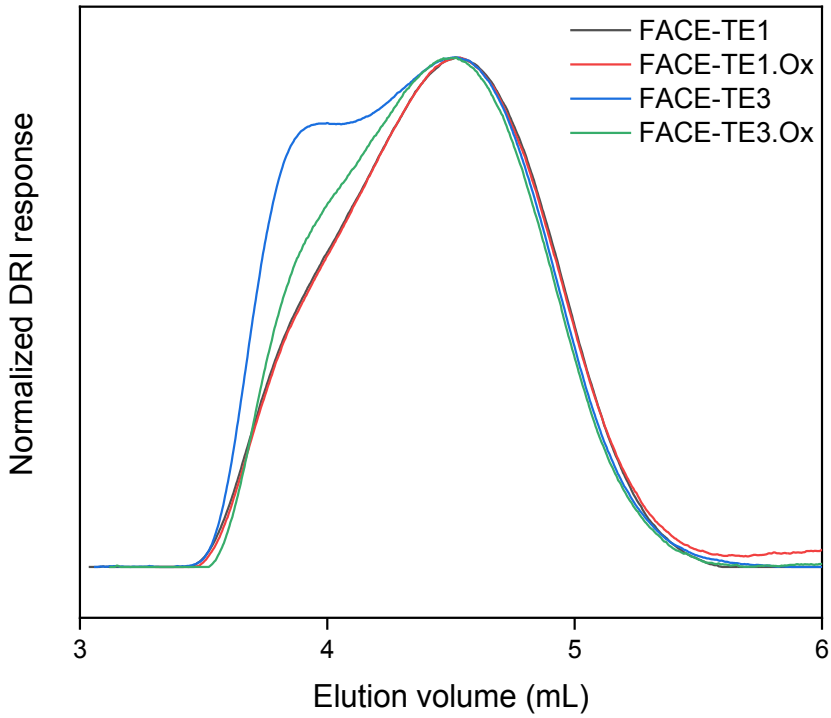

Figure 75: SEC traces of **FACE-TE1**, **FACE-TE1.Ox**, **FACE-TE3** and **FACE-TE3.Ox**.

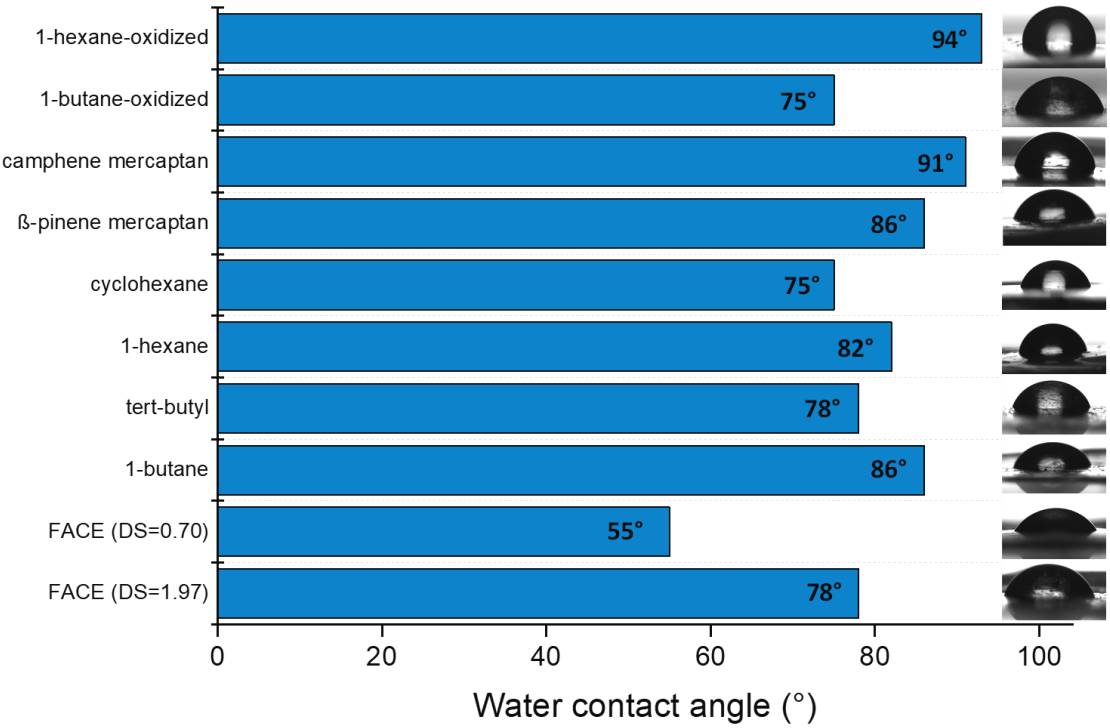

Figure 76: Water contact angle measurements of the synthesized products.

Synthesis of β-Pinene mercaptan

(-)-β-Pinene (5.00 g, 36.7 mmol) was placed into a round bottom flask and thioacetic acid (3.28 mL, 45.9 mmol) was added slowly. Reaction mixture was stirred at room temperature for 5 hours. After completion of the reaction, excess thioacetic acid was removed under reduced pressure. Subsequently, methanol (15.0 mL, 367 mmol) and concentrated sulfuric acid (0.097 mL, 1.83 mmol) were added, and the reaction mixture was stirred at 60 °C for 18 hours. Methanol was removed under reduced pressure and organic layer was extracted by ethyl acetate. Organic layer was washed with saturated $NaHCO_3$ solution three times and dried over sodium sulfate. After filtration, solvent was removed under reduced pressure. Mercaptopinene was obtain as a mixture of stereoisomers in a purity of 98%. (2% of thioester of pinene, from GC measurements) and used without further purification in the subsequent thiol-ene modification. (Yield: 89%)

ATR-IR: ν (cm^{-1}) = 2985, 2910, 2865, 1468, 1428, 1383, 1366, 1269, 1248, 1229, 1142, 956, 865, 776, 755, 713, 613. ^1H NMR (400 MHz, $CDCl_3$) δ (ppm) = 2.64-2.54,(m,2H), 2.41-2.32 (m, 1H), 2.18-2.09 (m, 1H), 1.99-1.81 (m, 3H), 1.53-1.42 (m, 2H), 1.33-1.24 (m, 1H), 1.19 (s, 3H), 0.97 (s, 3H), 0.90-0.88 (d, 1H). ^{13}C NMR (101 MHz, $CDCl_3$) δ (ppm) = 45.48, 45.43, 41.47, 33.43, 31.58, 28.13, 27.07, 26.23, 23.37, 22.01.

HRMS-EI m/z: $[M-H]^+$ calculated for $[C_{10}H_{17}S]^+$: 169.1045, found 169.1044.

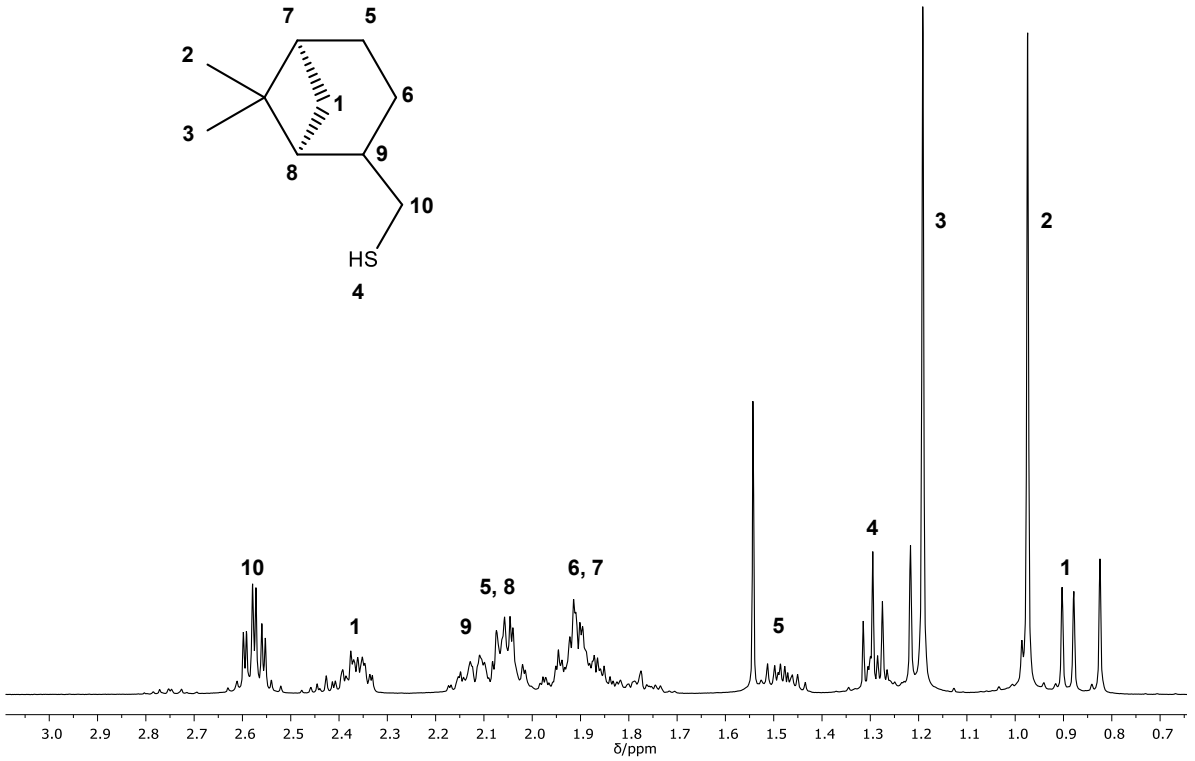

Figure 77: ^{1}H NMR spectrum of (β)-pinene mercaptan.

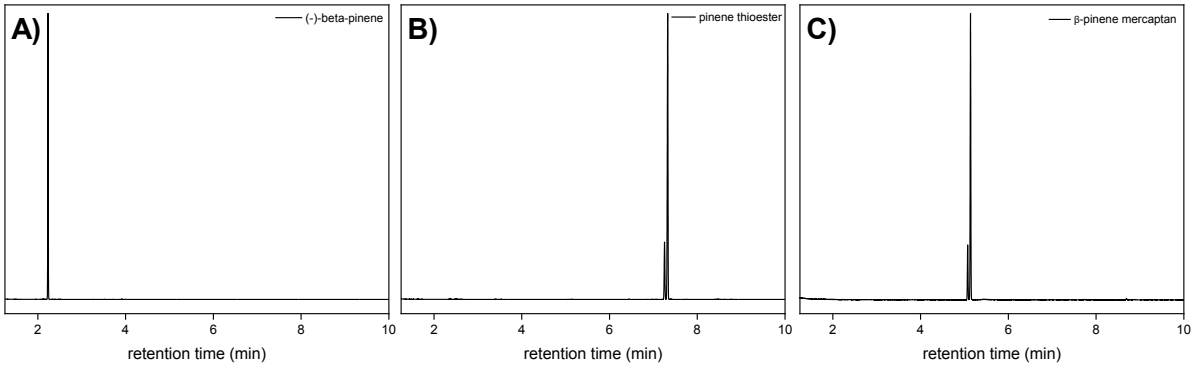

Figure 78: GC chromatograms of **A)** (-)-β-pinene, **B)** β-pinene thioester and **C)** β-pinene mercaptan.

Synthesis of camphene mercaptan

(+)-Camphene (5.00 g, 36.7 mmol) was placed into a round bottom flask and thioacetic acid (3.28 mL, 45.9 mmol) was added slowly. Reaction mixture was stirred at room temperature for 5 hours. After completion of the reaction, excess thioacetic acid was removed under reduced pressure. Subsequently, methanol (15.0 mL, 367 mmol) and concentrated sulfuric acid (0.097 mL, 1.83 mmol) were added, and the

reaction mixture was stirred at 60 °C for 18 hours. Methanol was removed under reduced pressure and organic layer was extracted by ethyl acetate. Organic layer was washed with saturated $NaHCO_3$ solution three times and dried over sodium sulfate. After filtration, solvent was removed under reduced pressure. Mercaptocamphene was obtain as a mixture of stereoisomers in a purity of 99%. (1% of thioester of pinene, from GC measurements) and used without further purification in the subsequent thiol-ene modification. (Yield: 92%)

ATR-IR: *v* (cm^{-1}) = 2951, 2932, 2876, 1739, 1693, 1460, 1387, 1363, 1325, 1299, 1247, 1210, 1152, 1111, 1078, 956, 892, 875, 722. ^1H NMR (400 MHz, $CDCl_3$) δ (ppm) = 2.57-2.45 (m, 2H), 2.35 (br, 1H), 1.77 (br, 1H), 1.66-1.60 (m, 1H), 1.59-1.50 (m, 2H), 1.33-1.22 (m, 4H), 1.21-1.15 (m, 1H), 0.98 (s, 3H), 0.84 (s, 3H). ^{13}C NMR (101 MHz, $CDCl_3$) δ (ppm) = 54.09, 49.52, 40.78, 37.91, 36.80, 32.50, 24.69, 22.83, 21.04, 19.84.

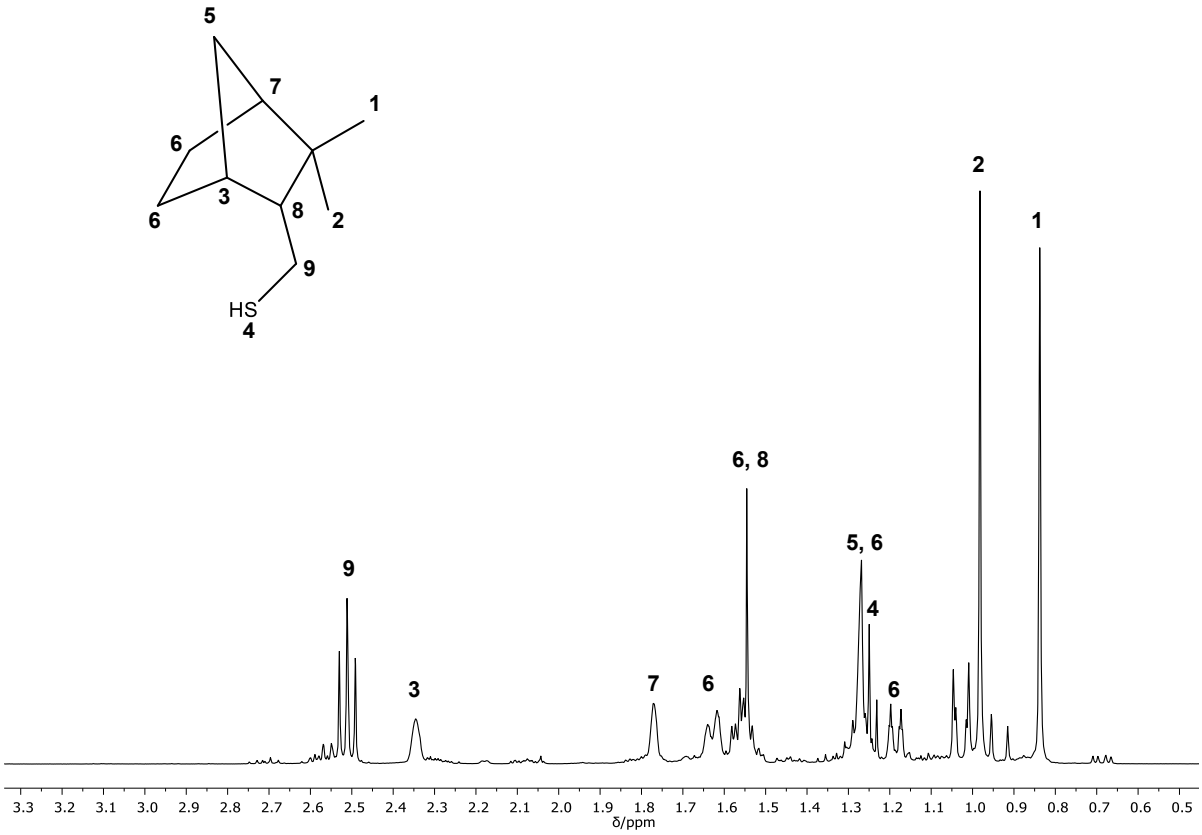

Figure 79: ^1H NMR spectrum of camphene mercaptan.

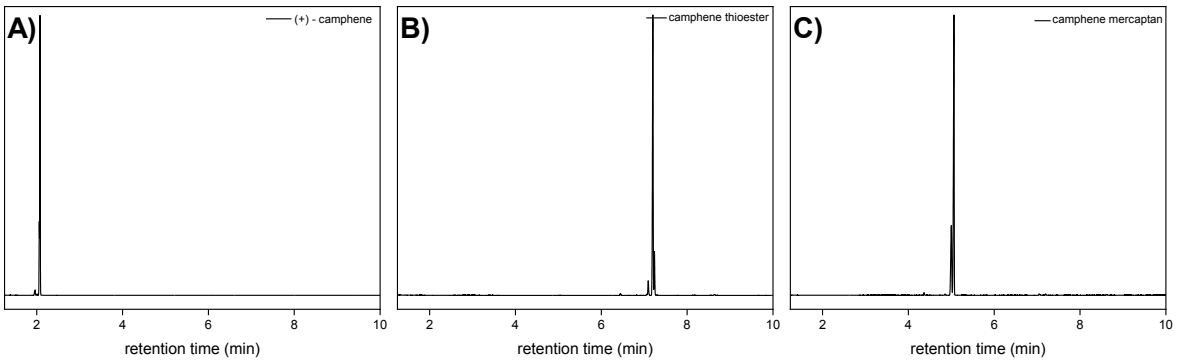

Figure 80: GC chromatograms of **A)** (+)-camphene, **B)** camphene thioester and **C)** camphene mercaptan.

Synthesis of model compound 1

Methyl 10-undecenoate (1.00 mL, 4.44 mmol), 1-butanethiol (0.476 mL, 4.44 mmol) and 2,2-dimethoxy-2-phenylacetophenone (DMPA) (56.8 mg, 0.222 mmol) were mixed in a round bottom flask and stirred under UV light (365 nm) overnight. Purification of the product was done by column chromatography with a mixture of cyclohexane and ethyl acetate, 9:1 with a yield of 97%.

ATR-IR: ν (cm^{-1}) = 2924, 2852, 1740, 1458, 1435, 1361, 1246, 1195, 1168, 1121, 1102, 1011, 913, 880, 746, 721. ^{1}H NMR (400 MHz, $CDCl_3$) δ (ppm) = 3.65 (s, 3H), 2.48 (m, 4H), 2.28 (t, J = 7.5 Hz, 2H), 1.65-1.49 (m, 6H), 1.45-1.32 (m, 4H), 1.31-1.20 (m, 10H), 0.90 (t, 3H). ^{31}C NMR (101 MHz, $CDCl_3$) δ (ppm) = 174.48, 51.59, 34.26, 32.33, 32.01, 31.99, 29.88, 29.59, 29.52, 29.37, 29.28, 29.09,13.86.

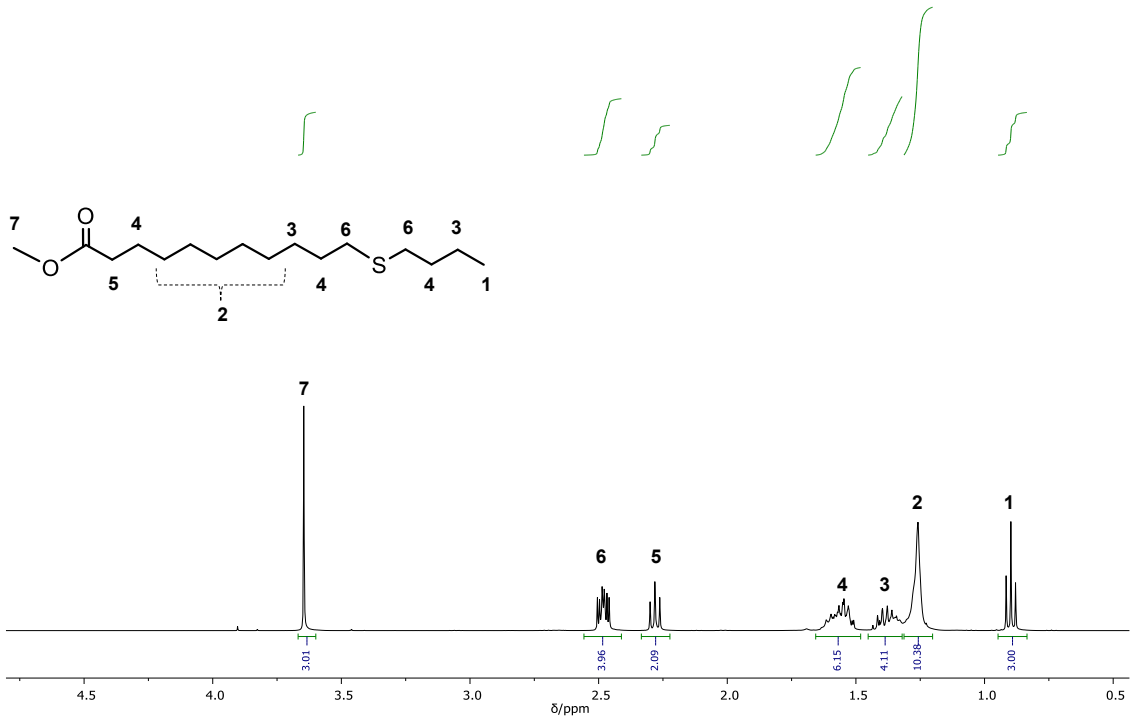

Figure 81: ^{1}H NMR spectrum of model compound 1.

Synthesis of model compound 2

Model compound 1 (500 mg, 1.73 mmol) was dissolved in 2 mL THF and *meta*-chloroperoxybenzoic acid (1.5 g, 8.65 mmol) was added. The reaction mixture was stirred at room temperature overnight. In order to quench remaining oxidizing agent, saturated sodium sulfite solution was added, and the organic layer was extracted by ethyl acetate. The aqueous layer was extracted two additional times. The combined organic layers were washed with 1 M sodium hydroxide solution and dried over sodium sulfate. After filtration, solvent was removed under reduced pressure and product was obtained with 95% yield.

ATR-IR: ν (cm^{-1}) = 2953, 2910, 2871, 2848, 1738, 1470, 1437, 1380, 1314, 1283, 1256, 1201, 1174, 1135, 1096, 1022, 1001, 970, 884, 773, 732, 717, 596, 514, 499, 483, 444, 419. ^{1}H NMR (400 MHz, $CDCl_3$) δ (ppm) = 3.66 (s, 3H), 2.94 (m, 4H), 2.30 (t, J = 7.6 Hz, 2H), 1.87-1.76 (m, 4H), 1.66-1.57 (m, 2H), 1.53-1.37 (m, 4H), 1.36-1.23 (m, 10H), 0.97 (t, J = 7.5 Hz, 3H). ^{13}C NMR (101 MHz, $CDCl_3$) δ (ppm) = 174.46,

52.87, 52.63, 51.60, 34.23, 29.40, 29.31, 29.23, 29.17, 28.65, 25.06, 24.09, 22.08, 21.94, 13.70.

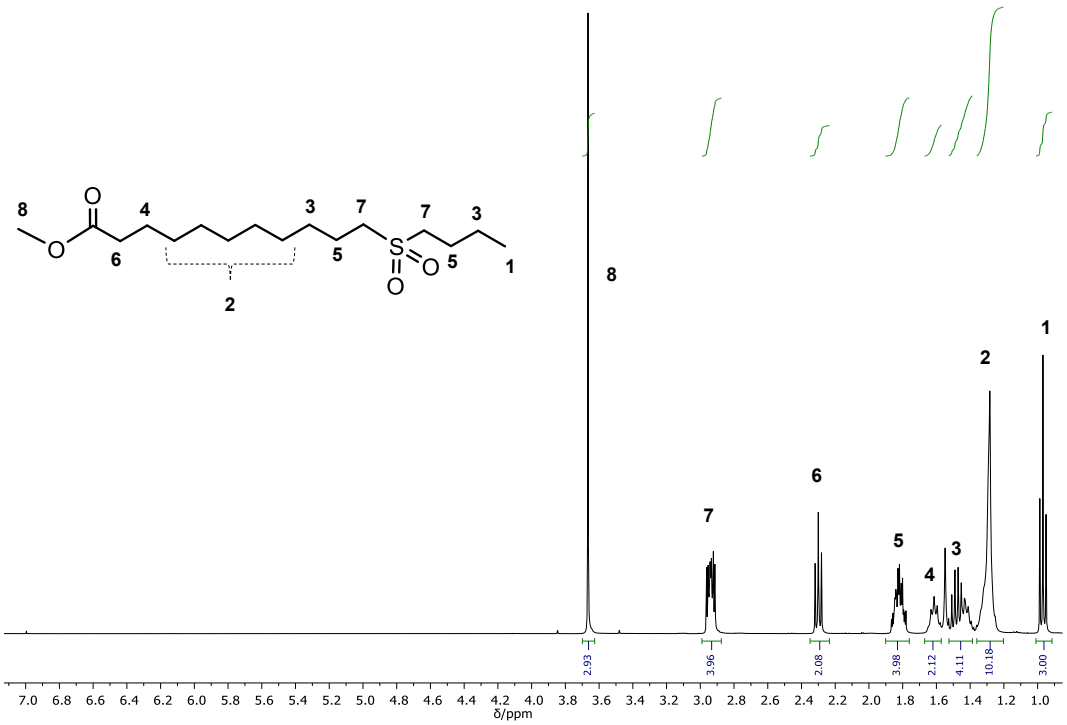

Figure 82: ^{1}H NMR spectrum of model compound 2.

7 Appendix

7.1 Abbreviations

Admim	1-*N*-allyl-2,3-dimethylimidazolium bromide
AGU	Anhydroglucose unit
AMIM	1-Allyl-3-methylimidazolium
ATR-IR	Attenuated total reflectance infrared spectroscopy
BMIM	1-Butyl-3-methylimidazolium
C_4dmim	1-*N*-butyldimethylimidazolium chloride
CMC	carboxymethyl cellulose
COSY	Correlated spectroscopy
Đ	Dispersity
DABCO	1,4-Diazabicyclo[2.2.2]octane
DAC	2,3-Dialdeyhde cellulose
DBN	1,5-Diazabicyclo[4.3.0]non-5-ene
DBU	1,8-Diazabicyclo5.4.0]undec-7-ene
DEC	Diethyl carbonate
DHPM	3,4-Dihydropyrimidin-2-(*1H*)-one
DMAc	Dimethylacetamide
DMAP	4-Dimethylaminopryridine
DMC	Dimethyl carbonate
DMPA	2,2-dimethoxy-2-phenylacetophenone
DMSO	Dimethyl sulfoxide
DO	Degree of oxidation
DP	Degree of polymerization
DS	Degree of substitution
DSC	Differential scanning calorimetry
E	Young's modulus

EMIM	1-*N*-ethyl-3-methylimidazolium
Eq	Equivalents
FACE	Fatty acid cellulose ester
GC	Gas chromatography
HFIP	Hexafluoroisopropanol
HMIM	1-Hexyl-3-methyl imidazolium
IL	Ionic liquid
MCC	Microcrystalline cellulose
*m*CPBA	*meta*-chloroperoxybenzoic acid
MCR	Multicomponent reactions
M_n	Number average molecular weight
MTBD	7-Methyl-1,5,7-triazabicyclo[4.4.0]dec-5-ene
M_w	Weight average molecular weight
NCC	Nanocrystalline cellulose
NFC	Nanofibrillated cellulose
NMMO	*N*-methylmorpholine-*N*-oxide
NMR	Nuclear magnetic resonance
OMIM	1-Octyl-3-methyl imidazolium
P_{8881}	Trioctylphosphonium
P-3CR	Passerini three component reaction
PCL	Polycaprolactone
PEG	Polyethylene glycol
PHA	Polyhydroxyalkanoates
PLA	Polylactic acid
p-TSA	*p*-toluenesulfonic acid
ROP	Ring opening polymerization
SAA	Starch acetoacetate
SBP	Starch Biginelli polymer

SEC	Size exclusion chromatography
t-BAA	*tert*-Butyl acetoacetate
TBAF	Tetrabutylammonium fluoride
TBD	1,5,7-Triazabiycylo[4.4.0]dec-5-ene
TEMPO	(2,2,6,6-Tetramethylpiperidin-1-yl)oxyl
TFA	Trifluoroacetic acid
T_g	Glass transition temperature
TGA	Thermogravimetric analysis
THD	2,2,6-Trimethyl-4H-1,3-dioxin-4-one
THF	Tetrahydrofuran
TMG	1,1,3,3-Tetramethylguadinine
TPS	Thermoplastic starch
Ugi-4CR	Ugi four component reaction
UV	Ultraviolet

7.2 List of Figures

7.3 List of Tables

7.4 Publications

[3] E. Esen, P. Hädinger, M. A. R. Meier, *Sustainable fatty acid modification of cellulose in a CO_2-based switchable solvent system and subsequent thiol-ene modification*, *Biomacromolecules,* **2020**.

[2] E. Esen, M. A. R. Meier, *Sustainable functionalization of 2,3-dialdehyde cellulose via the Passerini three component reaction*, *ACS Sustainable Chem. Eng.*, **2020**, 8, 41, 15755

[1] E. Esen, M. A. R. Meier, *Modification of starch via the Biginelli reaction*, *Macromol. Rapid Commun.*, **2020**, 41, 1900375.

7.5 Conference Contributions

Modification of starch via the Biginelli reaction, Oral presentation at the Macromolecular Colloquium Freiburg 2020, 26-28th February 2020, Freiburg, Germany.

Modification of starch via the Biginelli reaction, Poster presentation at the 6th International Symposium Frontiers in Polymer Science, 5-8th May 2019, Budapest, Hungary.

Modification of starch via the Biginelli reaction, Poster presentation at the 10th Workshop on Fats and Oils as Renewable Feedstock for the Chemical Industry, 17-19th March 2019, Karlsruhe, Germany.

8 Bibliography

[1] retrieved 15.10.2020, World Population Prospects 2019, can be found under https://population.un.org/wpp/Publications/Files/WPP2019_Highlights.pdf.

[2] retrieved 23.10.2020, Statistical Review of World Energy 2020, can be found under https://www.bp.com/content/dam/bp/business-sites/en/global/corporate/pdfs/energy-economics/statistical-review/bp-stats-review-2020-full-report.pdf.

[3] retrieved 23.10.2020, Plastics- the Facts 2019, can be found under https://www.plasticseurope.org/application/files/9715/7129/9584/FINAL_web_version_Plastics_the_facts2019_14102019.pdf.

[4] retrieved 18.10.2020, The New Plastics Economy, can be found under http://www3.weforum.org/docs/WEF_The_New_Plastics_Economy.pdf..

[5] retrieved 21.10.2020, the 2030 Agenda for Sustainable Development, can be found under https://sustainabledevelopment.un.org/post2015/transformingourworld.

[6] P. T. Anastas, J. B. Zimmerman, ACS Publications, **2003**.

[7] M. Pelckmans, T. Renders, S. Van de Vyver, B. F. Sels, *Green Chem.* **2017**, *19*, 5303-5331.

[8] Y. Zhu, C. Romain, C. K. Williams, *Nature* **2016**, *540*, 354-362.

[9] R. A. Sheldon, *Green Chem.* **2014**, *16*, 950-963.

[10] D. Klemm, B. Heublein, H.-P. Fink, A. Bohn, *Angew. Chem. Int. Ed.* **2005**, *44*, 3358-3393.

[11] A. Payen, *C.R. Hebd. Seances Acad. Sci.* **1838**, *7*, 1052.

[12] A. Payen, *C.R. Hebd. Seances Acad. Sci.* **1838**, *7*, 1125.

[13] H. Staudinger, *Ber. Dtsch. Chem. Ges.* **1920**, *53*, 1073.

[14] J. W. Hyatt, *Billiard-balls*, **1865**, US Patent 50,539.

[15] W. G. Ferrier, *Acta Cryst* **1963**, *16*, 1023-1031.

[16] H. Tao, N. Lavoine, F. Jiang, J. Tang, N. Lin, *Nanoscale Horizons* **2020**, *5*, 607-627.

[17] F. Lin, F. Cousin, J.-L. Putaux, B. Jean, *ACS Macro Lett.* **2019**, *8*, 345-351.

[18] H. Kamitakahara, Y. Enomoto, C. Hasegawa, F. Nakatsubo, *Cellulose* **2005**, *12*, 527-541.

[19] C. Tang, S. Spinney, Z. Shi, J. Tang, B. Peng, J. Luo, K. C. Tam, *Langmuir* **2018**, *34*, 12897-12905.

[20] S. Imlimthan, S. Otaru, O. Keinänen, A. Correia, K. Lintinen, H. A. Santos, A. J. Airaksinen, M. A. Kostiainen, M. Sarparanta, *Biomacromolecules* **2019**, *20*, 674-683.

[21] N.-H. Kim, T. Imai, M. Wada, J. Sugiyama, *Biomacromolecules* **2006**, *7*, 274-280.

[22] K. Heise, T. Koso, L. Pitkänen, A. Potthast, A. W. T. King, M. A. Kostiainen, E. Kontturi, *ACS Macro Lett.* **2019**, *8*, 1642-1647.

[23] K. Heise, G. Delepierre, A. W. T. King, M. A. Kostiainen, J. Zoppe, C. Weder, E. Kontturi, *Angew. Chem. Int. Ed.*, **2021**, 60, 6-87.

[24] A. Richter, D. Klemm, *Cellulose* **2003**, *10*, 133-138.

[25] T. Groth, W. Wagenknecht, *Biomaterials* **2001**, *22*, 2719-2729.

[26] D. Xu, B. Li, C. Tate, K. J. Edgar, *Cellulose* **2011**, *18*, 405-419.

[27] R. J. Moon, A. Martini, J. Nairn, J. Simonsen, J. Youngblood, *Chem. Soc. Rev.* **2011**, *40*, 3941-3994.

[28] D. Klemm, F. Kramer, S. Moritz, T. Lindström, M. Ankerfors, D. Gray, A. Dorris, *Angew. Chem. Int. Ed.* **2011**, *50*, 5438-5466.

[29] A. C. O'Sullivan, *Cellulose* **1997**, *4*, 173-207.

[30] R. H. Atallla, D. L. Vanderhart, *Science* **1984**, *223*, 283-285.

[31] T. Kuto, *Z. Physik. Chem B* **1941**, *49*, 235.

[32] H. A. Krässig, *Cellulose : Structure, Accessibility, and Reactivity*, Gordon and Breach Science Publisher, Yverdon, **1993**.

[33] D. Roy, M. Semsarilar, J. T. Guthrie, S. Perrier, *Chem. Soc. Rev.* **2009**, *38*, 2046-2064.

[34] Z. Zhang, J. Song, B. Han, *Chem. Rev.* **2017**, *117*, 6834-6880.

[35] V. Menon, M. Rao, *Prog. Energy Combust. Sci.* **2012**, *38*, 522-550.

[36] C. Li, X. Zhao, A. Wang, G. W. Huber, T. Zhang, *Chem. Rev.* **2015**, *115*, 11559-11624.

[37] B. M. Upton, A. M. Kasko, *Chem. Rev.* **2016**, *116*, 2275-2306.

[38] F. Cherubini, *Energy Convers. Manage.* **2010**, *51*, 1412-1421.

[39] F. H. Isikgor, C. R. Becer, *Polym. Chem.* **2015**, *6*, 4497-4559.

[40] C.-H. Zhou, X. Xia, C.-X. Lin, D.-S. Tong, J. Beltramini, *Chem. Soc. Rev.* **2011**, *40*, 5588-5617.

[41] T. Abbasi, S. A. Abbasi, *Renew. Sust. Energ. Rev.* **2010**, *14*, 919-937.

[42] M. Ek, G. Gellerstedt, G. Henriksson, *Pulping chemistry and technology, Vol. 2*, Walter de Gruyter, Berlin, **2009**.

[43] C. V. Stevens, R. Verhé, *Renewable bioresources: scope and modification for non-food applications*, John Wiley & Sons, **2004**.

[44] E. Sjostrom, *Wood Chemistry: Fundamentals and Applications*, Academic Press, California, **1993**.

[45] M. Ragnar, G. Henriksson, M. E. Lindström, M. Wimby, R. Süttinger, *Ullmann's Encyclopedia of Industrial Chemistry* **2000**, 1-89.

[46] J. Zakzeski, P. C. A. Bruijnincx, A. L. Jongerius, B. M. Weckhuysen, *Chem. Rev.* **2010**, *110*, 3552-3599.

[47] C. F. Schoenbein, *Pogg. Ann* **1846**, *70*, 220.

[48] C. Schönbein, *Ber. Naturforsch. Ges. Basel* **1847**, *7*, 27.

[49] A. M. Chardonnet, **1884**, French Patent 165,349.

[50] J.-L. Wertz, O. Bédué, J. P. Mercier, *Cellulose science and technology*, EPFL press, **2010**.

[51] T. Heinze, T. Liebert, in *Polymer Science: A Comprehensive Reference* (Eds.: K. Matyjaszewski, M. Möller), Elsevier, Amsterdam, **2012**, pp. 83-152.

[52] J. Schuetzenberger, *Compt. rend. Acad. Sciences* **1865**, *61*, 485.

[53] K. J. Edgar, *Cellulose Esters, Organic*, Wiley, New York, **2004**.

[54] T. Heinze, O. A. El Seoud, A. Koschella, in *Cellulose Derivatives: Synthesis, Structure, and Properties*, Springer International Publishing, Cham, **2018**, pp. 39-172.

[55] M. T. Holtzapple, in *Encyclopedia of Food Sciences and Nutrition (Second Edition)* (Ed.: B. Caballero), Academic Press, Oxford, **2003**, pp. 998-1007.

[56] T. Heinze, O. A. El Seoud, A. Koschella, in *Cellulose Derivatives: Synthesis, Structure, and Properties*, Springer International Publishing, Cham, **2018**, pp. 479-531.

[57] E. C. Yackel, W. O. Kenyon, *J. Am. Chem. Soc.* **1942**, *64*, 121-127.

[58] E. E. Johansson, J. Lind, *J. Wood Chem. Technol.* **2005**, *25*, 171-186.

[59] T. J. Painter, *Carbohydr. Res.* **1977**, *55*, 95-103.

[60] I. Borisov, E. Shirokova, R. K. Mudarisova, R. Muslukhov, Y. S. Zimin, S. Medvedeva, G. Tolstikov, Y. B. Monakov, *Russ. Chem. Bull.* **2004**, *53*, 318-324.

[61] M. S. Manhas, F. Mohammed, *Colloids Surf. A Physicochem. Eng. Asp.* **2007**, *295*, 165-171.

[62] P. Calvini, A. Gorassini, G. Luciano, E. Franceschi, *Vib. Spectrosc* **2006**, *40*, 177-183.

[63] U.-J. Kim, S. Kuga, M. Wada, T. Okano, T. Kondo, *Biomacromolecules* **2000**, *1*, 488-492.

[64] A. E. J. de Nooy, A. C. Besemer, H. van Bekkum, *Recl. Trav. Chim. Pays-Bas* **1994**, *113*, 165-166.

[65] R. A. A. Muzzarelli, C. Muzzarelli, A. Cosani, M. Terbojevich, *Carbohydr. Polym.* **1999**, *39*, 361-367.

[66] C. Tahiri, M. R. Vignon, *Cellulose* **2000**, *7*, 177-188.

[67] S. Camy, S. Montanari, A. Rattaz, M. Vignon, J. S. Condoret, *The Journal of Supercritical Fluids* **2009**, *51*, 188-196.

[68] T. Saito, Y. Nishiyama, J.-L. Putaux, M. Vignon, A. Isogai, *Biomacromolecules* **2006**, *7*, 1687-1691.

[69] T. Saito, Y. Okita, T. T. Nge, J. Sugiyama, A. Isogai, *Carbohydr. Polym.* **2006**, *65*, 435-440.

[70] Y. Jin, K. J. Edler, F. Marken, J. L. Scott, *Green Chem.* **2014**, *16*, 3322-3327.

[71] C. Geng, Z. Zhao, Z. Xue, P. Xu, Y. Xia, *Molecules* **2019**, *24*, 1947.

[72] S. Gomez-Bujedo, E. Fleury, M. R. Vignon, *Biomacromolecules* **2004**, *5*, 565-571.

[73] N. Bordenave, S. Grelier, V. Coma, *Biomacromolecules* **2008**, *9*, 2377-2382.

[74] T. Saito, A. Isogai, *Colloids Surf. A Physicochem. Eng. Asp.* **2006**, *289*, 219-225.

[75] D. J. Mendoza, C. Browne, V. S. Raghuwanshi, G. P. Simon, G. Garnier, *Carbohydr. Polym.* **2019**, *226*, 115292.

[76] S. Coseri, G. Biliuta, L. F. Zemljič, J. S. Srndovic, P. T. Larsson, S. Strnad, T. Kreže, A. Naderi, T. Lindström, *RSC Advances* **2015**, *5*, 85889-85897.

[77] E. Schacht, M. Nobels, S. Vansteenkiste, J. Demeester, J. Franssen, A. Lemahieu, *Polym. Gels Networks* **1993**, *1*, 213-224.

[78] D. Bruneel, E. Schacht, *Polymer* **1993**, *34*, 2628-2632.

[79] A. J. Varma, Y. K. Jamdade, V. M. Nadkarni, *Polym. Degrad. Stab.* **1985**, *13*, 91-98.

[80] U.-J. Kim, M. Wada, S. Kuga, *Carbohydr. Polym.* **2004**, *56*, 7-10.

[81] E. Maekawa, *J. Appl. Polym. Sci.* **1991**, *43*, 417-422.

[82] J. A. Sirviö, A. Kolehmainen, M. Visanko, H. Liimatainen, J. Niinimäki, O. E. O. Hormi, *ACS Appl. Mater. Interfaces* **2014**, *6*, 14384-14390.

[83] H. Zhang, P. Liu, S. M. Musa, C. Mai, K. Zhang, *ACS Sustainable Chem. Eng.* **2019**, *7*, 10452-10459.

[84] M. Wu, S. Kuga, *J. Appl. Polym. Sci.* **2006**, *100*, 1668-1672.

[85] J. Sirvio, U. Hyvakko, H. Liimatainen, J. Niinimaki, O. Hormi, *Carbohydr. Polym.* **2011**, *83*, 1293-1297.

[86] J. Sirviö, H. Liimatainen, J. Niinimäki, O. Hormi, *Carbohydr. Polym.* **2011**, *86*, 260-265.

[87] H. Liimatainen, J. Sirviö, H. Pajari, O. Hormi, J. Niinimäki, *J. Wood Chem. Technol.* **2013**, *33*, 258-266.

[88] S. Koprivica, M. Siller, T. Hosoya, W. Roggenstein, T. Rosenau, A. Potthast, *ChemSusChem* **2016**, *9*, 825-833.

[89] S. F. Plappert, S. Quraishi, N. Pircher, K. S. Mikkonen, S. Veigel, K. M. Klinger, A. Potthast, T. Rosenau, F. W. Liebner, *Biomacromolecules* **2018**, *19*, 2969-2978.

[90] L. Münster, J. Vícha, J. Klofáč, M. Masař, P. Kucharczyk, I. Kuřitka, *Cellulose* **2017**, *24*, 2753-2766.

[91] G. Yan, X. Zhang, M. Li, X. Zhao, X. Zeng, Y. Sun, X. Tang, T. Lei, L. Lin, *ACS Sustainable Chem. Eng.* **2019**, *7*, 2151-2159.

[92] Q. G. Fan, D. M. Lewis, K. N. Tapley, *J. Appl. Polym. Sci.* **2001**, *82*, 1195-1202.

[93] H. Spedding, *Journal of the Chemical Society (Resumed)* **1960**, 3147-3152.

[94] U.-J. Kim, S. Kuga, *Cellulose* **2000**, *7*, 287-297.

[95] E. Maekawa, T. Koshijima, *J. Appl. Polym. Sci.* **1984**, *29*, 2289-2297.

[96] P. A. Larsson, L. A. Berglund, L. Wågberg, *Biomacromolecules* **2014**, *15*, 2218-2223.

[97] P. A. Larsson, L. A. Berglund, L. Wågberg, *Cellulose* **2014**, *21*, 323-333.

[98] W. Kasai, T. Morooka, M. Ek, *Cellulose* **2014**, *21*, 769-776.

[99] U.-J. Kim, S. Kuga, *J. Chromatogr. A* **2001**, *919*, 29-37.

[100] X. Huang, G. Dognani, P. Hadi, M. Yang, A. E. Job, B. S. Hsiao, *ACS Sustainable Chem. Eng.* **2020**, *8*, 4734-4744.

[101] L. Jin, W. Li, Q. Xu, Q. Sun, *Cellulose* **2015**, *22*, 2443-2456.

[102] P. Liu, C. Mai, K. Zhang, *ACS Sustainable Chem. Eng.* **2017**, *5*, 5313-5319.

[103] J. Sirviö, A. Honka, H. Liimatainen, J. Niinimäki, O. Hormi, *Carbohydr. Polym.* **2011**, *86*, 266-270.

[104] M. Visanko, H. Liimatainen, J. A. Sirviö, J. P. Heiskanen, J. Niinimäki, O. Hormi, *Biomacromolecules* **2014**, *15*, 2769-2775.

[105] Z. Sabzalian, M. N. Alam, T. G. M. van de Ven, *Cellulose* **2014**, *21*, 1381-1393.

[106] T. Nikolic, M. Kostic, J. Praskalo, B. Pejic, Z. Petronijevic, P. Skundric, *Carbohydr. Polym.* **2010**, *82*, 976-981.

[107] N. Isobe, D.-S. Lee, Y.-J. Kwon, S. Kimura, S. Kuga, M. Wada, U.-J. Kim, *Cellulose* **2011**, *18*, 1251.

[108] M. Lv, X. Ma, D. P. Anderson, P. R. Chang, *Cellulose* **2018**, *25*, 233-243.

[109] R. Wu, B.-H. He, G.-L. Zhao, L.-Y. Qian, X.-F. Li, *Carbohydr. Polym.* **2013**, *97*, 523-529.

[110] S. V. Kanth, A. Ramaraj, J. R. Rao, B. U. Nair, *Process Biochem.* **2009**, *44*, 869-874.

[111] K. Song, H. Xu, K. Xie, Y. Yang, *ACS Sustainable Chem. Eng.* **2017**, *5*, 5669-5678.

[112] M. N. Alam, L. P. Christopher, *ACS Sustainable Chem. Eng.* **2018**, *6*, 8736-8742.

[113] U.-J. Kim, Y. R. Lee, T. H. Kang, J. W. Choi, S. Kimura, M. Wada, *Carbohydr. Polym.* **2017**, *163*, 34-42.

[114] S. Han, M. Lee, *J. Appl. Polym. Sci.* **2009**, *112*, 709-714.

[115] A. Codou, N. Guigo, L. Heux, N. Sbirrazzuoli, *Compos. Sci. Technol.* **2015**, *117*, 54-61.

[116] E. Schweizer, *J. Prakt.Chem.* **1857**, *72*, 109-111.

[117] C. F. Cross, E. J. Bevan, C. Beadle, *Viscose syndicate*, **1892**, British Patent 8,700.

[118] L. W. McKeen, in *The Effect of UV Light and Weather on Plastics and Elastomers (Fourth Edition)* (Ed.: L. W. McKeen), William Andrew Publishing, **2019**, pp. 425-438.

[119] D. L. Johnson, *Compounds dissolved in cyclic amine oxides*, **1969**, US Patent 3447956A.

[120] C. L. McCormick, D. K. Lichatowich, *Journal of Polymer Science: Polymer Letters Edition* **1979**, *17*, 479-484.

[121] C. Graenacher, *Cellulose solution*, **1934**, US Patent 1,943,176.

[122] G. T. Ciacco, T. F. Liebert, E. Frollini, T. J. Heinze, *Cellulose* **2003**, *10*, 125-132.

[123] M. T. Clough, *Green Chem.* **2017**, *19*, 4754-4768.

[124] A. W. T. King, J. Asikkala, I. Mutikainen, P. Järvi, I. Kilpeläinen, *Angew. Chem. Int. Ed.* **2011**, *50*, 6301-6305.

[125] J. Zhang, J. Wu, J. Yu, X. Zhang, J. He, J. Zhang, *Materials Chemistry Frontiers* **2017**, *1*, 1273-1290.

[126] M. Gericke, P. Fardim, T. Heinze, *Molecules* **2012**, *17*, 7458-7502.

[127] J. Wu, J. Zhang, H. Zhang, J. He, Q. Ren, M. Guo, *Biomacromolecules* **2004**, *5*, 266-268.

[128] Y. Luan, J. Zhang, M. Zhan, J. Wu, J. Zhang, J. He, *Carbohydr. Polym.* **2013**, *92*, 307-311.

[129] S. Barthel, T. Heinze, *Green Chem.* **2006**, *8*, 301-306.

[130] T. Kakko, A. W. T. King, I. Kilpeläinen, *Cellulose* **2017**, *24*, 5341-5354.

[131] A. Parviainen, R. Wahlström, U. Liimatainen, T. Liitiä, S. Rovio, J. K. J. Helminen, U. Hyväkkö, A. W. T. King, A. Suurnäkki, I. Kilpeläinen, *RSC Advances* **2015**, *5*, 69728-69737.

[132] O. Jogunola, V. Eta, M. Hedenström, O. Sundman, T. Salmi, J.-P. Mikkola, *Carbohydr. Polym.* **2016**, *135*, 341-348.

[133] C. F. Liu, R. C. Sun, A. P. Zhang, J. L. Ren, Z. C. Geng, *Polym. Degrad. Stab.* **2006**, *91*, 3040-3047.

[134] W. Li, A. Jin, C. Liu, R. Sun, A. Zhang, J. Kennedy, *Carbohydr. Polym.* **2009**, *78*, 389-395.

[135] S. R. Labafzadeh, K. J. Helminen, I. Kilpeläinen, A. W. T. King, *ChemSusChem* **2015**, *8*, 77-81.

[136] S. Paunonen, *Biores.*, **2013**, *8*, 3098-3121.

[137] Z. Söyler, M. A. R. Meier, *Green Chem.* **2017**, *19*, 3899-3907.

[138] P. G. Jessop, D. J. Heldebrant, X. Li, C. A. Eckert, C. L. Liotta, *Nature* **2005**, *436*, 1102-1102.

[139] H. Xie, X. Yu, Y. Yang, Z. K. Zhao, *Green Chem.* **2014**, *16*, 2422-2427.

[140] Q. Zhang, N. S. Oztekin, J. Barrault, K. De Oliveira Vigier, F. Jérôme, *ChemSusChem* **2013**, *6*, 593-596.

[141] K. N. Onwukamike, T. Tassaing, S. Grelier, E. Grau, H. Cramail, M. A. R. Meier, *ACS Sustainable Chem. Eng.* **2018**, *6*, 1496-1503.

[142] Y. Yang, H. Xie, E. Liu, *Green Chem.* **2014**, *16*, 3018-3023.

[143] Y. Yang, L. Song, C. Peng, E. Liu, H. Xie, *Green Chem.* **2015**, *17*, 2758-2763.

[144] L. Song, Y. Yang, H. Xie, E. Liu, *ChemSusChem* **2015**, *8*, 3217-3221.

[145] Z. Söyler, K. N. Onwukamike, S. Grelier, E. Grau, H. Cramail, M. A. R. Meier, *Green Chem.* **2018**, *20*, 214-224.

[146] X. Yin, C. Yu, X. Zhang, J. Yang, Q. Lin, J. Wang, Q. Zhu, *Polym. Bull.* **2011**, *67*, 401-412.

[147] M. Pei, X. Peng, Y. Shen, Y. Yang, Y. Guo, Q. Zheng, H. Xie, H. Sun, *Green Chem.* **2020**, *22*, 707-717.

[148] K. N. Onwukamike, S. Grelier, E. Grau, H. Cramail, M. A. R. Meier, *ACS Sustainable Chem. Eng.* **2018**, *6*, 8826-8835.

[149] H. Chen, F. Yang, J. Du, H. Xie, L. Zhang, Y. Guo, Q. Xu, Q. Zheng, N. Li, Y. Liu, *Cellulose* **2018**, *25*, 6935-6945.

[150] K. N. Onwukamike, L. Lapuyade, L. Maillé, S. Grelier, E. Grau, H. Cramail, M. A. R. Meier, *ACS Sustainable Chem. Eng.* **2019**, *7*, 3329-3338.

[151] L. Jin, J. Gan, G. Hu, L. Cai, Z. Li, L. Zhang, Q. Zheng, H. Xie, *Polymers* **2019**, *11*, 994.

[152] H. J. Endres, A. Siebert-Raths, in *Polymer Science: A Comprehensive Reference* (Eds.: K. Matyjaszewski, M. Möller), Elsevier, Amsterdam, **2012**, pp. 317-353.

[153] W. R. Morrison, J. Karkalas, in *Methods in Plant Biochemistry, Vol. 2* (Ed.: P. M. Dey), Academic Press, **1990**, pp. 323-352.

[154] W. Bergthaller, J. Hollmann, in *Comprehensive Glycoscience* (Ed.: H. Kamerling), Elsevier, Oxford, **2007**, pp. 579-612.

[155] R. F. Tester, J. Karkalas, X. Qi, *J. Cereal Sci.* **2004**, *39*, 151-165.

[156] A. Buléon, P. Colonna, V. Planchot, S. Ball, *Int. J. Biol. Macromol.* **1998**, *23*, 85-112.

[157] J. F. Robyt, in *Glycoscience: Chemistry and Chemical Biology* (Eds.: B. O. Fraser-Reid, K. Tatsuta, J. Thiem), Springer Berlin Heidelberg, Berlin, Heidelberg, **2008**, pp. 1437-1472.

[158] D. French, in *Starch: Chemistry and Technology (Second Edition)* (Eds.: R. L. Whistler, J. N. Bemiller, E. F. Paschall), Academic Press, San Diego, **1984**, pp. 183-247.

[159] C. M. Brites, C. A. L. d. Santos, A. S. Bagulho, M. L. Beirão-da-Costa, *Eur. Food Res. Technol.* **2008**, *226*, 1205-1212.

[160] T. J. Schoch, *J. Am. Chem. Soc.* **1942**, *64*, 2957-2961.

[161] S. Kim, J. L. Willett, *Starch - Stärke* **2004**, *56*, 29-36.

[162] D. Lourdin, H. Bizot, P. Colonna, *J. Appl. Polym. Sci.* **1997**, *63*, 1047-1053.

[163] D. Lourdin, L. Coignard, H. Bizot, P. Colonna, *Polymer* **1997**, *38*, 5401-5406.

[164] J.-l. Wang, F. Cheng, P.-x. Zhu, *Carbohydr. Polym.* **2014**, *101*, 1109-1115.

[165] H. Liu, D. Chaudhary, G. Ingram, J. John, *J. Polym. Sci., Part B: Polym. Phys.* **2011**, *49*, 1041-1049.

[166] R. L. Whistler, in *Starch: Chemistry and Technology (Second Edition)* (Eds.: R. L. Whistler, J. N. Bemiller, E. F. Paschall), Academic Press, San Diego, **1984**, pp. 1-9.

[167] C. Rivard, L. Moens, K. Roberts, J. Brigham, S. Kelley, *Enzyme Microb. Technol.* **1995**, *17*, 848-852.

[168] J. Zhou, L. Ren, J. Tong, Y. Ma, *J. Appl. Polym. Sci.* **2009**, *114*, 940-947.

[169] Y.-S. Jeon, A. V. Lowell, R. A. Gross, *Starch - Stärke* **1999**, *51*, 90-93.

[170] T. Liebert, W. M. Kulicke, T. Heinze, *React. Funct. Polym.* **2008**, *68*, 1-11.

[171] R. L. Shogren, A. Biswas, *Carbohydr. Polym.* **2010**, *81*, 149-151.

[172] L. Junistia, A. K. Sugih, R. Manurung, F. Picchioni, L. P. B. M. Janssen, H. J. Heeres, *Starch - Stärke* **2008**, *60*, 667-675.

[173] A. D. Sagar, E. W. Merrill, *J. Appl. Polym. Sci.* **1995**, *58*, 1647-1656.

[174] Z. Söyler, M. A. R. Meier, *ChemSusChem* **2017**, *10*, 182-188.

[175] K. B. Wesslén, B. Wesslén, *Carbohydr. Polym.* **2002**, *47*, 303-311.

[176] A. Bayazeed, S. Farag, S. Shaarawy, A. Hebeish, *Starch - Stärke* **1998**, *50*, 89-93.

[177] L. Kuniak, R. H. Marchessault, *Starch - Stärke* **1972**, *24*, 110-116.

[178] P. G. Seligra, C. Medina Jaramillo, L. Famá, S. Goyanes, *Carbohydr. Polym.* **2016**, *138*, 66-74.

[179] P.-H. Elchinger, D. Montplaisir, R. Zerrouki, *Carbohydr. Polym.* **2012**, *87*, 1886-1890.

[180] M. Çelik, *Journal of Polymer Research* **2006**, *13*, 427-432.

[181] L. Rahman, S. Silong, W. M. Zin, M. Z. A. Rahman, M. Ahmad, J. Haron, *J. Appl. Polym. Sci.* **2000**, *76*, 516-523.

[182] P. S. Chang, J. F. Robyt, *J. Carbohydr. Chem.* **1996**, *15*, 819-830.

[183] R. L. Whistler, R. Schweiger, *J. Am. Chem. Soc.* **1957**, *79*, 6460-6464.

[184] F. Felton, *Cereal Chem.* **1938**, *15*, 678.

[185] E. L. Jackson, C. Hudson, *J. Am. Chem. Soc.* **1938**, *60*, 989-991.

[186] R. E. Wing, J. L. Willett, *Ind Crops Prod* **1997**, *7*, 45-52.

[187] R. Mani, M. Bhattacharya, *Eur. Polym. J.* **2001**, *37*, 515-526.

[188] S.-Y. Yang, C.-Y. Huang, *J. Appl. Polym. Sci.* **2008**, *109*, 2452-2459.

[189] C.-H. Kim, E.-J. Choi, J.-K. Park, *J. Appl. Polym. Sci.* **2000**, *77*, 2049-2056.

[190] C. Bastioli, A. Cerutti, I. Guanella, G. Romano, M. Tosin, *Journal of environmental polymer degradation* **1995**, *3*, 81-95.

[191] Y. Parulekar, A. K. Mohanty, *Macromol. Mater. Eng.* **2007**, *292*, 1218-1228.

[192] J. W. Park, S. S. Im, S. H. Kim, Y. H. Kim, *Polymer Engineering & Science* **2000**, *40*, 2539-2550.

[193] A. Dömling, I. Ugi, *Angew. Chem. Int. Ed.* **2000**, *39*, 3168-3210.

[194] A. Dömling, *Chem. Rev.* **2006**, *106*, 17-89.

[195] S. Brauch, S. S. van Berkel, B. Westermann, *Chem. Soc. Rev.* **2013**, *42*, 4948-4962.

[196] A. Sehlinger, M. A. R. Meier, in *Multi-Component and Sequential Reactions in Polymer Synthesis* (Ed.: P. Theato), Springer International Publishing, Cham, **2015**, pp. 61-86.

[197] A. Llevot, A. C. Boukis, S. Oelmann, K. Wetzel, M. A. R. Meier, in *Polymer Synthesis Based on Triple-bond Building Blocks* (Eds.: B. Z. Tang, R. Hu), Springer International Publishing, Cham, **2018**, pp. 127-155.

[198] A. Strecker, *Justus Liebigs Ann. Chem.* **1850**, *75*, 27-45.

[199] A. Hantzsch, *Justus Liebigs Ann. Chem.* **1882**, *215*, 1-82.

[200] A. Hantzsch, *Ber. Dtsch. Chem. Ges.* **1890**, *23*, 1474-1476.

[201] P. Biginelli, *Ber. Dtsch. Chem. Ges.* **1891**, *24*, 1317-1319.

[202] C. Mannich, W. Krösche, *Arch. Pharm.* **1912**, *250*, 647-667.

[203] F. Asinger, *Angew. Chem* **1956**, *68*, 376-389.

[204] P. Biginelli, *Ber Deutsch Chem Ges* **1893**, *26*, 447-450.

[205] C. O. Kappe, *J. Org. Chem.* **1997**, *62*, 7201-7204.

[206] C. O. Kappe, *Eur. J. Med. Chem.* **2000**, *35*, 1043-1052.

[207] G. C. Rovnyak, K. S. Atwal, A. Hedberg, S. D. Kimball, S. Moreland, J. Z. Gougoutas, B. C. O'Reilly, J. Schwartz, M. F. Malley, *J. Med. Chem.* **1992**, *35*, 3254-3263.

[208] S. Suresh, J. S. Sandhu, *ChemInform* **2012**, *43*, no-no.

[209] R. W. Lewis, J. Mabry, J. G. Polisar, K. P. Eagen, B. Ganem, G. P. Hess, *Biochemistry* **2010**, *49*, 4841-4851.

[210] M. Passerini, L. Simone, *Gazz. Chim. Ital.* **1921**, *51* 126-129.

[211] I. Ugi, R. Meyr, C. Steinbruckner, *Angew. Chem.* **1959**, *71*, 373-388.

[212] I. Ugi, C. Steinbrückner, *Angew. Chem.* **1960**, *72*, 267-268.

[213] I. Ugi, R. Meyr, *Chem. Ber.* **1961**, *94*, 2229-2233.

[214] R. H. Baker, D. Stanonis, *J. Am. Chem. Soc.* **1951**, *73*, 699-702.

[215] E. Esen, M. A. R. Meier, *Macromol. Rapid Commun.* **2020**, *41*, 1900375.

[216] A. E. J. de Nooy, D. Capitani, G. Masci, V. Crescenzi, *Biomacromolecules* **2000**, *1*, 259-267.

[217] A. E. J. de Nooy, G. Masci, V. Crescenzi, *Macromolecules* **1999**, *32*, 1318-1320.

[218] Y. Y. Khine, S. Ganda, M. H. Stenzel, *ACS Macro Lett.* **2018**, *7*, 412-418.

[219] A. Pettignano, A. Daunay, C. Moreau, B. Cathala, A. Charlot, E. Fleury, *ACS Sustainable Chem. Eng.* **2019**, *7*, 14685-14696.

[220] E. Esen, M. A. R. Meier, *ACS Sustainable Chem. Eng.* **2020**.

[221] L. Rong, M. Zeng, H. Liu, B. Wang, Z. Mao, H. Xu, L. Zhang, Y. Zhong, J. Yuan, X. Sui, *Carbohydr. Polym.* **2019**, *209*, 223-229.

[222] P. Verma, S. Pal, S. Chauhan, A. Mishra, I. Sinha, S. Singh, V. Srivastava, *J. Mol. Struct.* **2020**, *1203*, 127410.

[223] R. Bonyasi, M. Gholinejad, F. Saadati, C. Nájera, *New J. Chem.* **2018**, *42*, 3078-3086.

[224] Â. de Fátima, T. C. Braga, L. d. S. Neto, B. S. Terra, B. G. F. Oliveira, D. L. da Silva, L. V. Modolo, *J. Adv. Res.* **2015**, *6*, 363-373.

[225] H. Liu, X. Sui, H. Xu, L. Zhang, Y. Zhong, Z. Mao, *Macromol. Mater. Eng.* **2016**, *301*, 725-732.

[226] H. Würfel, M. Kayser, T. Heinze, *Cellulose* **2018**, *25*, 4919-4928.

[227] A. W. T. King, J. Jalomäki, M. Granström, D. S. Argyropoulos, S. Heikkinen, I. Kilpeläinen, *Anal. Methods* **2010**, *2*, 1499-1505.

[228] A. C. Boukis, A. Llevot, M. A. R. Meier, *Macromol. Rapid Commun.* **2016**, *37*, 643-649.

[229] G. Maiti, P. Kundu, C. Guin, *Tetrahedron Lett.* **2003**, *44*, 2757-2758.

[230] W. Fan, Y. Queneau, F. Popowycz, *Green Chem.* **2018**, *20*, 485-492.

[231] Y. Jiugao, W. Ning, M. Xiaofei, *Starch - Stärke* **2005**, *57*, 494-504.

[232] R. Shi, Z. Zhang, Q. Liu, Y. Han, L. Zhang, D. Chen, W. Tian, *Carbohydr. Polym.* **2007**, *69*, 748-755.

[233] S. Estevez-Areco, L. Guz, L. Famá, R. Candal, S. Goyanes, *Food Hydrocoll.* **2019**, *96*, 518-528.

[234] A. López-Córdoba, C. Medina-Jaramillo, D. Piñeros-Hernandez, S. Goyanes, *Food Hydrocoll.* **2017**, *71*, 26-34.

[235] M. C. Pirrung, K. D. Sarma, *J. Am. Chem. Soc.* **2004**, *126*, 444-445.

[236] O. Kreye, T. Tóth, M. A. R. Meier, *J. Am. Chem. Soc.* **2011**, *133*, 1790-1792.

[237] K. A. Waibel, R. Nickisch, N. Möhl, R. Seim, M. A. R. Meier, *Green Chem.* **2020**, *22*, 933-941.

[238] S. Hell, K. Ohkawa, H. Amer, A. Potthast, T. Rosenau, *J. Wood Chem. Technol.* **2018**, *38*, 96-110.

[239] I. Sulaeva, K. M. Klinger, H. Amer, U. Henniges, T. Rosenau, A. Potthast, *Cellulose* **2015**, *22*, 3569-3581.

[240] A. J. Varma, V. B. Chavan, *Cellulose* **1995**, *2*, 41-49.

[241] U.-J. Kim, S. Kuga, *Thermochim. Acta* **2001**, *369*, 79-85.

[242] E. Esen, P. Hädinger, M. A. R. Meier, *Biomacromolecules* **2020**.

[243] K. Jedvert, T. Heinze, *J. Polym. Eng.* **2017**, *37*, 845.

[244] W. G. Glasser, *Macromol. Symp.* **2004**, *208*, 371-394.

[245] T. Kulomaa, J. Matikainen, P. Karhunen, M. Heikkilä, J. Fiskari, I. Kilpeläinen, *RSC Advances* **2015**, *5*, 80702-80708.

[246] P. Wang, B. Y. Tao, *J. Environ. Polym. Degrad.* **1995**, *3*, 115-119.

[247] L. Crépy, L. Chaveriat, J. Banoub, P. Martin, N. Joly, *ChemSusChem* **2009**, *2*, 165-170.

[248] S. Thiebaud, M. E. Borredon, *Bioresour. Technol.* **1995**, *52*, 169-173.

[249] Y. Wang, T. Heinze, K. Zhang, *Nanoscale* **2016**, *8*, 648-657.

[250] N. Joly, R. Granet, P. Branland, B. Verneuil, P. Krausz, *J. Appl. Polym. Sci.* **2005**, *97*, 1266-1278.

[251] Y. Zhou, D.-y. Min, Z. Wang, Y. Yang, S. Kuga, *BioResources* **2014**, *9*, 8.

[252] M. Jebrane, N. Terziev, I. Heinmaa, *Biomacromolecules* **2017**, *18*, 498-504.

[253] L. P. Hinner, J. L. Wissner, A. Beurer, B. A. Nebel, B. Hauer, *Green Chem.* **2016**, *18*, 6099-6107.

[254] A. Nakamura, M. Tokunaga, *Tetrahedron Lett.* **2008**, *49*, 3729-3732.

[255] R. E. Murray, *Transvinylation reaction*, **1991**, US Patent 4,981,973.

[256] J. Ziriakus, T. K. Zimmermann., A. Pöthig, M. Drees, S. Haslinger, D. Jantke, F. E. Kühn, *Adv. Synth. Catal.* **2013**, *355*, 2845-2859.

[257] A. Schenzel, A. Hufendiek, C. Barner-Kowollik, M. A. R. Meier, *Green Chem.* **2014**, *16*, 3266-3271.

[258] C. Satgé, R. Granet, B. Verneuil, P. Branland, P. Krausz, *C. R. Chim.* **2004**, *7*, 135-142.

[259] C. S. Marvel, L. E. Olson, *J. Polym. Sci.* **1957**, *26*, 23-28.

[260] M. Firdaus, M. A. R. Meier, U. Biermann, J. O. Metzger, *Eur. J. Lipid Sci. Technol.* **2014**, *116*, 31-36.

[261] M. Desroches, S. Caillol, V. Lapinte, R. Auvergne, B. Boutevin, *Macromolecules* **2011**, *44*, 2489-2500.

[262] A. Sehlinger, R. Schneider, M. A. R. Meier, *Eur. Polym. J.* **2014**, *50*, 150-157.

[263] S. Oelmann, A. Travanut, D. Barther, M. Romero, S. M. Howdle, C. Alexander, M. A. R. Meier, *Biomacromolecules* **2019**, *20*, 90-101.

[264] S. Fujii, T. J. McCarthy, *Langmuir* **2016**, *32*, 765-771.